THE MINOR PLANET BULLETIN

BULLETIN OF THE MINOR PLANETS SECTION OF THE ASSOCIATION OF LUNAR AND PLANETARY OBSERVERS

VOLUME 49, NUMBER 2, A.D. 2022 APRIL-JUNE

SECTION NEWS: ROBERT STEPHENS NAMED ASSOCIATE COORDINATOR OF THE MINOR PLANETS SECTION

Frederick Pilcher, Coordinator
ALPO Minor Planets Section

I am pleased to announce that Robert Stephens has accepted an invitation to the position of Associate Coordinator of the Minor Planets Section of the ALPO. As Associate Coordinator, Bob will assist and advise Coordinator Frederick Pilcher on the affairs of the Minor Planets Section. Pilcher anticipates retiring as Section Coordinator at an undetermined date a few years hence. At that time Stephens will advance to Section Coordinator.

Bob started observing asteroid lightcurves in 1999 and in the more than 20 subsequent years he has authored or co-authored over 300 research papers, including almost 1100 asteroid lightcurves, and 18 binary asteroid discoveries. He is a Full Member of the American Astronomical Society and a member of its Division for Planetary Sciences. Stephens is Treasurer of both the American Association of Variable Star Observers and the Society for Astronomical Sciences. He is also past President and past Treasurer of the Riverside Astronomical Society. Asteroid (39890) Bobstephens was named in his honor by the International Astronomical Union.

Please join me in welcoming Bob to this new role and in offering thanks for agreeing to this service.

CALL FOR OBSERVATIONS

Frederick Pilcher
4438 Organ Mesa Loop
Las Cruces, NM 88011 USA
fpilcher35@gmail.com

Observers who have made visual, photographic, or CCD measurements of positions of minor planets in calendar year 2021 are encouraged to report them to this author on or before 2022 April 1. This will be the deadline for receipt of reports, for which results can be included in the "General Report of Position Observations for 2021," to be published in *MPB* Vol. 49, No. 3.

CALL FOR MINOR PLANET OBSERVERS TO JOIN THE ALPO EXOPLANET SECTION

Jerry Hubbell
Acting Coordinator, Exoplanet Section
Association of Lunar and Planetary Observers (ALPO)
Mark Slade Remote Observatory (MSRO) W54
Wilderness, VA USA
jerry.hubbell@alpo-astronomy.org

This is a call for interested minor planet observers to join in the effort to observe exoplanets as a member of the Exoplanet Section of the Association of Lunar and Planetary Observers (ALPO). Minor planet observers already possess a large part of the requisite skills and knowledge to perform effective observations and provide high-quality data.

In November 2020, the ALPO Board of Directors approved the formation of the Exoplanet Section and appointed this author as the Acting Coordinator. The initial mission of the Exoplanet Section is to train members in the current techniques used to obtain high quality data and perform the high-precision measurements needed to not only detect exoplanets using the transit method, but also to model the measured exoplanet orbit. This modeling will help to refine the ephemerides of the exoplanet and contribute valuable data needed to fully understand these new celestial bodies.

The Exoplanet Section was originally formed with the following groups:

1. Instrumentation Group
2. Observing Program Group
3. Analysis & Modeling Group
4. Exoplanet Data Reporting Group
5. Exoplanet Observation Training Group

The primary goal of the Instrumentation Group is to define and demonstrate valid instrument configurations and components including the selection of off-the-shelf instruments, the determination of configuration settings and parameters, and researching the use and application of new instrument systems, sub-systems, and components. Additional work is needed to understand and measure the different sources of error due to the instruments used for the observation of exoplanet transits.

The primary goal of the Observing Program Group is to provide the needed resources for members to be able to easily identify exoplanets to observe and develop the information needed to acquire the observations and do the analysis of the observations for specific exoplanets. Processes and procedures will also be developed to coordinate observations of specific exoplanet transit events between our members.

The Analysis and Modeling group members are interested in learning how to process the data acquired during their own observation runs or may be interested in processing and analyzing other member's data. It is expected that the group members will develop and improve data processing and analysis techniques and perhaps develop new and improved exoplanet transit modeling tools. A large part of this group's members may be dedicated to computer-based analysis and modeling automation tools in the future.

The primary role of the Exoplanet Data Reporting Group is to coordinate the transfer of data and analysis results to those external professional and other organizations that want and need the exoplanet observation data our members create. The reporting group will also manage and archive all member data and analysis results in a standard format suitable for searching and for the development of papers based on the exoplanet members' observations. Finally, the Reporting Group will coordinate the work of our members with professional exoplanet observing programs to provide pro/am opportunities, to contribute to real research, and to realize the opportunity to get published in professional papers.

The Exoplanet Observation Training Group will provide members with documents, procedures, presentations, and other training material developed by the section needed to learn how to observe and analyze transit data and report exoplanet transit observations. The Training Group members will also maintain contact with the larger exoplanet observing community to bring "best practices" and relevant information back to the exoplanet section for implementation as desired.

The purpose of this "Call for Observers" brief is to solicit interested minor planet observers to join the Observing Program Group and provide observations of exoplanet transits using the techniques and procedures developed by the Exoplanet Section. Your contributions in reviewing procedures and further developing and refining techniques are also welcome.

Here are a few resources to get you started in finding targets to start your planning. The resources here are used by the TESS Follow-up Observation Program (TFOP) members. The astronomers at the MSRO are on the TFOP team as part of the SG1 group (Seeing-limited Observing group) managed by Dr. Karen Collins, Harvard & Smithsonian Center for Astrophysics.

The ExoFOP-TESS for the TESS TOI and KELT-FP observations:

https://exofop.ipac.caltech.edu/tess

You must apply for your own ExoFOP-TESS account:

https://exofop.ipac.caltech.edu/account.html

The TESS Transit Finder (TTF) is used to find events for your location on the night(s) of interest:

http://astro.swarthmore.edu/telescope/tess/find_tess_transits.cgi

TESS Observations Coordinator (TOC) is used to list your planned observations to let other SG1 team members know what you are planning to observe:

http://www.astro.louisville.edu/tessplanner

Your inquires are welcome! Please contact Jerry Hubbell at jerry.hubbell@alpo-astronomy.org if you are interested in joining the ALPO Exoplanet Section, or if you would like more information.

[EDITOR'S NOTE: It is with great enthusiasm that the Minor Planets Section Coordinator and *Minor Planet Bulletin* Editor endorse this invitation for experienced minor planet observers to also consider contributing their expertise and efforts toward the exciting and emerging science of exoplanet photometry.]

ROTATION PERIOD DETERMINATION FOR ASTEROID 849 ARA

Nick Sioulas
NOAK Observatory (L02)
Stavraki Ioannina, Greece
nsioulas@hotmail.com

(Received: 2021 October 28)

Photometric observations of the main-belt asteroid 849 Ara were conducted from the NOAK Observatory, in Greece in order to determine its synodic rotation periods. The results are: P = 4.119 ± 0.001 h, A = 0.18 mag.

Asteroid 849 Ara (A915 UB) was discovered by Russian astronomer Sergey Belyavsky on February 09, 1912 at the Simeis Observatory on the Crimean Peninsula. It is an outer main-belt asteroid with a semi-major axis of 3.147AU, eccentricity 0.201, inclination 19.523° and an orbital period of 5.58 years. Its absolute magnitude is $H = 8.2$ (MPO473773).

We report observations of 849 Ara performed at the NOAK Observatory, Ioannina Greece (MPC-International Astronomical Union code L02), using a 0.25m Newtonian Skywatcher optical tube operating at f/4.7. The optical tube is mounted on NEQ6 Skywatcher robotic mount and equipped with ATIK 460exm CCD camera. It is a high Quantum Efficiency CCD. No filters were used for better signal-to-noise. Exposure time for all images was 2 minutes. The images binned at 1×1 yielding an image scale of 0.78 arcsec/pixel and the field of view 35.77'× 28.61'. In these fields, the asteroid and five comparison stars were measured for differential photometry.

All images were reduced in the standard manner using nightly flatfield files as well as dark-current and bias images. Photometric measurements and lightcurve analysis were performed using *MPO Canopus* (version 10.8.1.1; Warner, 2019). The *Cartes Du Ciel* was used as the planetarium software with the most recent ephemerides downloaded from the Minor Planet Center and *Artemis Capture* was used for image capture.

The period analysis shows a solution for the rotational period of $P = 4.119 \pm 0.001$ h with an amplitude $A = 0.18 \pm 0.03$ mag, which is close to the previously published results in the asteroid lightcurve database 4.116 h (LCDB; Warner et al., 2009).

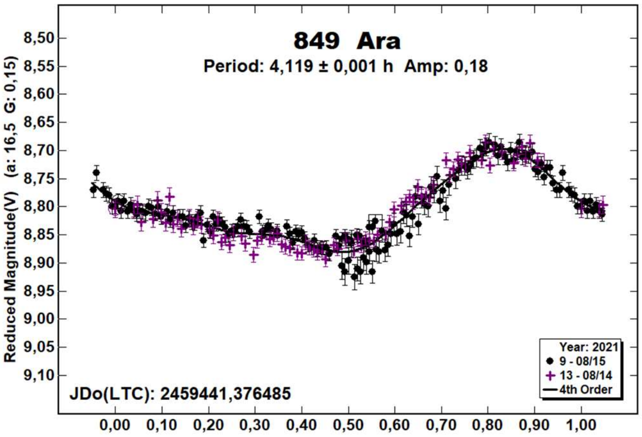

References

Harris, A.W.; Young, J.W.; Scaltriti, F.; Zappala, V. (1984). "Lightcurves and phase relations of the asteroids 82 Alkmene and 444 Gyptis." *Icarus* **57**, 251-258.

JPL (2020). Small Body Database Browser. *https://ssd.jpl.nasa.gov*

MPC (2020). Database Search. *https://minorplanetcenter.net/db_search/*

Warner, B.D.; Harris, A.W.; Pravec, P. (2009). "The Asteroid Lightcurve Database." *Icarus* **202**, 134-146. Updated 2019 Aug. *http://www.minorplanet.info/lightcurvedatabase.html*

Warner, B.D. (2019). MPO Software, *MPO Canopus* v10.8.1.1. Bdw Publishing. *http://minorplanetobserver.com*

Number	Name	yyyy mm/dd	Phase	L_{PAB}	B_{PAB}	Period(h)	P.E.	Amp	A.E.	Grp
849	Ara	2021 08/14-08/15	16.9,16.7	0.7	19.7	4.119	0.001	0.18	0.03	MB-O

Table I. Observing circumstances and results. The phase angle is given for the first and last date. If preceded by an asterisk, the phase angle reached an extrema during the period. L_{PAB} and B_{PAB} are the approximate phase angle bisector longitude/latitude at mid-date range (see Harris et al., 1984). Grp is the asteroid family/group (Warner et al., 2009).

ROTATIONAL PERIOD DETERMINATION OF 5987 LIVIOGRATTON

Maurizio Scardella, Angelo Tomassini, Fernando Pierri
ATA (Associazione Tuscolana di Astronomia)
“F. Fuligni” Observatory (MPC code D06)
Via Lazio, 14 - Rocca di Papa (RM) - 00040 - ITALY
nikkor5@gmail.com

(Received: 2022 January 6)

We report observations of the main-belt asteroid 5987 Liviogratton in September 2021. Our results show P = 3.2 ± 0.1 h with an amplitude of A = 0.19 mag.

Discovered in June 1975 at Felix Aguilar Observatory (Argentina) the main-belt asteroid 5987 Liviogratton was selected for our measurements owing to historical reasons. Our Association (ATA) is dedicated to Prof. Livio Gratton who lived and worked near the site where our astronomical observatory is located. The observations were carried out from “F. Fuligni” Observatory located in the Astronomical Park “Livio Gratton” during two nights in September 2021. The telescope used is a Meade 0.35-m f/10 ACF telescope equipped with SBIG ST8-XE CCD camera. All images were unfiltered and were dark and flat-field calibrated with *Maxim DL*. The analysis of the lightcurve was made with a differential photometry technique extrapolating the best polynomial of approximation of the observations, using the *MPO Canopus* (Warner, 2012). The derived synodic period determined has been P = 3.2 ± 0.1 h with an amplitude of A = 0.19 mag.

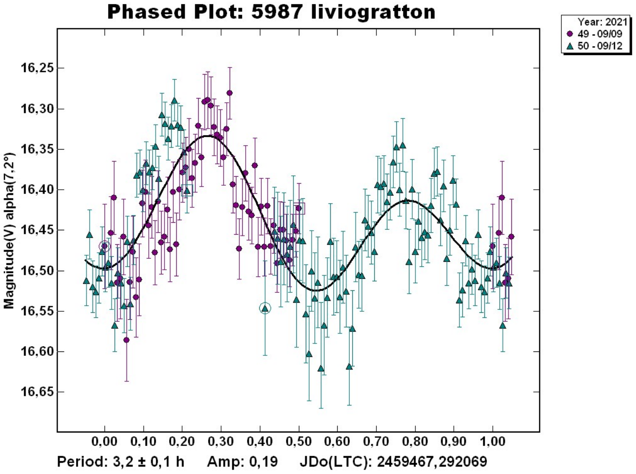

Acknowledgement

We would like to thank Simone Nodari and Samuele Piscitello for their help in take image frames and maintenance of the ATA observatory instruments.

References

Harris, A.W.; Young, J.W.; Scaltriti, F.; Zappala, V. (1984). “Lightcurves and phase relations of the asteroids 82 Alkmene and 444 Gyptis.” *Icarus* **57**, 251-258.

Warner, B.D.; Harris, A.W.; Pravec, P. (2009). “The Asteroid Lightcurve Database.” *Icarus* **202**, 134-146. Updated 2021 June. *https://minorplanet.info/php/lcdb.php*

Warner, B.D. (2012). MPO Software, Canopus version 10.4.1.9. Bdw Publishing, *http://minorplanetobserver.com/*

Number	Name	2021 mm/dd	Pts	Phase	L_{PAB}	B_{PAB}	Period(h)	P.E.	Amp	A.E.	Grp
5987	Liviogratton	09/09-09/12	158	7.2,8.7	335	0.5	3.2	0.1	0.19	0.02	MBA

Table I. Observing circumstances and results. Pts is the number of data points. The phase angle is given for the first and last date. L_{PAB} and B_{PAB} are the approximate phase angle bisector longitude and latitude at mid-date range (see Harris et al., 1984). Grp is the asteroid family/group (Warner et al., 2009).

SYNODIC AND SIDEREAL ROTATION PERIODS OF KORONIS FAMILY MEMBER (1762) RUSSELL

Stephen M. Slivan, Abigail Colclasure, Inés Escobedo,
Aidan Henopp, Rory Knight, Andi Mitchell
Massachusetts Institute of Technology,
Dept. of Earth, Atmospheric, and Planetary Sciences
77 Mass. Ave. Rm. 54-427, Cambridge, MA 02139
slivan@mit.edu

Francis P. Wilkin
Union College Dept. of Physics and Astronomy
Schenectady, NY

(Received: 2021 November 10)

Rotation lightcurves of Koronis asteroid family member (1762) Russell were observed in 2021, yielding a synodic rotation period of 12.7946 ± 0.0004 h. The precision is shown to be sufficient to unambiguously count sidereal rotations across the entire data set of available Russell lightcurves, and constrain the sidereal rotation period to 12.79381 ± 0.00007 h prograde.

Koronis family member (1762) Russell was observed in 2021 as part of an ongoing observing program to study rotation properties of the family's brighter objects (Slivan et al., 2008). Previous lightcurve observations of Russell from 2014 have been reported by Cooney et al. (2015), spanning 44 days with a derived rotation period of 12.797 ± 0.007 h. Subsequent statistical analyses of "sparse data" from photometric surveys have produced solutions for sidereal periods and pole locations that are not consistent with each other within their estimated errors (Ďurech et al., 2018a; Ďurech and Hanuš, 2018b). The new observations were made to improve the determination of the synodic rotation period, by obtaining a set of lightcurves spanning a relatively long calendar interval of several lunations during the 2021 apparition (Slivan, 2012).

Nightly observing information is summarized in Table I, and details about the instruments used are given in Table II. Observations prior to the Sep. 8 opposition were made using telescopes at the Wallace Astrophysical Observatory in Westford, MA. Processing and measurement of the images were as described by Slivan et al. (2008), except that for these observations made using smaller telescopes the choices of synthetic aperture sizes for the on-chip relative photometry were guided by the experience of Howell (1989). Observations near and after opposition were made remotely using the CHI-1 telescope of Telescope Live in Rio Hurtado, Chile, for which candidate nights during the post-opposition lunation were identified specifically to overlap the best pre-opposition coverage of rotation phase. The CHI-1 images were measured using *AstroImageJ*, and comparison stars having APASS DR10 catalog colors similar to solar were used to minimize systematic errors in the zero-point calibration to r' magnitudes.

The calibrated r' data were reduced to unit distances. A fit of the Lumme-Bowell model (Bowell et al., 1989) to the brightnesses of the well-observed lightcurve maximum was used to determine the slope parameter of $G_{r'} = 0.285$ used to account for changing solar phase angle in producing the composite lightcurve (Fig. 1).

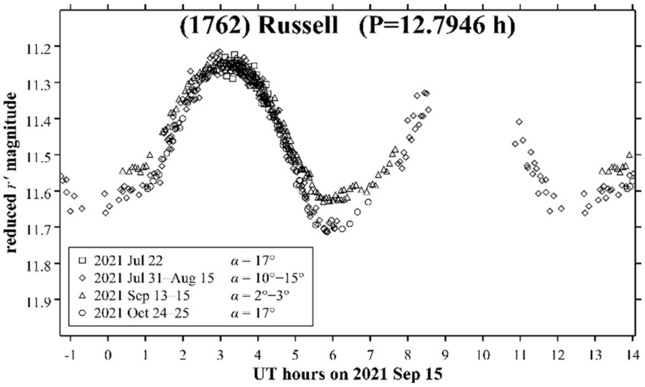

Figure 1. Folded composite lightcurve of (1762) Russell during four lunations of its 2021 apparition, light-time corrected, showing one rotation period plus the earliest and latest 10% repeated. The estimated error in the *r′* zero-point calibration is 0.03 mag. Nights of relative photometry have been shifted in brightness to form a self-consistent composite with the calibrated *r′* lightcurves. Solar phase angles *α* of the observations are given in the legend, and changing depth of the lightcurve minima with solar phase angle is apparent.

The best information to improve the period comes from the observations on Jul. 31 and on Oct. 25, which recorded the same rotation phase brightness increase and lightcurve maximum 86 days apart at comparable solar phase angles. The derived synodic period 12.7946 ± 0.0004 h is consistent with the previously published synodic period.

The "sieve algorithm" of Slivan (2013) is used here to test whether the improved period precision is sufficient to unambiguously count sidereal rotations across the entire available lightcurve data set. In addition to the lightcurves from 2014 and 2021, observations of Russell made in 2019 and 2020 by the ATLAS astrometric survey (Tonry et al., 2018) are suitable for folded composite lightcurves and are publicly available online from the MPC astrometry Web site; the epochs measured for all four apparitions are given in Table III.

The initial constraint on the sidereal period for the algorithm is based on the best synodic period, but at the precision level of the new determination, the change in viewing aspect during the time interval spanning the observations upon which it is based also is significant and needs to be accounted for. Instead of dividing the time interval by the integer number of elapsed synodic rotations N, a range of sidereal periods allowing for the maximum possible effect of the aspect change is calculated by using $N \pm (\Delta\lambda_{PAB}/360°)$ as the divisor where $\Delta\lambda_{PAB}$ is the change in ecliptic longitude of the phase angle bisector. In this case $N = 161$ rotations and $\Delta\lambda_{PAB} = 3.5°$ allowing a range of possible sidereal periods up to 0.0008 h shorter and longer than the synodic period, which when combined with 2.5× the period error to include a ~99% confidence interval, yields an initial constraint range half-width of 0.0018 h. The algorithm results (Fig. 2) confirm an unambiguous solution that corresponds to 5202 sidereal rotations during the maximum epoch interval, leaving unknown only the sign of the fractional part that depends on the direction of spin.

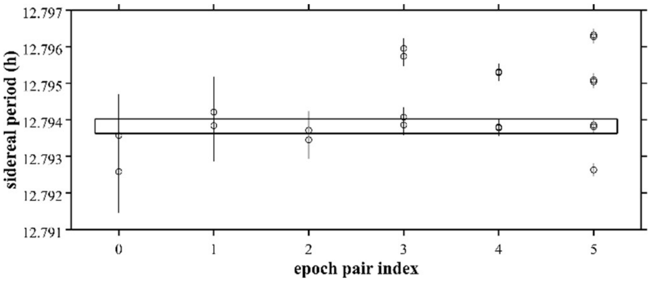

Figure 2: Single range of possible sidereal rotation periods of (1762) Russell allowed by the epochs in Table III as described in the text. The epoch measurement adopted errors are 28 min which is 1.5× the maximum observed asymmetry of the timing of the maxima in the composite lightcurves. Each horizontal coordinate index marks the time interval between a pair of epochs, with longer intervals to the right. Open circles and vertical bars represent sidereal periods and period ranges, respectively, calculated from every possible number of rotations that could elapse during the interval. The thin horizontal rectangle identifies the single range of periods that is allowed by all six time intervals.

Distinguishing between the two corresponding possible sidereal period ranges - one each prograde and retrograde, overlapping - requires knowing the direction of spin. Although the available data do not confidently fully locate the pole, there is enough information for sidereal photometric astrometry (Slivan, 2014; Drummond et al., 1988) to identify prograde rotation, for which the corresponding allowed range for the sidereal period from the sieve algorithm is 12.79363 to 12.79399 h. Adopting the associated period result from the algorithm, with the allowed range as an estimate of a ~99% confidence interval (half-width 2.5σ), yields a sidereal period of 12.79381 ± 0.00007 h prograde. The period result is consistent with that of Ďurech et al. (2018a) but not Ďurech and Hanuš (2018b).

UT date 2021	Tel. ID	Filter	Solar phase angle(°)	PAB λ (°)
Jul 22.2	WAO-4	*R*	17.2	343.8
Jul 31.3	WAO-3	*R*	14.9	344.6
Aug 01.2	WAO-3,4	*R*	14.7	344.7
Aug 03.2	WAO-3	*R*	14.1	344.9
Aug 07.2	WAO-2	*R*	12.9	345.1
Aug 14.2	WAO-2,4	*R*	10.5	345.5
Aug 15.3	WAO-2,3	*R*	10.1	345.6
Sep 13.1	CHI-1	*r′*	1.9	346.0
Sep 14.2	CHI-1	*r′*	2.4	346.0
Sep 15.1	CHI-1	*r′*	2.8	346.0
Oct 24.1	CHI-1	*r′*	16.6	348.0
Oct 25.1	CHI-1	*r′*	16.9	348.1

Table I: Nightly observing information, with rows grouped by lunation. Columns are: UT date at lightcurve mid-time, telescope ID (see Table II), filter used (Cousins R; Sloan r'), solar phase angle, and J2000 ecliptic longitude of the phase angle bisector.

Tel. ID	Dia. (m)	CCD camera	FOV (′)	Bin	Scale (″/pix)	Int. (s)
WAO-2	0.36	SBIG STL-1001	22×22	1×1	1.26	180
WAO-3	0.36	SBIG STL-1001	20×20	1×1	1.18	180
WAO-4	0.36	SBIG STL-1001	21×21	1×1	1.25	180
CHI-1	0.61	FLI-PL9000	32×32	2×2	1.24	240

Table II: Telescopes and cameras information. Columns are: telescope ID, telescope diameter, CCD camera, detector field of view, image binning used, binned image scale, and image integration time used.

UT epoch	PAB λ,β(°)	Data reference
2014 Mar 23 1.23 h	164.4 +0.3	Cooney et al. 2015
2019 Mar 14 1.46 h	174.7 +0.7	ATLAS-MLO *o*-band
2020 May 31 5.29 h	253.0 +2.8	ATLAS-MLO *o*-band
2021 Oct 25 2.76 h	348.1 -0.8	this paper

Table III: Summary of (1762) Russell lightcurve epochs, in each case locating a maximum from the second harmonic of a Fourier series model that was fit to lightcurves. λ,β are J2000 ecliptic longitude and latitude of the phase angle bisector. Photometry from the ATLAS-MLO survey (Tonry et al., 2018) was retrieved from the MPC Orbits/Observations Database.

Acknowledgements

We thank Dr. Michael Person and Timothy Brothers for allocation of telescope time at Wallace and for observer instruction and support. The student observers were supported by a grant from MIT's Undergraduate Research Opportunities Program. We thank Ernesto Guido at Telescope Live for very timely assistance with the remote observing. F. Wilkin received funding from the Faculty Research Grant at Union College. This work has made use of the AAVSO Photometric All-Sky Survey (APASS), funded by the Robert Martin Ayers Sciences Fund and NSF AST-1412587. This work also has made use of data and services provided by the International Astronomical Union's Minor Planet Center; specifically, the brightnesses accompanying astrometry from the Asteroid Terrestrial-impact Last Alert System (ATLAS) survey observing program.

References

Bowell, E.; Hapke, B.; Domingue, D.; Lumme, K.; Peltoniemi, J.; Harris, A.W. (1989). "Application of Photometric Models to Asteroids." In *Asteroids II* (R.P. Binzel; T. Gehrels; M.S. Matthews, eds.) pp. 524-556. Appendix: The IAU Two-Parameter Magnitude System for Asteroids. U. of Arizona Press, Tucson, AZ.

Cooney, W.R.; Gross, J.; Terrell, D.; Klinglesmith, D.A.; Hanowell, J. (2015). "Rotation Period and Lightcurve of 1762 Russell." *Minor Planet Bull.* **42**, 66–67.

Drummond, J.D.; Weidenschilling, S.J.; Chapman, C.R.; Davis, D.R. (1988). "Photometric geodesy of main-belt asteroids. II. Analysis of lightcurves for poles, periods, and shapes." *Icarus* **76**, 19-77.

Number	**Name**	**yyyy mm/dd**	**Phase**	**L_{PAB}**	**B_{PAB}**	**Period(h)**	**P.E.**	**Amp**	**A.E.**
1762	Russell	2021 07/22-10/25	*17.2,16.9	346	0	12.7946	0.0004	0.46	0.03

Table IV. Observing circumstances and results. Solar phase angle is given for the first and last dates; the asterisk indicates that the phase angle reached a minimum within that interval. L_{PAB} and B_{PAB} are the phase angle bisector longitude and latitude at mid-date range.

Ďurech, J.; Hanuš, J.; Alí-Lagoa, V. (2018a). “Asteroid models reconstructed from the Lowell Photometric Database and WISE data.” *Astron. Astrophys.* **617**, A57.

Ďurech, J.; Hanuš, J. (2018b). “Reconstruction of asteroid spin states from Gaia DR2 photometry.” *Astron. Astrophys.* **620**, A91.

Howell, S.B. (1989). “Two-dimensional Aperture Photometry: Signal-to-noise Ratio of Point-source Observations and Optimal Data-extraction Techniques.” *PASP* **101**, 616-622.

Slivan, S.M.; Binzel, R.P.; Boroumand, S.C.; Pan, M.W.; Simpson, C.M.; Tanabe, J.T.; Villastrigo, R.M.; Yen, L.L.; Ditteon, R.P.; Pray, D.P.; Stephens, R.D. (2008). “Rotation Rates in the Koronis Family, Complete to $H \approx 11.2$.” *Icarus* **195**, 226-276.

Slivan, S.M. (2012). “Epoch Data in Sidereal Period Determination. I. Initial Constraint from Closest Epochs.” *Minor Planet Bull.* **39**, 204-206.

Slivan, S.M. (2013). “Epoch Data in Sidereal Period Determination. II. Combining Epochs from Different Apparitions.” *Minor Planet Bull.* **40**, 45-48.

Slivan, S.M. (2014). “Sidereal Photometric Astrometry as Efficient Initial Search for Spin Vector.” *Minor Planet Bull.* **41**, 282-284.

Tonry, J.L.; Denneau, L.; Heinze, A.N.; Stalder, B.; Smith, K.W.; Smartt, S.J.; Stubbs, C.W.; Weiland, H.J.; Rest, A. (2018). “ATLAS: A High-cadence All-sky Survey System.” *PASP* **130**, 064505.

PHOTOMETRIC OBSERVATIONS AND DATA ANALYSIS OF NEA BINARY ASTEROID 5143 HERACLES

Brian D. Warner
Center for Solar System Studies / MoreData!
446 Sycamore Ave.
Eaton, CO 80615 USA
brian@MinorPlanetObserver.com

Robert D. Stephens
Center for Solar System Studies / MoreData!
Rancho Cucamonga, CA 91730

(Received: 2022 January 12)

Analysis of CCD photometric observations of the known binary asteroid 5143 Heracles (Taylor et al., 2012) was conducted at the Center for Solar System Studies based on observations obtained in 2021 October and November. A secure period of P1 = 2.70776 ± 0.00006 h was established for the rotation of the primary. The secondary period is ambiguous and depends on whether or not the rotation of the secondary is locked to its orbital period. Our analysis favors an independently rotating secondary with P2 = 46.41 h.

Observations of the near-Earth asteroid 5143 Heracles were made at the Center for Solar System Studies in 2021 October and November. They were made with a 0.35-m f/9.1 Schmidt-Cassegrain and FLI Microline CCD camera. The camera uses a KAF-1001E chip, which has a 1024×1024×24m array of pixels. The combination gives a field-of-view of about 25×25 arcminutes and image scale of 1.5 arcsec/pixel. The analysis of our data follows below.

All lightcurve observations were unfiltered since a clear filter can cause a 0.1-0.3 mag loss. The exposure duration varied depending on the asteroid’s brightness and sky motion. Guiding on a field star sometimes resulted in a trailed image for the asteroid.

Measurements were made using *MPO Canopus*. The Comp Star Selector utility in *MPO Canopus* found up to five comparison stars of near solar-color for differential photometry. To reduce the number of adjusted nightly zero points and their amounts, the analysis of the 2021 data used the ATLAS catalog r´ (SR) magnitudes (Tonry et al., 2018). The rare zero-point adjustments ≥ ±0.03 mag may be related in part to using unfiltered observations, poor centroiding of the reference stars, not correcting for second-order extinction, or selecting a star that is an unresolved pair.

The Y-axis values are ATLAS SR “sky” (catalog) magnitudes. The two values in the parentheses are the phase angle (a) and the value of *G* used to normalize the data to the comparison stars used in the earliest session. This, in effect, corrected all the observations to seem to have been made at a single fixed date/time and phase angle, leaving any variations due only to the asteroid’s rotation and/or albedo changes. The X-axis shows rotational phase from -0.05 to 1.05. If the plot includes the amplitude, e.g., “Amp: 0.65”, this is the amplitude of the Fourier model curve and *not necessarily the adopted amplitude for the lightcurve*.

References to previous works were taken from the asteroid lightcurve database (Warner et al., 2009), known as “LCDB” from here on. Since most listed rotation periods for the primary were very similar, only a few of the LCDB references have been used.

5143 Heracles is a known binary, first suspected by Pilcher et al. (2012) based on optical observations in 2021 November and then confirmed with radar observations in December of that year (Taylor et al., 2012).

The most notable feature when plotting the raw data was an apparently long period. We tried different values for the phase slope parameter (*G*), the default 0.15 and then 0.40. The latter was close to that derived from IR observations, e.g., Thomas et al. (2011) and Usui et al. (2011). As discussed below, using *G* = 0.40 kept nightly zero-point adjustments to less than ±0.03 mag while using *G* = 0.15 required more frequent adjustments of up to ±0.07 mag. These are generally much larger than when using SR magnitudes from the ATLAS catalog (Tonry et al., 2018).

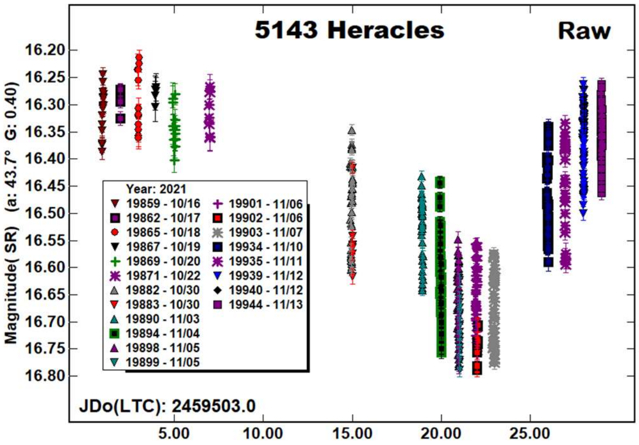

The search for a longer period in the data led to a period spectrum indicating a number of possible solutions. It was not the value of *G* but the number of orders in the Fourier search that had the more pronounced effect on the period search. We used 4th order to keep the undulations of the secondary period lightcurves in check.

Based on the raw data plot, we first opted to search for a long period between 40-50 hours. This was contradictory to the premise that the satellite was tidally locked to its orbital period but Taylor et al. (2012) did allow that an orbital period of 40-57 h was possible if the satellite rotation period was not also that of its orbital period.

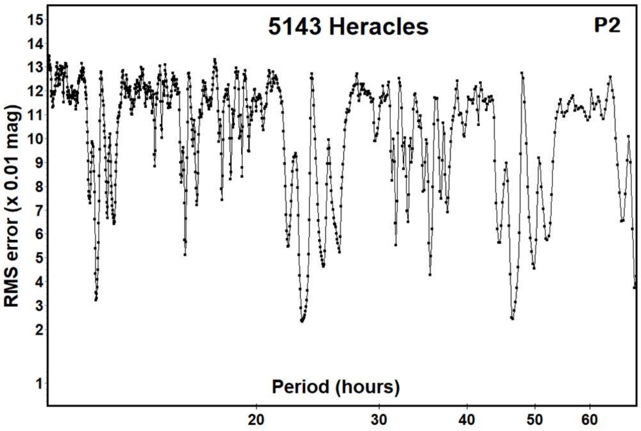

After finding the primary rotation period and a secondary period of about 46 hours, we then forced the secondary period to a range of 13-18 h, the range considered more likely by Taylor et al. (2012). In both cases, a value of *G* = 0.40 was used because, as mentioned above, this reduced the nightly zero-point adjustments to acceptable and more typical values. We could and did try using *G* = 0.15 and allowed substantial zero-point adjustments. Even so, the quality of the two lightcurves was considerably diminished.

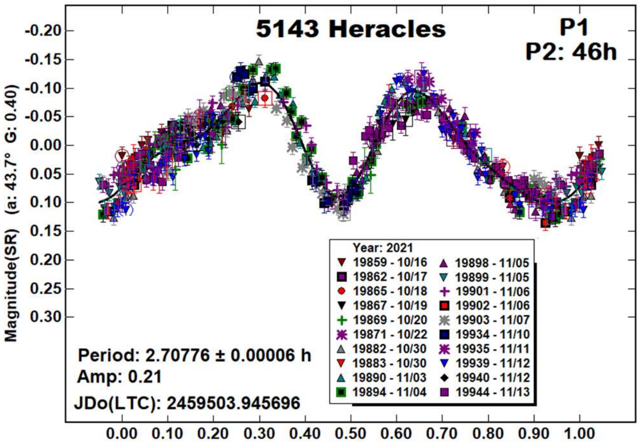

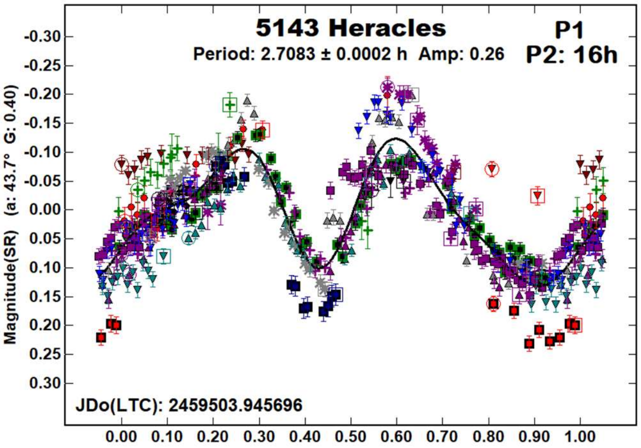

The two plots for the primary rotation period (P_1) show a dramatic difference in the quality of the fit between using a secondary period of about 46 h or 16 h. In this comparison, the zero-point adjustments were kept at the values used to find the higher-quality solution (P1, P2: 46h), i.e., ≤ ±0.03 mag. Even when allowing much larger adjustments, there was not much improvement in the P_1 and P_2 plots when using P_2 = 16 h.

The two plots for the secondary period show a similar, dramatic difference in the quality of the lightcurve fits depending on the adopted period. Given the better fits to the P_1 and P_2 lightcurves, which do not appear to be the result of a *fit by exclusion*, i.e., minimizing the number of overlapping data points, the longer secondary period, P_2 = 46.43 h, has been adopted for this work.

Looking at the results from other optical campaigns, Vaduvescu et al. (2017), using data from the 2016 apparition, found a secondary period of 17.114 h, which is more in line with the assumed tidally-locked satellite. Previous observations (Warner, 2017; 2018) found periods of 2.704 h and 2.758 h, respectively, for the primary but there were no obvious signs of a satellite in those data.

Number	Name	2021 mm/dd	Phase	L_{PAB}	B_{PAB}	Period(h)	P.E.	Amp	A.E.	Grp
5143	Heracles	10/16-11/13	43.6,78.5	87	18	2.70776	0.00006	0.21	0.02	NEA
						46.41	0.01	0.37	0.03	

Table II. Observing circumstances. The first line gives the primary period for the system. The second line gives the secondary period. The phase angle (α) is given at the start and end of each date range. An asterisk indicates that the phase angle reached a maximum or minimum during the period. L_{PAB} and B_{PAB} are, respectively the average phase angle bisector longitude and latitude (see Harris et al.,1984). For the Grp/Dr column, the first line gives the group/family: NEA: Near-Earth asteroid.

The next time the asteroid is V < 18 is in 2023 October. Maybe then the asteroid's true nature and parameters can be confirmed.

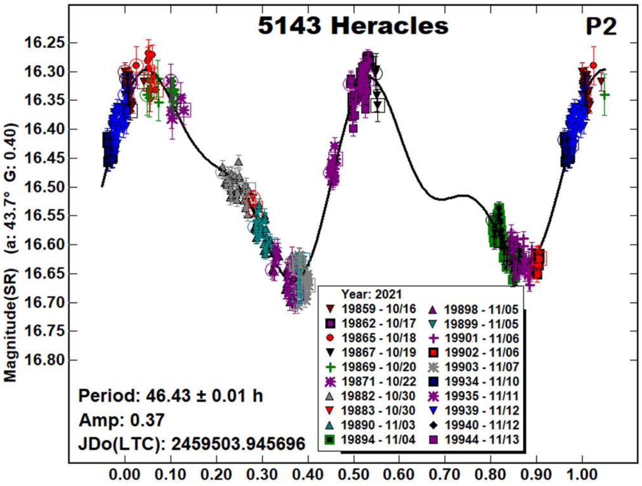

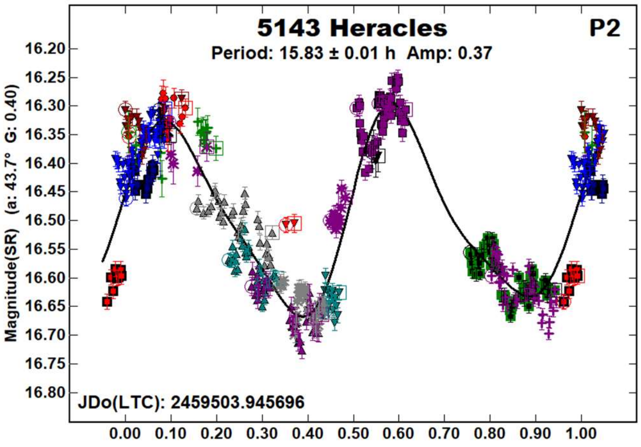

Acknowledgements

The authors gratefully acknowledge Shoemaker NEO Grants from the Planetary Society (2007, 2013). These were used to purchase some of the telescopes and CCD cameras used in this research. This work includes data from the Asteroid Terrestrial-impact Last Alert System (ATLAS) project. ATLAS is primarily funded to search for near earth asteroids through NASA grants NN12AR55G, 80NSSC18K0284, and 80NSSC18K1575; byproducts of the NEO search include images and catalogs from the survey area. The ATLAS science products have been made possible through the contributions of the University of Hawaii Institute for Astronomy, the Queen's University Belfast, the Space Telescope Science Institute, and the South African Astronomical Observatory. This paper made use of the services provided by the SAO/NASA Astrophysics Data System, which is operated by the Smithsonian Astrophysical Observatory under NASA Cooperative Agreement 80NSSC211M0056.

References

Harris, A.W.; Young, J.W.; Scaltriti, F.; Zappala, V. (1984). "Lightcurves and phase relations of the asteroids 82 Alkmene and 444 Gyptis." *Icarus* **57**, 251-258.

Pilcher, F.; Briggs, J.W.; Franco, L.; Inasaridze, R.Y.; Krugly, Y.N.; Molotiv, I.E.; Klinglesmith III, D.A.; Pollock, J.; Pravec, P. (2012). "Rotation Period Determination of 5143 Heracles." *Minor Planet Bull.* **39**, 148-151.

Taylor, P.; Nolan, M.C.; Howell, E.S. (2012). "5143 Heracles." *CBET* **3176**.

Thomas, C.A.; Trilling, D.E.; Emery, J.P.; Mueller, M.; Hora, J.L.; Benner, L.A.M.; Bhattacharya, B.; Bottke, W.F.; Chesley, S.; Delbo, M.; Fazio, G.; Harris, A.W.; Mainzer, A.; Mommert, M.; Morbidelli, A.; Penprase, B.; Smith, H.A.; Spahr, T.B.; Stansberry, J.A. (2011). "ExploreNEOs. V. Average Albedo by Taxonomic Complex in the Near-Earth Population." *Astron. J.* **142**, A85.

Tonry, J.L.; Denneau, L.; Flewelling, H.; Heinze, A.N.; Onken, C.A.; Smartt, S.J.; Stalder, B.; Weiland, H.J.; Wolf, C. (2018). "The ATLAS All-Sky Stellar Reference Catalog." *Ap. J.* **867**, A105.

Usui, F.; Kuroda, D.; Muller, T.G.; Hasegawa, S.; Ishiguro, M.; Ootsubo, T.; Ishihara, D.; Kataza, H.; Takita, S.; Oyabu, S.; Ueno, M.; Matsuhara, H.; Onaka, T. (2011). "Asteroid Catalog Using Akari: AKARI/IRC Mid-Infrared Asteroid Survey." *Pub. Astron. Soc. Japan* **63**, 1117-1138.

Vaduvescu, O.; Aznar, A.M.; Tudor, V.; Predatu, M. and 23 co-authors. (2017). "The EURONEAR Lightcurve Survey of Near-Earth Asteroids." *Earth, Moon, and Planets* **120**, 41-100.

Warner, B.D., Harris, A.W., Pravec, P. (2009). "The Asteroid Lightcurve Database." *Icarus* **202**, 134-146. Updated 2021 May. *http://www.minorplanet.info/lightcurvedatabase.html*

Warner, B.D. (2017). "Near-Earth Asteroid Lightcurve Analysis at CS3-Palmer Divide Station: 2016 July-September." *Minor Planet Bull.* **44**, 22-36.

Warner, B.D. (2018). "Near-Earth Asteroid Lightcurve Analysis at CS3-Palmer Divide Station: 2017 July Through October." *Minor Planet Bull.* **45**, 19-34.

LIGHTCURVE FOR KORONIS FAMILY MEMBER 2498 TSESEVICH

Francis P. Wilkin
Department of Physics and Astronomy, Union College
807 Union St., Schenectady NY 12308
wilkinf@union.edu

Rebecca Z. Schechter
Niskayuna, NY

(Received: 2022 Jan 15)

Observations of the Koronis-family asteroid 2498 Tsesevich were obtained on five nights in 2021 at the 0.61m Chi-1 telescope of El Sauce Observatory. We obtained a doubly-periodic lightcurve with period 2.8737 ± 0.0002 h and an amplitude in Sloan r´ (SR) of 0.26 ± 0.04 mag.

Observations were performed from 2021 April-July in Sloan r´ filter on the Chi-1 (0.61 m) telescope at El Sauce Observatory in the Rio Hurtado Valley, Chile, operated by Telescope Live. Target selection and ephemeris were based upon the Koronis family asteroids web tool (Slivan 2003). The FLI PL9000 CCD camera was cooled to -25º C and the 12 μm pixels with 1×1 binning yielded an image scale of 0.62 arcsec/pix. Images were processed for bias, dark and flat field corrections. Photometry was performed using *AstroImageJ* using on-chip comparison stars of solar color (B-V = 0.63) to red (0.6 < B-V < 1.0) stars.

For the three consecutive nights in April, target motion was sufficiently small to use the same on-chip comparison stars. Using NASA Horizons ephemeris, all photometry was corrected for light travel time, unit distances, and solar phase angle using $G = 0.15$. The absolute calibration is based on catalog magnitudes from the APASS10 survey tied to the April observations. Small shifts in scale were subsequently applied to the June 18 and July 24 magnitudes to obtain a consistent, composited lightcurve. We derived an amplitude, in magnitudes, from trough to peak, $A = 0.26 \pm 0.04$ mag and synodic period $P = 2.8737 \pm 0.0002$ h, which is consistent within the uncertainties with that of Fauerbach and Brown (2019) from the 2017 apparition, who obtained $P = 2.864 \pm 0.019$ h. A singly-periodic fit with one-half this period was strongly disfavored by the July 24 dataset when examined alone because one and a half periods were observed. Our data covered the full rotation curve and yield a considerably more precise period due to the nearly 3-month observation span.

We checked our results by comparing to publicly available data from the Minor Planet Center from the Asteroid Terrestrial-impact Last Alert System (ATLAS; Tonry et al., 2018) program during 2021 in the o filter (orange, 560-820 nm). Corrections for light travel time, unit distance, and solar phase angle were performed and the data were shifted for clarity. The two resulting lightcurves show substantial similarity. The ATLAS data allowed us to consider other values of *G*. The lightcurve becomes noticeably more scattered for *G* values outside the range 0.15 ± 0.03.

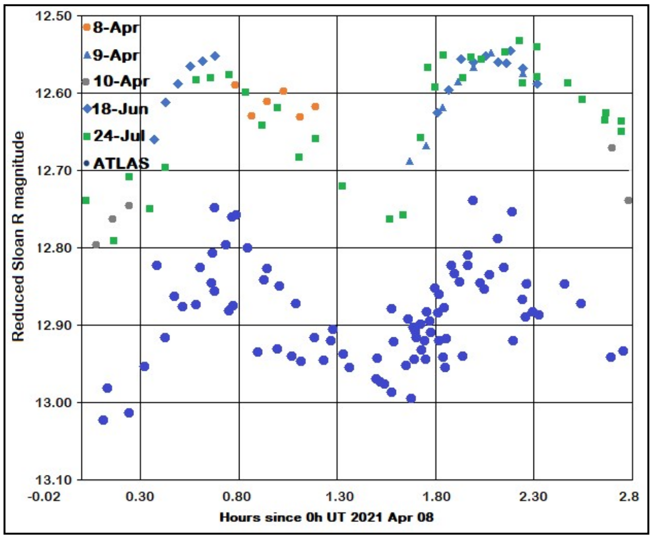

Acknowledgements

We thank Dr. Stephen Slivan for helpful advice during the course of this study. FPW is grateful for funding from the Union College Faculty Research Fund and the Department of Physics and Astronomy. This work made use of the AAVSO Photometric All-Sky Survey (APASS), funded by the Robert Martin Ayers Sciences Fund and NSF AST-1412587. This work has also made use of data and services provided by the International Astronomical Union's Minor Planet Center; specifically, the brightnesses accompanying astrometry from the Asteroid Terrestrial-impact Last Alert System (ATLAS) survey observing program.

References

Fauerbach, M.; Brown, A. (2019). “Rotational Period Determination for Asteroids 2498 Tsesevich, (16024) 1999 CT101, (46304) 2001 OZ62.” *Minor Planet Bulletin* **46**, 19-20.

Harris, A.W.; Young, J.W.; Scaltriti, F.; Zappala, V. (1984). “Lightcurves and phase relations of the asteroids 82 Alkmene and 444 Gyptis.” *Icarus* **57**, 251-258.

Slivan, S. (2003). “A Web-based tool to calculate observability of Koronis program asteroids.” *Minor Planet Bulletin* **30**, 71.

Tonry, J.L.; Denneau, L.; Heinze, A.N.; Stalder, B.; Smith, K.W.; Smartt, S.J.; Stubbs, C.W.; Weiland, H.J.; Rest, A. (2018). “ATLAS: A High-cadence All-sky Survey System.” *PASP* **130**, 064505.

Warner, B.D.; Harris, A.W.; Pravec, P. (2009). “The Asteroid Lightcurve Database.” *Icarus* **202**, 134-146. Updated 2016 Sep. *http://www.minorplanet.info/lightcurvedatabase.html*

Number	Name	yyyy mm/dd	Phase	L_{PAB}	B_{PAB}	Period(h)	P.E.	Amp	A.E.	Grp
2498	Tsesevich	2021 04/8-7/24	*17.5,17.1	253	-2	2.8737	0.0002	0.26	0.04	MB-Kor

Table I. Observing circumstances and results. The phase angle is given for the first and last date. If preceded by an asterisk, the phase angle reached an extremum during the period. L_{PAB} and B_{PAB} are the approximate phase angle bisector longitude/latitude at mid-date range (see Harris et al., 1984). Grp is the asteroid family/group (Warner et al., 2009).

ROTATIONAL PERIOD DETERMINATION AND TAXONOMIC CLASSIFICATION FOR ASTEROID 8080 INTEL

Nico Montigiani, Massimiliano Mannucci
Osservatorio Astronomico Margherita Hack (A57)
Florence, ITALY
info@astrofilifiorentini.it

(Received: 2021 November 4)

CCD photometric observation of outer main-belt asteroid 8080 Intel was obtained in order to measure the rotation period and find the color indexes B-V and V-R. These measures were performed during five different nights on 2021 Oct 9, 10, 11, 13 and 14 using the instrumentation available at the Osservatorio Astronomico Margherita Hack located on the hills near Florence (Italy).

Asteroid 8080 Intel was discovered by CERGA, Centre de Recherches en Géodynamique et Astrométrie, on November 17, 1987, from Caussols (France). It is named after the Intel 8080 microprocessor, ancestor of a series of microprocessor chips fundamental to the "PC revolution". It was chosen from the Asteroid Lightcurve Data Exchange Format (ALCDEF, 2020). It is an outer main-belt asteroid with a semi-major axis of 2.861 AU, eccentricity 0.2862, inclination 9.427°, and an orbital period of 4.84 years. Its absolute magnitude is H = 13.14 (JPL, 2021; MPC, 2021).

CCD photometric observations were carried out in 2021 October at the Osservatorio Astronomico Margherita Hack (A57). We used a 0.35-m f/8,25 Schmidt-Cassegrain telescope, a SBIG ST10 XME CCD camera, clear filter and B, V, Rc photometric filters. The pixel scale was 1 arcsec when binned at 2×2 pixels. Data processing and analysis were done with *MPO Canopus* (Warner, 2017). All the images were calibrated with dark and flat field frames using *Astroart 6.0*. Table I shows the observing circumstances and results.

Our observations were conducted in two different steps. The first step consisted in collecting 222 data points with clear filter in four different nights (2021 Oct 9, 10, 11 and 13). The derived synodic period was P = 3.5337 ± 0.0003 h with an amplitude of A = 0.36 ± 0.03 mag (Warner, 2006). Moreover, we consulted the asteroid lightcurve database (LCDB; Warner et al., 2009) and we found two previous calculated periods: P = 3.54 +/- 0.01 h (Chang et al., 2014) and P = 3.533 +/- 0.0019 h (Waszczak et al., 2015). The period we found seems to be in good agreement with the previous mentioned periods.

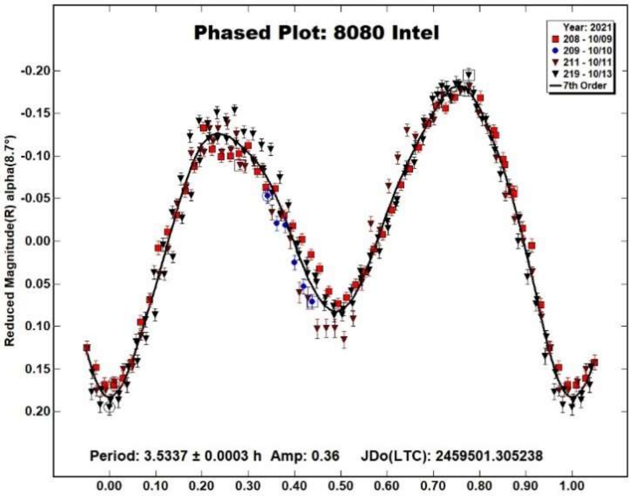

Figure 1. Phased lightcurve of 8080 Intel.

In the second step we collected further 50 data points during one night (2021 Oct 14) using filter V, Rc and B. This allowed us to determine the color indexes (V-R) = 0.46 +/- 0.03 and (B-V) = 0.75 +/- 0.05. These values are consistent with a moderate albedo M-type taxonomic class (Shevchenko and Lupishko, 1998), moreover the semi-major axis (a) of 8080 Intel is compatible with this taxonomic class (Gradie and Tedesco, 1982). We didn't find any other bibliographic reference where the taxonomic class has been derived by color indexes, in order to compare our results with others.

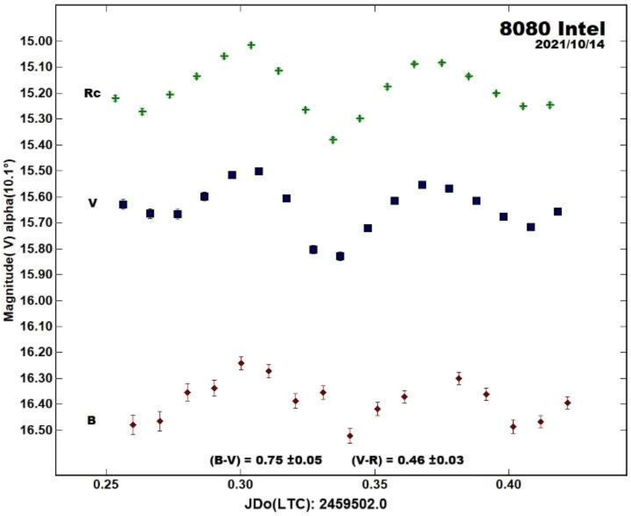

Figure 2. (B-V) and (V-R) raw plot of 8080 Intel.

Number	Name	2021 mm/dd	Pts	Phase	L_{PAB}	B_{PAB}	Period(h)	P.E.	Amp	A.E.	Grp
8080	Intel	09/10-13/10	222	8.7-9.8	11.3	12.7	3.5337	±0.0003	0.36	0.03	OMB

Table I. Observing circumstances and results. Pts is the number of data points. The phase angle is given for the first and last date. L_{PAB} and B_{PAB} are the approximate phase angle bisector longitude and latitude at mid-date range (see Harris et al., 1984). Grp is the asteroid family/group (Warner et al., 2009).

References

ALCDEF (2020). Asteroid Lightcurve Data Exchange Format database. *http://www.alcdef.org/*

Chang, C.-K.; Ip, W.-H.; Lin, H.-W.; Cheng, Y.-C.; Ngeow, C.-C.; Yang, T.-C.; Waszczak, A.; Kulkarni, S.R.; Levitan, D.; Sesar, B.; Laher, R.; Surace, J.; Price, T.A. and the PTF Team (2014). "313 New Asteroid Rotation Periods from Palomar Transient Factory Observations." *Ap. J.,* **788**, id 17.

Gradie J.; Tedesco E. (1982). "Compositional structure of the asteroid belt." *Science Reprint Series* **216**, 1405-1407.

Harris, A.W.; Young, J.W.; Scaltriti, F.; Zappala, V. (1984). "Lightcurves and phase relations of the asteroids 82 Alkmene and 444 Gyptis." *Icarus* **57**, 251-258.

JPL (2021). Small-Body Database Browser.
http://ssd.jpl.nasa.gov/sbdb.cgi#top

MPC (2021). MPC Database.
http://www.minorplanetcenter.net/db_search/

Shevchenko, V.G.; Lupishko, D.F. (1998). "Optical Properties of Asteroids from Photometric Data." *Solar System Research* **32**, 220.

Warner, B.D. (2006). *A Practical Guide to Lightcurve Photometry and Analysis (2nd edition)*. Springer, New York.

Warner, B.D.; Harris, A.W.; Pravec, P. (2009). "The Asteroid Lightcurve Database." *Icarus* **202**, 134-146. Updated 2018 June. *http://www.minorplanet.info/lightcurvedatabase.html*

Warner, B.D. (2017). MPO Software, MPO Canopus v10.7.7.0. Bdw Publishing. *http://minorplanetobserver.com*

Waszczak, A.; Chang, C.-K.; Ofek, E.O.; Laher, R.; Masci, F.; Levitan, D.; Surace, J.; Cheng, Y.-C.; Ip, W.-H.; Kinoshita, D.; Helou, G.; Prince, T.A.; Kulkarni, S. (2015). "Asteroid Light Curves from the Palomar Transient Factory Survey: Rotation Periods and Phase Functions from Sparse Photometry." *A. J.* **150**, A75.

ROTATION PERIOD FOR ASTEROID (125072) 2001 UG

Stephen C. Percy
The Studios Observatory (Z52)
Grantham, U.K.
mail@opussoftware.co.uk

(Received: 2022 January 27)

CMOS photometric observations of asteroid (125072) 2001 UG were performed by the author at The Studios Observatory in January 2022. The synodic rotation period was determined as 9.27 ± 0.01 h with amplitude 0.68 ± 0.04 mag.

Asteroid (125072) 2001 UG (=1985 YO1 = 1998 WU33) is in a Mars crossing orbit. It was discovered at Socorro on 2001 October 16 by LINEAR. A search of the asteroid lightcurve database (LCDB, Warner et al., 2009) indicates no previous reported rotation period for this asteroid.

We report observations performed at The Studios Observatory, Grantham, U.K. (Z52) using a Meade 14" (0.36 m) LX200 ACF OTA operating at f/10 with a Takahashi FS-102 4" f/8 refractor as guide scope. The OTAs are mounted on a Paramount MEII robotic mount. The 14" OTA is equipped with Moonlite CSL 2.5-inch large format motorized focuser and a QHY600M cooled CMOS camera (binned 2×2). A Chroma 50mm square Clear filter was used for all observations. All guiding was carried out using a ZWO ASI1600M-Cooled CMOS camera binned 2×2. The main imaging QHY600M camera is based on a 36mm × 24mm Sony IMX455 sensor with 3.76um pixels. The image scale, after 2×2 binning, was 0.448 arcsecs per pixel.

Sequence Generator Pro was used for all image centering, capture, and focusing. *PHD2* was used for all guiding. *TheSkyX Professional* software was used for all telescope control and initial focusing. *TheSkyX Professional* was also used to calibrate all science images using bias, dark, dark-for-flat, and flat-field frames. All flat-field images were obtained using a wall-mounted whiteboard illuminated by an A4-size electroluminescent (EL) panel. A recent library of bias, dark and dark-for-flat frames was used in the calibration process, no scaling of dark frames was necessary.

All data processing of the calibrated images and subsequent period analysis was performed using *MPO Canopus* (BDW Publishing 2018). Differential photometry measurements were performed using the Comp Star Selector (CSS) and Star-B-Gone procedures of *MPO Canopus*. Unless otherwise stated the asteroid and five solar-like stars were used for all photometric comparisons. The Sony IMX455 sensor has a peak spectral response in the green visual band so V band magnitudes and V-R colour indexes were used throughout the data processing.

The asteroid's magnitude ranged from 16.2 V to 16.3 V during the observing period. Period analysis was performed using the Fourier analysis algorithm (FALC) of *MPO Canopus* developed by Alan Harris (Harris et al., 1989). All likely periods from 1 hour onwards were examined.

Number	Name	2022 mm/dd	Phase	L_{PAB}	B_{PAB}	Period(h)	P.E.	Amp	A.E.	Grp
125072	2001 UG	01/13-01/20	13.0,18.1	102	6.5	9.27	0.01	0.68	0.04	MC

Table 1. Observing circumstances and results. The phase angle is given for the first and last date. If preceded by an asterisk, the phase angle reached an extrema during the period. L_{PAB} and B_{PAB} are the approximate phase angle bisector longitude/latitude at mid-date range (see Harris et al., 1984). Grp is the asteroid family/group (Warner et al., 2009).

A total of 39 h 58 m of observations were performed over a four-night period from 2022 January 13-20. A total of 571 data points were used in the period analysis.

The observing schedule for this project and calibrated data are summarized in Table 1. All new data have been deposited in the ALCDEF database. The resulting phased plot and period spectrum are illustrated below.

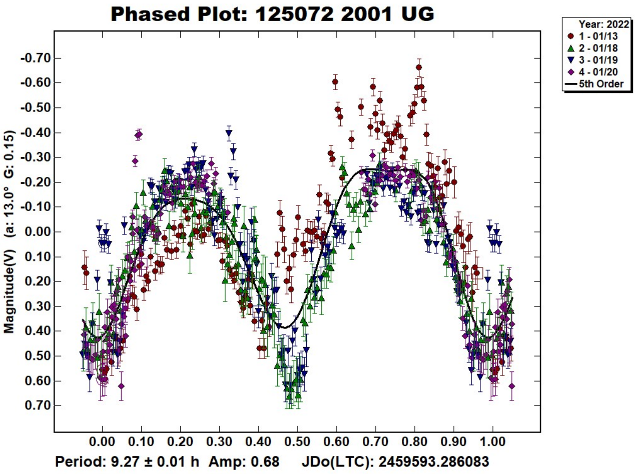

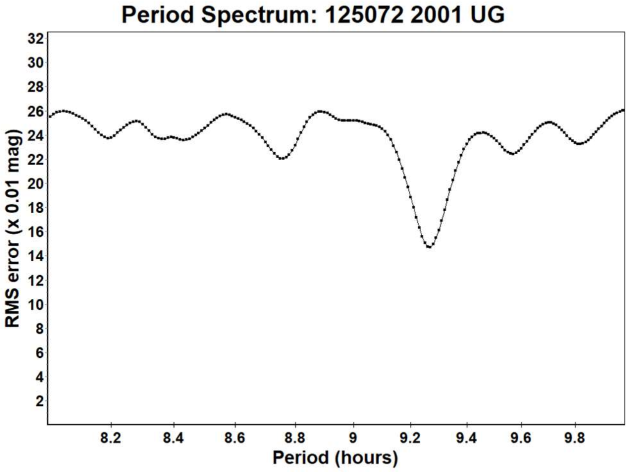

Acknowledgements

This research has made use of data and services provided by the International Astronomical Union's Minor Planet Center.

https://www.minorplanetcenter.net/iau/mpc.html

This research was made possible in part based on data from the MPCOSC3-2MASS catalog (a product of the Two Micron All Sky Survey), UCAC4 (the fourth U.S. Naval Observatory CCD Astrograph Catalog), and the AAVSO Photometric All-Sky Survey (APASS), funded by the Robert Martin Ayers Sciences Fund. The author would like to express his gratitude to Brian D. Warner for his *MPO Canopus* software and support, along with the 2nd edition of his book 'A Practical Guide to Lightcurve Photometry and Analysis'. Both have been invaluable in this research.

References

Harris, A.W.; Young, J.W.; Scaltriti, F.; Zappala, V. (1984). "Lightcurves and phase relations of the asteroids 82 Alkmene and 444 Gyptis." *Icarus* **57**, 251-258.

Harris, A.W.; Young, J.W.; Contreiras, L.; Dockweiler, T.; Belkora, L.; Salo, H.; Harris, W.D.; Bowell, E.; Poutanen, M.; Binzel, R.P.; Tholen, D.J.; Wang, S. (1989). "Phase relations of high albedo asteroids: The unusual opposition brightening of 44 Nysa and 64 Angelina." *Icarus* **81**, 365-374.

Warner, B.D.; Harris, A.W.; Pravec, P. (2009). "The Asteroid Lightcurve Database." *Icarus* **202**, 134-146. Updated 2016 Sep. *https://www.minorplanet.info/php/alcdef.php*

Warner, B.D. (2018). MPO Software, MPO Canopus v10.7.11.3. BDW Publishing. *http://www.minorplanetobserver.com/MPOSoftware/MPOCanopus.htm*

Software Bisque TheSkyX Professional software website. *https://www.bisque.com/product-category/software/*

Sequence Generator Pro by Main Sequence Software. *https://www.sequencegeneratorpro.com/*

PHD2 by Open PHD Guiding. *https://openphdguiding.org/*

SMALL, FAST ROTATOR ASTEROID 2018 GG

Braden J. Larsen
Physics Department, University of Maryland
College Park, Maryland
blarsen@umd.edu

M. T. Read, M. J. Brucker
Lunar and Planetary Laboratory
Tucson, Arizona

C. W. Morgan, J. A. Larsen
Physics Department, U.S. Naval Academy
Annapolis, Maryland

(Received: 2021 November 30)

We report results from April 2018 measurements from Kitt Peak National Observatory showing near-Earth asteroid 2018 GG to be a fast rotator. From three data series, the lightcurve analysis suggests that the asteroid has a rotational period of 0.0223 ± 0.0001 h and 0.33 magnitude amplitude; with a small possibility of the period being 0.023 h.

Near-Earth asteroid 2018 GG was discovered on April 6th, 2018, by the Catalina Sky Survey. It was last observed on September 6th, 2018, but it has a high probability of being recovered on its next apparition. 2018 GG is a 30m Apollo asteroid with a semi-major axis of 2.18 AU, an eccentricity of 0.606, an inclination of 7.17 degrees, an orbital period of 3.21 years, and an absolute magnitude of H = 24.73 (JPL 2021).

Just a few nights after its discovery, on 2018 April 10, Mike Read of Spacewatch took a lightcurve of 2018 GG with their 1.8m telescope as a test. The data were never reduced but were rediscovered during the process of archiving the images for submission to NASA's PDS. As a dataset accessible during COVID-19, the data were reduced as a part of a College Park Scholars Capstone.

The image data we analyzed was obtained at Kitt Peak National Observatory Tucson, Arizona (MPC code: 291) using the *Spacewatch* 1.8m Prime Focus optical tube operating at f/2.75. A PL3041-LC CCD camera with a Schott OG-515 long-pass filter in the beam. Exposure time for the images was set between 2-3 seconds. The camera was binned at 1 × 1 with a plate scale of 0.63 arcsecond/pixel and a field of view of 21.5 × 21.5 arcmin. The asteroid and five comparison stars were measured for the differential photometry. Three separate data time series were collected over multiple intervals of several hours with gaps. They began at 7:37 pm, 10:15 pm, and 1:21 am, respectively.

The images were reduced in *AstroImageJ* (version 4.0.0.1; Collins, 2017) using night sky flats as well as biases. Photometric measurement and light curve analysis were performed using *MPO Canopus* (version 10.7.12.9; Warner, 2019). The *UCAC4* all-sky star catalog (Zacharias 2013) was used to complete the astrometry for each separate data set. Differential photometry was accomplished through the standard catalog included in *MPO Canopus*, MPOSC3 (Warner 2019).

On the night of the observation, the object was extremely faint, about 18th magnitude, and moving with a high sky plane, 46 arcsec/min. Due to the high orbital velocity, the exposure time was decreased to reduce the chance of period smearing. A second-order fit of all three datasets simultaneously yielded a rotational period of 0.0223 ± 0.0001 h with an amplitude of 0.32 ± 0.11 mag. The indicated period is the strongest in the power spectrum with a small possibility of a period of 0.023 h with less significance in the power spectrum.

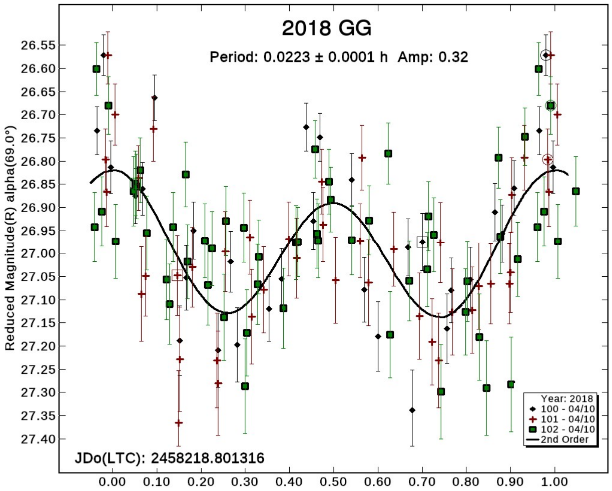

Acknowledgements

The authors thank the University of Arizona Spacewatch Project, United States Naval Academy, and University of Maryland Science Discovery and the Universe program for this amazing opportunity despite the conditions that have arisen from COVID-19. Special thanks to Dr. Melissa Brucker for the opportunity to work with the data, Prof. Chris Morgan and Prof. Jeff Larsen for the mentorship that they provided in the data analysis process, and Dr. Alan Peel and Ms. Erin Thomson for their guidance on how to pursue a professional project.

References

Collins, K.; Kielkopf, J.; Stassun, K.; Hessman, F. (2017). "AstroImageJ: Image Processing and Photometric Extraction for Ultra-Precise Astronomical Light Curves.". *A.J., **153(2)**, 77.*

JPL (2021). Small Body Database. *https://ssd.jpl.nasa.gov/*

Warner, B.D.; Harris, A.W.; Pravec, P. (2009). "The Asteroid Lightcurve Database." *Icarus* **202**, 134-146. Updated 2016 Sep. *http://www.minorplanet.info/lightcurvedatabase.html*

Warner, B.D (2019). MPO Software, MPO Canopus v 10.7.12.9. Bdw Publishing. *http://mniorplanetoberver.com*

Zacharias, N.; Finch, C.; Girard, T.; Henden, A.; Bartlett, J.; Monet, D.; Zacharias, M. (2013). "The Fourth US Naval Observatory CCD Astrograph Catalog (UCAC4)." *A.J., **145(2)**, 44.*

Name	yyyy mm/dd	Phase	L_{PAB}	B_{PAB}	Period(h)	P.E.	Amp	A.E.	Grp
2018 GG	2018 04/10	69.0	170.6	16.1	0.0223	0.0001	0.32	0.11	NEA

Table I. Observing circumstances and results. The phase angle is given for the observation date. L_{PAB} and B_{PAB} are the approximate phase angle bisector longitude/latitude at mid-date range (see Harris et al., 1984). Grp is the asteroid family/group (Warner et al., 2009).

6764 KIRILLAVROV:
A BINARY ASTEROID

Tom Polakis
Command Module Observatory (MPC V02)
121 W. Alameda Dr.
Tempe, AZ 85282
tpolakis@cox.net

Julian Oey
Blue Mountains Observatory (MPC Q68)
JBL Observatory (MPC Q67)
94 Rawson Pde. Leura, NSW, AUSTRALIA
Julianoey1@optusnet.com.au

Milagros Colazo
Estación Astrofísica de Bosque Alegre (MPC 821)
(EABA-UNC), ARGENTINA
Instituto de Astronomía Teórica y Experimental
(IATE-CONICET), ARGENTINA
milirita.colazovinovo@gmail.com

(Received: 2021 November 26)

Mutual events appearing in the lightcurve of 6764 Kirrillavrov unambiguously show that it is a binary asteroid with a rotation period of 4.739 ± 0.001 h, and an orbital period of 30.41 ± 0.01 h. Follow-up observations conducted during the 2021 opposition did not detect the mutual events due to unfavorable viewing geometry. Further observations during subsequent oppositions are encouraged.

While the primary purpose of the Transiting Exoplanet Survey Satellite (TESS) is detection of exoplanets, its images are also useful for the construction of lightcurves for asteroids. Pál et al. (2020) obtained 9912 such lightcurves. In addition to supplying 15 documents containing raw and phased lightcurves for all of these objects, the authors made available the raw photometry data.

Main-belt asteroids typically spend 2 to 4 weeks in the TESS frames, which are gathered with a cadence of 30 minutes. This is often sufficient coverage for determination of rotational periods. Since these periods are shown in The Asteroid Lightcurve Database (LCDB; Warner et al., 2009), they form a suitable basis for comparing results.

This principal author's discovery of the binary nature of 1803 Zwicky (Polakis, 2021) led to an inspection of the TESS raw and phased data. Pál et al. published only the short rotation period of roughly 2.7 hours, but their raw lightcurve contained a clear signature of deep, mutual events occurring with an interval of greater than 14 hours. This prompted a review of thousands of raw TESS lightcurves for similar mutual event signatures that the authors may have missed.

The raw TESS lightcurve of 6764 Kirillavrov, gathered over the course of 26 days, contains such a signature. Pál et al. published a rotation period of 30.4318 ± 0.0005 h. Their data shown in Figure 1 was downloaded, and a dual-period search in *MPO Canopus* (Warner 2020) revealed that this is in fact an orbital period overlaid on a shorter rotation period of lesser amplitude. The rotation and orbital periods derived from the TESS data are 4.740 ± 0.002 h and 30.41 ± 0.01 h, and amplitudes are 0.08 and 0.25 mag, respectively. These rotation and orbital lightcurves appear in Figures 2 and 3.

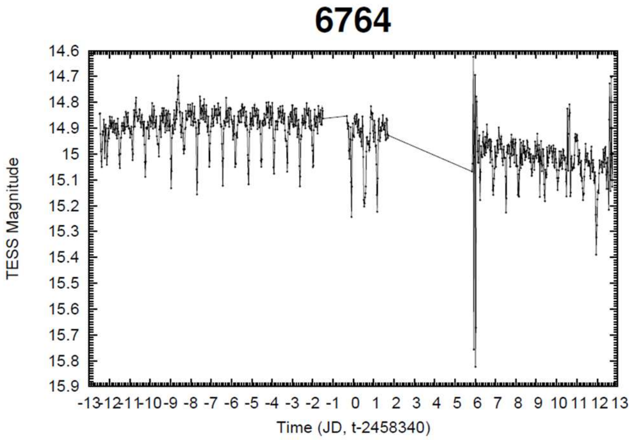

Figure 1. TESS data: raw lightcurve.

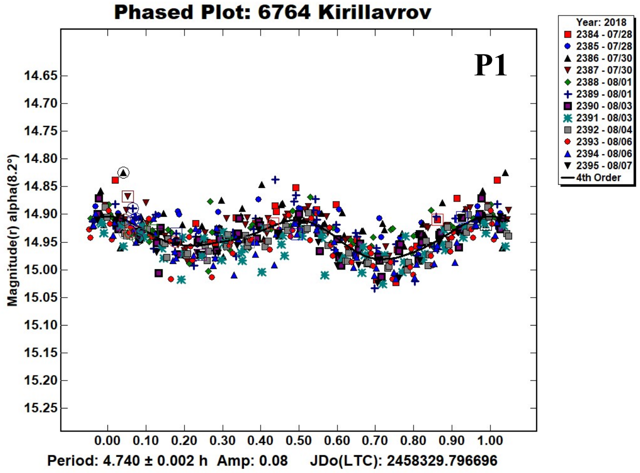

Figure 2. TESS data: phased lightcurve showing rotation period.

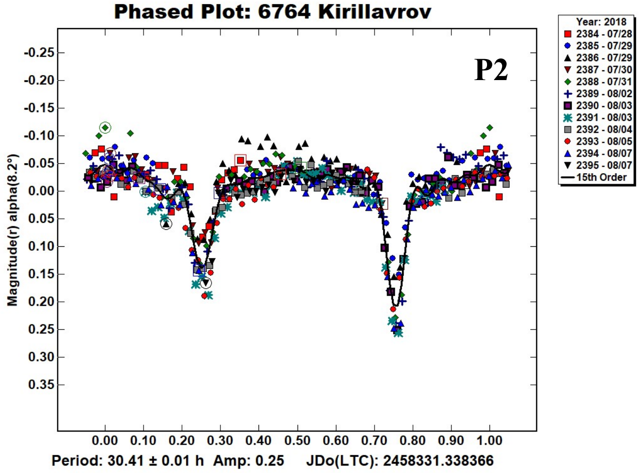

Figure 3. TESS data: phased lightcurve showing orbital period.

Brian Skiff (private communication) provided an agreeing rotation period of 4.737 ± 0.002 h, using data acquired in 2014 March. The LCDB shows the orbital period of Behrend et al. (2020web): 30.43 ± 0.05 h. Their web site states, "Provisional: binary asteroid in season of eclipses."

Number	Name	yy/mm/dd	Phase	L_{PAB}	B_{PAB}	Period(h)	P.E.	Amp	A.E.	Grp
6764	Kirillavrov	21/04/13-04/18	12.2,6.0	222	-3	4.739	0.001	0.08	0.03	FLOR
						30.41	0.01	0.25	0.06	

Table I. Observing circumstances and results. The first line gives the primary (adopted) period for the system. The second line gives the secondary period. The phase angle is given for the first and last date. If preceded by an asterisk, the phase angle reached an extrema during the period. L_{PAB} and B_{PAB} are the approximate phase angle bisector longitude/latitude at mid-date range (see Harris et al., 1984). Grp is the asteroid family/group (Warner et al., 2009).

6764 Kirillavrov came to opposition in 2021 May at magnitude 15. Unfortunately for northern observers, the declination was -21°. Observers in the Southern Hemisphere were solicited for observations. Julian Oey in Australia and Milagros Colazo in Argentina kindly obliged, providing data from ten nights.

CCD photometric observations by Oey (MPC code Q68) were conducted on six nights between 2021 April 18 and 24, using a 0.35m Schmidt Cassegrain telescope, SBIG ST8XME camera, and a clear filter. Image scale was 0.88 arcsec/pixel. Exposure time was 3 minutes.

Colazo (MPC code 821) performed her observations during four nights from 2021 April 12 through 15 with a 1.5m Newtonian telescope, Apogee Alta F16M camera, and without filter. Her images have a scale of 0.74 arcsec/pixel. She used an exposure time of 80 seconds.

Both observers provided all of their photometric data to the principal author for reduction. The data reduction and period analysis were done using *MPO Canopus* (Warner, 2020). The clear-filtered images were reduced to Sloan r´ to minimize error with respect to a color term. Comparison star magnitudes were obtained from the ATLAS catalog (Tonry et al., 2018), which is incorporated directly into *MPO Canopus*. Period determination was done using the *MPO Canopus* Fourier-type FALC fitting method (cf. Harris et al., 1989). Phased lightcurves show the maximum at phase zero. Magnitudes in these plots are apparent and scaled by MPO Canopus to the first night.

A raw plot of the full dataset is provided in Figure 4, followed by a phased lightcurve in Figure 5.

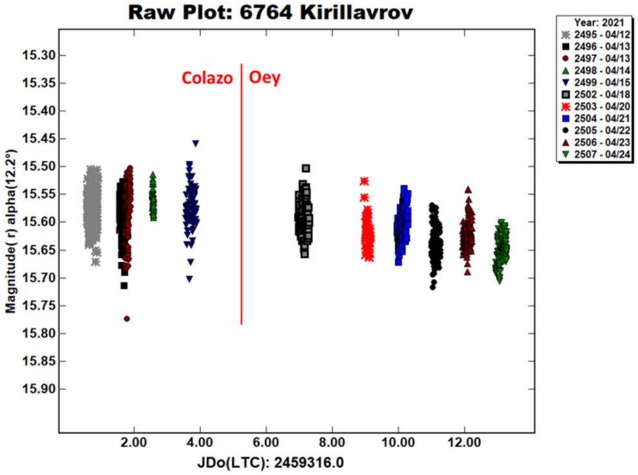

Figure 4. Colazo and Oey data: raw lightcurve.

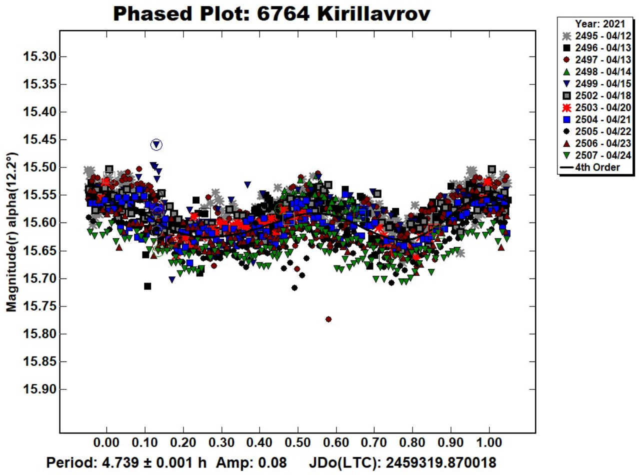

Figure 5. 2021 Colazo and Oey data: phased lightcurve.

Within the data scatter, mutual events were not detected during the ten nights during which data was gathered. The duration and frequency of these data were more than sufficient to capture some mutual events. It can only be concluded that the unfavorable viewing geometry resulted in misses rather than eclipses and occultations, at least within the precision of the scatter. The dense coverage does enable a refinement of the rotation period to 4.739 ± 0.001 h, with an RMS scatter on the fit of 0.034 mag. Results are summarized in Table I.

Since 2014, we now have four data sets for this asteroid, with two of them exhibiting mutual events. Table II summarizes PAB values for the four sets. Note that the Skiff data was sparse, so it is insufficient to conclude that mutual events did not occur.

Lightcurve	Date	Events?	PAB (°)	
			Lon	Lat
Skiff	3/28/2014	?	183	3
TESS	8/2/2018	Y	313	-10
Behrend	1/19/2020	Y	85	8
Colazo & Oey	4/18/2021	N	221	-3

Table II. Viewing geometry for four datasets

Looking forward, the next two oppositions will favor northern observers. A summary of future oppositions through 2025 is presented in Table III. Follow-up observing with the aim of detecting mutual events is encouraged.

Opposition Date	Declination (°)	Magnitude	PAB (°)	
			Lon	Lat
2022 Nov 05	20	16.3	42	4
2024 Feb 24	17	16.0	154	7
2025 Sep 14	-9	15.7	350	-5

Table III. Observing circumstances for upcoming oppositions

Acknowledgements

The authors would like to express gratitude to Brian Skiff for his indispensable mentoring in data acquisition and reduction. Thanks also go out to Brian Warner for support of his *MPO Canopus* software package. Petr Pravec provided helpful guidance. The research work at Blue Mountains Observatory is supported by the 2018 Shoemaker NEO Grant.

References

Behrend, R. (2020web). Observatoire de Geneve web site. *http://obswww.unige.ch/~behrend/page_cou.html*

Harris, A.W.; Young, J.W.; Scaltriti, F.; Zappala, V. (1984). “Lightcurves and phase relations of the asteroids 82 Alkmene and 444 Gyptis.” *Icarus* **57**, 251-258.

Harris, A.W.; Young, J.W.; Bowell, E.; Martin, L.J.; Millis, R.L.; Poutanen, M.; Scaltriti, F.; Zappala, V.; Schober, H.J.; Debehogne, H.; Zeigler, K.W. (1989). “Photoelectric Observations of Asteroids 3, 24, 60, 261, and 863.” *Icarus* **77**, 171-186.

Pál, A.; Szakáts, R.; Kiss, C.; Bódi, A.; Bognár, Z.; Kalup, C.; Kiss, L.L.; Marton, G.; Molnár, L.; Plachy, E.; Sárneczky, K.; Szabó, G.M.; Szabó, R. (2020). “Solar System Objects Observed with TESS - First Data Release: Bright Main-belt and Trojan Asteroids from the Southern Survey.” *Ap. J.* **247**, A26.

Polakis, T. (2021). “1803 Zwicky, A Confirmed Binary Asteroid.” *Minor Planet Bull.* **48**, 272-273.

Tonry, J.L.; Denneau, L.; Flewelling, H.; Heinze, A.N.; Onken, C.A.; Smartt, S.J.; Stalder, B.; Weiland, H.J.; Wolf, C. (2018). “The ATLAS All-Sky Stellar Reference Catalog.” *Astrophys. J.* **867**, A105.

Warner, B.D.; Harris, A.W.; Pravec, P. (2009). “The Asteroid Lightcurve Database.” *Icarus* **202**, 134-146. Updated 2020 Aug. *http://www.minorplanet.info/lightcurvedatabase.html*

Warner. B.D. (2020). *MPO Canopus* software. *http://bdwpublishing.com*

NEAR-EARTH ASTEROID LIGHTCURVE ANALYSIS AT THE CENTER FOR SOLAR SYSTEM STUDIES: 2021 OCTOBER-DECEMBER

Brian D. Warner
Center for Solar System Studies (CS3)
446 Sycamore Ave.
Eaton, CO 80615 USA
brian@MinorPlanetObserver.com

Robert D. Stephens
Center for Solar System Studies (CS3)
Rancho Cucamonga, CA

(Received: 2022 January 12)

Lightcurves of 16 near-Earth asteroids (NEAs) obtained at the Center for Solar System Studies (CS3) from 2021 October through December were analyzed for rotation period, peak-to-peak amplitude, and signs of satellites or tumbling. The minor planets (87024) 2000 JS66 and 2019 XS were found to be in a tumbling state.

CCD photometric observations of 16 near-Earth asteroids (NEAs) were made at the Center for Solar System Studies (CS3) from 2021 October through December. Table I lists the telescopes and CCD cameras that were available to make observations.

Up to nine telescopes can be used but seven is more common. All the cameras use CCD chips from the KAF blue-enhanced family and so have essentially the same response. The pixel scales ranged from 1.24-1.60 arcsec/pixel.

Telescopes	Cameras
0.30-m *f*/10 Schmidt-Cass	FLI Microline 1001E
0.35-m *f*/9.1 Schmidt-Cass	FLI Proline 1001E
0.40-m *f*/10 Schmidt-Cass	SBIG STL-1001E
0.40-m *f*/10 Schmidt-Cass	
0.50-m *f*/8.1 Ritchey-Chrétien	

Table I. List of available telescopes and CCD cameras at CS3. The exact combination for each telescope/camera pair can vary due to maintenance or specific needs.

All lightcurve observations were unfiltered since a clear filter can cause a 0.1-0.3 mag loss. The exposure duration varied depending on the asteroid’s brightness and sky motion. Guiding on a field star sometimes resulted in a trailed image for the asteroid.

Measurements were made using *MPO Canopus*. The Comp Star Selector utility in *MPO Canopus* found up to five comparison stars of near solar-color for differential photometry. To reduce the number of times and amounts of adjusting nightly zero points, we use the ATLAS catalog r´ (SR) magnitudes (Tonry et al., 2018). Those adjustments are usually $|\Delta| \leq 0.03$ mag. The larger corrections, which are rare, may have been related in part to using unfiltered observations, poor centroiding of the reference stars, and not correcting for second-order extinction. Another cause may be selecting what appears to be a single star but is actually an unresolved pair.

The Y-axis values are ATLAS SR “sky” (catalog) magnitudes. The two values in the parentheses are the phase angle (a) and the value of *G* used to normalize the data to the comparison stars used in the earliest session. This, in effect, corrected all the observations to seem to have been made at a single fixed date/time and phase angle, leaving any variations due only to the asteroid’s rotation and/or albedo changes. The X-axis shows rotational phase from -0.05 to 1.05. If the plot includes the amplitude, e.g., “Amp: 0.65”, this is the amplitude of the Fourier model curve and *not necessarily the adopted amplitude for the lightcurve*.

“LCDB” substitutes for “Warner et al. (2009)” from here on.

1862 Apollo. A rotation period of about 3.065 h has been long-established for this namesake of a subclass of NEAs (e.g., Harris et al., 1987). The amplitude during late-2021 observations (0.61 mag) at CS3 was about mid-way between the known extremes of 0.15 to 1.15 mag.

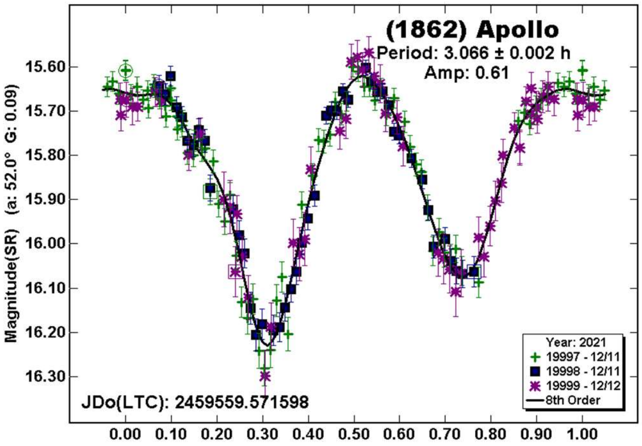

3200 Phaethon. There are numerous rotation periods listed in the LCDB, all of about 3.60 h, e.g., Pravec et al. (2004web, 3.6048 h).

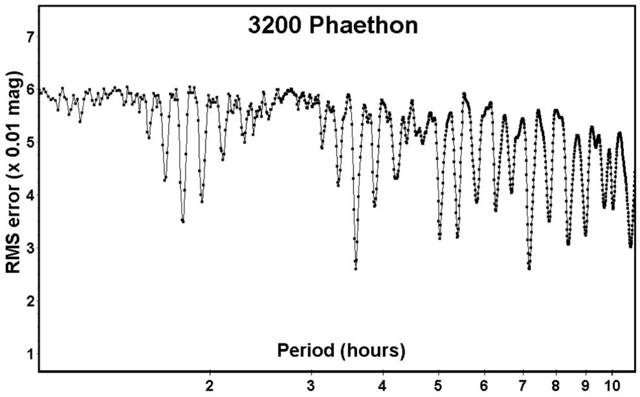

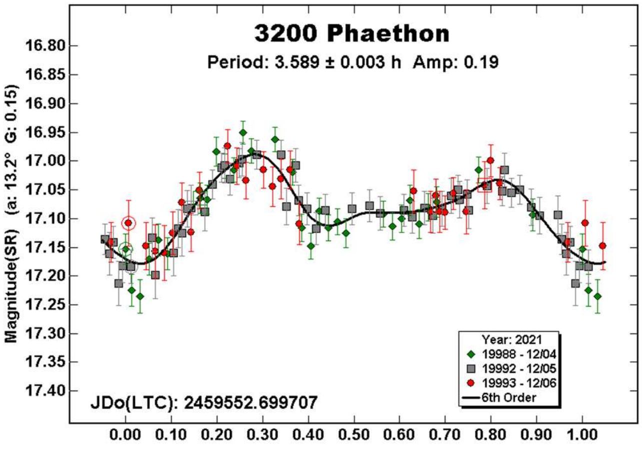

As discussed in Harris et al. (2014), the low amplitude and phase angle make solutions other than bimodal a possibility. This is borne out by the period spectrum, which shows a number of nearly equal solutions. The 3.589 h period is considered to be the correct result.

3361 Orpheus. Wisniewski (1991) has the earliest entry in the LCDB with a period of 3.58 h. Subsequent results (e.g., Pravec et al., 2019web) shortened the period to near 3.538 h. The result using the most recent CS3 data in good agreement with the shorter period.

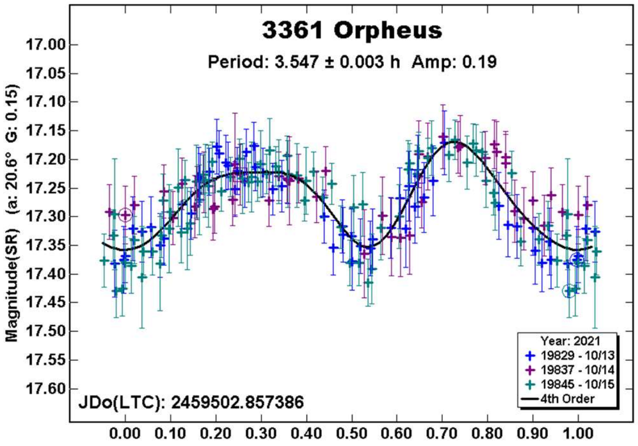

4660 Nereus. Pravec et al. (2021web) found Nereus to be tumbling, with periods of 15.4749 h and 12.457 h. There were insufficient data to try to duplicate those results but they may explain the lower amplitude near 0.2 rotation phase on some nights.

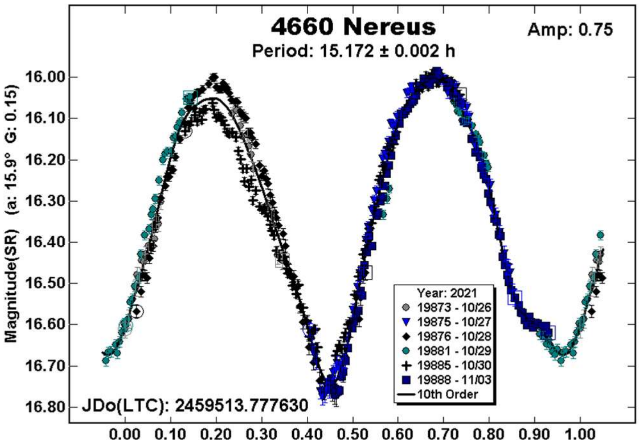

7358 Oze. Previous solutions for Oze have included 5.433 h (Skiff et al., 2012), 24.4 h (Skiff et al., 2019), and 125.8 h (this work). The period spectrum using the CS3 data lacked a clear solution.

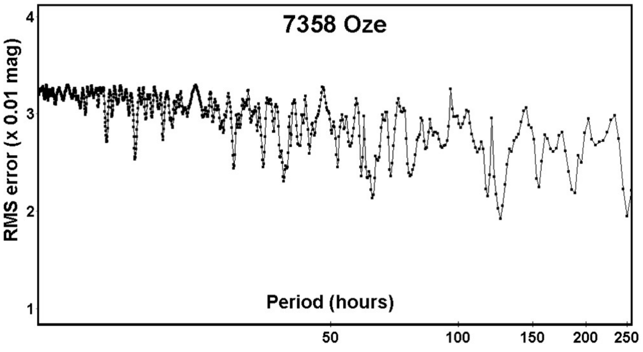

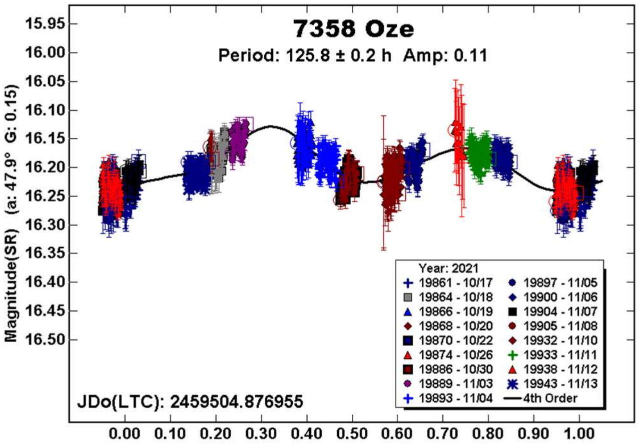

The two shorter periods have a close to 23:1 or 5:1 ratio with the period reported here. This could be a good indication of *rotational aliasing*, which is when the true number of rotations over the total duration of a data set is ambiguous.

12711 Tukmit. The only previous period in the LCDB is from Pravec et al. (2000web), who found 3.4848 h.

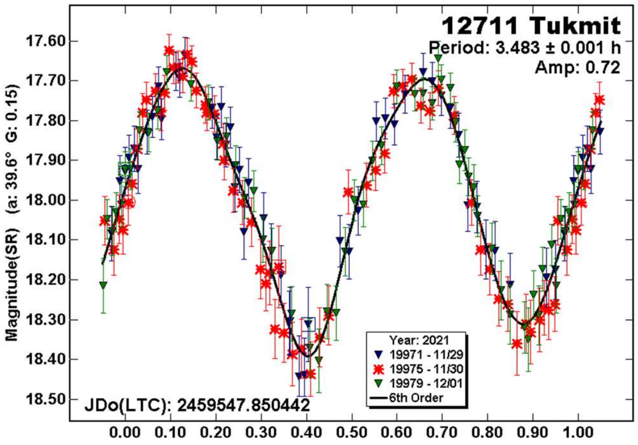

(18882) 1999 YN4. This appears to be the first reported rotation period of 1999 YN4. Despite the low amplitude and almost symmetrical halves of the lightcurve, the half period of 1.173 h doesn't seem likely given the diameter of 1.8 km. A higher modal lightcurve, and longer period, cannot be formally excluded (Harris et al., 2014).

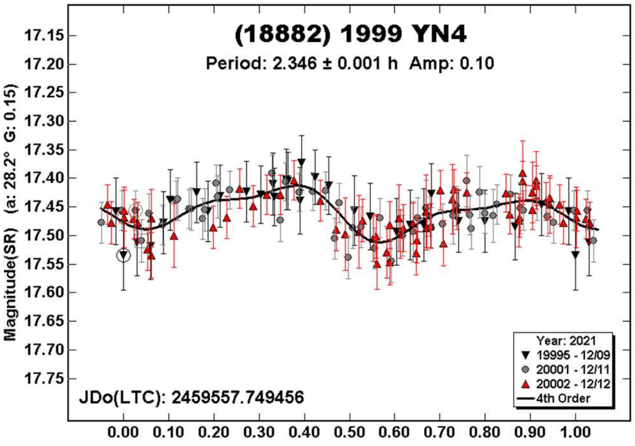

20460 Robwhiteley. The period spectrum using the latest CS3 data shows an essentially unique solution of 2.751 h; this is in good agreement with a previous result of 2.7209 h (Warner, 2018) and that of Pravec et al. (2017web; 2.7228 h), who also reported indications, unconfirmed, of a satellite.

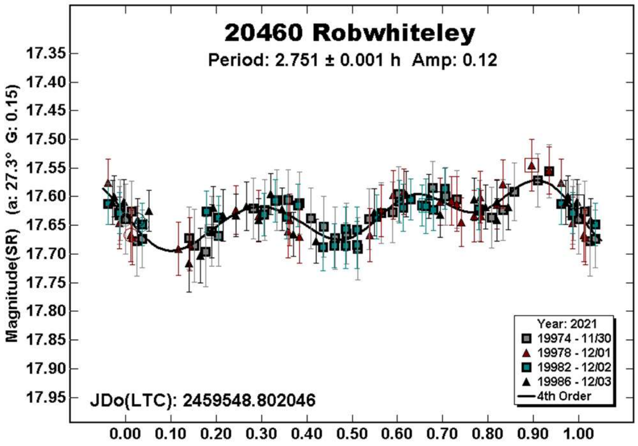

(87024) 2000 JS66. Pravec et al. (2021web) determined this NEA to be in non-principal axis rotation (NPAR), otherwise known as *tumbling*. They reported two periods of 28.2 h and 37.2 and a PAR of -2 (see Pravec et al., 2005; 2014).

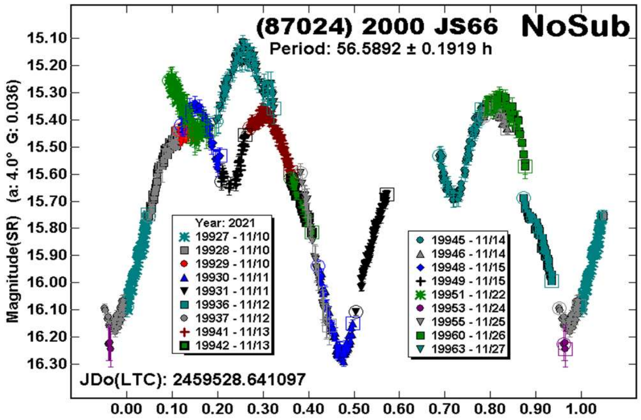

It was apparent from the raw data and attempts to find a single period (NoSub) that the asteroid was tumbling. *MPO Canopus,* even though it is not properly designed to handle tumbling asteroids, was used to try to extract possible two-period solutions. It was only after finding three periods and subtracting pairs, e.g., subtract P_2 and P_3 to find P_1, that the data would closely fit Fourier curves that did not have completely improbable shapes.

Interestingly, the dominant period is almost exactly double the "primary" period found by Pravec et al. (2021web). However, the close asymmetry of the two halves in the P_1 and P_2 plots means the half periods are possible. This would put the dominant period given here close to that found by Pravec et al. (2021web).

The value of P_3 = 39.46 h is close to the second period found by Pravec et al. (2021web). While the CS3 results differ significantly in some respects, they provide independent confirmation that the asteroid is tumbling.

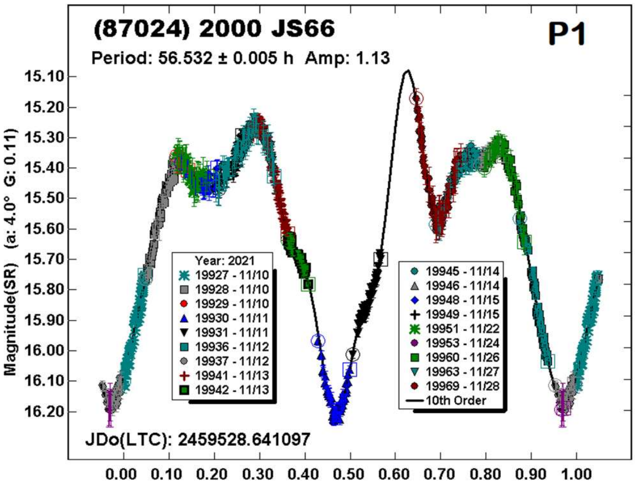

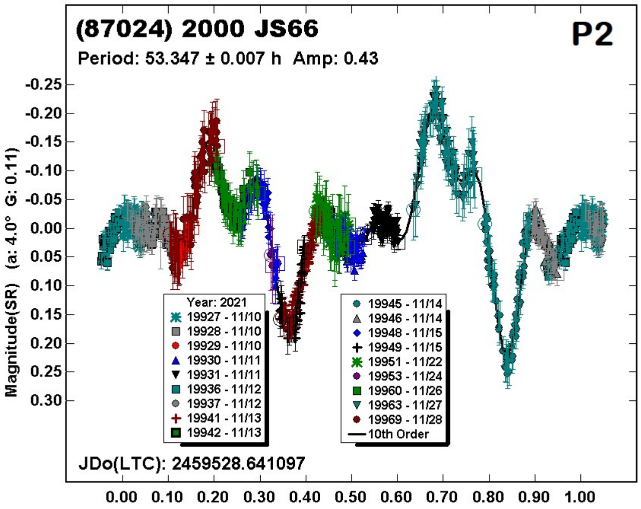

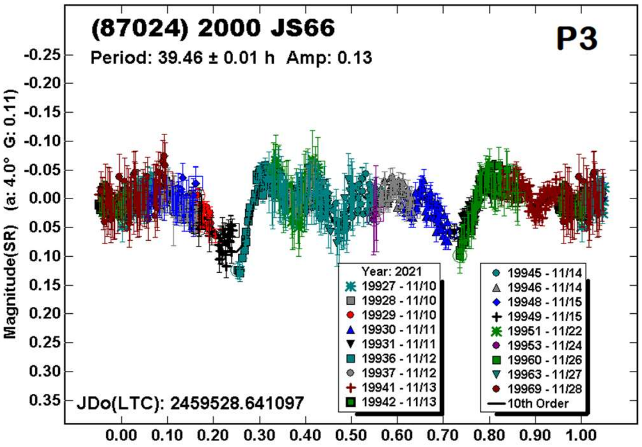

(137062) 1998 WM. The only previously reported period in the LCDB is 2.58 h (Vaduvescu et al., 2017). The period spectrum shows several possible solutions, which is not unexpected for a low amplitude lightcurve at moderate phase angles (Harris et al., 2014).

The more common solutions, shown below, correspond to a monomodal lightcurve, $P = 2.469$ h, and a bimodal lightcurve at the doubled period of $P = 4.934$ h. The shorter period is adopted for this work since it and the estimated diameter make the asteroid fall just below the so-called "spin barrier," a more typical location for many small NEAs.

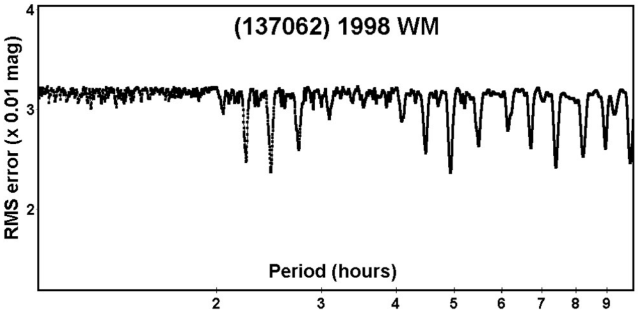

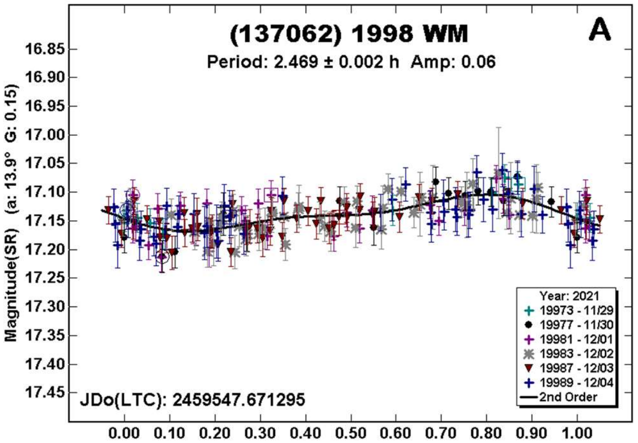

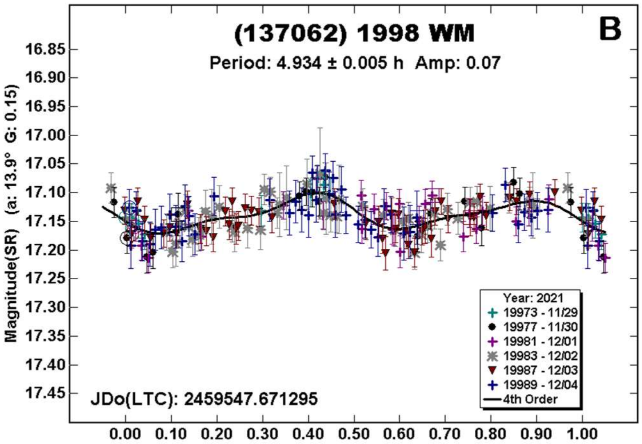

(137805) 1999 YK5. The latest solution is in fairly good agreement with a previous result of 3.930 h (Warner, 2016a). It was not possible to get a satisfactory fit to 3.468 h (Aznar et al., 2018).

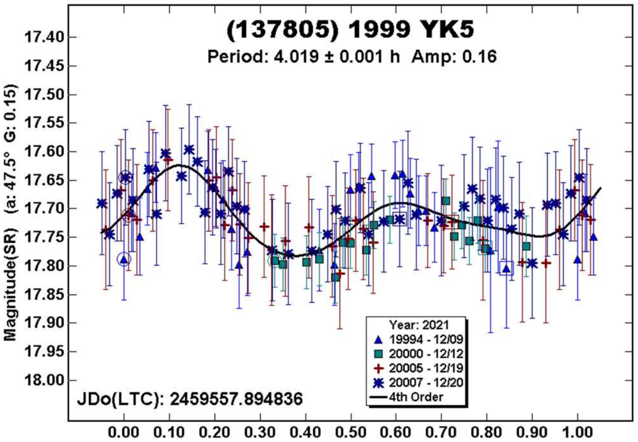

(285571) 2000 PQ9. Colazo et al. (2022) and Behrend (2021web) both reported periods near 3.74 h. Assuming the ATLAS catalog magnitudes allowed near-zero zero-point adjustments, a long-period solution of 119.6 h was found using the CS3 data.

A shorter period superimposed on the long-period curve, if it exists, could not be extracted from the noise. A dual-period solution with $P_{Shorter} < 10$ h, might fit with the suspected class of very wide binary asteroids (e.g., see Warner, 2016b).

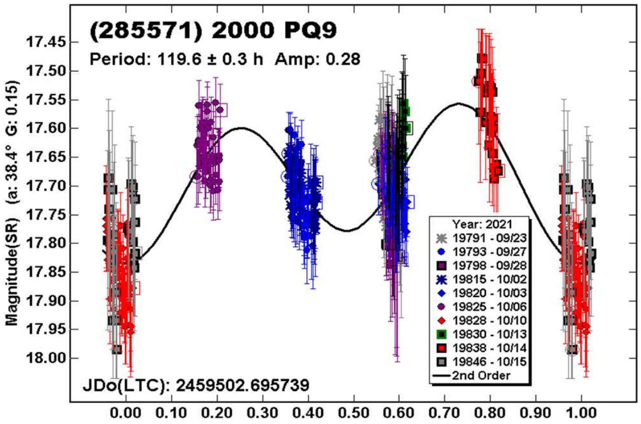

1999 FJ21. This NEA was followed for four consecutive nights in 2021 October. This provided a good demonstration of the evolution of a lightcurve over a relatively short number of days. As the phase angle increased from 11.5° on Oct 13 to 22° on Oct 16, the depth of the first minimum (about 0.35 rotation phase) increased as did the overall amplitude of the lightcurve. The latter is an expected trait (Zappala et al., 1990).

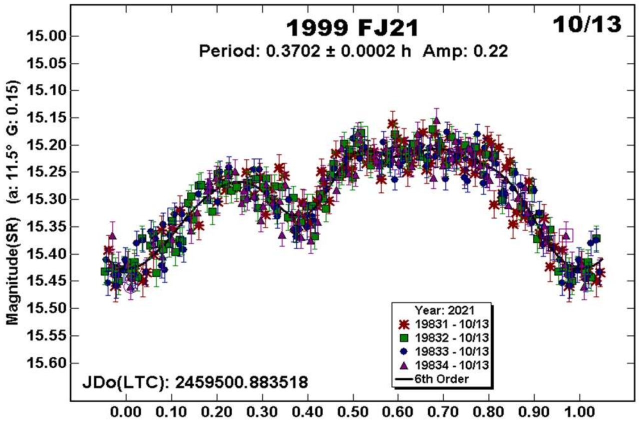

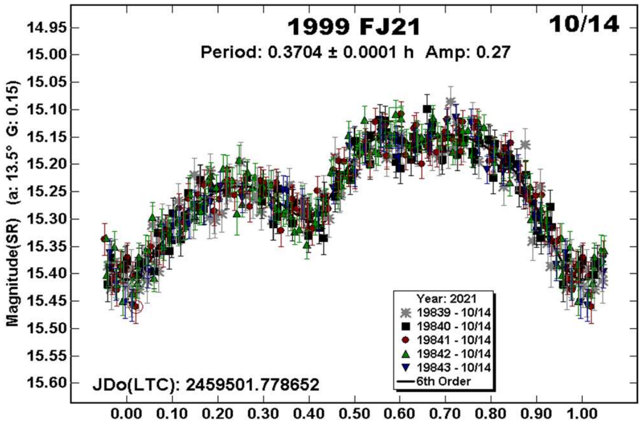

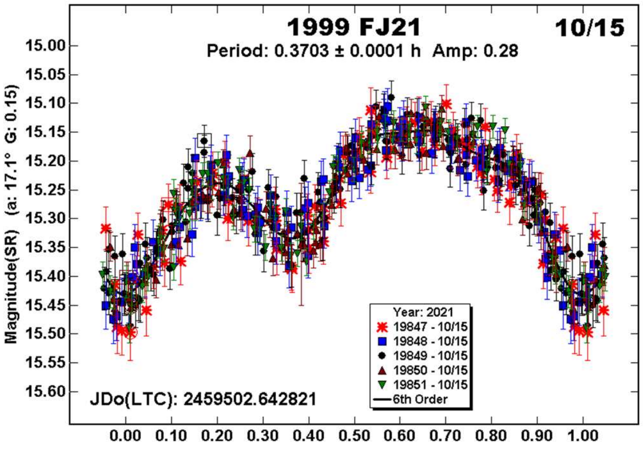

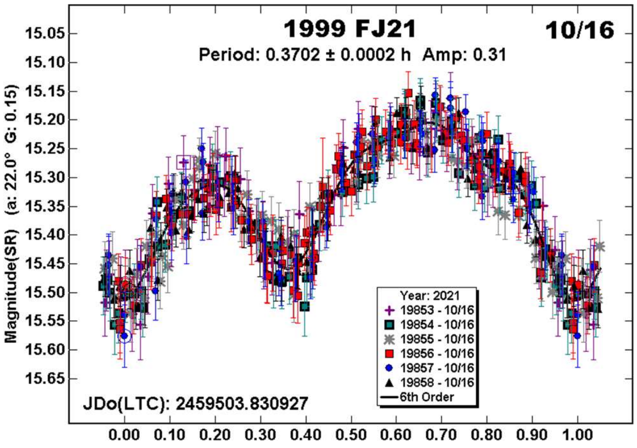

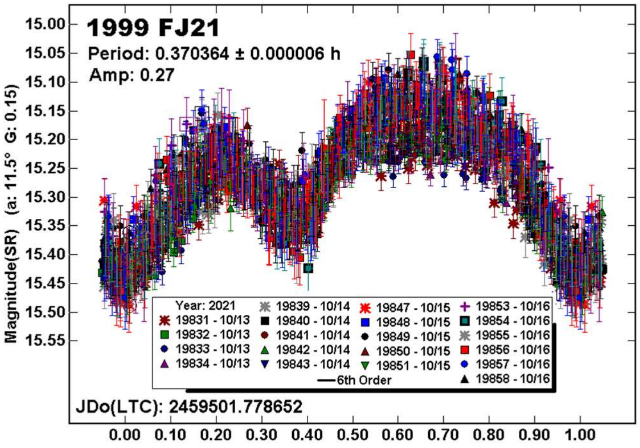

While combing the four nights into a single set covered up the changes in the lightcurve, it did provide a longer baseline to establish a more precise synodic period of 0.370364 h, or – with a 5-sigma error bar – 1333 ± 0.1 s.

2019 XS. The raw plot was reminiscent of previous examples of tumbling where two periods could be combined to what appeared a single period but with an unlikely lightcurve shape (see Harris et al., 2014). However, no single period provided a reasonable fit to the CS3 data obtained on the night of 2021 November 10.

Knowing the limitations of *MPO Canopus* for analyzing tumbling asteroids, an attempt was made to find a dual-period solution. This led to a dominant period of 2.35 h and a secondary period of 3.01 h. The two periods should not be taken as the actual periods of rotation and precession (Pravec et al., 2005; 2014).

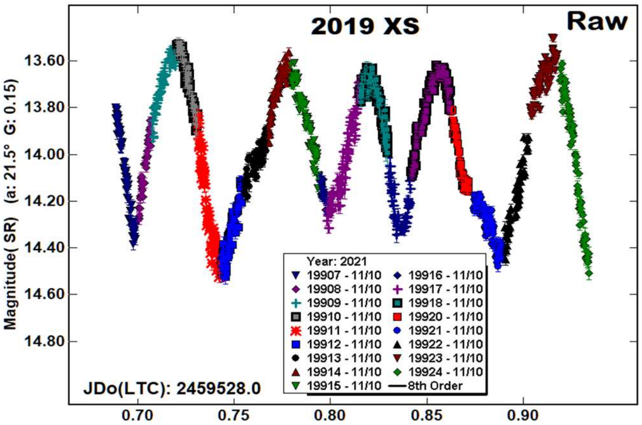

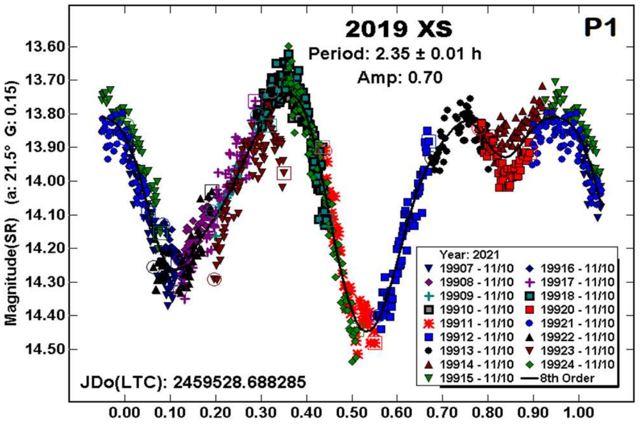

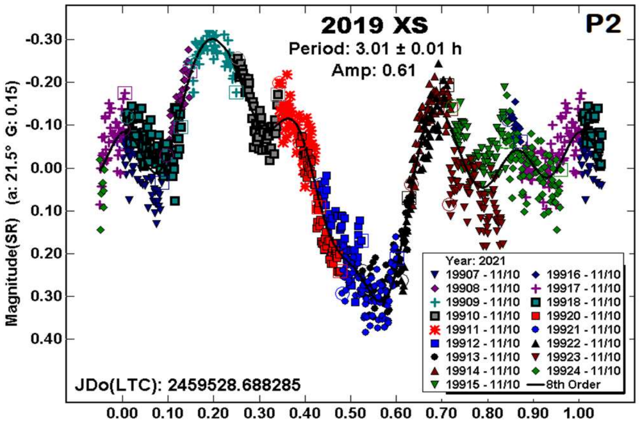

2021 JQ24. There were no previous entries of any kind in the LCDB for this NEA with an estimated diameter of 0.8 km. Given the noise in the data and the almost three-week span of the data set, it is possible that the actual period is an integral (or 0.5) multiple or divisor of the period reported here.

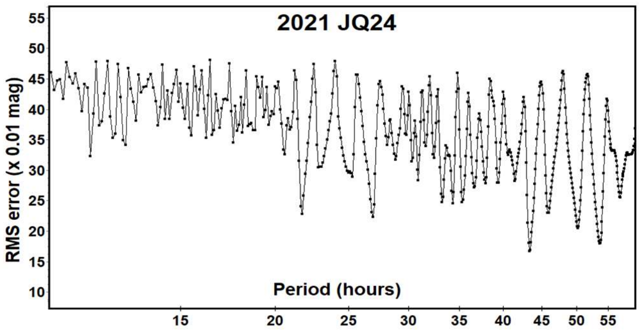

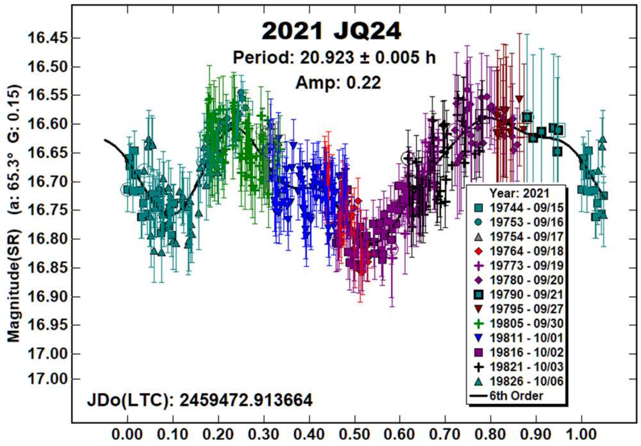

2021 LQ24. Pravec et al. (2021web) reported this to be a tumbling asteroid with periods of 25.39 h and 15.6 h. The data set was insufficient to duplicate those results but a dominant period of 17.1 h was found.

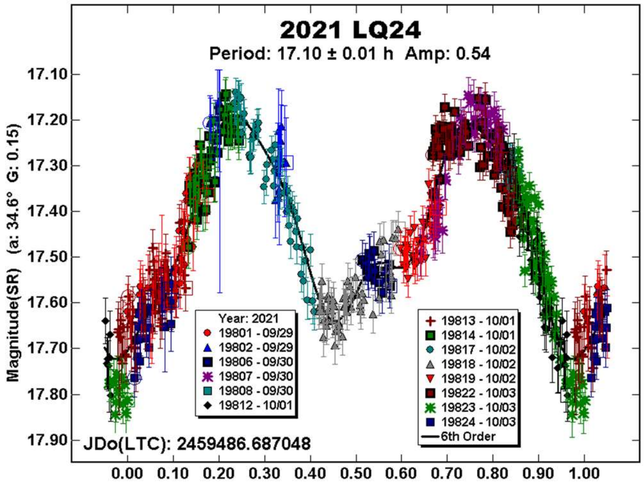

Acknowledgements

The authors gratefully acknowledge Shoemaker NEO Grants from the Planetary Society (2007, 2013). These were used to purchase some of the telescopes and CCD cameras used in this research. This work includes data from the Asteroid Terrestrial-impact Last Alert System (ATLAS) project. ATLAS is primarily funded to search for near earth asteroids through NASA grants NN12AR55G, 80NSSC18K0284, and 80NSSC18K1575; byproducts of the NEO search include images and catalogs from the survey area. The ATLAS science products have been made possible through the contributions of the University of Hawaii Institute for Astronomy, the Queen's University Belfast, the Space Telescope Science Institute, and the South African Astronomical Observatory. This paper made use of the services provided by the SAO/NASA Astrophysics Data System, which is operated by the Smithsonian Astrophysical Observatory under NASA Cooperative Agreement 80NSSC211M0056.

References

References from web sites should be considered transitory, unless from an agency with a long lifetime expectancy. Sites run by private individuals, even if on an institutional web site, do not necessarily fall into this category.

Number	Name	2021 mm/dd	Phase	L_{PAB}	B_{PAB}	Period(h)	P.E.	Amp	A.E.
1862	Apollo	12/11-12/12	51.8,50.9	39	8	3.066	0.002	0.61	0.03
3200	Phaethon	12/04-12/06	13.2,14.3	53	14	3.589	0.003	0.19	0.02
3361	Orpheus	10/13-10/15	20.7,19.3	35	-2	3.547	0.003	0.19	0.02
4660	Nereus	10/26-11/03	16.0,12.7	45	5	15.172	0.002	0.75	0.03
7358	Oze	10/17-11/13	48.0,35.4	91	2	125.8	0.2	0.11	0.01
12711	Tukmit	11/29-11/30	39.6,39.4	119	18	3.483	0.001	0.72	0.04
18882	1999 YN4	12/09-12/12	28.2,26.8	105	22	2.346	0.001	0.10	0.02
20460	Robwhiteley	11/30-12/03	27.3,26.5	110	3	2.751	0.001	0.12	0.02
87024	2000 JS66	11/10-11/27	*3.8,21.5	49	-3	56.532	0.005	1.08	0.05
						53.347	0.007	0.43	0.03
						39.46	0.01	0.13	0.02
137062	1998 WM	11/29-12/04	14.0,18.1	58	13	2.469	0.002	0.06	0.01
137805	1999 YK5	12/09-12/20	47.5,44.4	123	28	4.019	0.001	0.16	0.03
285571	2000 PQ9	09/23-10/15	38.3,32.4	123	29	119.6	0.6	0.30	0.05
	1999 FJ21	10/13-10/16	11.7,23.1	13	3	0.370364	0.000006	0.27	0.03
	2019 XS	11/10-11/10	18.7	43	-8	^{T}2.35	0.01	0.70	0.03
						3.01	0.01	0.61	0.03
	2021 JQ24	09/15-10/06	65.3,63.8	43	-17	20.923	0.005	0.22	0.03
	2021 LQ24	09/28-10/03	34.7,34.2	21	17	17.10	0.01	0.54	0.03

Table II. Observing circumstances and analysis results. ^{T}Dominant period of a likely tumbler. The phase angle (α) is given at the start and end of each date range. If there is an asterisk before the first phase value, the phase angle reached a maximum or minimum during the period. L_{PAB} and B_{PAB} are, respectively the average phase angle bisector longitude and latitude (see Harris et al.,1984).

Aznar, A.M.; Predatu, M.; Vaduvescu, O.; Oey, J. (2018). "EURONEAR - First Light Curves and Physical Properties of Near-Earth Asteroids." arXiv:1801.09420. *Romanian J. Phys.* **62**, 904.

Behrend, R. (2021web). Observatoire de Geneve web site. *http://obswww.unige.ch/~behrend/page_cou.html*

Colazo, M.; Morales, M.; Fornari, C.; Chapman, A. and 20 co-authors (2022). "Photometry and Light Curve Analysis of Eight Asteroids by GORA's Observatories." *Minor Planet Bull.* **49**, 48-51.

Harris, A.W.; Young, J.W.; Scaltriti, F.; Zappala, V. (1984). "Lightcurves and phase relations of the asteroids 82 Alkmene and 444 Gyptis." *Icarus* **57**, 251-258.

Harris, A.W.; Young, J.W.; Goguen, J.; Hammel, H.B.; Hahn, G. (1987). "Photoelectir lightcurves of the asteroid 1862 Apollo." *Icarus* **70**, 246-256.

Harris, A.W.; Pravec, P.; Galad, A.; Skiff, B.A.; Warner, B.D.; Vilagi, J.; Gajdos, S.; Carbognani, A.; Hornoch, K.; Kusnirak, P.; Cooney, W.R.; Gross, J.; Terrell, D.; Higgins, D.; Bowell, E.; Koehn, B.W. (2014). "On the maximum amplitude of harmonics on an asteroid lightcurve." *Icarus* **235**, 55-59.

Pravec, P.; Wolf, M.; Sarounova, L. (2000web; 2004web; 2017web; 2019web; 2021web). *http://www.asu.cas.cz/~ppravec/neo.htm*

Pravec, P.; Harris, A.W.; Scheirich, P.; Kušnirák, P.; Šarounová, L.; Hergenrother, C.W.; Mottola, S.; Hicks, M.D.; Masi, G.; Krugly, Yu.N.; Shevchenko, V.G.; Nolan, M.C.; Howell, E.S.; Kaasalainen, M.; Galád, A.; Brown, P.; Degraff, D.R.; Lambert, J.V.; Cooney, W.R.; Foglia, S. (2005). "Tumbling asteroids." *Icarus* **173**, 108-131.

Pravec, P.; Scheirich, P.; Durech, J.; Pollock, J.; Kusnirak, P.; Hornoch, K.; Galad, A.; Vokrouhlicky, D.; Harris, A.W.; Jehin, E.; Manfroid, J.; Opitom, C.; Gillon, M.; Colas, F.; Oey, J.; Vrastil, J.; Reichart, D.; Ivarsen, K.; Haislip, J.; LaCluyze, A. (2014). "The tumbling state of (99942) Apophis." *Icarus* **233**, 48-60.

Skiff, B.A.; Bowell, E.; Koehn, B.W.; Sanborn, J.J.; McLelland, K.P.; Warner, B.D. (2012). "Lowell Observatory Near-Earth Asteroid Photometry Survey (NEAPS) - 2008 May through 2008 December." *Minor Planet Bull.* **39**, 111-130.

Skiff, B.A.; McLelland, K.P.; Sanborn, J.J.; Pravec, P.; Koehn, B.W. (2019). "Lowell Observatory Near-Earth Asteroid Photometric Survey (NEAPS): Paper 3." *Minor Planet Bull.* **46**, 238-265.

Tonry, J.L.; Denneau, L.; Flewelling, H.; Heinze, A.N.; Onken, C.A.; Smartt, S.J.; Stalder, B.; Weiland, H.J.; Wolf, C. (2018). "The ATLAS All-Sky Stellar Reference Catalog." *Ap. J.* **867**, A105.

Vaduvescu, O.; Aznar, A.M.; Tudor, V.; Predatu, M.; and 23 co-authors (2017). "The EUROENAR Lightcurve Survey of Near-Earth Asteroids." *Earth, Moon, and Planets* **120**, 41-100.

Warner, B.D.; Harris, A.W.; Pravec, P. (2009). "The Asteroid Lightcurve Database." *Icarus* **202**, 134-146. Updated 2021 June. *http://www.minorplanet.info/lightcurvedatabase.html*

Warner, B.D. (2016a). "NearEarth Asteroid Lightcurve Analysis at CS3-Palmer Divide Station." *Minor Planet Bull.* **43**, 240-250.

Warner, B.D. (2016b). "Three Additional Candidates for the Group of Very Wide Binaries." *Minor Planet Bul.* **43**, 306-309.

Warner, B.D. (2018). "Near-Earth Asteroid Lightcurve Analysis at CS3-Palmer Divide Station: 2017 July Through October." *Minor Planet Bull.* **45**, 19-34.

Wisniewski, W.Z. (1991), "Physical studies of small asteroids I. Lightcurves and taxonomy of 10 asteroids." *Icarus* **90**, 117-122.

Zappala, V.; Cellini, A.; Barucci, A.M.; Fulchignoni, M.; Lupishko, D.E. (1990). "An anlaysis of the amplitude-phase relationship among asteroids." *Astron. Astrophys.* **231**, 548-560.

LIGHTCURVE ANALYSIS FOR ELEVEN NEAR-EARTH ASTEROIDS

Peter Birtwhistle
Great Shefford Observatory
Phlox Cottage, Wantage Road
Great Shefford, Berkshire, RG17 7DA
United Kingdom
peter@birtwhistle.org.uk

(Received: 2021 December 14. Revised: 2022 February 5)

Lightcurves and amplitudes for eleven near-Earth asteroids observed from Great Shefford Observatory during close approaches in 2021 are reported: 2021 LC1, 2021 QB3, 2021 RA, 2021 RB1, 2021 RS2, 2021 RG19, 2021 TT10, 2021 US1, 2021 UW1, 2021 VL3 and 2021 VQ26. Most are fast or superfast rotators including two ultra-fast rotators with periods < 1 minute and one shows indications of tumbling.

Photometric observations of near-Earth asteroids during close approaches to Earth between June and November 2021 were made at Great Shefford Observatory using a 0.40-m Schmidt-Cassegrain and Apogee Alta U47+ CCD camera. All observations were made unfiltered and with the telescope operating with a focal reducer at f/6. The 1K×1K, 13-micron CCD was binned 2×2 resulting in an image scale of 2.16 arc seconds/pixel. All the images were calibrated with dark and flat frames and *Astrometrica* (Raab, 2018) was used to measure photometry using APASS Johnson V band data from the UCAC4 catalogue (Zacharias et al., 2013) and G band data from the Gaia DR 2 catalogue (Brown et al., 2018). *MPO Canopus* (Warner, 2021), incorporating the Fourier algorithm developed by Harris (Harris et al., 1989) was used for lightcurve analysis.

No previously reported results for any of the objects reported here have been found in the Asteroid Lightcurve Database (from here on referred to as LCDB; Warner et al., 2009), from searches via the Astrophysics Data System (ADS, 2021) or from wider searches. All size estimates are calculated using H values from the Small-Body Database Lookup (from here on referred to as SBDB; JPL 2021), using an assumed albedo for NEAs of 0.2 (LCDB readme.pdf file) and are therefore uncertain and offered for relative comparison only.

2021 LC1. The ZTF team at Palomar discovered this Aten 31 hours before an approach to 3 Lunar Distances (LD) on 2021 June 5.5 UTC (Pettarin et al., 2021). With H = 26.53 in the SBDB it has an estimated size of 15 m. It was observed for 3.7 h while still inbound, at a range of ~3.5 LD, about 12 hours before passing Earth. Its apparent speed increased from 115-133 arcsec/min during that time and exposures were limited to 5.6 s or shorter. The telescope was repositioned a total of 19 times during the session and although relatively faint on individual images, no short-term variation was obvious as it crossed individual fields, however longer term (tens of minutes) variation was noted. The images were then stacked using *Astrometrica*, with 3 stacks being formed from the images collected from each of the 19 separate fields with the maximum elapsed time from the start of the first exposure to the end of the last used in any stack being 165 s. The raw plot shows fragments of a lightcurve, with two ~2 mag amplitude rises and indications of three maxima over ~3.6 h. The period spectrum shows the first of the three most significant RMS minima at 1.9 h and this period is adopted to generate the bimodal phased plot, though as this implies there was only partial coverage of less than 2 revolutions, this solution should be regarded as uncertain.

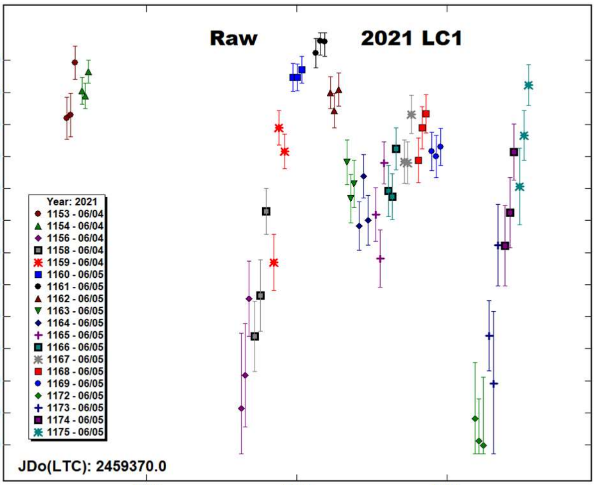

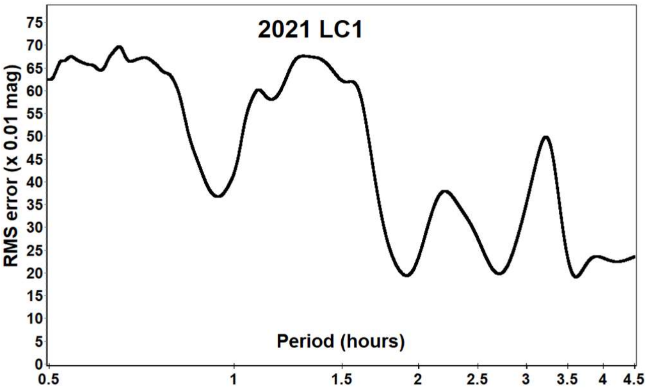

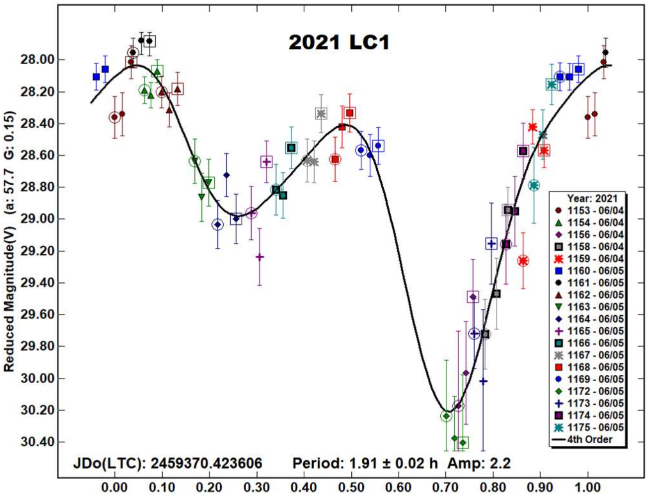

2021 QB3. The SBDB lists this Apollo with H = 23.77, equating to a diameter of ~52 m. It was an ATLAS-MLO discovery from 2021 Aug 31.3 UTC (Melnikov et al., 2021a) and made an approach to 1.7 LD of Earth on 2021 Sep 3.0 UTC, reaching mag +13 for 40 hours following that passage. 811 images were obtained over a period of 2.1 h starting 2021 Sep 3.93 UTC using exposures of 5.2 and 5.6 s and an initial solution resulted in a bimodal lightcurve of period 0.3630 h with an amplitude of 0.5. This figure is marked as PAR (Principal Axis Rotation) but shows strong indications of low amplitude non-principal axis rotation.

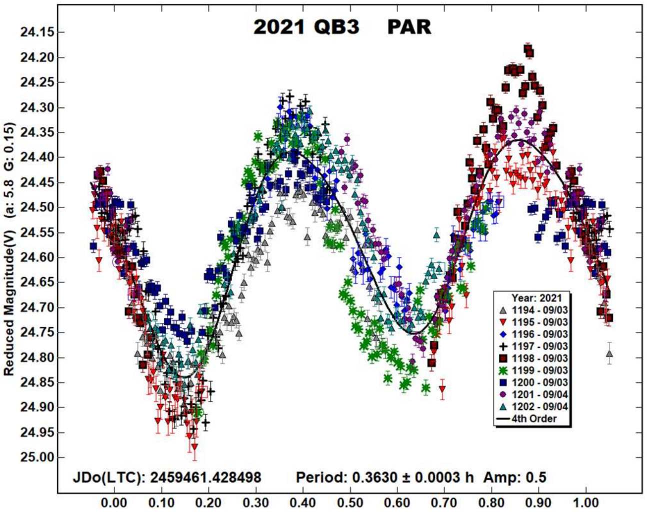

An attempt to solve for two periods in Canopus using its Dual-Period search functionality resulted in a second period of 0.3206 h with amplitude 0.12 being derived, the two lightcurves given here marked as P1 and P2.

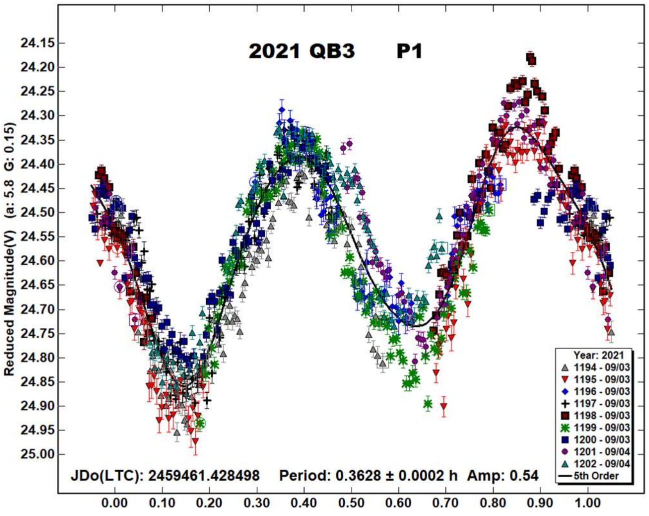

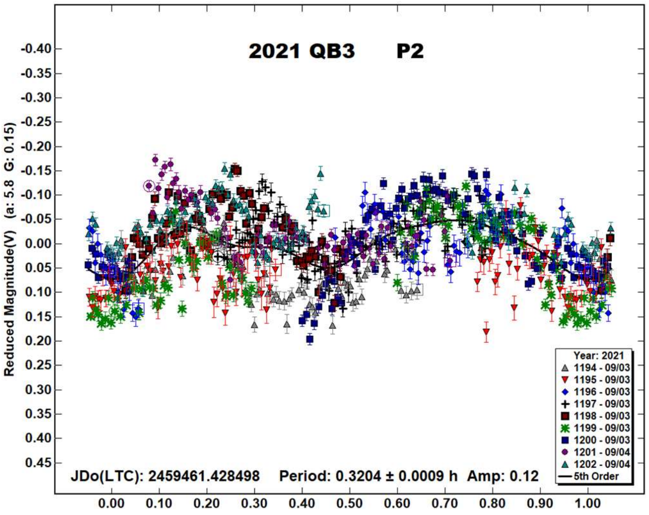

The large scatter in the P2 lightcurve and the reduced but still remaining systematic trends in the P1 lightcurve indicate problems with the NPAR fit and a plot of the measurements with the calculated curve from the NPAR solution superimposed shows the observed variations are represented only moderately well. It is expected that 2021 QB3 may be rated with a PAR code of -2 "NPA rotation detected based on deviations from a single period but the second period is not resolved" (Petr Pravec, personal communication).

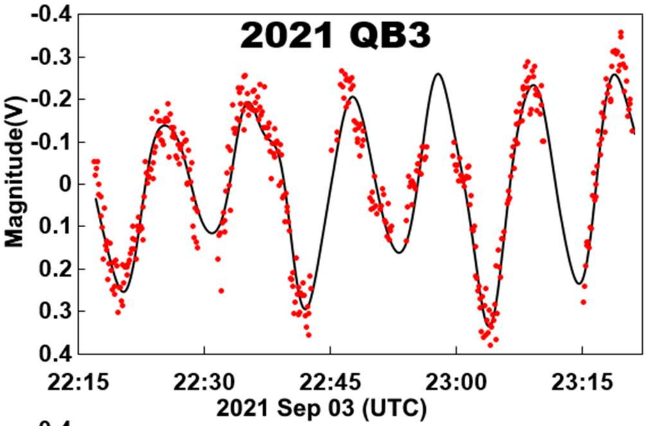

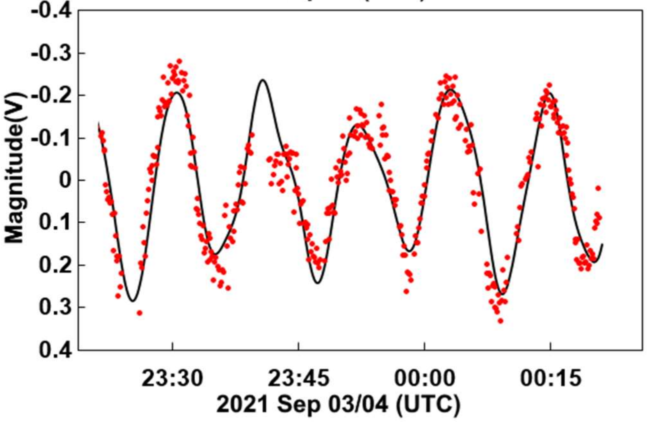

2021 RA. This Apollo was discovered at mag +15 and declination -44° on 2021 Sep 2.05 UTC by the SONEAR team in Brazil, already receding after an approach to within 3 LD some 13 h beforehand (Foglia et al., 2021a). The value of H given in the SBDB is 24.70, suggesting an approximate diameter of 34 m. It had already faded by about 1 mag when observed from Great Shefford starting at 2021 Sep 4.02 UTC. Over a period of 1.65 h, 531 exposures of 8 s duration were taken with the telescope needing repositioning 3 times. The period spectrum indicates a solution at 0.34 h gives the best fit, the resulting trimodal lightcurve is given as well as a bimodal solution at 0.22 h, but the shorter period is clearly an inferior fit.

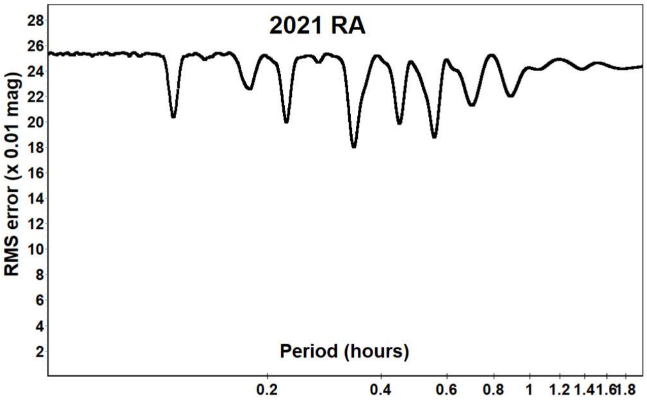

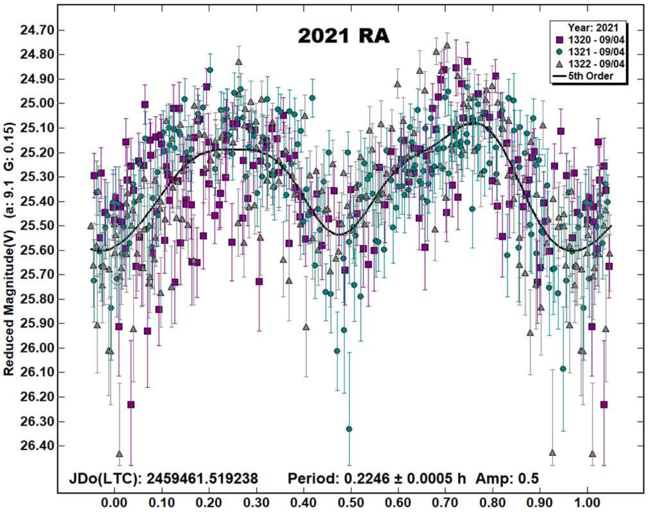

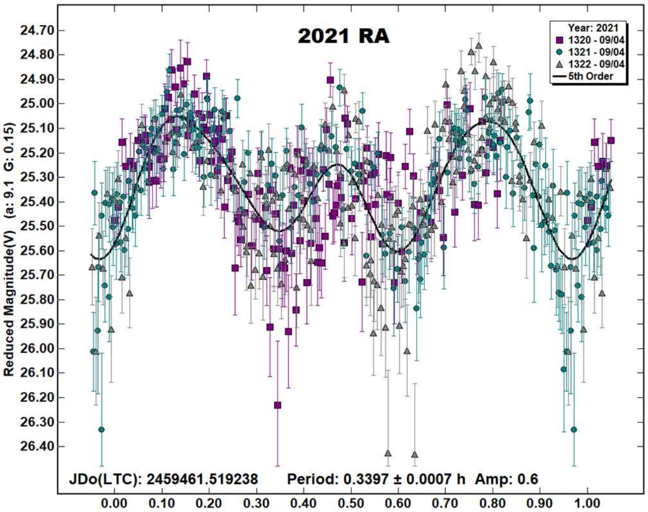

2021 RB1. Another discovery by the SONEAR team in Brazil, this Amor object was found on 2021 Sep 5.2 UTC and passed Earth at 8 LD about 30 hours later (Foglia et al., 2021b). The SBDB lists it with H = 24.06, equating to an approximate diameter of 46 m. It was under observation for 2.4 h starting at 2021 Sep 5.97 UTC and again for 3.9 h starting 2021 Sep 6.90 UTC and a total of 2527 images were obtained with exposures ranging from 2 - 7 s. 2021 RB1 was 16th mag throughout that period, sky conditions were occasionally only fair. The resulting noisy lightcurve from measuring individual images revealed no short period variation but did show a ~0.4 mag amplitude variation over the several hours it was observed on each of the two nights. The images were then combined into 109 stacked images and measured using *Astrometrica* before analysing with *MPO Canopus*. The period spectrum, covering the range 1 - 10 h reveals multiple solutions giving similar fits to the data in the range 2.5 - 6 h, the strongest bimodal solution, at 2.925 h is adopted here as the most plausible. The maximum elapsed time from the start of the first exposure to the end of the last used in any stack was 200 s, significantly less than the derived period, indicating lightcurve smoothing was negligible (Pravec et al., 2000).

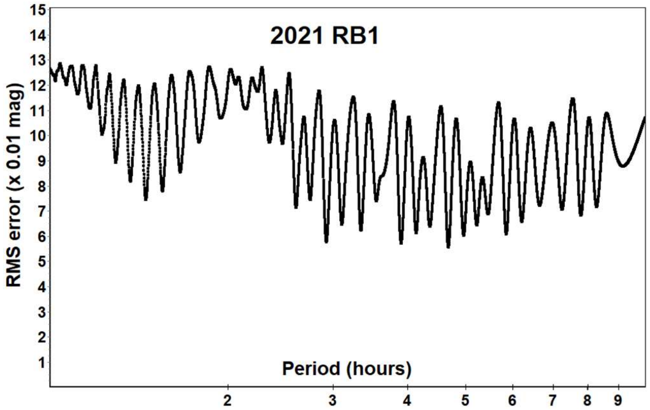

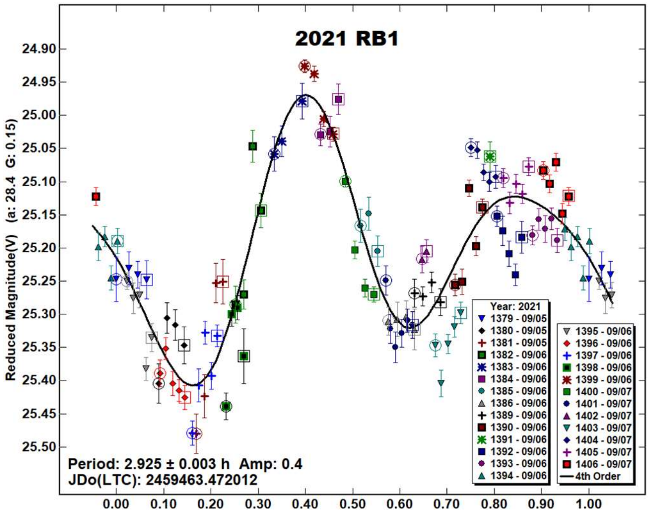

2021 RS2. The SBDB lists this Apollo with an H value of 30.35, suggesting a diameter of just 3 m and it was discovered by the Mt. Lemmon survey on 2021 Sep 7.26 UTC, 25 hours before making a very close approach to Earth at a distance of 0.06 LD (Melnikov et al., 2021b). It was under observation, initially for 15 mins starting at 2021 Sep 8.05 UTC, then 1.4 hours later for a further 55 mins and during that period halved its distance from Earth, to 0.56 LD. Exposures were kept between 4 and 5.6 s as the apparent speed increased from 40 to 100 arcsec/min. The apparent magnitude brightened from +18 to +17 and the amount of noise in the resulting photometric measures is large. However, especially during the latter stages, large variations in magnitude were obvious between consecutive exposures, taken with a cadence of ~6 s. The period spectrum covering periods from 11 to 360 s shows a set of very sharply defined RMS minima, the trimodal solution at 0.01809 h giving the lowest RMS figure, but only different to the bimodal solution's RMS by 0.01 mag and with the overall amount of noise in the measures being ~0.35 mag the bimodal solution at 0.012 h is selected here as being the most likely. This indicates that during the 1.4 h it was being observed it completed 119 revolutions. With the longest exposures used being 12.9% of the rotation period the amplitude attributable to the second harmonic would have been reduced due to lightcurve smoothing by 0.09 mag (Pravec et al., 2000), considerably less than the observed uncertainty in the amplitude.

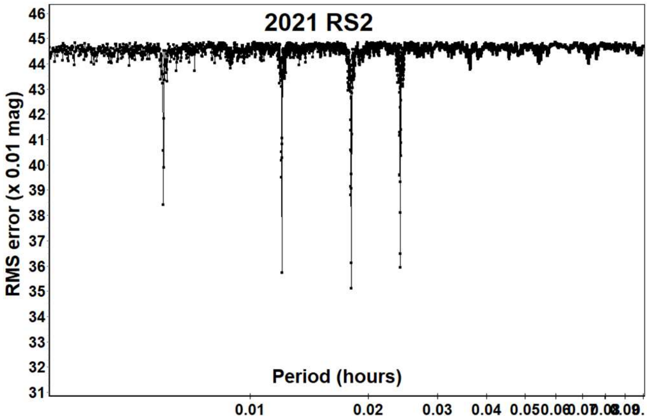

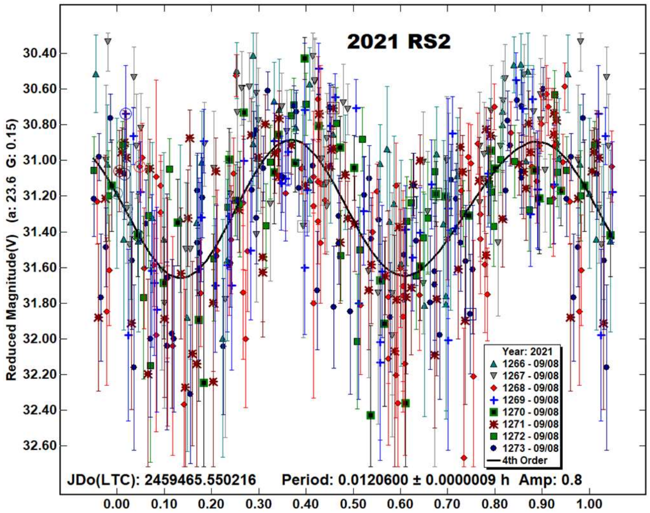

2021 RG19. The Pan-STARRS team discovered this Apollo at mag +22, with over two weeks lead time before it made an approach to 2 LD of Earth on 2021 Sep 28.92 UTC (Bulger et al., 2021). It was observed for 1.7 h starting at 2021 Sep 27.80 UTC and two hours later observed for another 2.0 h, when it was 16th mag and at a range of 4 LD. 1084 images were obtained with exposures ranging from 5.3 - 7.1 s with the telescope being repositioned 15 times due to the apparent speed, accelerating from 55 to 75 arcsec/min. The SBDB value of H = 24.73 translates to an approximate diameter of 34 m. 2021 RG19 could be seen to fade abruptly about every minute on individual images and the period spectrum shows the strongest solution at 0.031760 h (= 1.9 min.) is bimodal with a 0.8 mag amplitude. Over the 3.7 h of data collection, 2021 RG19 completed 116 rotations.

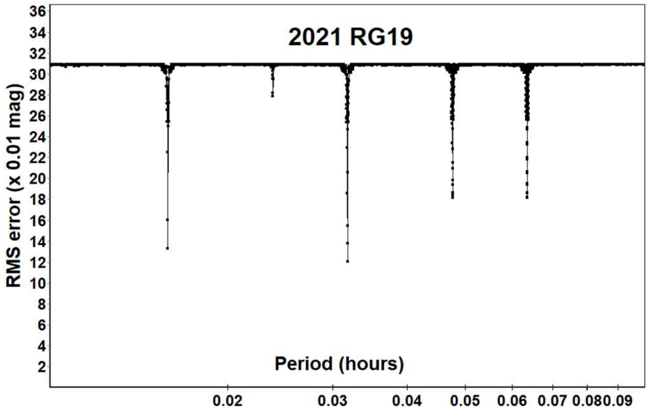

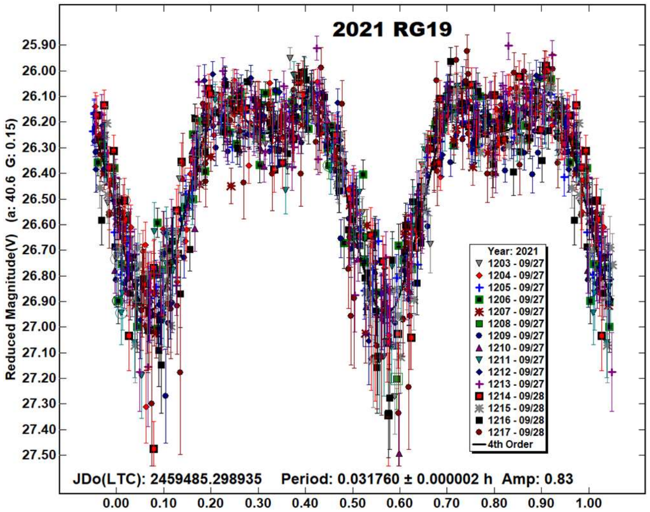

2021 TT10. The Mauna Loa ATLAS telescope discovered this Apollo on images taken on 2021 Oct 11.4 UTC, 4 hours after an approach to 1.7 LD from Earth (Bacci et al., 2021a). Pre-discovery positions were subsequently reported by the Catalina Sky Survey from 2 hours before closest approach, some 76° distant from the ATLAS positions. With the SBDB listing 2021 TT10 with a value of H = 23.41 this is likely to be the largest of the objects being reported here, with an estimated size of 62 m. It was observed for 2.1 h on the discovery date when it was 16th mag and moving at 20 arcsec/min. Exposures ranged from 7 - 12 s and 350 images were taken, with the telescope being repositioned 6 times. Analysis with Canopus revealed only short period solutions and the period spectrum, covering the range 1 - 7.2 min shows the strongest solution at 0.03646 h. The phased lightcurve indicates a low amplitude bimodal curve. The longest exposure as a fraction of the period is 0.09 and therefore no significant lightcurve smoothing is expected to be present (Pravec et al., 2000). 58 revolutions were completed during the period of observation.

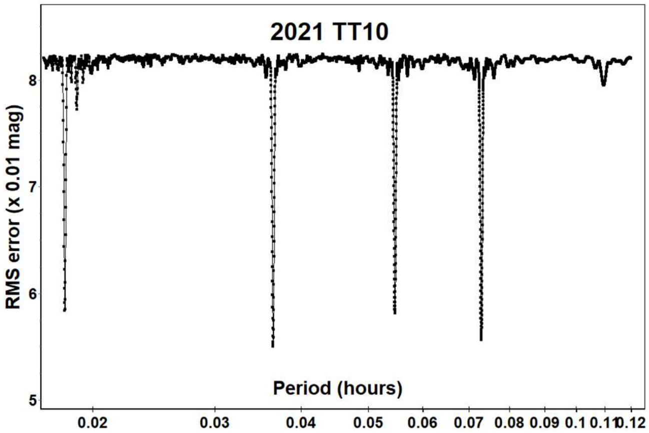

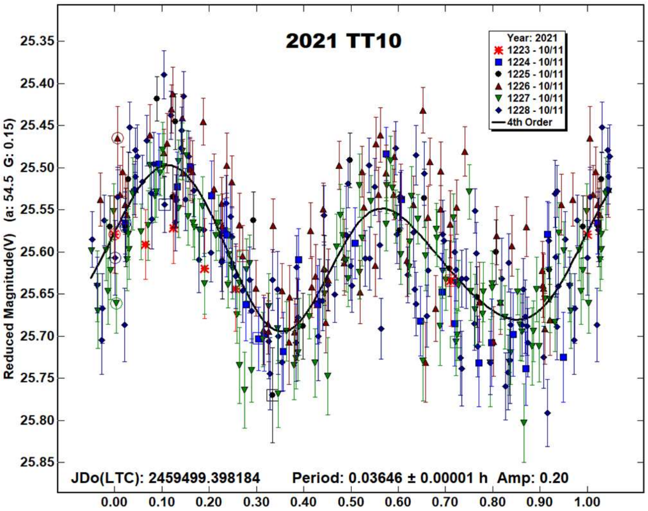

2021 US1. Another Apollo, discovered by the Mt. Lemmon survey on 2021 Oct 26.1 UTC on its way in to an approach to within 2 LD on 2021 Nov 2.97 UTC (Panterotto et al., 2021). It was observed for 1.3 h through the point of closest approach, apparent speed was not excessive, at 43 arcsec/min, with the telescope requiring repositioning 7 times, but it was rather faint at mag +17. The SBDB gives the value for absolute magnitude H as 27.79, inferring a diameter of approximately 8 m. 645 images were obtained with exposures of 2, 4 and 6 s and these measured and used to produce a lightcurve in *MPO Canopus*. As expected, there was a large amount of noise in the measurements but a bimodal solution with period 119 s was apparent. The optimal exposure to record the strongest signal for a minor planet with a bimodal lightcurve and rotation period of P is 0.185 P (Pravec et al., 2000), in this case 0.185 × 119 s = 22 s. The images from each of the 7 fields were examined and divided up into sets for stacking with *Astrometrica*, each set chosen so that the elapsed time from start of the first exposure to end of the last was 22 s or less. This resulted in 151 stacks combining on average 4.3 images in each. The measurements from these stacks were then imported into Canopus and the resulting period spectrum showing the solution at 0.03307 h being the strongest. The likely effect of forcing the effective integration time to be 0.185 P is to decrease the amplitude due to the second harmonic by 0.06 mag (Pravec et al., 2000), indicating that the amplitude without any lightcurve smoothing would be ~0.30 mag.

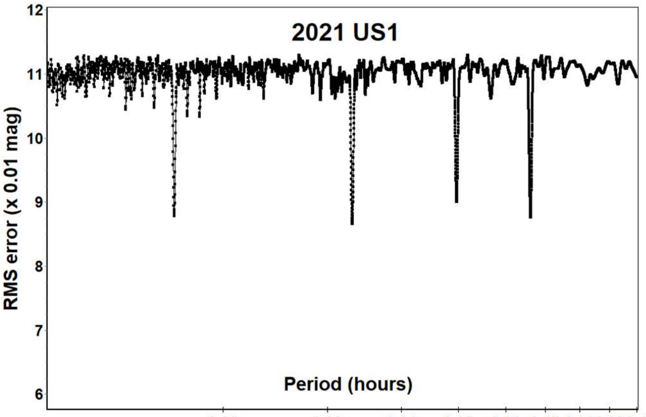

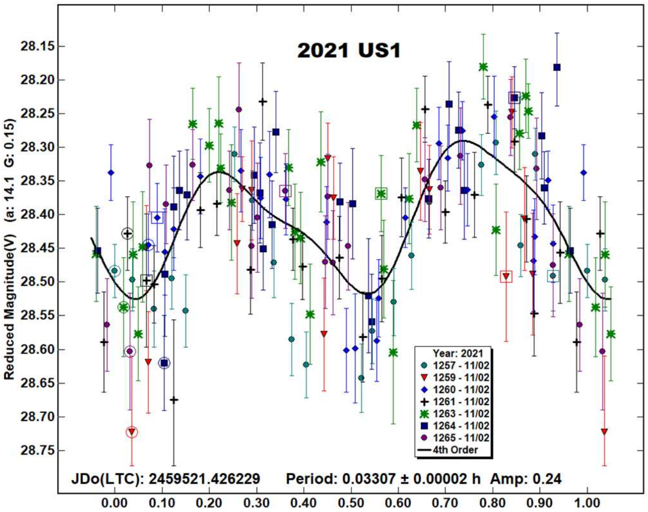

2021 UW1. This Apollo was another discovered by the Mt. Lemmon Survey, one day after 2021 US1 and due to pass Earth at 1 LD on 2021 Oct 30.85 UTC (Bacci et al., 2021b). It was observed for 43 minutes within 2 hours of closest approach at large phase angles (85 - 90°) with the apparent speed increasing from 420 to 440 arcsec/min and exposure lengths were limited to 0.9 s throughout. A total of 396 measurable images were obtained and large variations in brightness were obvious between consecutive exposures, indicating a very fast rotation period. The period spectrum shows a number of ultra-fast solutions below 60 s, the strongest being at 0.0058620 h (= 21 s) and the next strongest at half that value at 0.0029308 h. Both lightcurves are given here, but the longer period with a more complex curve appears to fit the data significantly better and is adopted here as the correct period. 2021 UW1 has an estimated diameter of 17 m based on the value of H = 26.15 in the SBDB. It completed 121 revolutions during the time it was under observation.

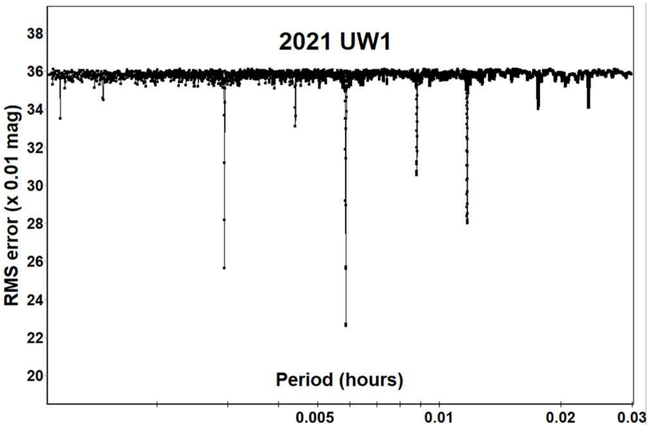

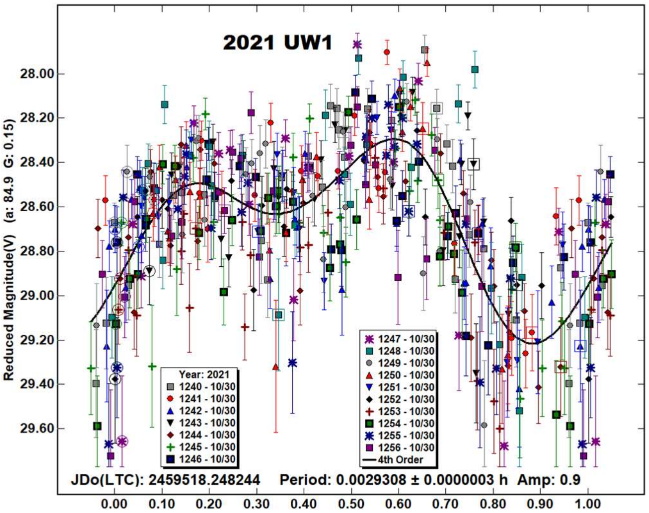

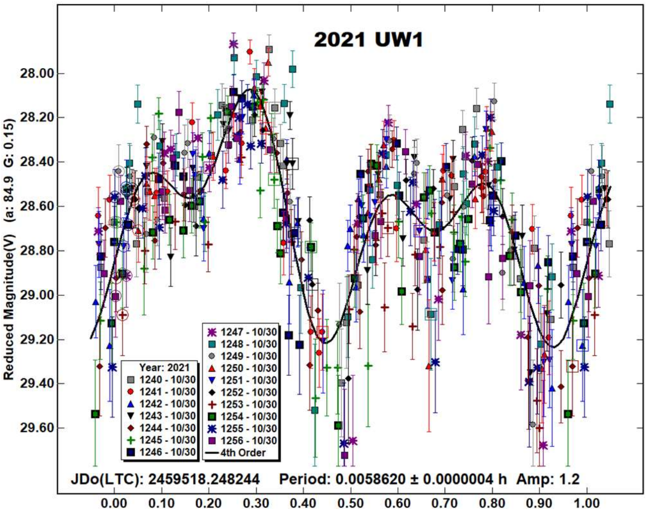

2021 VL3. This Apollo was discovered by the ATLAS telescope on Haleakala on 2021 Nov 7.45 UTC, 22 hours before passing Earth at 0.4 LD (Barni et al., 2021). The SBDB lists it with H = 28.43, equating to an estimated size of 6_m. It was observed for 1.4 h starting at 2021 Nov 7.95 UTC at 15th mag and with the apparent speed increasing from 160 to 190 arcsec/min during that period the telescope had to be repositioned 13 times, resulting in 745 measurable images being obtained, taken with exposures ranging between 2.3 and 2.7 s. Small adjustments to the zero-points of the 13 sessions were made in *MPO Canopus* to minimise the overall RMS fit of the lightcurve, with the RMS of those adjustments being 0.056 mag. The RMS of the four potential solutions revealed in the period spectrum are equal to within 0.0004 mag and the bimodal lightcurve is presented here with a period of 5.4 minutes and amplitude of 0.4.

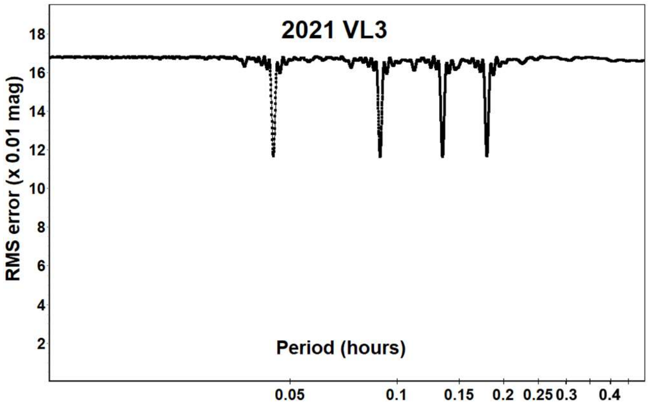

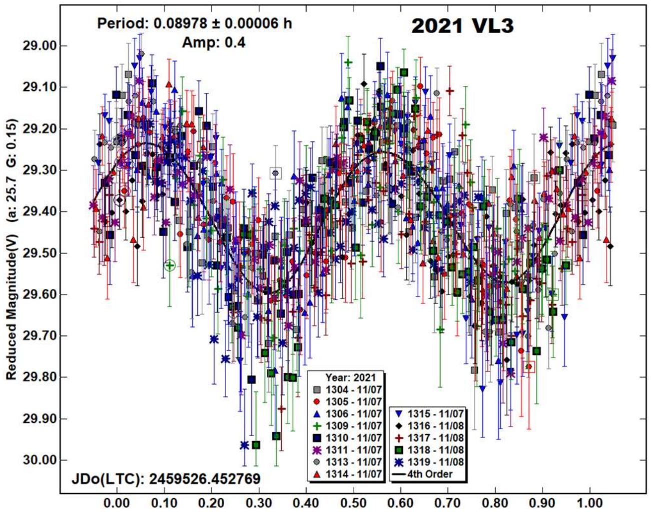

2021 VQ26. The Mt. Lemmon survey discovered this Apollo on 2021 Nov 15.1 UTC about 1 week before an approach to 4.6 LD (Buzzi et al., 2021). It was observed extensively from Great Shefford starting on 2021 Nov 21.8 for 5.3 h and 2021 Nov 22.7 UTC for 8.4 h with a total of 3837 measurable images being obtained, with the telescope being repositioned 47 times, the apparent magnitude rose from +16 to +15 over the two nights. With an apparent speed of 63 - 70 arcsec/min exposures were kept to 6.1 s or shorter. On initial examination no very short-term magnitude changes was evident but variation was seen over tens of minutes, so the images were then stacked in *Astrometrica* with the time from start of first exposure to end of last exposure in any one stack being kept to 240 seconds or less. The last three sessions measured (numbered 1375, 1376 and 1377 in the following plots) would not solve with the UCAC4 catalogue, instead G-band magnitudes were measured using the Gaia DR 2 catalogue and converted to V band by using the adjustment of 0.28 used by the MPC (MPC, 2021). A raw plot, with the observed magnitudes reduced to unit distance and adjusted for phase angle, assuming the phase slope parameter G = 0.15 indicates that an almost complete rotation with unequal minima may have been captured on the second night, assuming a bimodal curve. The partial curve on the first night includes one minimum, with a similar shape to the first minima on the second night, though it appears to be about 0.1 mag brighter. However, the phase angle decreased from 43.0 - 37.9° on the first night but had reduced to 21.4 - 17.2° on the second night, so levelling between the two nights will be sensitive to the value of G adopted in the HG magnitude system parameters used in the reduction.

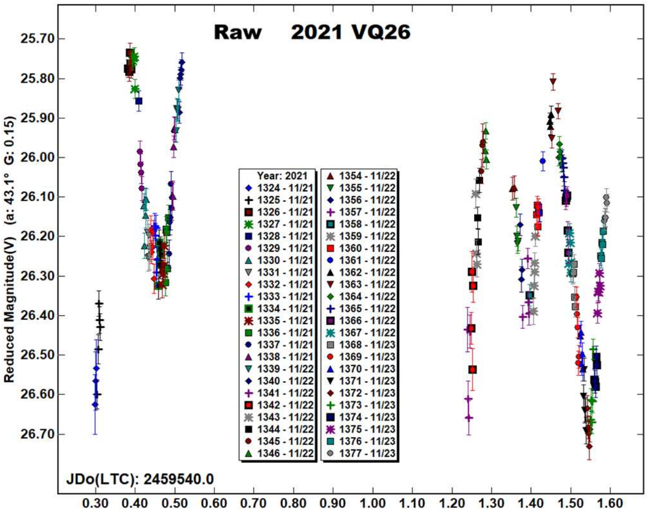

The period spectrum over a range of 1 – 24 h shows a set of similar RMS minima starting with a bimodal solution at 7.6 h, which with the limited coverage obtained is chosen as likely to be the correct period.

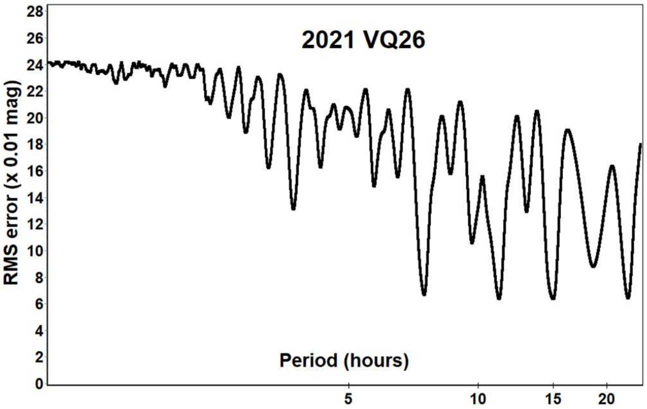

MPO Canopus was used to vary the value of G to minimise the fit between the two nights of data, the best fit was obtained using G = 0.26 and is given here:

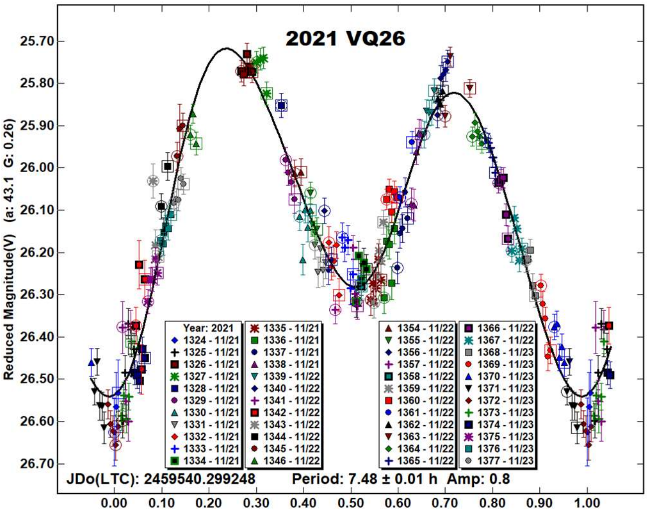

Acknowledgements

The author would like to again thank Petr Pravec for his help on the analysis of tumbling asteroids.

The author also gratefully acknowledges a Gene Shoemaker NEO Grant from the Planetary Society (2005) and a Ridley Grant from the British Astronomical Association (2005), both of which facilitated upgrades to observatory equipment used in this study.

References

ADS (2021). Astrophysics Data System. *https://ui.adsabs.harvard.edu/*

Bacci, P.; Maestripieri, M.; Tesi, L.; Fagioli, G.; Fuls, D.C.; Gray, B.; Rankin, D.; Shelly, F.C.; Dupouy, P.; de Vanssay, J.B.; Losse, F.; Briggs, D.; Birtwhistle, P.; Morra, G.; Denneau, L. and 7 colleagues (2021a). “2021 TT10” MPEC 2021-T227. *https://minorplanetcenter.net/mpec/K21/K21TM7.html*

Bacci, P.; Maestripieri, M.; Tesi, L.; Fagioli, G.; Foglia, S.; Galli, G.; Brucker, M.J.; Panterotto, G.; Pettarin, E.; Dupouy, P.; Camarasa, J.; Jahn, J.; Urbanik, M.; Urbanik, S.; Fuls, D.C. and 20 colleagues (2021b). “2021 UW1” MPEC 2021-U150. *https://minorplanetcenter.net/mpec/K21/K21UF0.html*

Barni, S.; Colzani, E.; Sicoli, P.; Pettarin, E.; Ikari, Y.; Birtwhistle, P.; Korlevic, K.; Okumura, S.; Nimura, T.; Denneau, L.; Tonry, J.; Weiland, H.; Fitzsimmons, A.; Robinson, J.; Erasmus, N. and 4 colleagues (2021), “2021 VL3” MPEC 2021-V151. *https://minorplanetcenter.net/mpec/K21/K21VF1.html*

Brown, A.G.A. et al. (Gaia collaboration) (2018). “Gaia Data Release 2: Summary of the contents and survey properties.” *Astronomy & Astrophysics* **616**, A1.

Bulger, J.; Lowe, T.; Schultz, A.; Smith, I.; Chambers, K.; Chastel, S.; de Boer, T.; Fairlamb, J.; Gao, H.; Huber, M.; Lin, C.-C.; Magnier, E.; Ramanjooloo, Y.; Wainscoat, R.; Weryk, R. and 3 colleagues (2021). “2021 RG19” MPEC 2021-S03. *https://minorplanetcenter.net/mpec/K21/K21S03.html*

Buzzi, L.; Wierzchos, K.W.; Christensen, E.J.; Farneth, G.A.; Fuls, D.C.; Gibbs, A.R.; Grauer, A.D.; Groeller, H.; Kowalski, R.A.; Larson, S.M.; Leonard, G.J.; Rankin, D.; Seaman, R.L.; Shelly, F.C. (2021). “2021 VQ26” MPEC 2021-W21. *https://minorplanetcenter.net/mpec/K21/K21W21.html*

Foglia, S.; Galli, G.; Glassey, R.B.; Panterotto, G.; Pettarin, E.; Leonard, G.J.; Christensen, E.J.; Farneth, G.A.; Fuls, D.C.; Gibbs, A.R.; Grauer, A.D.; Groeller, H.; Kowalski, R.A.; Larson, S.M.; Pruyne, T.A. and 20 colleagues (2021a). “2021 RA” MPEC 2021-R43. *https://minorplanetcenter.net/mpec/K21/K21R43.html*

Foglia, S.; Galli, G.; Tichy, M.; Ticha, J.; Honkova, M.; Pettarin, E.; Dupouy, P.; de Vanssay, J.B.; Urbanik, M.; Briggs, D.; Birtwhistle, P.; Korlevic, K.; Dementiev, T.O.; Tanasiychuk, Y.V.; Kozhukhov, A.M. and 14 colleagues (2021b). “2021 RB1” MPEC 2021-R97. *https://minorplanetcenter.net/mpec/K21/K21R97.html*

Harris, A.W.; Young, J.W.; Scaltriti, F.; Zappala, V. (1984). “Lightcurves and phase relations of the asteroids 82 Alkmene and 444 Gyptis.” *Icarus* **57**, 251-258.

Harris, A.W.; Young, J.W.; Bowell, E.; Martin, L.J.; Millis, R.L.; Poutanen, M.; Scaltriti, F.; Zappala, V.; Schober, H.J.; Debehogne, H.; Zeigler, K. (1989). "Photoelectric Observations of Asteroids 3, 24, 60, 261, and 863." *Icarus* **77**, 171-186.

JPL (2021). Small-Body Database Lookup.
https://ssd.jpl.nasa.gov/tools/sbdb_lookup.html

Kwiatkowski, T.; Buckley, D.A.H.; O'Donoghue, D.; Crause, L.; Crawford, S.; Hashimoto, Y.; Kniazev, A.; Loaring, N.; Romero Colmenero, E.; Sefako, R.; Still, M.; Vaisanen, P. (2010). "Photometric survey of the very small near-Earth asteroids with the SALT telescope - I. Lightcurves and periods for 14 objects." *Astronomy & Astrophysics* **509**, A94.

Melnikov, S.; Hoegner, C.; Laux, U.; Ludwig, F.; Stecklum, B.; Bacci, P.; Maestripieri, M.; Tesi, L.; Fagioli, G.; Buzzi, L.; Pettarin, E.; Dupouy, P.; Emmerich, M.; Melchert, S.; Ruocco, N. and 16 colleagues (2021a). "2021 QB3" MPEC 2021-R13.
https://minorplanetcenter.net/mpec/K21/K21R13.html

Melnikov, S.; Hoegner, C.; Laux, U.; Ludwig, F.; Stecklum, B.; Tichy, M.; Ticha, J.; Honkova, M.; Wierzchos, K.W.; Christensen, E.J.; Farneth, G.A.; Fuls, D.C.; Gibbs, A.R.; Grauer, A.D.; Groeller, H. and 9 colleagues (2021b). "2021 RS2" MPEC 2021-R141.
https://minorplanetcenter.net/mpec/K21/K21RE1.html

MPC (2021). V-band correction table
https://minorplanetcenter.net/iau/info/BandConversion.txt
linked from:
https://minorplanetcenter.net/iau/info/OpticalObs.html

Panterotto, G.; Pettarin, E.; Dupouy, P.; de Vanssay, J.B.; Fuls, D.C.; Christensen, E.J.; Farneth, G.A.; Gibbs, A.R.; Grauer, A.D.; Groeller, H.; Kowalski, R.A.; Larson, S.M.; Leonard, G.J.; Rankin, D.; Seaman, R.L. and 14 colleagues (2021). "2021 US1" MPEC 2021-U146.
https://minorplanetcenter.net/mpec/K21/K21UE6.html

Pettarin, E.; Felber, T.; Bolin, B.T.; Bhalerao, V.; Cheng, Y.-L.; Copperwheat, C.M.; Deshmukh, K.P.; Hsu, C.-Y.; Lin, Z.-Y.; Purdum, J.; Royle, S.; Sharma, K.; Zhai, C.; Z.T.F. Collaboration; Duev, D.A. and 8 colleagues (2021). "2021 LC1" MPEC 2021-L55.
https://minorplanetcenter.net/mpec/K21/K21L55.html

Pravec, P.; Hergenrother, C.; Whiteley, R.; Sarounova, L.; Kusnirak, P.; Wolf, M. (2000). "Fast Rotating Asteroids 1999 TY2, 1999 SF10, and 1998 WB2." *Icarus* **147**, 477-486.

Pravec, P.; Harris, A.W.; Scheirich, P.; Kušnirák, P.; Šarounová, L.; Hergenrother, C.W.; Mottola, S.; Hicks, M.D.; Masi, G.; Krugly, Yu.N.; Shevchenko, V.G.; Nolan, M.C.; Howell, E S.; Kaasalainen, M.; Galád, A. and 5 colleagues. (2005). "Tumbling Asteroids." *Icarus* **173**, 108-131.

Raab, H. (2018). Astrometrica software, version 4.12.0.448. *http://www.astrometrica.at/*

Warner, B.D.; Harris, A.W.; Pravec, P. (2009). "The Asteroid Lightcurve Database." *Icarus* **202**, 134-146. Updated 2021 June. *https://minplanobs.org/mpinfo/php/lcdb.php*

Warner, B.D. (2021). MPO Software, Canopus version 10.8.4.11. Bdw Publishing, Colorado Springs, CO.

Zacharias, N.; Finch, C.T.; Girard, T.M.; Henden, A.; Bartlett, J.L.; Monet, D.G.; Zacharias, M.I. (2013). "The Fourth US Naval Observatory CCD Astrograph Catalog (UCAC4)." *The Astronomical Journal* **145**, 44-57.

Number	Name	Integration times	Max intg./ Period	Min a/b	Points	Fields
	2021 LC1	165$^{\Sigma}$	0.024	2.0	57	19
	2021 QB3	5.2-5.6	0.010	1.5	811	9
	2021 RA	8	0.007	1.5	531	3
	2021 RB1	200$^{\Sigma}$	0.019	1.2	109	26
	2021 RS2	4-5.6	0.129	1.5	439	8
	2021 RG19	5.3-7.1	0.062	1.4	1084	15
	2021 TT10	7,8,12	0.091	1.1	350	6
	2021 US1	22$^{\Sigma}$	0.185	1.2	151	7
	2021 UW1	0.9	0.043	1.3	396	17
	2021 VL3	2.3-2.7	0.008	1.2	745	13
	2021 VQ26	240$^{\Sigma}$	0.009	1.5	199	47

Table I. Ancillary information, listing the integration times used (seconds), the fraction of the period represented by the longest integration time (Pravec et al., 2000), the calculated minimum elongation of the asteroid (Kwiatkowski et al., 2010), the number of data points used in the analysis and the number of times the telescope was repositioned to different fields.
Note: Σ = Longest elapsed integration time for stacked images (start of first to end of last exposure used).

Number	Name	yyyy mm/ dd	Phase	L_{PAB}	B_{PAB}	Period(h)	P.E.	Amp	A.E	PAR	H
	2021 LC1	2021 06/04-06/05	57.5,63.8	233	23	1.91	0.02	2.2	0.4		26.53
	2021 QB3	2021 09/03-09/04	5.6,8.0	344	-2	0.3628	0.0002	0.5	0.1	-2	23.77
						0.3204	0.0009	0.1	0.1		
	2021 RA	2021 09/04-09/04	9.1,9.2	346	-1	0.3397	0.0007	0.6	0.3		24.70
	2021 RB1	2021 09/05-09/07	28.5,30.3	357	3	2.925	0.003	0.4	0.1		24.06
	2021 RS2	2021 09/08-09/08	23.1,24.9	348	12	0.0120600	0.0000009	0.8	0.5		30.35
	2021 RG19	2021 09/27-09/28	40.4,43.6	11	20	0.031760	0.000002	0.8	0.2		24.73
	2021 TT10	2021 10/11-10/11	54.5,54.9	23	28	0.03646	0.00001	0.2	0.1		23.41
	2021 US1	2021 11/02-11/02	14.0,14.8	47	2	0.03307	0.00002	0.2	0.1		27.79
	2021 UW1	2021 10/30-10/30	85.2,90.3	358	21	0.0058620	0.0000004	1.2	0.3		26.15
	2021 VL3	2021 11/07-11/08	26.5,23.3	35	-7	0.08978	0.00006	0.4	0.2		28.43
	2021 VQ26	2021 11/21-11/23	43.0,17.1	52	11	7.48	0.01	0.8	0.1		24.33

Table II. Observing circumstances and results. Where more than one line is given, these include periods determined for NPA rotation. The phase angle is given for the first and last date. If preceded by an asterisk, the phase angle reached an extrema during the period. L_{PAB} and B_{PAB} are the approximate phase angle bisector longitude/latitude at mid-date range (see Harris et al., 1984). PAR is the expected Principal Axis Rotation quality detection code (Pravec et al., 2005) and H is the absolute magnitude at 1 au from Sun and Earth taken from the Small-Body Database Lookup (JPL, 2021).

LIGHTCURVE ANALYSIS OF 10 V-TYPE ASTEROIDS

Matthew C. Nowinski
Department of Physics & Astronomy
George Mason University
Fairfax, VA, USA 22030
mnowinsk@gmu.edu

Tyler R. Linder
Astronomical Research Institute
tlinder34@gmail.com

Daniel E. Reichart, Joshua B. Haislip,
Vladimir V. Kouprianov, Justin P. Moore
Skynet Robotic Telescope Network
University of North Carolina
269 Phillips Hall, CB #3255
Chapel Hill, NC, USA

(Received: 2021 Dec 26)

Lightcurves for ten asteroids of taxonomic type V, potential impact debris from 4 Vesta, are presented. This analysis is based on observations conducted from 2016 November through 2017 June.

Photometric observations of ten V-type asteroids were performed using three observatories: Stone Edge Observatory (SEO) in Sonoma, CA, USA; Cerro Tololo Inter-American Observatory (CTIO) in La Serena, Chile; and Yerkes Observatory in Williams Bay, WI, USA. Telescope, camera, and image specifications for each of these facilities are presented in Table I. All images used in this analysis were obtained between 2016 November and 2017 June. Data processing and analysis were done with *MPO Canopus* (Warner, 2019).

The targets for this study were selected from a set of asteroids categorized by Carvano et al. (2010) with a V_p-type taxonomic class. This taxonomy was developed based on optical photometric observations from the Sloan Digital Sky Survey (SDSS) Moving Object Catalogue (MOC4) (Ivezić et al., 2010). The V_p-type taxonomic class is so named because of its photometric similarities with 4 Vesta; hence, these asteroids represent a population of potential impact debris from that parent body. Several of the target asteroids for this study were also included in a near-infrared spectroscopic investigation conducted by Hardersen et al. (2014, 2015). The orbital and physical properties of the ten target asteroids are shown in Table II. Table III summarizes the observing circumstances and the results of this study.

3648 Raffinetti was discovered in 1957 at the La Plata Observatory near Buenos Aires, Argentina. The asteroid was named after Virgilio Raffinetti (1869-1946), the observatory's director from 1889 to 1905. The asteroid was observed using the CTIO-PROMPT6 telescope. Measurements were obtained for a total of approximately 15 hours using exposure times of 120 seconds and an open filter (*i.e.*, no filter). The derived rotational period was $P = 5.1757 \pm 0.0006$ h with an amplitude of $A = 0.16 \pm 0.007$ mag. Galdies (2022) published a similar result of $P = 5.177 \pm 0.001$ h.

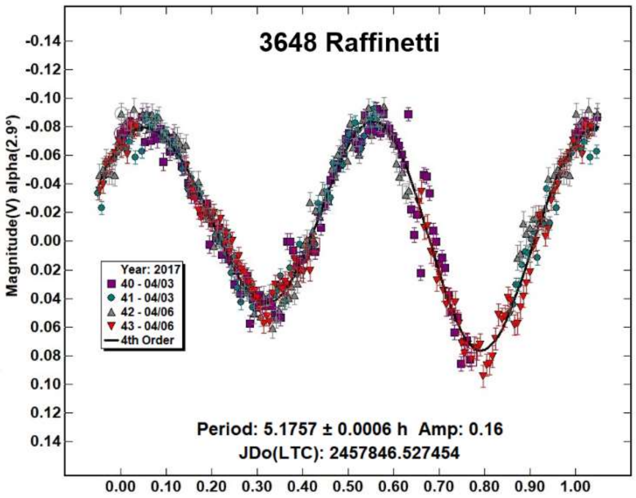

5235 Jean-Loup was discovered in 1990 at the Palomar Observatory, CA, USA. The asteroid was named after French astronaut Jean-Loup Jacques Marie Chrétien (1938-). 5235 Jean-Loup was observed using the CTIO-PROMPT6 telescope. Measurements were obtained for a total of approximately 9.5 hours using exposure times of 120 seconds and an open filter. The derived rotational period was $P = 2.4523 \pm 0.0004$ h with an amplitude of $A = 0.11 \pm 0.006$ mag. Oszkiewicz et al. (2020) published a similar result of $P = 2.4524 \pm 0.0001$ h.

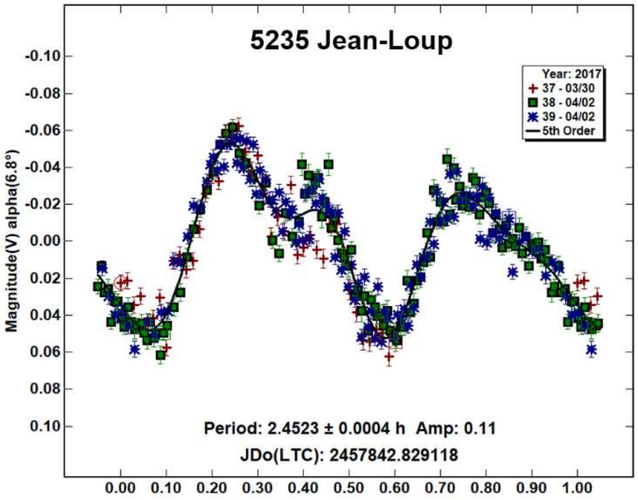

9223 Leifandersson was discovered in 1995 by the University of Arizona's SPACEWATCH group at the Kitt Peak National Observatory, AZ, USA. The asteroid was named after Swedish astronomer Leif Erland Andersson (1943-1979), who calculated the pole orientation of the planet Pluto. 9223 Leifandersson was observed using both the SEO and CTIO-PROMPT6 telescopes. Measurements were obtained for a total of approximately 23 hours using exposure times of (1) 120 seconds and a clear filter for SEO, and (2) 180 seconds and an open filter for CTIO-PROMPT6. The derived rotational period was $P = 3.75834 \pm 0.00018$ h with an amplitude of $A = 0.33 \pm 0.028$ mag. Waszczak et al. (2015) published a similar result of $P = 3.758 \pm 0.0014$ h.

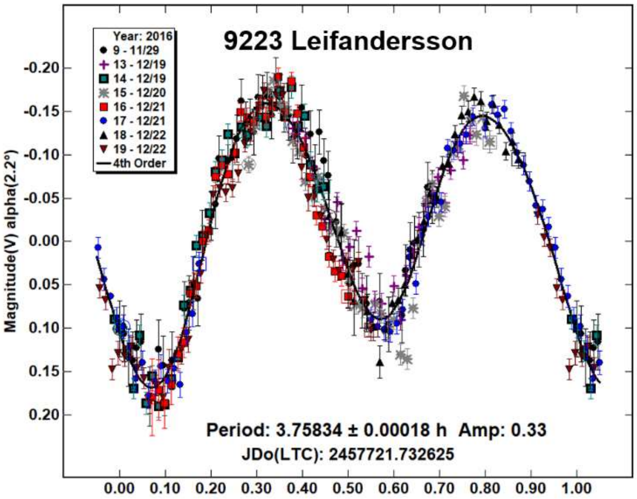

(11699) 1998 FL105 was discovered in 1998 by MIT's Lincoln Near Earth Asteroid Research (LINEAR) program in Soccoro, NM, USA. (11699) 1998 FL105 was observed using both the CTIO-PROMPT3 and CTIO-PROMPT6 telescopes. Measurements were obtained for a total of approximately 15 hours using individual exposure times of (1) 30 seconds and a clear filter for CTIO-PROMPT3, and (2) 80 seconds and an open filter for CTIO-PROMPT6. The derived rotational period was *P* = 4.09625 ± 0.00075 h with an amplitude of *A* = 0.58 ± 0.042 mag. A review of the literature found no previously published lightcurve results for (11699) 1998 FL105.

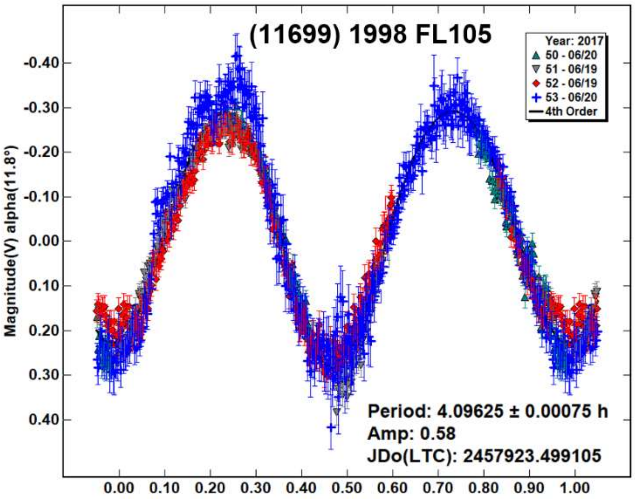

12073 Larimer was discovered in 1998 by LINEAR. The asteroid was named after Curtis James Larimer (1986-), a 2002 awardee of the Intel International Science and Engineering Fair (ISEF). 12073 Larimer was observed using the CTIO-PROMPT6 telescope. Measurements were obtained for a total of approximately 11 hours using individual exposure times of 120 seconds and an open filter. The derived rotational period was *P* = 9.4892 ± 0.0064 h with an amplitude of *A* = 0.35 ± 0.019 mag. A review of the literature found no previously published lightcurve results for 12073 Larimer.

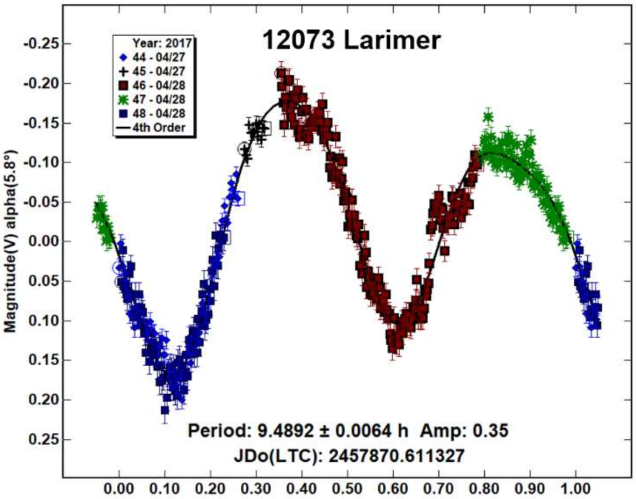

(15121) 2000 EN14 was discovered in 2000 by Korado Korlević at the Višnjan Observatory, Croatia. (15121) 2000 EN14 was observed using the CTIO-PROMPT6 telescope. Measurements were obtained for a total of approximately 15 hours using individual exposure times of 120 seconds and an open filter. The derived rotational period was *P* = 5.5822 ± 0.0005 h with an amplitude of *A* = 0.71 ± 0.020 mag. Yeh et al. (2020) estimated a longer period (by approximately 0.22 h or 4%) of *P* = 5.80 ± 0.06 h based on 14 observations by the China Near-Earth Object Survey Telescope (CNEOST).

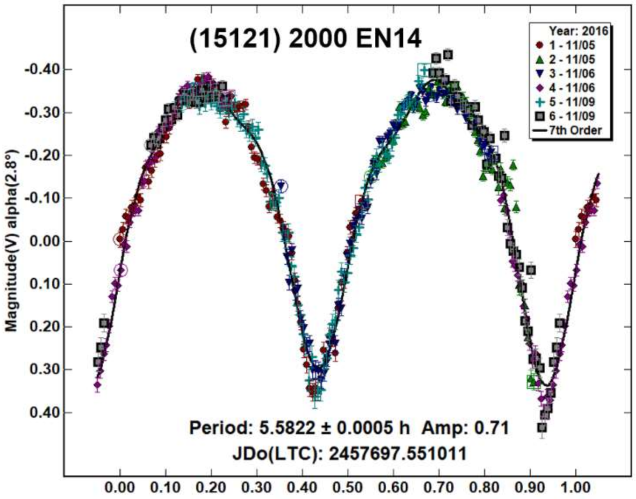

16452 Goldfinger was discovered in 1998 by Carolyn Shoemaker at the Palomar Observatory, CA. The asteroid was named after Pauline J. ("PJ") Goldfinger (1964-), an adaptive-optics operator at the observatory who helped to organize the glass plate archive of the observatory's famous Schmidt Oschin telescope. 16452 Goldfinger was observed using the CTIO-PROMPT6 telescope. Measurements were obtained for a total of approximately 14 hours using individual exposure times of 120 (on 2017 February 27) and 180 seconds (all other dates) and an open filter. The derived rotational period was *P* = 3.8836 ± 0.0004 h with an amplitude of *A* = 0.31 ± 0.014 mag. Dose (2021) published a similar result of *P* = 3.884 ± 0.001 h.

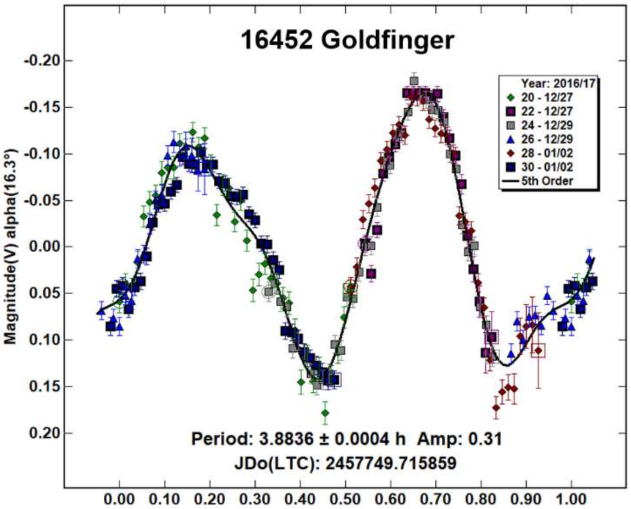

20557 Davidkulka was discovered in 1999 by LINEAR. The asteroid was named after David Kulka, a mentor at the 2004 Discovery Channel Young Scientist Challenge. 20557 Davidkulka was observed using both the CTIO-PROMPT1 and CTIO-PROMPT6 telescopes. Measurements were obtained for a total of approximately 16 hours using exposure times of (1) 35 seconds and a clear filter for CTIO-PROMPT1, and (2) 120 seconds and an open filter for CTIO-PROMPT6. The derived rotational period was $P = 5.8410 \pm 0.0005$ h with an amplitude of $A = 0.30 \pm 0.028$ mag. Durech et al. (2019) estimated a shorter period (by approximately 0.5 h or 9%) of 5.295743 ± 0.000002 h based on photometric data from the Lowell Observatory and the Gaia Data Release 2.

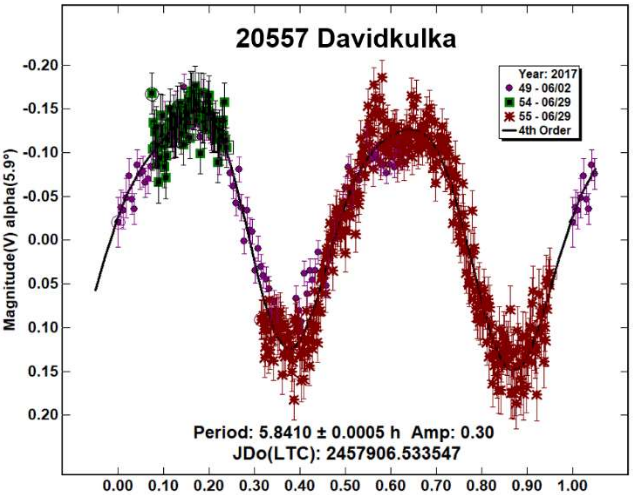

(29796) 1999 CW77 was discovered in 1999 by LINEAR. (29796) 1999 CW was observed using the Yerkes-41 telescope. Measurements were obtained for a total of approximately 16 hours using exposure times of 120 seconds and a clear filter. The derived rotational period was $P = 6.4707 \pm 0.0022$ h with an amplitude of $A = 0.19 \pm 0.013$ mag. A review of the literature found no previously published lightcurve results for (29796) 1999 CW.

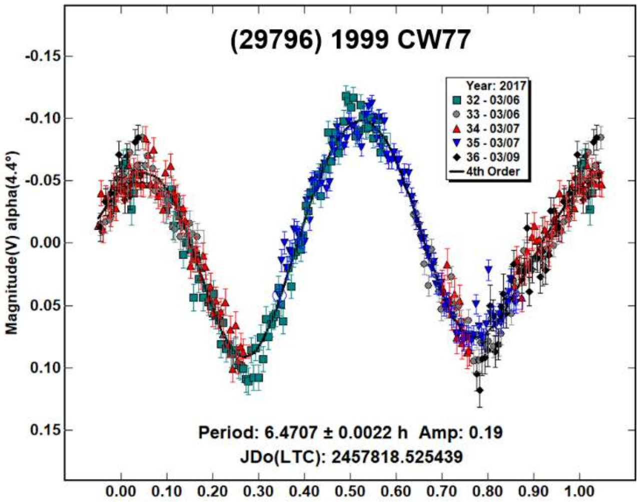

(35821) 1999 JW50 was discovered in 1999 by LINEAR. (35821) 1999 JW50 was observed using the CTIO-PROMPT6 telescope. Measurements were obtained for a total of approximately 14 hours using exposure times of 120 and 80 (3 December 2016) seconds and an open filter. The derived rotational period was $P = 4.9295 \pm 0.0005$ h with an amplitude of $A = 0.74 \pm 0.013$ mag. Waszczak (2015) published a similar result of $P = 4.931 \pm 0.1177$ h.

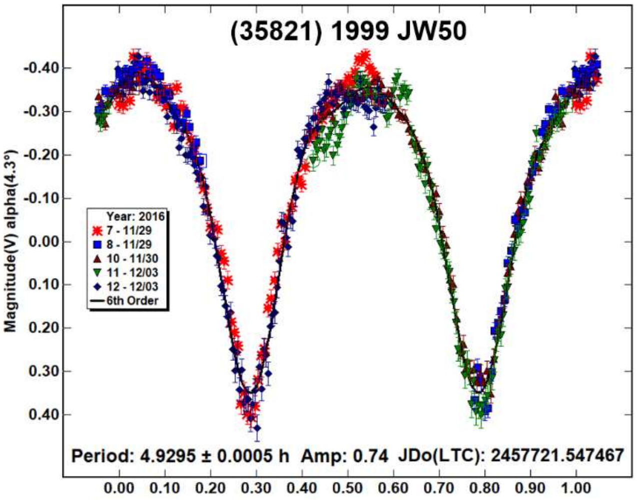

Acknowledgements

The first author would like to thank the University of North Dakota's Department of Space Studies, and particularly Paul Hardersen and Ron Fevig for their mentorship during the master's degree associated with this study. Special thanks also to Vivian Hoette, Kate Meredith, and Amanda Pagul for their tremendous support, encouragement, and use of the Yerkes Observatory. Finally, the first author would like to acknowledge the McQuown Trust for providing access to the Stone Edge Observatory.

Observatory	Code	Telescope	Aperture	Focal Ratio	Filter	CCD	Binning	Resolution	Image Scale
SEO	G52	RC	0.51 m	f/8.1	Clear	FLI CG230	2x2	1024x1024	1.50 arcsec/pixel
CTIO-PROMPT 1/3	807	DK	0.6 m	f/6.6	Clear	Alta F47	2x2	512x512	1.34 arcsec/pixel
CTIO-PROMPT 6	807	RC	0.41 m	f/17.3	Open	Aspen CG230	2x2	1024x1024	0.87 arcsec/pixel
Yerkes-41	754	Cass.	1.0 m	f/8.2	Clear	SBIG STL-1001E	1x1	1024x1024	0.61 arcsec/pixel

Table I. Facilities used to perform the observations presented in this paper. Resolution and image scale are provided according to the specified binning.

Number	a (AU)	i (°)	e	H	D (km)	p_V
3648	2.42	7.90	0.11	13.0	5.31	0.609
5235	2.30	4.85	0.14	12.7	7.39	0.301
9223	2.30	3.41	0.07	13.5	4.50	0.381
11699	2.40	5.08	0.08	13.1	6.71	0.227
12073	2.42	6.24	0.09	14.0	2.95	0.465
15121	2.35	3.57	0.16	15.0	3.55	0.169
16452	2.41	6.29	0.08	13.4	4.33	0.344
20557	2.38	6.27	0.10	14.1	3.95	0.179
29796	2.34	7.87	0.07	13.9	4.85	0.248
35821	2.48	5.95	0.13	14.3	N/A	N/A

Table II. Orbital parameters and physical properties for the target asteroids. Diameter (*D*) and visible albedo (p_V) values are from Masiero et al. (2011).

References

Carvano, J.M.; Hasselmann, P.H.; Lazzaro, D.; Mothe-Diniz, T. (2010). "SDSS-based taxonomic classification and orbital distribution of main belt asteroids." *Astronomy and Astrophysics* **510**, 1-12.

Dose, E. (2021). "Lightcurves of Fourteen Asteroids." *Minor Planet Bulletin* **48**, 228-233.

Durech, J.; Hanus, J.; Vanco, R. (2019). "Inversion of asteroid photometry from Gaia DR2 and the Lowell Observatory photometric database." *Astronomy and Astrophysics* **631** A2, 4pp.

Galdies, C. (2022). "Photometric Observations of Main-Belt Asteroids 2229 Mezzarco, 3648 Raffinetti and 3919 Maryanning." *Minor Planet Bulletin* **49**, 1-2.

Hardersen, P.S.; Reddy, V.; Roberts, R.; Mainzer, A. (2014). "More chips off of Asteroid (4) Vesta: Characterization of eight Vestoids and their HED meteorite analogs." *Icarus* **242**, 269-282.

Hardersen, P.S.; Reddy, V.; Roberts, R. (2015). "Vestoids, Part II: The basaltic nature and HED meteorite analogs for eight Vp-type asteroids and their associations with (4) Vesta." *Astrophys. J. Suppl. Ser.* **221**, 19.

Harris, A.W.; Young, J.W.; Scaltriti, F.; Zappala, V. (1984). "Lightcurves and phase relations of the asteroids 82 Alkmene and 444 Gyptis." *Icarus* **57**, 251-258.

Ivezić, Ž.; Jurić, M.; Lupton, R. (2010). "Sloan Digital Sky Survey (SDSS) Moving Object Catalog 4th Release." *EAR-A-I0035-3-SDSSMOC-V3.0.*

Masiero, J. and 17 colleagues (2011). "Main Belt Asteroids with WISE/NEOWISE. I. Preliminary Albedos and Diameters." *Astrophys. J.* **741**, 68.

Oszkiewicz, D.; Troianskyi, V.; Föhring, D. and 19 colleagues (2020). "Spin rates of V-type asteroids." *Astronomy and Astrophysics* **643**, A117.

Warner, B.D.; Harris, A.W.; Pravec, P. (2009). "The Asteroid Lightcurve Database." *Icarus* **202**, 134-146. Updated 2016 Sep. *http://www.minorplanet.info/lightcurvedatabase.html*

Warner, B.D. (2019). *MPO Canopus* Software, version 10.8.1.1. BDW Publishing. *http://www.bdwpublishing.com*

Waszczak, A.; Chang, C.-K.; Ofek, E.O.; Laher, R.; Masci, F.; Levitan, D.; Surace, J.; Cheng, Y.-C.; Ip, W.-H.; Kinoshita, D.; Helou, G.; Prince, T.A.; Kulkarni, S. (2015). "Asteroid Light Curves from the Palomar Transient Factory Survey: Rotation Periods and Phase Functions from Sparse Photometry," *The Astronomical Journal* **150**, Issue 3, article id. 75, 35pp.

Yeh, T.-S. Li, B.; Chang, C.-K.; Zhao, H.-B.; Ji, J.-H.; Lin, Z.-Y.; Ip, W.-H. (2020). "The Asteroid Rotation Period Survey Using the China Near-Earth Object Survey Telescope (CNEOST)." *Astronomical Journal* **160,** Issue 2, article id. 73, 18pp.

Number	Name	yyyy mm/dd	Phase	L_{PAB}	B_{PAB}	Period(h)	P.E.	Amp	A.E.	Grp
3648	Raffinetti	2017 4/3-4/6	2.9,1.6	198	-2	5.1757	0.0006	0.16	0.007	MB-M
5235	Jean-Loup	2017 3/30-4/2	6.9,5.6	200	-6	2.4523	0.0004	0.11	0.006	Flora
9223	Leifandersson	2016 11/29-12/22	2.1,12.7	63	-1	3.7583	0.0002	0.33	0.028	MB-M
11699	1998 FL105	2017 6/19-6/20	11.8,12.3	248	-5	4.0963	0.0008	0.58	0.042	Vesta
12073	Larimer	2017 4/27-4/28	5.9,5.4	227	+4	9.4892	0.0064	0.35	0.019	Vesta
15121	2000 EN14	2016 11/5-11/6	2.8,2.9	43	-4	5.5822	0.0005	0.71	0.020	MB-M
16452	Goldfinger	2016 12/27-2017 1/2	16.4,14.0	127	+5	3.8836	0.0004	0.31	0.014	Vesta
20557	Davidkulka	2017 6/2-6/29	6.0,13.1	256	+9	5.8410	0.0005	0.30	0.028	Vesta
29796	1999 CW77	2017 3/6-3/9	4.4,4.5	166	-7	6.4707	0.0022	0.19	0.013	MB-M
35821	1999 JW50	2016 11/29-12/03	4.2,5.5	64	-7	4.9295	0.0005	0.74	0.013	Vesta

Table III. Observing circumstances and results. The phase angle is given for the first and last date. If preceded by an asterisk, the phase angle reached an extrema during the period. L_{PAB} and B_{PAB} are the approximate phase angle bisector longitude/latitude at mid-date range (see Harris et al., 1984). Grp is the asteroid family/group (Warner et al., 2009).

LIGHTCURVE ANALYSIS OF HILDA ASTEROIDS AT THE CENTER FOR SOLAR SYSTEM STUDIES: 2021 SEPTEMBER-DECEMBER

Brian D. Warner
Center for Solar System Studies (CS3)
446 Sycamore Ave.
Eaton, CO 80615 USA
brian@MinorPlanetObserver.com

Robert D. Stephens
Center for Solar System Studies (CS3)
Rancho Cucamonga, CA

(Received: 2022 January 12)

CCD photometric observations of five Hilda asteroids made between 2021 September-December. Data analysis found that four were in simple principal axis rotation, i.e., a single rotation period could be found. On the other hand, revised analysis of data obtained in 2018 for 1748 Mauderli showed potential signs of a satellite.

CCD photometric observations of five Hilda asteroid were carried out at the Center for Solar System Studies (CS3) from 2021 September through December as part of an ongoing study of the family/group that is located between the outer main-belt and Jupiter Trojans in a 3:2 orbital resonance with Jupiter. The goal is to determine the spin rate statistics of the Hildas and to find pole and shape models when possible. We also look to examine the degree of influence that the YORP (Yarkovsky-O'Keefe-Radzievskii-Paddack) effect (Rubincam, 2000) has on distant objects and to compare the spin rate distribution against the Jupiter Trojans, which can provide evidence that the Hildas are more "comet-like" than main-belt asteroids.

Telescopes	Cameras
0.30-m *f*/6.3 Schmidt-Cass	FLI Microline 1001E
0.35-m *f*/9.1 Schmidt-Cass	FLI Proline 1001E
0.35-m *f*/11 Schmidt-Cass	SBIG STL-1001E
0.40-m f/10 Schmidt-Cass	
0.50-m *f*/8.1 Ritchey-Chrétien	

Table I. List of available telescopes and CCD cameras at CS3. The exact combination for each telescope/camera pair can vary due to maintenance or specific needs.

Table I lists the telescopes and CCD cameras that are combined to make observations. Up to nine telescopes are commonly used for observations. All the cameras use CCD chips from the KAF blue-enhanced family and so have essentially the same response. The pixel scales ranged from 1.24-1.60 arcsec/pixel. All lightcurve observations were unfiltered since a clear filter can result in a 0.1-0.3 magnitude loss. The exposures varied depending on the asteroid's brightness.

To reduce the number of times and amounts of adjusting nightly zero-points, the ATLAS catalog r´ (SR) magnitudes (Tonry et al., 2018) are used. Those adjustments are usually ≤ ±0.03 mag. The rare greater corrections may have been related in part to using unfiltered observations, poor centroiding of the reference stars, and not correcting for second-order extinction. Another cause may be selecting what appears to be a single star but is actually an unresolved pair.

The Y-axis values are ATLAS SR "sky" (catalog) magnitudes. The two values in the parentheses are the phase angle (a) and the value of *G* used to normalize the data to the comparison stars used in the earliest session. This, in effect, made all the observations seem to be made at a single fixed date/time and phase angle, leaving any variations due only to the asteroid's rotation and/or albedo changes. The X-axis shows rotational phase from -0.05 to 1.05. If the plot includes the amplitude, e.g., "Amp: 0.65", this is the amplitude of the Fourier model curve and *not necessarily the adopted amplitude for the lightcurve*.

For brevity, only some of the previous results are referenced. A more complete listing is in the asteroid lightcurve database (Warner et al., 2009; "LCDB" from here on).

1162 Larissa. There are several previously reported periods in the LCDB for Larissa, including Warner and Stephens (2021; 6.53 h). All previous results had very similar periods, save Dahlgren et al. (1998), who found a period of 13.0 h.

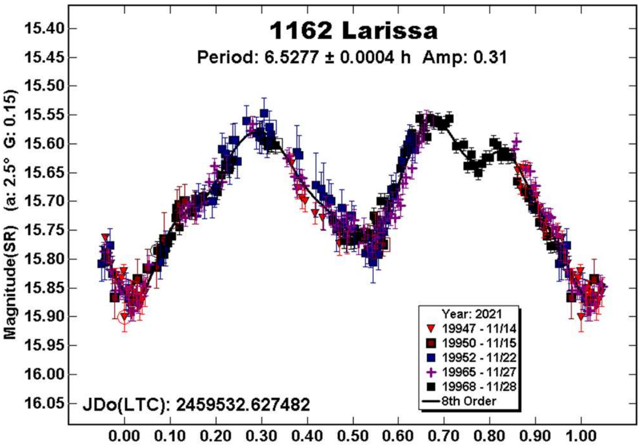

1180 Rita. Dahlgren et al. (1998) found a period of 14.902 h. In a previous paper (Warner and Stephens, 2017a), a period of 13.090 h was found, but subsequent review of those results revised the period to 14.928 h using data from 2017 and 14.849 h using data from 2018 (Warner and Stephens, 2018). The most recent CS3 result is consistent with Dahlgren et al. (1998) and the revised periods.

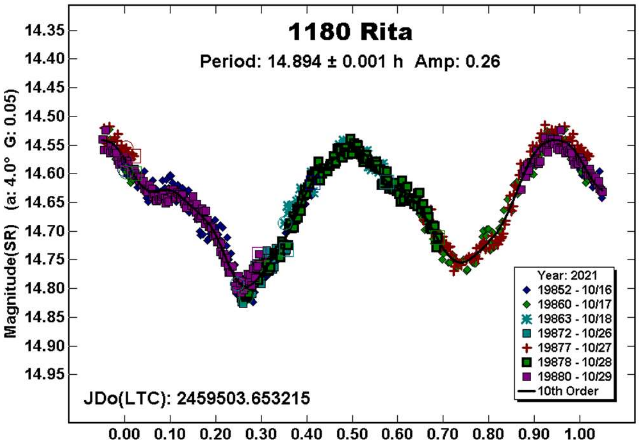

1748 Mauderli. Dahlgren et al. (1998) found a period of 6.00 h. Data obtained at CS3 in 2017 found a shorter period of 5.552 h (Warner and Stephens, 2017b). When observed again in 2018 (Warner and Stephens, 2018), a period of 5.320 h was found and the 2017 result was reconfirmed to within 0.001 h. Both appear to be wrong.

Romanishin has observed Mauderli several times, the most recent being in 2020 (Romanishin, 2021). Using data from four apparitions, he was able to establish that the true period was close to 6.00 h and a period near 5.55 h was implausible. He also reported signs of a second period in his 2018 data but its origin was not established. Based on the Romanishin (2021) results, the period search using the 2021 CS3 data was confined to near 6 h. The result of 5.994 h is in good agreement with Romanishin (2021).

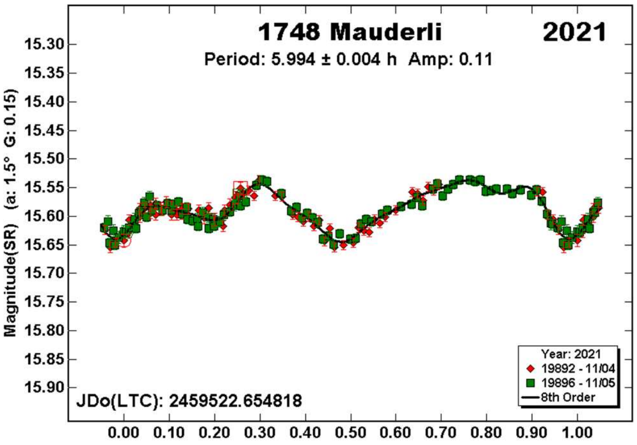

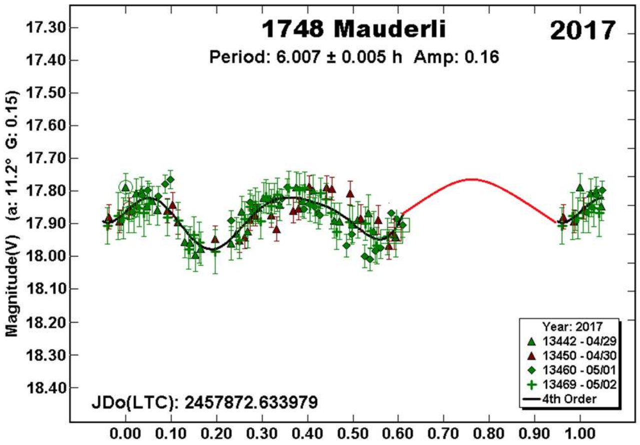

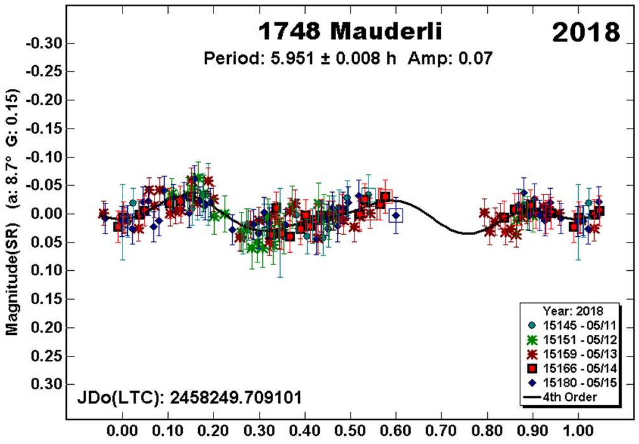

The data from 2017 and 2018 were analyzed anew, but forcing a period solution near 6 h. The gap in the 2017 data sent the Fourier curve soaring to unrealistic heights. The red line in that plot is an attempt to complete the curve.

A suspicious secondary period was found in the 2018 data set. The period was 37.9 h but the coverage is too sparse to consider it a valid solution. The best that can be said is that after two possible sightings (2014 and 2018), future observers should be aware of the possibility of a satellite, or at least a second period, and obtain high-quality data.

1877 Marsden. Dahlgren et al. (1998) found a period of 14.4 h. In 2018 (Warner and Stephens, 2018), a period of 13.18 h was found, which *seemed* at the time to be more likely correct. Pal et al. (2020) used dense TESS lightcurve data to find 14.4319 h. The analysis of the most recent CS3 data set yields a similar period of 14.412 h. Attempts to force the 2018 data to a period near 14.4 h and the 2021 data to a period near 13.18 h were fruitless.

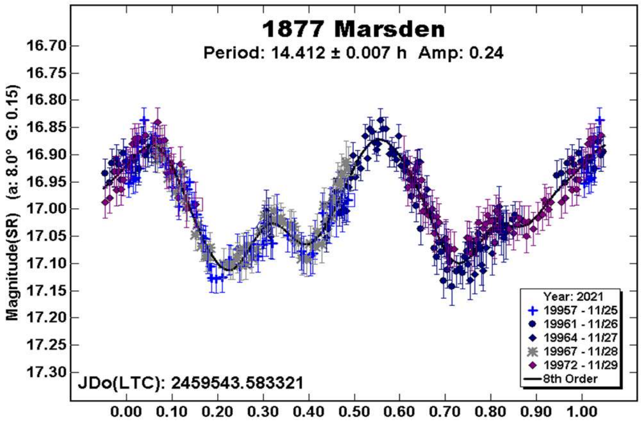

8086 Peterthomas. The results from the latest data set yield a period that is highly consistent with previous results in the LCDB.

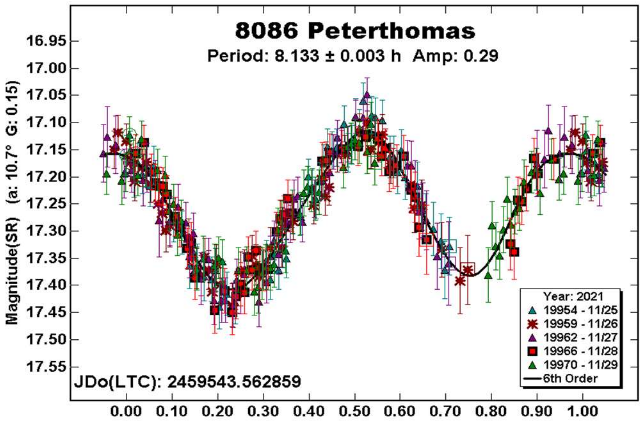

Acknowledgements

This work includes data from the Asteroid Terrestrial-impact Last Alert System (ATLAS) project. ATLAS is primarily funded to search for near earth asteroids through NASA grants NN12AR55G, 80NSSC18K0284, and 80NSSC18K1575; byproducts of the NEO search include images and catalogs from the survey area. The ATLAS science products have been made possible through the contributions of the University of Hawaii Institute for Astronomy, the Queen's University Belfast, the Space Telescope Science Institute, and the South African Astronomical Observatory. The authors gratefully acknowledge Shoemaker NEO Grants from the Planetary Society (2007, 2013). These were used to purchase some of the telescopes and CCD cameras used in this research.

Number	Name	2021/mm/dd	Phase	L_{PAB}	B_{PAB}	Period(h)	P.E.	Amp	A.E.
1162	Larissa	11/14-11/28	2.6,6.0	60	1	6.5277	0.0004	0.31	0.02
1180	Rita	10/16-10/29	4.0,7.1	12	-8	14.894	0.001	0.25	0.02
1748	Mauderli	2021/11/04-11/05	1.5,1.3	44	-4	5.994	0.004	0.11	0.01
		2017/04/29-05/02	11.2,11.4	159	2	^{R}6.007	0.005	0.16	0.02
		2018/05/11-05/15	8.7,9.5	194	4	^{R}5.951	0.008	0.07	0.01
1877	Marsden	11/25-11/29	8.0,8.7	37	15	14.412	0.007	0.24	0.02
8086	Peterthomas	11/25-11/29	10.8,11.6	26	1	8.133	0.003	0.29	0.02

Table II. Observing circumstances. ^{R}Revised period. The phase angle (α) is given at the start and end of each date range. L_{PAB} and B_{PAB} are the average phase angle bisector longitude and latitude (see Harris *et al.*, 1984).

References

Dahlgren, M.; Lahulla, J.F.; Lagerkvist, C.-I.; Lagerros, J.; Mottola, S.; Erikson, A.; Gonano-Beurer, M.; Di Martino, M. (1998). “A Study of Hilda Asteroids. V. Lightcurves of 47 Hilda Asteroids.” *Icarus* **133**, 247-285.

Harris, A.W.; Young, J.W.; Scaltriti, F.; Zappala, V. (1984). “Lightcurves and phase relations of the asteroids 82 Alkmene and 444 Gyptis.” *Icarus* **57**, 251-258.

Pal, A.; Szakats, R.; Kiss, C.; Bodi, A.; Bognar, Z.; Kalup, C.; Kiss, L.L.; Marton, G.; Molnar, L.; Plachy, E.; Sárneczky, K.; Szabo, G.M.; Szabo, R. (2020). “Solar System Objects Observed with TESS - First Data Release: Bright Main-belt and Trojan Asteroids from the Southern Survey.” *Ap. J. Supl. Ser.* **247**, id.26.

Romanashin, W. (2021). “Lightcurves of Three Hildas.” *Minor Planet Bull*. **48**, 15-16.

Rubincam, D.P. (2000). “Relative Spin-up and Spin-down of Small Asteroids.” *Icarus* **148**, 2-11.

Tonry, J.L.; Denneau, L.; Flewelling, H.; Heinze, A.N.; Onken, C.A.; Smartt, S.J.; Stalder, B.; Weiland, H.J.; Wolf, C. (2018). “The ATLAS All-Sky Stellar Reference Catalog.” *Astrophys. J.* **867**, A105.

Warner, B.D.; Harris, A.W.; Pravec, P. (2009). “The Asteroid Lightcurve Database.” *Icarus* **202**, 134-146. Updated 2021 June. *http://www.minorplanet.info/lightcurvedatabase.html*

Warner, B.D.; Stephens, R.D. (2017a). “Lightcurve Analysis of Hilda Asteroids at the Center for Solar System Studies: 2016 December thru 2017 April.” *Minor Planet Bull*. **44**, 220-222.

Warner, B.D.; Stephens, R.D. (2017b). “Lightcurve Analysis of Hilda Asteroids at the Center for Solar System Studies: 2017 April thru July.” *Minor Planet Bull*. **44**, 331-334.

Warner, B.D.; Stephens, R.D. (2018). “Lightcurve Analysis of Hilda Asteroids at the Center for Solar System Studies: 2018 April-June.” *Minor Planet Bull*. **45**, 390-393.

Warner, B.D.; Stephens, R.D. (2021). “Lightcurve Analysis of Hilda Asteroids at The Center for Solar System Studies: 2020 August - September.” *Minor Planet Bull*. **48**, 17-19.

LIGHTCURVE ANALYSIS FOR TWO MAIN BELT ASTEROIDS

Giovanni Battista Casalnuovo
Filzi School Observatory D12
Laives, ITALY
gb.minorplanet@gmail.com

(Received: 2022 January 9)

Photometric observations of two main-belt asteroids, (7637) 1984 DN and (49483) 1999 BP13, were made at the Filzi School Observatory (School in country Laives - Italy) MPC code D12.

CCD photometric observations, were made at the Filzi School Observatory, all are without filter (clear). All images were obtained with a 0.35m reflector telescope reduced to *f*/8.0, a QHY9 CCD camera, and then calibrated with dark and flat-field frames. The pixel scale was 1.56 arcsec when binned at 4×4 pixels. All exposures were 120 seconds. The computer clock was synchronized with an Internet time server before each session. Differential photometry and period analysis were done using *MPO Canopus* version 10.7.12.9 (Warner, 2018). Solar type stars from CMC15 catalog in R band were used as comparison stars.

(7637) 1984 DN. This main-belt asteroid was reported as a lightcurve photometry opportunity for 2021 March on the MinorPlanet.info web site (*http://www.minorplanet.info/lightcurvedatabase.html*; hereafter referenced as MPI). It was discovered in the year 1984 by H. Debehogne at La Silla. It is a main-belt asteroid with a semi-major axis of 2.55 AU, eccentricity 0.21, inclination 7.50 deg, and orbital period of 4.09 yr. Its absolute magnitude is H= 13.49 It was studied for four nights. The derived synodic period was P = 7.332 ± 0.001 h with an amplitude of A = 0.62 ± 0.05 mag. There were no entries in the LCDB (Warner et al., 2009) for this asteroid.

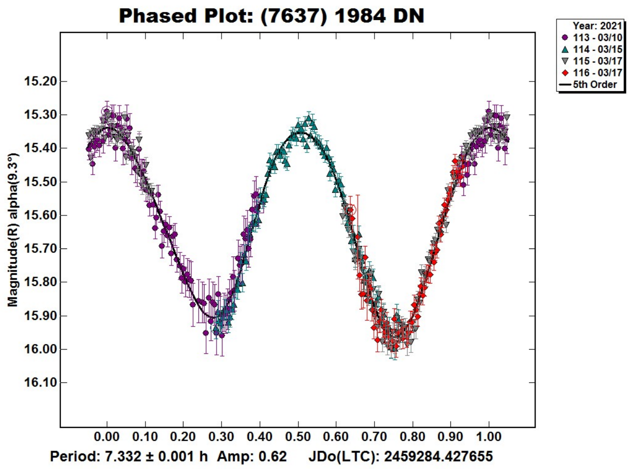

(49483) 1999 BP13. This main-belt asteroid was also reported as a lightcurve photometry opportunity for 2021 February on the MPI. It was discovered in the year 1999 by K. Korlevic at Visnjan. It is a main belt asteroid, with a semi-major axis of 2.69 AU, eccentricity 0.23, inclination 6.63 deg, and orbital period of 4.41 yr. Its absolute magnitude is H= 13.17. It was studied for seven nights; the derived synodic period was P = 6.362 ± 0.002 h with an amplitude of A = 0.25 ± 0.08 mag. Marchini et al. (2021). reported a period of 6.365 h., which is in very close agreement with the result given here.

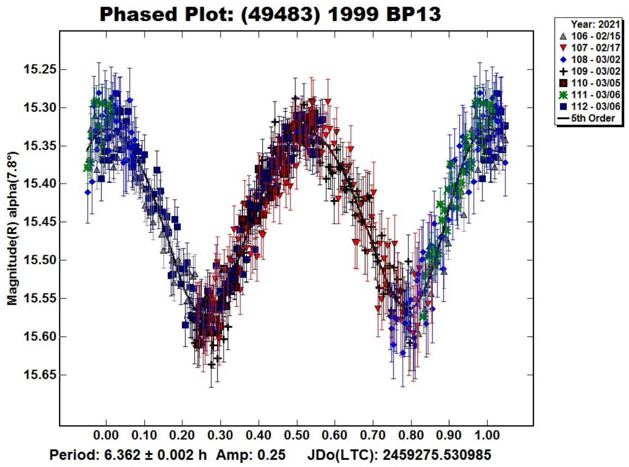

References

Harris, A.W.; Young, J.W.; Scaltriti, F.; Zappala, V. (1984). "Lightcurves and phase relations of the asteroids 82 Alkmene and 444 Gyptis." *Icarus* **57**, 251-258.

Marchini, A.; Cavaglioni, L.; Privitera, C.A.; Papini, R.; Salvaggio, F. (2021) "Rotation Period Determination for Asteroids 2243 Lonnrot, (10859) 1995 GJ7, (18640) 1998 EF9 and (49483) 1999 BP13." *Minor Planet Bulletin* **48**, 206-208.

Warner, B.D.; Harris, A.W.; Pravec, P. (2009). "The Asteroid Lightcurve Database." *Icarus* **202**, 134-146. Updated 2018 June. *http://www.minorplanet.info/lightcurvedatabase.html*

Warner, B.D. (2018). MPO Software. MPO Canopus version 10.7.12.9. *Bdw Publishing. http://minorplanetobserver.com*

Number	Name	yyyy mm/dd	Phase		L_{PAB}	B_{PAB}	Period(h)	P.E.	Amp	A.E.	Grp
7637	1984 DN	2021 03/10-03/17	9.7	6.3	184.3	5.3	7.332	0.001	0.62	0.05	MB
49483	1999 BP13	2021 02/15-03/06	8.3	2.2	161.0	-0.1	6.362	0.002	0.42	0.08	MB

Table I. Observing circumstances and results. The phase angle is given for the first and last date. If preceded by an asterisk, the phase angle reached an extrema during the period. L_{PAB} and B_{PAB} are the approximate phase angle bisector longitude/latitude at mid-date range (see Harris et al., 1984). Grp is the asteroid family/group (Warner et al., 2009).

PHOTOMETRY AND LIGHTCURVE ANALYSIS OF 1774 KULIKOV, 7145 LINZEXU, 11099 SONODAMASAKI AND (16024) 1999 CT101

Michael Fauerbach
Florida Gulf Coast University
and SARA Observatories
10501 FGCU Blvd.
Ft. Myers, FL33965-6565
mfauerba@fgcu.edu

Matthew Fauerbach
NYU
Tandon School of Engineering
6 MetroTech Center
Brooklyn, NY 11201

(Received: 2022 January 7)

Photometric observations of four main belt asteroids were obtained on four nights 2021 August 9 to 2021 October 6. The following rotational periods were determined: 1774 Kulikov, 3.831 ± 0.001 h; 7145 Linzexu, 2.905 ± 0.004 h; 11099 Sonodamasaki, 7.247 ± 0.001 h and (16024) 1999 CT101, 2.791 ± 0.001 h.

We report on photometric observations obtained with the 0.6m telescope of the Southeastern Association for Research in Astronomy (SARA) consortium at Cerro Tololo Inter-American Observatory. The telescope is coupled with an Andor iKon-L series CCD. A detailed description of the instrumentation and setup can be found in the paper by Keel et al. (2017). The data was calibrated using *MaximDL* and photometric analysis was performed using *MPO Canopus* (Warner, 2017). All four asteroids were observed by FGCU's Asteroid Research Group previously and are shape modelling targets of our group.

1774 Kulikov is a member of the Koronis family. The asteroid was observed on two nights, roughly three weeks apart. The derived rotational period of 3.831 ± 0.001 h with an amplitude of 0.35 mag is in good agreement with the result previously obtained by our group (Fauerbach and Nelson, 2019, 3.832 h; Fauerbach, 2019b, 3.823 h) and the result reported by Ďurech et al. (2016, 3.830791 h).

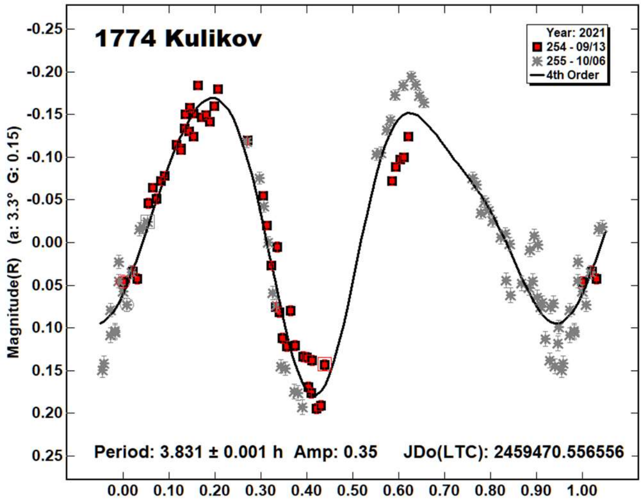

7145 Linzexu is an inner main-belt asteroid. Our analysis yields a rotational period of 2.905 ± 0.004 h with an amplitude of 0.10 mag. This is not in agreement with Pál et al. (2020, 13.7126 h) derived from TESS data, but in excellent agreement with previous publications by Ditteon and West (2011, 2.905 h) as well as our previous results (Fauerbach and Fauerbach, 2019, 2.905 h).

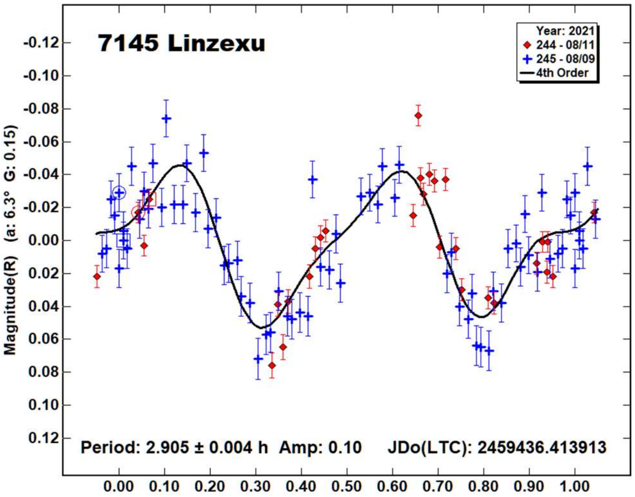

11099 Sonodamasaki is a member of the Klio family. The asteroid was observed on two nights, roughly three weeks apart. Our analysis yields a rotational period of 7.247 ± 0.001 h with an amplitude of 0.35 mag. This is in good agreement with previous measurements by Behrend et al. (2021web, 7.238 h), Ďurech et al. (2018, 7.24714 h), Waszczak et al. (2015, 7.248 h) as well as our previous result (Fauerbach, 2019a, 7.251 h).

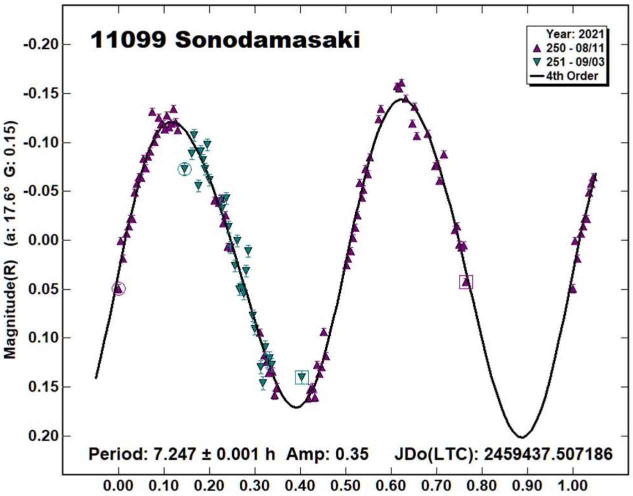

(16024) 1999 CT101 is a member of the Maria family. We observed (16024) 1999 CT101 for three nights over the period of a month. Our analysis yields a rotational period of 2.791 ± 0.001 h with an amplitude of 0.19 mag. This is in good agreement with the result by Waszczak et al. (2015, 2.804 h) as well as our previous result (Fauerbach and Brown, 2019, 2.786 h).

Number	Name	yyyy mm/dd	Phase	L_{PAB}	B_{PAB}	Period(h)	P.E.	Amp	A.E.
1774	Kulikov	2021 09/13,10/06	3.3,11.8	343	0.3	3.831	0.001	0.35	0.03
7145	Linzexu	2021 08/09,08/11	5.6,6.3	308	8.8	2.905	0.004	0.10	0.02
11099	Sonodamasaki	2021 08/11,09/03	17.6,25.2	301	-14.3	7.247	0.001	0.35	0.03
16024	1999 CT101	2021 09/03,10/06	5.7,12.4	348	-5.7	2.791	0.001	0.19	0.02

Table I. Observing circumstances and results. The phase angle is given for the first and last date. If preceded by an asterisk, the phase angle reached an extrema during the period. L_{PAB} and B_{PAB} are the approximate phase angle bisector longitude/latitude at mid-date range (see Harris et al., 1984).

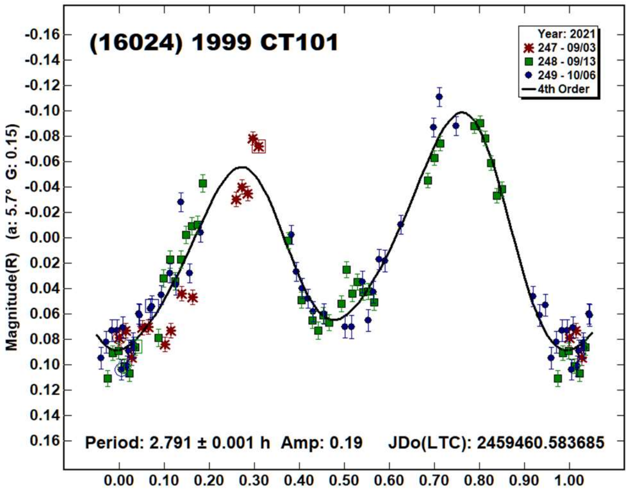

References

Behrend, R. (2021web). Observatoire de Geneve web site. *http://obswww.unige.ch/~behrend/page_cou.html*

Ditteon, R.; West, J. (2011) "Asteroid Lightcurve Analysis at the Oakley Southern Observatory: 2011 January thru April." *Minor Planet Bulletin* **38**, 214-217.

Ďurech, J.; Hanuš, J.; Oszkiewicz, D.; Vančo, R. (2016). "Asteroid models from the Lowell photometric database." *Astronomy & Astrophysics* **587**, A48.

Ďurech, J.; Hanuš, J.; Alí-Lagoa, V. (2018). "Asteroid models reconstructed from the Lowell Photometric Database and WISE data." *Astronomy & Astrophysics* **617**, A57.

Fauerbach, M. (2019a). "Photometric Observations for 8 Main-belt Asteroids: 2017 April - May." *Minor Planet Bulletin* **46**, 15-19.

Fauerbach, M. (2019b). "Photometric Observations for 7 Main-belt Asteroids: 2019 February - May." *Minor Planet Bulletin* **46**, 418-421.

Fauerbach, M.; Brown, A. (2019). "Rotational Period Determination for Asteroids 2498 Tsesevich, (16024) 1999 CT101, (46304) 2001 OZ62." *Minor Planet Bulletin* **46**, 19-20.

Fauerbach, M.; Fauerbach, M. (2019). "Lightcurve Analysis of Asteroids 131 Vala, 1184 Gaea, 7145 Linzexu and 26355 Grueber." *Minor Planet Bulletin* **46**, 236-237.

Fauerbach, M.; Nelson, K.M. (2019). "Photometric Observations of 1007 Pawlowia, 1774 Kulikov, 2764 Moeller, 5110 Belgirate, (8505) 1990 YK, and (34459) 2000 SC91." *Minor Planet Bulletin* **46**, 21-23.

Harris, A.W.; Young, J.W.; Scaltriti, F.; Zappala, V. (1984). "Lightcurves and phase relations of the asteroids 82 Alkmene and 444 Gyptis." *Icarus* **57**, 251-258.

Keel, W.C.; Oswalt, T.; Mack, P.; Henson, G.; Hillwig, T.; Batcheldor, D.; Berrington, R.; De Pree, C.; Hartmann, D.; Leake, M.; Licandro, J.; Murphy, B.; Webb, J.; Wood, M.A. (2017). "The Remote Observatories of the Southeastern Association for Research in Astronomy (SARA)." *PASP* **129**:015002 (12pp). *http://iopscience.iop.org/article/10.1088/1538-3873/129/971/015002/pdf*

Pál, A.; Szakáts, R.; Kiss, C.; Bódi, A.; Bognár, Z.; Kalup, C.; Kiss, L.L.; Marton, G.; Molnár, L.; Plachy, E.; Sárneczky, K.; Szabó, G. M.; Szabó, R. (2020). "Solar System Objects Observed with TESS - First Data Release: Bright Main-belt and Trojan Asteroids from the Southern Survey," *The Astrophysical Journal Supplement Series*, **247**:26 (9pp).

Warner, B.D. (2017). MPO Canopus software version 10.7.10.0. *http://www.bdwpublishing.com*

Waszczak, A.; Chang, C.-K.; Ofek, E.O.; Laher, R.; Masci, F.; Levitan, D.; Surace, J.; Cheng, Y.-C.; Ip, W.-H.; Kinoshita, D.; Helou, G.; Prince, T.A.; Kulkarni, S. (2015). "Asteroid Light Curves from the Palomar Transient Factory Survey: Rotation Periods and Phase Functions from Sparse Photometry," *The Astronomical Journal* **150**, Issue 3, article id. 75, 35pp.

MAIN-BELT ASTEROIDS OBSERVED FROM CS3: 2021 SEPTEMBER – 2022 JANUARY

Robert D. Stephens
Center for Solar System Studies (CS3)
11355 Mount Johnson Ct., Rancho Cucamonga, CA 91737 USA
rstephens@foxandstephens.com

Brian D. Warner
Center for Solar System Studies (CS3)
Eaton, CO

(Received: 2022 January 12)

CCD photometric observations of five main-belt asteroids were obtained at the Center for Solar System Studies (CS3) from 2021 September to 2022 January.

The Center for Solar System Studies (CS3) has nine telescopes which are normally used in program asteroid family studies. The focus is on near-Earth asteroids, Jovian Trojans and Hildas. When a nearly full moon is too close to the family targets being studied, targets of opportunity amongst the main-belt families were selected.

Table I lists the telescopes and CCD cameras that were used to make the observations. Images were unbinned with no filter and had master flats and darks applied. The exposures depended upon various factors including magnitude of the target, sky motion, and Moon illumination.

Telescope	Camera
0.30-m f/6.3 Schmidt-Cass	SBIG 1001E
0.35-m f/9.1 Schmidt-Cass	FLI Microline 1001E
0.35-m f/9.1 Schmidt-Cass	FLI Microline 1001E
0.35-m f/9.1 Schmidt-Cass	FLI Microline 1001E
0.40-m f/10 Schmidt-Cass	FLI Proline 1001E
0.40-m f/10 Schmidt-Cass	FLI Proline 1001E
0.50-m F8.1 R-C	FLI Proline 1001E

Table I: List of CS3 telescope/CCD camera combinations.

Image processing, measurement, and period analysis were done using *MPO Canopus* (Bdw Publishing), which incorporates the Fourier analysis algorithm (FALC) developed by Harris (Harris et al., 1989). The Comp Star Selector feature in *MPO Canopus* was used to limit the comparison stars to near solar color. Night-to-night calibration was done using field stars from the ATLAS catalog (Tonry et al., 2018), which has Sloan *griz* magnitudes that were derived from the GAIA and Pan-STARR catalogs and are "native" magnitudes of the catalog. Those adjustments are usually ≤ ±0.03 mag. The rare greater corrections may have been related in part to using unfiltered observations, poor centroiding of the reference stars, and not correcting for second-order extinction.

The Y-axis values are ATLAS SR "sky" magnitudes. The two values in the parentheses are the phase angle (a) and the value of *G* used to normalize the data to the comparison stars used in the earliest session. This, in effect, made all the observations seem to be made at a single fixed date/time and phase angle, leaving any variations due only to the asteroid's rotation and/or albedo changes. The X-axis shows rotational phase from -0.05 to 1.05. If the plot includes the amplitude, e.g., "Amp: 0.65", this is the amplitude of the Fourier model curve and *not necessarily the adopted amplitude for the lightcurve*.

For brevity, only some of the previously reported rotational periods may be referenced. A complete list is available at the asteroid lightcurve database (LCDB; Warner et al., 2009).

22 Kalliope. At the request of Josef Hanus (private communications) observations of this outer main-belt asteroid were made at CS3. It is a known binary. The times of observations were meant to observe mutual events between the two bodies.

On the first night, 2021 Nov 26, an attenuation seemed to be recorded and was near the predicted time. However, the attenuation was too shallow and too short to fit predictions based on accurate modeling. The cause for the attenuation was attributed to an artifact during star subtraction as the asteroid passed a star three magnitudes fainter. The Fates could not have been much less kind.

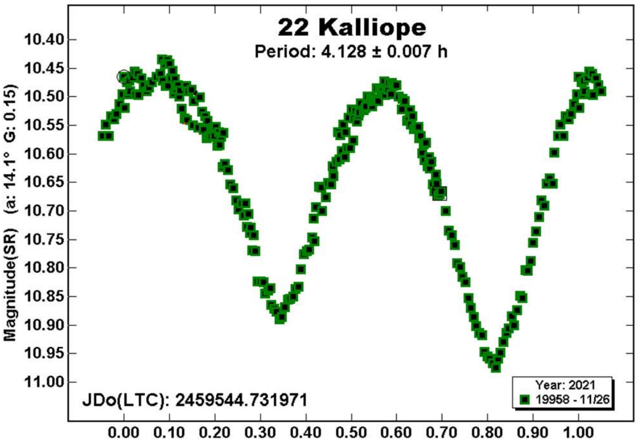

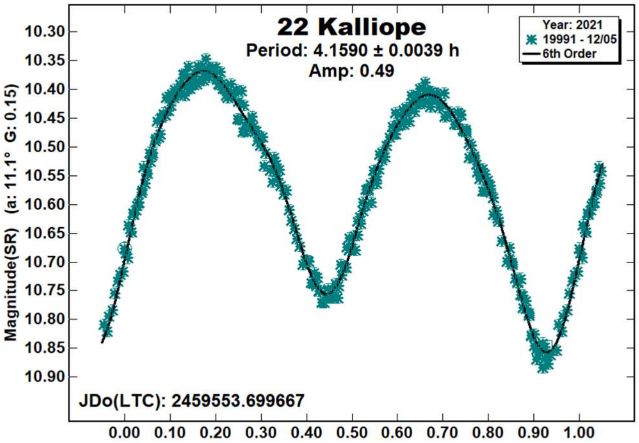

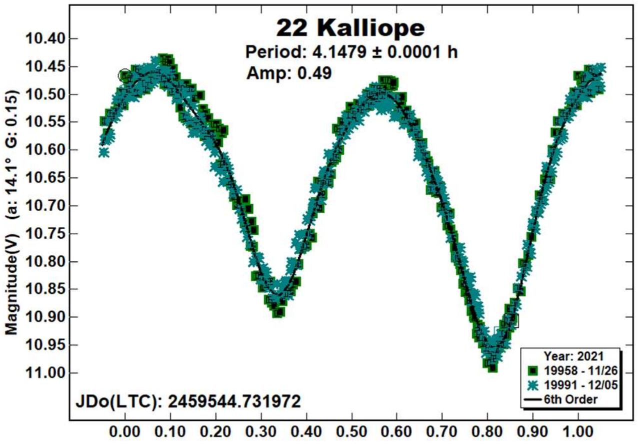

Follow-up observations on 2021 Dec 5 showed no attenuations, but the observations were made outside any predicted events so nothing unusual was expected.

Combining the two sets allowed finding a more accurate and precise synodic rotation period of 4.1479 h. This fits well with the many previous results found in the LCDB.

6249 Jennifer. This member of the Hungaria dynamical group has been observed many times in the past (Warner 2015 and references therein), each time reporting a period near 4.96 h. The results found this year are in good agreement.

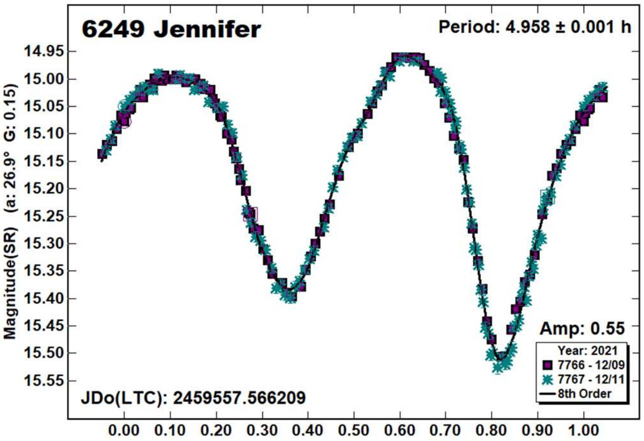

(12198) 1980 PJ1. The estimated diameter of this Mars-crosser (family 9103 in the LCDB) is 3 km. Carreño et al. (2019) reported a period 5.494 h. There were no other periods listed in the LCDB. The results using the 2021 data obtained at CS3 are in good agreement with Carreño et al. (2019).

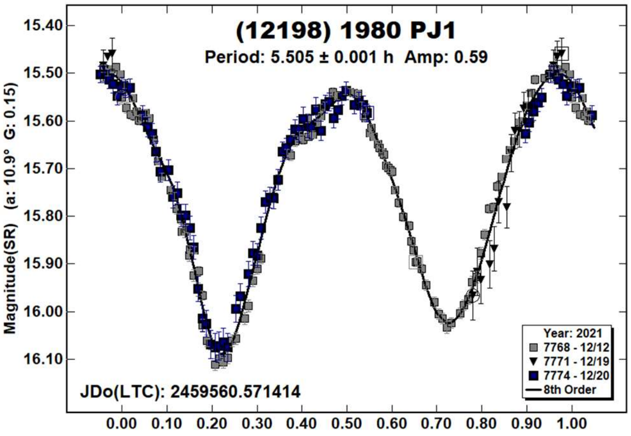

45687 Pranverahyseni. Observations were made at the request of its namesake, Pranvera Hyseni, a student at the University of Santa Cruz, who founded the organization *Astronomy Outreach of Kosovo* and is a leading advocate of amateur astronomy in her native country. The lightcurve was used to link a point in the curve to any changes in the asteroid's spectrum during rotation.

There were no previous results for a period in the LCDB. Masiero et al. (2021) used WISE data to find an estimated D = 13.14 km. Using H = 15.84 gave p_V = 0.039. This was a difficult target, being about SR = 18.55 mag. Fortunately, the amplitude was large enough to overcome the noise and, based the modest phase angle and amplitude, a bimodal solution was very likely (Harris et al., 2014).

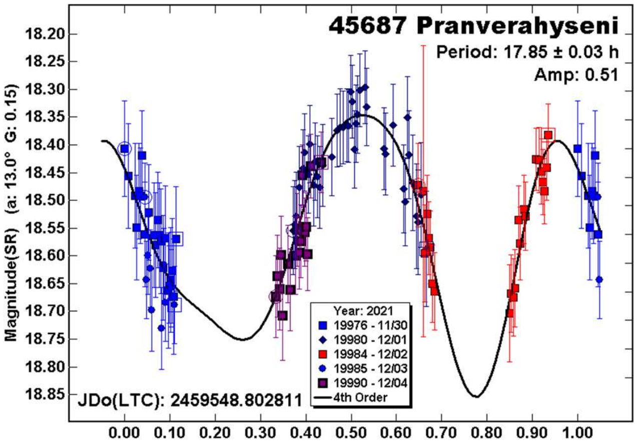

(52800) 1998 QT60. There were no previously-reported rotation periods in the LCDB for this Mars-crosser. With large gaps between successive sessions, it was fully expected that there would be numerous potential periods due to rotational aliasing, which is when the actual number of rotations over the total span of the data set is not known.

Different solutions presented themselves depending on the number of orders in the Fourier analysis. Using 4th and 6th orders found similar results for a somewhat symmetrical bimodal lightcurve. The true period may be tens of hours from what's reported here. At the least, it's been established that the asteroid is tumbling and so is a place with continuously restless days and nights.

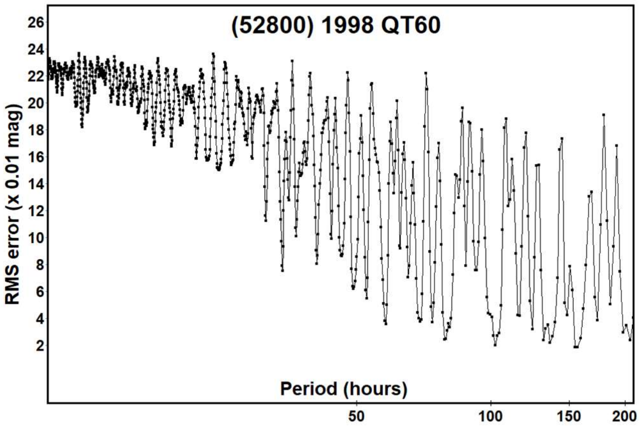

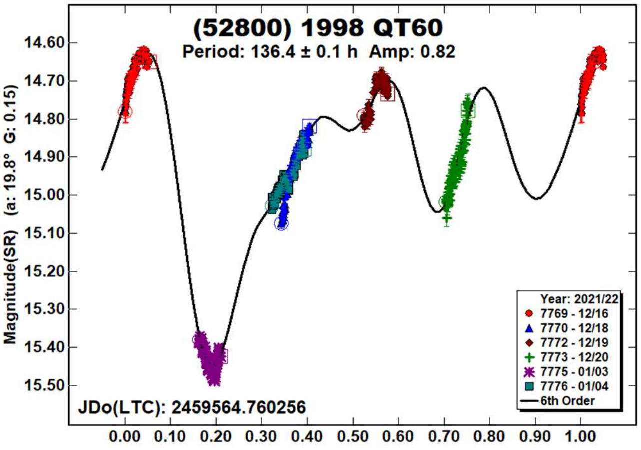

Number	Name	2021/mm/dd	Phase	L_{PAB}	B_{PAB}	Period(h)	P.E.	Amp	A.E.
22	Kalliope	11/26-12/05	14.1,11.1	97	7	4.1479	0.0001	0.49	0.03
6249	Jennifer	12/31-12/31	*20.3,19.7	0	0	4.958	0.001	0.55	0.02
12198	1980 PJ1	12/12-12/20	10.9,15.7	68	3	5.505	0.001	0.59	0.01
45687	Pranverahyseni	11/30-12/04	13.0,12.1	101	-19	17.85	0.03	0.51	0.05
52800	1998 QT60	12/16-01/04	19.9,7.5	106	12	^{T}136.4	0.1	0.82	0.03

Table II. Observing circumstances and results. ^{T}Dominant period for a tumbling asteroid. The phase angle is given for the first and last date. If preceded by an asterisk, the phase angle reached an extremum during the period. L_{PAB} and B_{PAB} are the approximate phase angle bisector longitude/latitude at mid-date range (see Harris et al., 1984).

Acknowledgements

This work includes data from the Asteroid Terrestrial-impact Last Alert System (ATLAS) project. ATLAS is primarily funded to search for near earth asteroids through NASA grants NN12AR55G, 80NSSC18K0284, and 80NSSC18K1575; byproducts of the NEO search include images and catalogs from the survey area. The ATLAS science products have been made possible through the contributions of the University of Hawaii Institute for Astronomy, the Queen's University Belfast, the Space Telescope Science Institute, and the South African Astronomical Observatory. The authors gratefully acknowledge Shoemaker NEO Grants from the Planetary Society (2007, 2013). These were used to purchase some of the telescopes and CCD cameras used in this research.

References

Carreño, A.; Arce, E.; Fornas, G.; Mas, V. (2019). "Eleven Main-belt Asteroids and One Near-Earth Asteroid Lightcurves at Asteroids Observers (OBAS) - MPPD: 2017 May - 2019 Jan." *Minor Planet Bul.* **46**, 200-203.

Harris, A.W.; Young, J.W.; Scaltriti, F.; Zappala, V. (1984). "Lightcurves and phase relations of the asteroids 82 Alkmene and 444 Gyptis." *Icarus* **57**, 251-258.

Harris, A.W.; Young, J.W.; Contreiras, L.; Dockweiler, T.; Belkora, L.; Salo, H.; Harris, W.D.; Bowell, E.; Poutanen, M.; Binzel, R.P.; Tholen, D.J.; Wang, S. (1989). "Phase relations of high albedo asteroids: The unusual opposition brightening of 44 Nysa and 64 Angelina." *Icarus* **81**, 365-374.

Harris, A.W.; Pravec, P.; Galad, A.; Skiff, B.A.; Warner, B.D.; Vilagi, J.; Gajdos, S.; Carbognani, A.; Hornoch, K.; Kusnirak, P.; Cooney, W.R.; Gross, J.; Terrell, D.; Higgins, D.; Bowell, E.; Koehn, B.W. (2014). "On the maximum amplitude of harmonics on an asteroid lightcurve." *Icarus* **235**, 55-59.

Masiero, J.R.; Mainzer, A.K.; Bauer, J.M.; Cutri, R.M.; Grav, T.; Kramer, E.; Pittichova, J.; Wright, E.L. (2021). "Asteroid Diameters and Albedos from NEOWISE Reactivation Mission Years Six and Severn." *Plan. Sci. J.* **2**, id.162.

Tonry, J.L.; Denneau, L.; Flewelling, H.; Heinze, A.N.; Onken, C.A.; Smartt, S.J.; Stalder, B.; Weiland, H.J.; Wolf, C. (2018). "The ATLAS All-Sky Stellar Reference Catalog." *Astrophys. J.* **867**, A105.

Warner, B.D.; Harris, A.W.; Pravec, P. (2009). "The Asteroid Lightcurve Database." *Icarus* **202**, 134-146. Updated 2021 August. *http://www.minorplanet.info/lightcurvedatabase.html*

Warner, B.D. (2015). "Asteroid Lightcurve Analysis at CS3-Palmer Divide Station: 2015 March-June." *Minor Planet Bul.* **42**, 267-276.

COLLABORATIVE ASTEROID PHOTOMETRY OF SIX MAIN-BELT ASTEROIDS

Stephen M. Brincat
Flarestar Observatory (MPC 171)
Fl.5/B, George Tayar Street,
San Gwann SGN 3160, MALTA
stephenbrincat@gmail.com

Charles Galdies
Znith Observatory
Naxxar NXR 2217, MALTA

Martin Mifsud
Manikata Observatory
Manikata MLH 5013, MALTA

Kevin Hills
Tacande Observatory
El Paso, La Palma, SPAIN

(Received 2021 Nov 17)

Synodic rotation periods of six main-belt asteroids were derived from photometric observations obtained from 2021 July 21 through November 2 from three observatories situated in Malta and one from Spain. We provide lightcurve rotation periods for (1713) Bancilhon, (2232) Altaj, (2458) Veniakaverin, (6681) Prokopovich, (6787) 1991 PF15, and (18863) 1999 RC191.

Photometric observations of six asteroids were carried out from four observatories located on the Maltese mainland and another located on the island of La Palma, Spain. Observations of asteroids for (1713) Bancilhon, (2232) Altaj, (2458) Veniakaverin, (6681) Prokopovich, and (6787) 1991 PF15 were obtained from the Maltese observatories, while the data for (18863) 1991 RC191 were obtained from Spain. Our observatories used the configurations shown in Table 1. All of our images were dark subtracted and flat-fielded.

All telescopes and cameras were controlled remotely over the internet either from a location near each telescope via *Sequence Generator Pro* (Binary Star Software) or through remote programing for the La Palma Observatory. Photometric reduction, lightcurve construction and analyses were derived through *MPO Canopus* software (Warner, 2017) where differential aperture photometry was used. The Comparison Star Selector (CSS) feature of *MPO Canopus* was used to select comparison stars of near-solar color. Our magnitude measurements were based on the ATLAS catalogue through the Red (r) bandpass.

Observatory	Tel	F	CCD	Observed
Flarestar (MPC171)	0.25m SCT	C	Moravian G2-1600	2232(3) 2458(4)
Znith	0.20m SCT	C	Moravian G2-1600	2232(2) 2458(2) 6681(3)
Manikata	0.20m SCT	C	SBIG ST-9	1713(2) 2232(3)
Tancade	0.50m CDK	Rc	QHY-600	18863(1)

Table I. Instruments used. The F column gives the filter. The Observed column gives the asteroid number and, in parentheses, the number of observing sessions contributed by the observatory. SCT: Schmidt- Cassegrain; CDK: Corrected Dall-Kirkham.

1713 Bancilhon is a main-belt asteroid that was discovered on 1951 September 27 by L. Boyer at Algiers Observatory. It is named in honor of the French astronomer Odette Bancilhon (1908 - 1998), who discovered the asteroid (1333) Cevenola from the same observatory (Schmadel, 2012). The estimated diameter of 5.716 ± 0.113 km based on an absolute magnitude *H* = 13.34. The semi-major axis = 2.223 au, the eccentricity = 0.184, and the orbital period = 3.32 years (JPL, 2021).

Bachilon was observed from Manikata Observatory during two nights on 2021 October 5 and November 2. Weather conditions prevented us from obtaining additional data during the interim period. Our results yielded a synodic period of 2.483 ± 0.001 h and amplitude of 0.24 ± 0.05 mag. The Lightcurve Database (LCDB from hereon; Warner et al., 2009) did not contain any references of the synodic period for this asteroid.

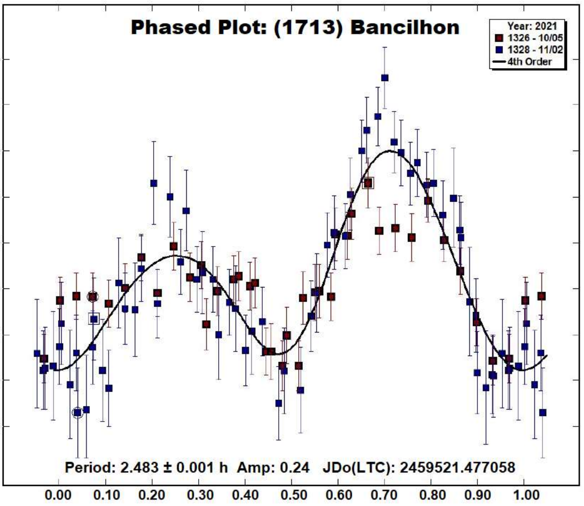

2232 Altaj (1969 RD2) is a main-belt asteroid that was discovered by B.A. Burnasheva at the Crimean Astrophysical Observatory on 1969 Sept. 15. It was named by the discoverer for the place of residence of her mother, Elena Andreevna Vasil'eva (Schmadel, 2012). Some orbital properties are semi-major axis = 2.668AU, eccentricity = 0.1433, and orbital period = 4.36 years (JPL, 2021). The JPL Small-Bodies Database Browser lists the diameter of 2232 Altaj as 11.780 ± 0.212 km based on an absolute magnitude *H* = 12.18.

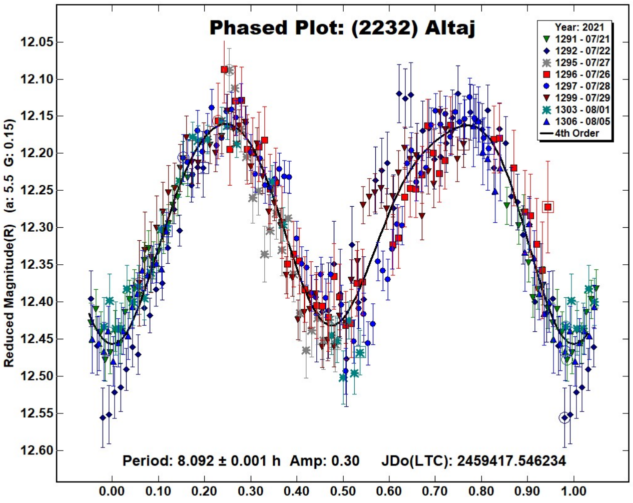

2232 Altaj was observed over eight nights from 2021 July 21 to August 5. Our analysis yielded a synodic rotation period of 8.092 ± 0.001 h and amplitude of 0.30 ± 0.06 mag. This is consistent with Ďurech et al. (2020).

2458 Veniakaverin (1977 RC7) is a main-belt asteroid that was discovered on 1977 Sep 11 by N. Chernykh at Nauchnyj. It was named after Soviet writer Veniamin Aleksandrovich Kaverin (1902-1989) (Schmadel, 2012). The estimated diameter is 22.764 ± 0.138 km based on an absolute magnitude of *H* = 12.05. The orbital semi-major axis is 3.131AU, the eccentricity is 0.144, and the orbital period is 5.54 years (JPL, 2021).

Observations were conducted by Flarestar and Znith Observatories over six nights from 2021 August 15 to September 2. Our analysis indicates a synodic period of 17.310 ± 0.006 h and amplitude of 0.32 ± 0.06 mag. The LCDB did not contain any references of the synodic period for this asteroid.

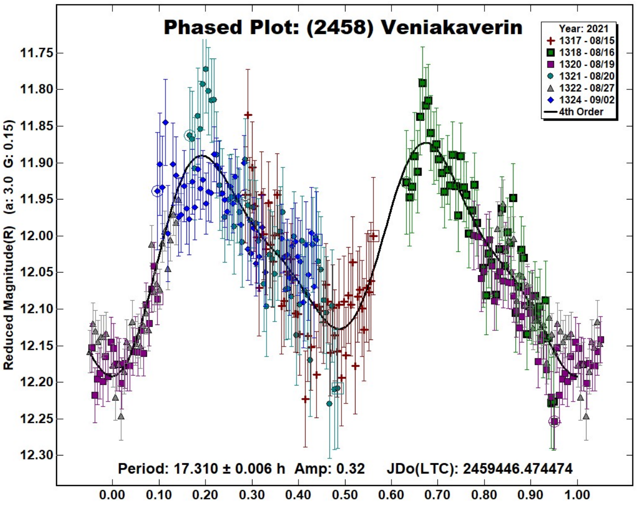

6681 Prokopovich (1972 RU3) is a main-belt asteroid that was discovered on 1972 Sep 6 by L.V. Zhuravleva at Nauchnyj. It is named after Feofan Prokopovich (1681-1736), a Ukrainian and Russian writer, archbishop, and associate of Peter the Great (Schmadel, 2012).

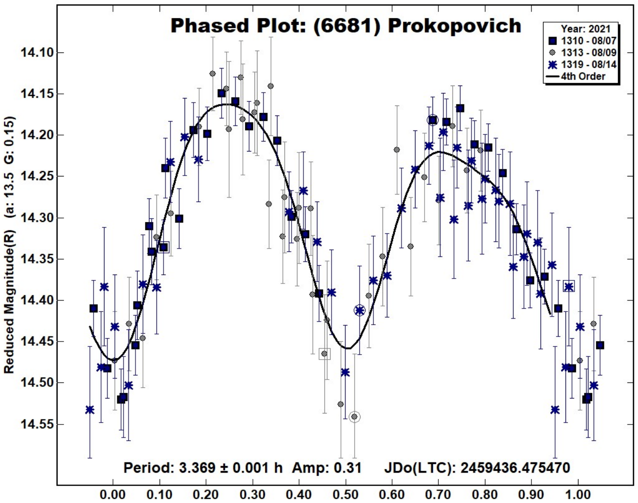

The estimated diameter is 4.288 ± 0.107 km based on an absolute magnitude of $H = 13.9$. The orbital semi-major axis is 2.205 au and the eccentricity is 0.146. The orbital period is about 3.27 years (JPL, 2021).

The Flora main-belt asteroid was observed by our group on three nights from 2021 August 7-14. Our analysis yields a rotation period of 3.369 ± 0.001 h with an amplitude of 0.31 ± 0.05 mag. The LCDB did not report any references regarding the synodic period for this asteroid.

(6787) 1991 PF15 is a main-belt asteroid that belongs to the Flora family. It was discovered on 1991 Aug 7 by H.E. Holt at Palomar (Schmadel, 2012). The estimated diameter is 4.865 ± 0.117 km based on $H = 13.57$. The orbital eccentricity is 0.1475 and the semi-major axis is 2.232 au. The orbital period is 3.34 years (JPL, 2021).

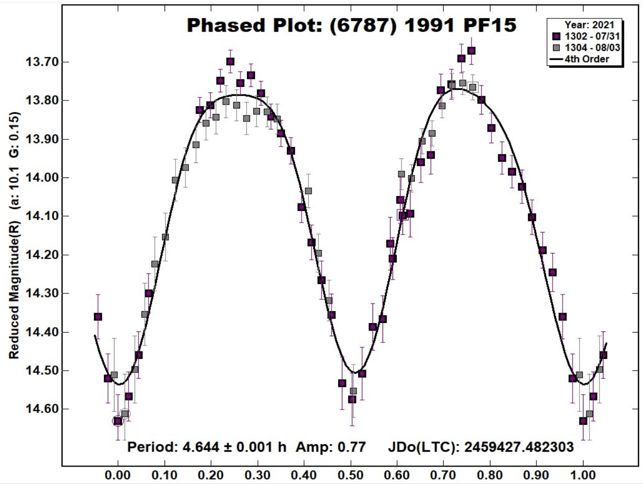

We observed 1991 PF15 on two nights from Manikata Observatory, Malta, and derived a synodic period of 4.644 ± 0.001 h with a lightcurve amplitude of amplitude of 0.77 ± 0.05 mag. This main-belt asteroid did not have any rotational period recorded in the LCDB.

(18863) 1999 RC191 is a main-belt asteroid that was discovered on 1999 September 11 by LINEAR at Socorro. The estimated diameter is 7.629 ± 0.133 km diameter based on an absolute magnitude of $H = 12.75$. The semi-major axis is 2.668 au and the eccentricity 0.176. The orbital period is 4.360 years (JPL, 2021).

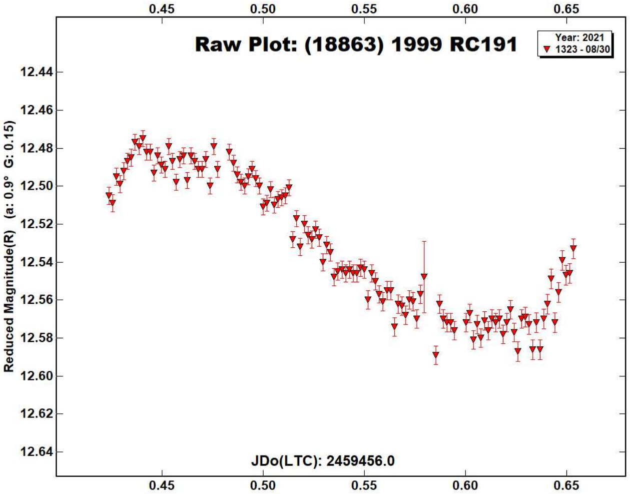

This asteroid was observed from Tacande Observatory on 2021 August 29 from 22:20 UT to 03:50 UT. Due to technical problems and weather conditions, we were unable to obtain additional data because the asteroid was too faint for our smaller instruments and the amplitude too low amplitude to overcome low SNR noise.

The data set of 119 data points provided limited coverage of the full lightcurve. This prevented finding a precise period solution but we did determine that a period of 11.6 h ± 0.1 h with an amplitude of 0.09 ± 0.01 mag based on half-period solution was possible. This main-belt asteroid did not have any rotational period recorded in the LCDB.

Acknowledgements

We would like to thank Brian Warner for his work in the development of *MPO Canopus* and for his efforts in maintaining the CALL website (Warner, 2009; 2016). This research has made use of the JPL's Small-Body Database.

Number	Name	2021 mm/dd	Phase	L_{PAB}	B_{PAB}	Period(h)	P.E.	Amp	A.E.	Grp
1713	Bancilhon	10/05-11/02	4.1,3.0,15.7	14	4	2.483	0.001	0.24	0.05	MB
2232	Altaj	07/21-08/05	5.4,2.9,4.2	308	5	8.092	0.001	0.30	0.06	MB
2458	Veniakaverin	08/15-09/02	3.1,4.7	330	-1	17.310	0.006	0.32	0.06	MB
6681	Prokopovich	08/07-08/14	13.1,9.5	333	-7	3.369	0.001	0.31	0.05	MB
6787	1991 PF15	07/31-08/03	10.2,8.5	323	4	4.644	0.001	0.77	0.05	MB
18863	1999 RC191	08/03	13.1	334	-1	11.6	0.1	0.09	0.01	MB

Table II. Observing circumstances and results. The phase angle is given for the first and last date. LPAB and BPAB are the approximate phase angle bisector longitude and latitude at mid-date range (see Harris et al., 1984). Grp is the asteroid family/group (Warner et al., 2009).

References

Ďurech, J.; Tonry, J.; Erasmus, N.; Denneau, L.; Heinze, A.N.; Flewelling, H.; Vančo, R. (2020). “Asteroid models reconstructed from ATLAS photometry.” *Astron. Astrophys.* **643**, A59.

Harris, A.W.; Young, J.W.; Scaltriti, F.; Zappala, V. (1984). “Lightcurves and phase relations of the asteroids 82 Alkmene and 444 Gyptis.” *Icarus* **57**, 251-258.

JPL (2021). Small-Body Database Browser - JPL Solar System Dynamics web site. Last accessed: 11 July 2021.
http://ssd.jpl.nasa.gov/sbdb.cgi

Schmadel, L.D. (2012). *Dictionary of Minor Planet Names (3rd edition)*. pp. 216, 288, 317, 807, 815. Springer, Berlin.

Warner, B.D.; Harris, A.W.; Pravec, P. (2009). “The asteroid lightcurve database.” *Icarus* **202**, 134-146. Updated 2021 June.
https://minplanobs.org/MPInfo/php/lcdbsummaryquery.php

Warner, B.D. (2016). *Collaborative Asteroid Lightcurve Link website*. Last accessed: 26 September 2018.
http://www.minorplanet.info/call.html

Warner, B.D. (2017). MPO Software, *MPO Canopus* version 10.7.10.0. Bdw Publishing.
http://www.minorplanetobserver.com/

DETERMINING THE LIGHTCURVES AND ROTATIONAL PERIODS OF FIVE MAIN BELT ASTEROIDS

Harum Ahmed
Kent Montgomery
Michael Cheek
Texas A&M University-Commerce
P.O. Box 3011
Commerce, TX 75429-3011
Kent.Montgomery@tamuc.edu

(Received: 2021 October 26)

Lightcurves and rotational periods were determined for the following five main belt asteroids: 3942 Churivannia, 2.516 ± 0.002 h; 4673 Bortle, 2.643 ± 0.001 h; 5186 Donalu, 3.154 ± 0.001 h; 8441 Lapponica, 3.285 ± 0.001 h; and 12259 Szukalski, 5.986 ± 0.001 h.

Introduction

The objective of this research was to determine the rotational periods for the following five asteroids: 3942 Churivannia, 4673 Bortle, 5186 Donalu, 8441 Lapponica, and 12259 Szukalski, by plotting their lightcurves derived from photometric data taken over several nights. These lightcurves were analyzed to determine the asteroid’s rotational period and from the shape of the lightcurve create a possible model of the asteroid.

Asteroid 3942 Churivannia was discovered by Chernykh, N. at the Crimean Astrophysical Observatory in 1977. It has an orbital eccentricity of 0.197 and a semi-major axis of 2.39 AU (JPL). Asteroid 4673 Bortle was discovered by Shoemaker, C.S. at the Palomar Observatory in 1988. The asteroid has an orbital eccentricity of 0.057 and a semi-major axis of 2.55 AU (JPL). Asteroid 5186 Donalu was discovered by Roman, B. at the Palomar Observatory in 1990. It has an orbital eccentricity of 0.084 and a semi-major axis of 2.58 AU (JPL). Asteroid 8441 Lapponica was discovered by C.J. van Houten and I. van Houten-Groeneveld at the Palomar Observatory in 1977. It has an orbital eccentricity of 0.139 and a semi-major axis of 2.19 AU (JPL). Asteroid 12259 Szukalski was discovered by E.W. Elst at the European Southern Observatory in 1989. It has an orbital eccentricity of 0.161 and a semi-major axis of 2.19 AU (JPL).

Asteroids were selected through the website which catalogs all known asteroids (CALL). The asteroid’s apparent magnitude, declination, and opposition date, were the criterion used to choose these asteroids. Asteroids at or near opposition were chosen to ensure the maximum amount of data each night. For the ideal signal to noise ratio, asteroids with magnitude of 16 or brighter were chosen. When observing asteroids in the northern hemisphere, asteroids with more positive declinations were chosen and when observing in the southern hemisphere, asteroids with more negative declinations were chosen.

Method

Two different telescopes were used to observe the asteroids. One telescope was the Texas A&M University-Commerce 0.7-m CDK 700 Planewave telescope equipped with an Andor iKon-XL CCD Camera located in Commerce, TX at a latitude of 33ºN. The CCD camera was thermoelectrically cooled to -40ºC to reduce background noise. The other telescope was part of the Southern Associate for Research in Astronomy (SARA) consortium. The SARA-CT 0.6-m telescope is also equipped with an Andor Ikon CCD Camera located in the southern hemisphere at the Cerro Tololo Observatory in Chile at a latitude of 30ºS. The camera was cooled to -85ºC to reduce background noise.

To calibrate the images, dark, flat, and bias frames were obtained at the beginning of each night. Dark frames were taken using the same exposure length as the respective light images, three minutes for each telescope. Flat field images were taken against the twilight sky at exposure times between five and thirty seconds were used. The flat field images were used to correct for anomalies in the optical path and non-uniformities across the chip. Both telescopes had a luminance filter between the telescope and camera. The luminance filter transmits most of the visible light from the target but blocks the infrared.

Images were reduced and aligned using the software *MaxIm DL* (Diffraction Limited). Once the images were reduced, the program *MPO Canopus v.10.3.0.0.* (Warner, 2011) was used to perform differential photometry. For each night of observations, five comparison stars were chosen within each of the images. Aperture photometry was then used to determine the brightness of the asteroid and the comparison stars. The average difference in mag. between the stars and asteroids was found for each image and then plotted versus time, to produce a lightcurve. When the asteroid passed a nearby star those observations were deleted from the lightcurve. A Fourier transform was then applied to the lightcurve to determine the asteroid's rotational period and associated error.

The processed lightcurve files were then exported into *MPO LCInvert* (Warner, 2011) to create notional 3D models for all five asteroids. The reduced and light-time corrected *MPO Canopus* files were converted into "Kaasalainen files" since they have a specific format utilized by the inversion algorithms of the program. A search was done with *MPO LCInvert* for the rotational period with the lowest chi-squared value, indicating the best period. For all five asteroids, the rotational periods found for the 3D models were within 0.01 hours of the original lightcurve periods. However, despite the seemingly accurate depiction of the 3D models, limited solar phase angle variations and limited ecliptic longitude coverage in the data means these shape models are simply initial estimates to encourage future observations. We can expect that these models may be subject to significant revision as more data become available.

Results

3942 Churivannia was imaged 170 times on 2021, July 15, and 172 times on 2021, July 16. Both nights used the SARA-CT telescope and the data resulted in a rotational period of 2.526 ± 0.002 h with an amplitude variance of 0.26 mag. No previous studies regarding the rotation period were found in either the JPL Small-Body Database or the Minor Planet Light Curve Database.

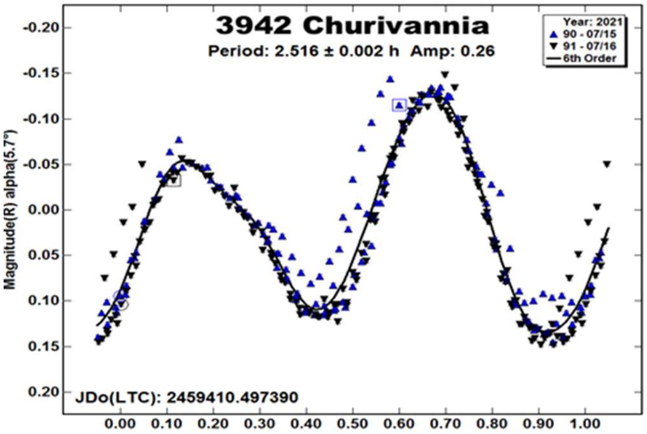

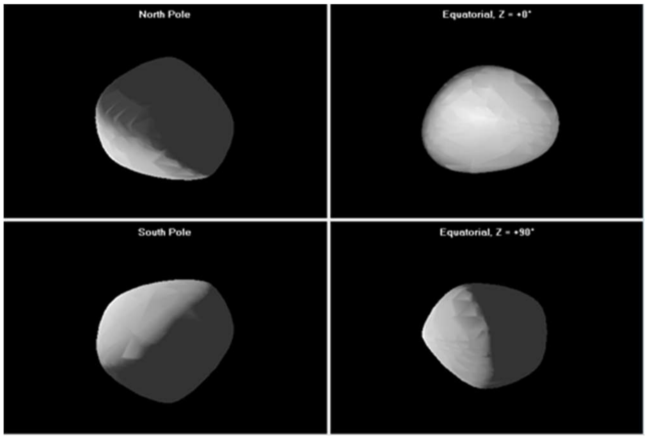

4673 Bortle Asteroid 4673 Bortle was imaged 101 times on 2021, June 17, and 97 times on 2021, June 19. Both nights used the TAMUC telescope and the data resulted in a rotational period of 2.643 ± 0.001 h with an amplitude variance of 0.17 mag. Behrend (2008web) found a similar period of 2.639 ± 0.00002 h with an amplitude of 0.16 mag. Kim et al. (2014) found a similar period of 2.64 ± 0.01 h with an amplitude of 0.16 mag. Behrend (2016web) found a similar period of 2.639 ± 0.0006 h with an amplitude of 0.15 mag. Pal et al. (2020) found a similar period of 2.640 ± 0.00005 h with an amplitude of 0.09 mag.

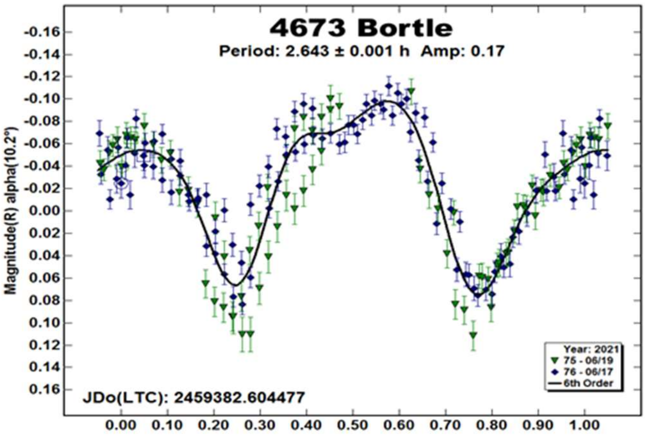

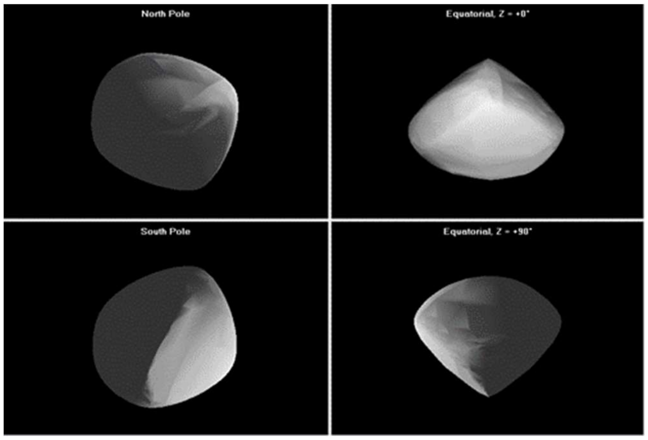
North Pole
Equatorial, Z = +0°
South Pole
Equatorial, Z = +90°

5186 Donalu was imaged 106 times on 2021, March 19, and 96 times on 2021, March 20. Both nights used the TAMUC telescope and the data resulted in a rotational period of 3.154 ± 0.001 h with an amplitude variance of 0.37 mag. Casalnuovo (2016) found a similar period of 3.15 ± 0.01 h with an amplitude of 0.25 mag. Benishek (2020) found a similar period of 3.153 ± 0.001 h with an amplitude of 0. 36 mag. Durech et al. (2020) also found a similar period of 3.153 ± 0.000005 h.

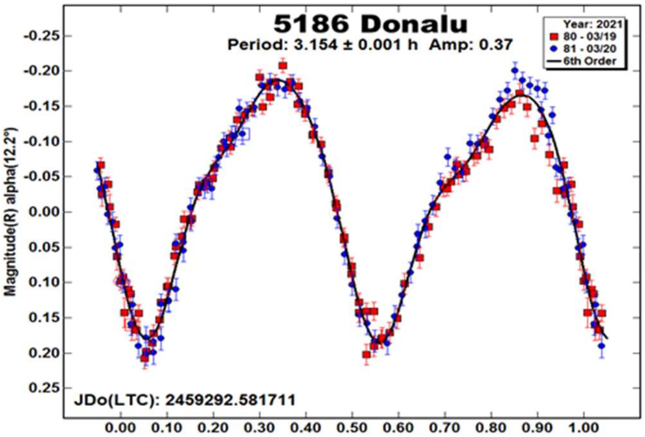

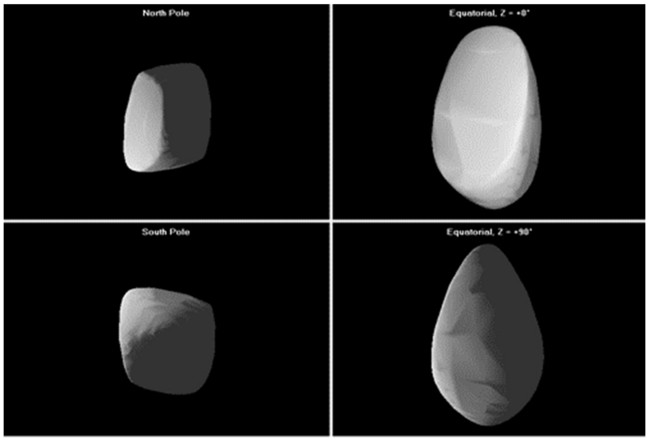
North Pole
Equatorial, Z = +0°
South Pole
Equatorial, Z = +90°

8441 Lapponica was imaged 120 times on 2021, March 4, and 125 times on 2021, March 8. Both nights used the TAMUC telescope and a rotational period of 3.285 ± 0.001 h was found with an amplitude variance of 0.35 mag. Behrend (2008web) found a similar period of 3.270 ± 0.01 h with an amplitude of 0.29 mag. Clark (2008) found a similar period of 3.275 ± 0.001 h with an amplitude of 0.50 mag. Benishek (2021) found a similar period of 3.285 ± 0.0003 h with an amplitude of 0.38 mag.

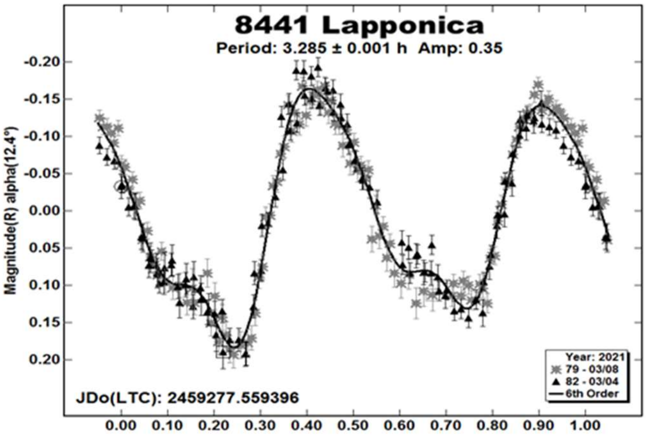

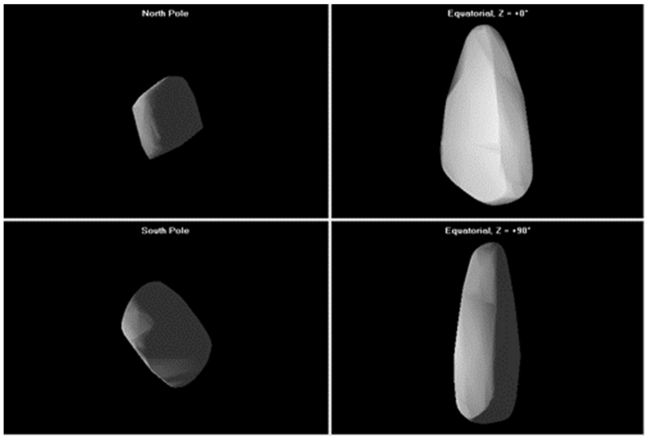
North Pole
Equatorial, Z = +0°
South Pole
Equatorial, Z = +90°

12259 Szukalski was imaged 91 times on 2021, July 4, and 98 times on 2021, July 5 both nights using the TAMUC telescope and it was also imaged 150 times on 2021, July 12 using the SARA-CT telescope. The data resulted in a rotational period of 5.986 ± 0.001 h with an amplitude variance of 1.00 mag. No previous studies regarding the rotational period were found either in the JPL Small-Body Database or the Minor Planet Light Curve Database.

Number	Name	2021 mm/dd	Phase	L_{PAB}	B_{PAB}	Period(h)	P.E.	Amp	A.E.	Grp
3942	Churivannia	2021 07/15-07/16	5.65,5.93	289.1	-7.1	2.516	0.002	0.26	0.01	MB-I
4673	Bortle	2021 06/17-06/19	9.55,10.18	247.9	11.2	2.643	0.001	0.17	0.02	MAR
5186	Donalu	2021 03/19-03/20	12.18,12.54	150.8	-1.1	3.154	0.001	0.37	0.01	MB-I
8441	Lapponica	2021 03/04-03/08	10.21,12.43	150.1	6.3	3.285	0.001	0.35	0.03	MB-I
12259	Szukalski	2021 07/05-07/11	6.10,9.04	277.6	5.6	5.986	0.001	1.00	0.02	MB-I

Table I. Observing circumstances and results. The phase angle is given for the first and last date. If preceded by an asterisk, the phase angle reached an extrema during the period. L_{PAB} and B_{PAB} are the approximate phase angle bisector longitude/latitude at mid-date range (see Harris et al., 1984). Grp is the asteroid family/group (Warner et al., 2009). Additional data is from *MPO Canopus v10.3.0.0.* (Warner, 2011).

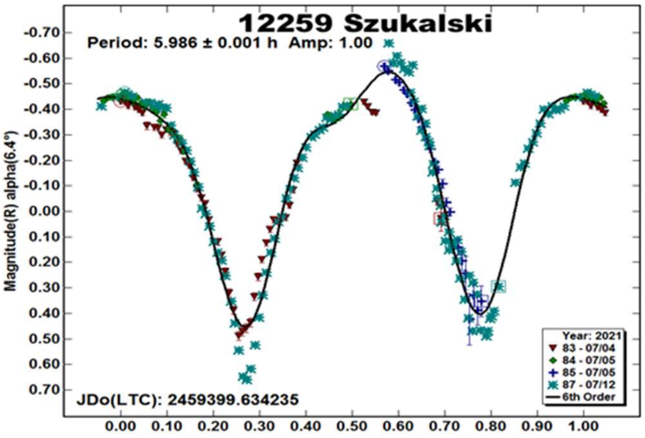

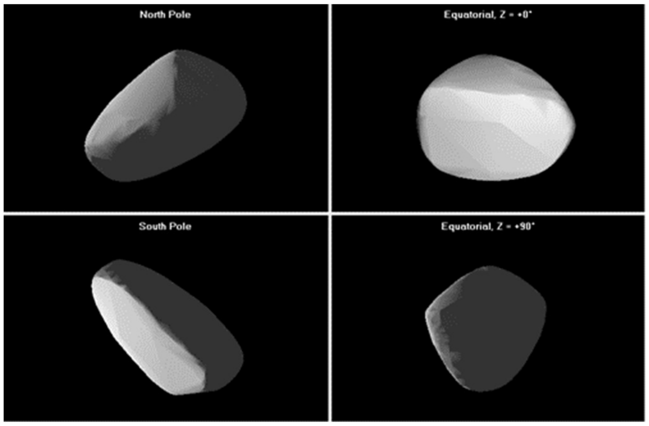

Acknowledgements

This research was supported by the Physics and Astronomy Research Experiences for Undergraduates (REU) Program at the Texas A&M University-Commerce funded by NSF Grant No. 2050277.

References

Behrend, R. (2008web, 2016web) Observatoire de Geneve web site. *http://obswww.unige.ch/~behrend/page_cou.html*

Benishek, V. (2020). "Photometry of 39 Asteroids at Sopot Astronomical Observatory: 2019 September - 2020 March." *Minor Planet Bulletin* **47**, 231-241.

Benishek, V. (2021). "Lightcurve and Rotation Period Determinations for 25 Asteroids." *Minor Planet Bull.* **48**, 280-285.

Casalnuovo, G.B. (2016). "Lightcurve Analysis for Nine Main Belt Asteroids." *Minor Planet Bulletin* **43**, 112-115.

Clark, M. (2008). "Asteroid Lightcurve Observations." *Minor Planet Bulletin* **35**, 152-154.

Collaborative Asteroid Lightcurve Link (CALL): Potential Lightcurve Targets.
http://www.minorplanet.info/PHP/call_OppLCDBQuery.php

Diffraction Limited MaxIm DL - Astronomy and Scientific Imaging Software.
https://diffractionlimited.com/product/maxim-dl/

Durech, J.; Tonry, J.; Erasmus, N.; Denneau, L.; Heinze, A.N.; Flewelling, H.; Vanco, R. (2020). "Asteroid models reconstructed from ATLAS photometry." *Astron. Astrophys*. **643**, A59, 5 pp.

Harris, A.W.; Young, J.W.; Scaltriti, F.; Zappala, V. (1984). "Lightcurves and phase relations of the asteroids 82 Alkmene and 444 Gyptis." *Icarus* **57**, 251-258.

JPL Small-Body Database Browser.
http://ssd.jpl.nasa.gov/sbdb.cgi#top

Kim, M.-J.; Choi, Y.-J.; Moon, H.-K. and 13 colleagues (2014). "Rotational properties of the maria asteroid family." *Astron. J.* **147**, A56.

Minor Planet Light Curve Database (LCDB).
https://minplanobs.org/MPInfo/php/lcdbsummaryquery.php

Pal, A.; Szakats, R.; Kiss, C.; Bodi, A.; Bognar, Z.; Kalup, C.; Kiss, L.L.; Marton, G.; Molnar, L.; Plachy, E.; Sárneczky, K.; Szabo, G.M.; Szabo, R. (2020). "Solar System Objects Observed with TESS - First Data Release: Bright Main-belt and Trojan Asteroids from the Southern Survey." *Ap. J. Supl. Ser.* **247**, id.26.

Warner, B.D., Harris, A.W., Pravec, P. (2009). "The Asteroid Lightcurve Database." Icarus **202**, 134-146. Updated 2021 June. *http://www.minorplanet.info/lightcurvedatabase.html*

Warner, B.D. (2011). MPO Canopus software Version 10.3.0.0. Bdw Publishing. *http://www.minorplanetobserver.com/*

LIGHTCURVE ANALYSIS OF L4 TROJAN ASTEROIDS AT THE CENTER FOR SOLAR SYSTEM STUDIES: 2021 OCTOBER TO DECEMBER

Robert D. Stephens
Center for Solar System Studies (CS3)
11355 Mount Johnson Ct., Rancho Cucamonga, CA 91737 USA
rstephens@foxandstephens.com

Brian D. Warner
Center for Solar System Studies (CS3)
Eaton, CO

(Received: 2022 January 12)

Lightcurves for five Jovian Trojan asteroids were obtained at the Center for Solar System Studies (CS3) from 2021 October to December.

For several years, the Center for Solar System Studies (CS3, MPC U81) has been conducting a study of Jovian Trojan asteroids. This paper reports CCD photometric observations of five Trojan asteroids from the L_4 (Greek) Lagrange point from 2021 October to December.

All observations were made using a 0.4-m f/10 Schmidt-Cassegrain telescope and an FLI Proline 1001E CCD camera. Images were unbinned with no filter and had master flats and darks applied. The exposures were 180 seconds.

Image processing, measurement, and period analysis were done using *MPO Canopus* (Bdw Publishing), which incorporates the Fourier analysis algorithm (FALC) developed by Harris (Harris et al., 1989). The Comp Star Selector feature in *MPO Canopus* was used to limit the comparison stars to near solar color. Night-to-night calibration was done using field stars from the ATLAS catalog (Tonry et al., 2018), which has Sloan *griz* magnitudes that were derived from the GAIA and Pan-STARR catalogs and are the "native" magnitudes of the catalog.

The Y-axis of lightcurves gives ATLAS SR "sky" (catalog) magnitudes. During period analysis, the magnitudes were normalized to the phase angle and value for *G* given in the parentheses. The X-axis rotational phase ranges from -0.05 to 1.05.

The amplitude indicated in the plots (e.g., Amp. 0.23) is the amplitude of the Fourier model curve and *not necessarily* the adopted amplitude of the lightcurve.

For brevity, only some of the previously reported rotational periods may be referenced. A complete list is available at the lightcurve database (LCDB; Warner et al., 2009).

3063 Makhaon. We observed this L_4 Trojan five times in the past (Stephens et al., 2021; and references therein). Mottola et al. (2011) also observed it twice. The results this year are in good agreement with those prior findings.

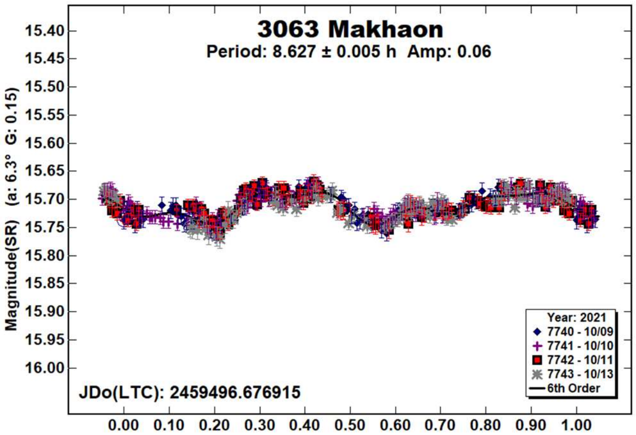

3596 Meriones. Periods for this L_4 Trojan have been reported twice in the past. Gonano et al. (1991) found a period of 12.96 h. Using data from the TESS spacecraft, Pál et al. (2020) found a period of 6.4178 h, seemingly a 1:2 alias of the Gonano result. Both reported a 0.15 mag amplitude. The results this year did not break the tie. The amplitude we observed was only 0.04 - 0.05 mag. With such a low amplitude, one cannot assume a bimodal shape to the lightcurve (Harris et al., 2014). The period spectrum shows many possible periods, with ones around 6.5 h and 13 h barely above the noise. This dataset cannot differentiate between the two possible periods, but we prefer the 6.54 h solution because it produces a bimodal lightcurve with a much better fit to the Fourier curve.

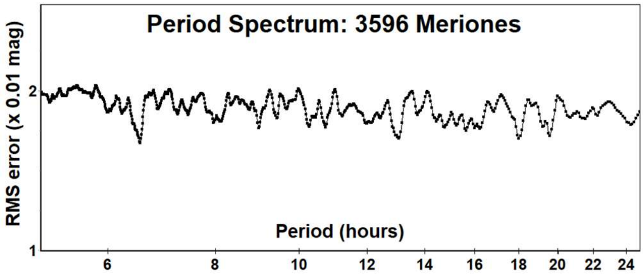

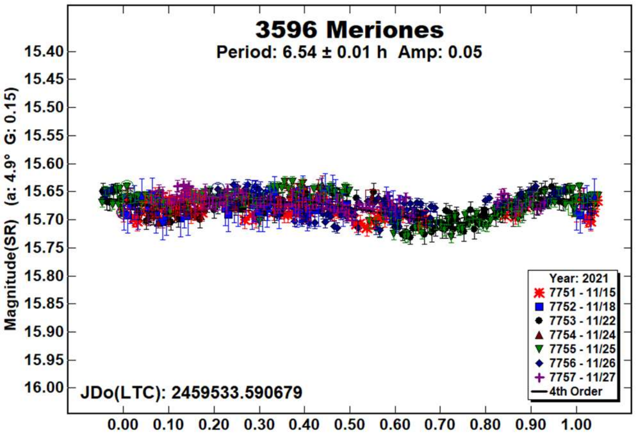

Number	Name	2021/mm/dd	Phase	L_{PAB}	B_{PAB}	Period(h)	P.E.	Amp	A.E.
3063	Makhaon	10/09-10/13	6.4,5.7	46	12	8.627	0.005	0.06	0.01
3596	Meriones	11/15-11/27	4.9,5.7	52	22	6.54	0.01	0.05	0.01
						[a]13.08	0.01	0.04	0.01
4063	Euforbo	10/14-10/16	6.6,6.3	42	-21	8.844	0.004	0.23	0.01
4068	Menestheus	2019/08/30-09/06	3.9,4.9	320	12	[r]14.319	0.003	0.52	0.02
		12/01-12/06	9.0,9.5	18	-8	14.301	0.007	0.28	0.02
4501	Eurypylos	11/28-11/30	2.3,2.8	55	1	6.931	0.004	0.31	0.03

Table I. Observing circumstances and results. [r]Restated previous period. [a]Alternative period. The phase angle is given for the first and last dates. If preceded by an asterisk, the phase angle reached an extremum during the period. L_{PAB} and B_{PAB} are the approximate phase angle bisector longitude/latitude at mid-date range (see Harris et al., 1984).

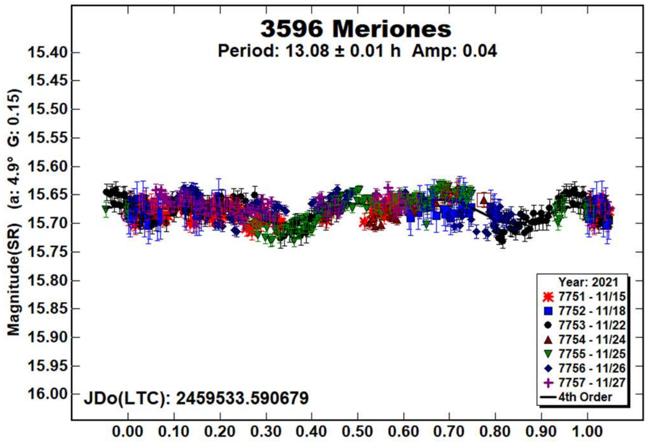

4063 Euforbo. This L_4 Trojan is estimated to be 102 km in size. A period has been reported several times in the past (Stephens et al., 2016; and references therein), each time finding it rotated every 8.84 h. The result this year is in good agreement with the prior results.

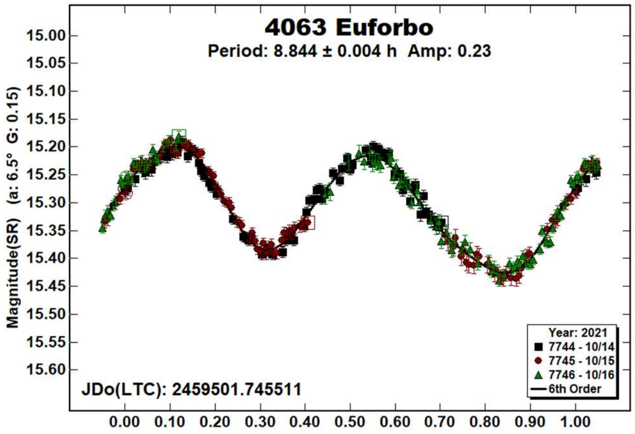

4068 Menestheus. A period for this L_4 Trojan has been reported several times in the past (e.g., Stephens and Warner, 2017), each time reporting a period near 14.3 h. In researching for this article, we found an unreported result of ours from 2019 September. The results from 2019 and 2021 are in good agreement with the prior findings.

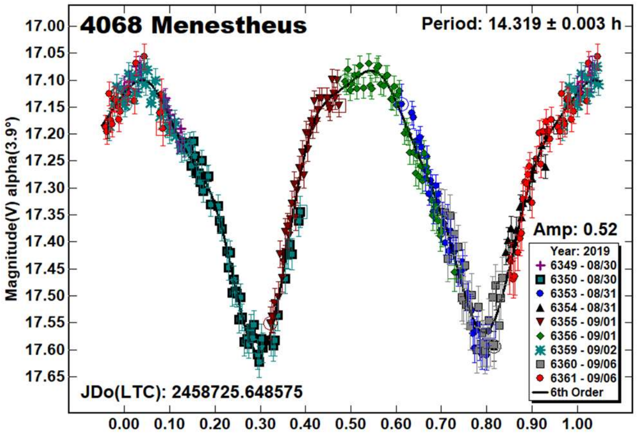

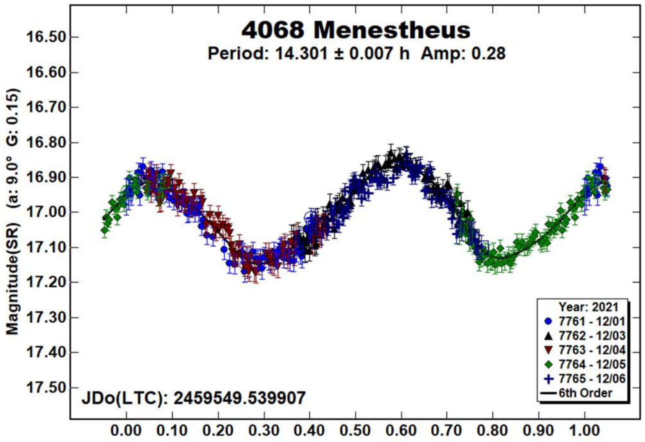

4501 Eurpylos. A period for this Trojan has been reported twice in the past (Stephens and Warner, 2020; and references therein). The period found this year is in good agreement with those prior results.

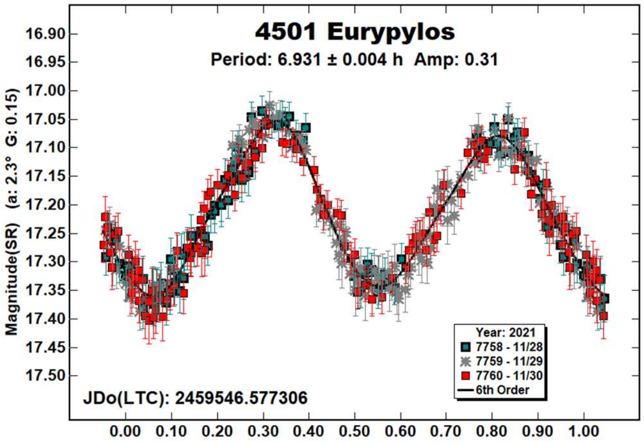

Acknowledgements

This work includes data from the Asteroid Terrestrial-impact Last Alert System (ATLAS) project. ATLAS is primarily funded to search for near earth asteroids through NASA grants NN12AR55G, 80NSSC18K0284, and 80NSSC18K1575; byproducts of the NEO search include images and catalogs from the survey area. The ATLAS science products have been made possible through the contributions of the University of Hawaii Institute for Astronomy, the Queen's University Belfast, the Space Telescope Science Institute, and the South African Astronomical Observatory. The purchase of a FLI-1001E CCD camera was made possible by a 2013 Gene Shoemaker NEO Grant from the Planetary Society.

References

Gonano, M.; di Martino, M.; Mottola, S.; Neukum, G. (1991). "Physical study of outer belt asteroids." *Adv. in Space Research.* **11**, 197-200.

Harris, A.W.; Young, J.W.; Scaltriti, F.; Zappala, V. (1984). "Lightcurves and phase relations of the asteroids 82 Alkmene and 444 Gyptis." *Icarus* **57**, 251-258.

Harris, A.W.; Young, J.W.; Bowell, E.; Martin, L.J.; Millis, R.L.; Poutanen, M.; Scaltriti, F.; Zappala, V.; Schober, H.J.; Debehogne, H.; Zeigler, K.W. (1989). "Photoelectric Observations of Asteroids 3, 24, 60, 261, and 863." *Icarus* **77**, 171-186.

Harris, A.W.; Pravec, P.; Galad, A.; Skiff, B.A.; Warner, B.D.; Vilagi, J.; Gajdos, S.; Carbognani, A.; Hornoch, K.; Kusnirak, P.; Cooney, W.R.; Gross, J.; Terrell, D.; Higgins, D.; Bowell, E.; Koehn, B.W. (2014). "On the maximum amplitude of harmonics on an asteroid lightcurve." *Icarus* **235**, 55-59.

Mottola, S.; Di Martino, M.; Erikson, A.; Gonano-Beurer, M.; Carbognani, A.; Carsenty, U.; Hahn, G.; Schober, H.; Lahulla, F.; Delbò, M.; Lagerkvist, C. (2011). "Rotational Properties of Jupiter Trojans. I. Light Curves of 80 Objects." *Astron. J.* **141**, A170.

Pál, A.; Szakáts, R.; Kiss, C.; Bódi, A.; Bognár, Z.; Kalup, C.; Kiss, L.L.; Marton, G.; Molnár, L.; Plachy, E.; Sárneczky, K.; Szabó, G.M.; Szabó, R. (2020). "Solar System Objects Observed with TESS - First Data Release: Bright Main-belt and Trojan Asteroids from the Southern Survey." *Ap. J.* **247**, A26.

Stephens, R.D.; Coley, D.R.; Warner, B.D.; French, L.M. (2016). "Lightcurves of Jovian Trojan Asteroids from the Center for Solar System Studies: L4 Greek Camp and Spies." *Minor Planet Bull.* **43**, 323-331.

Stephens, R.D.; Warner, B.D. (2017). "Lightcurve Analysis of L4 Trojan Asteroids at the Center for Solar System Studies 2017 April-June." *Minor Planet Bull.* **44**, 312-316.

Stephens, R.D.; Warner, B.D. (2020). "Lightcurve Analysis of L4 Trojan Asteroids at the Center for Solar System Studies: 2019 July to September." *Minor Planet Bull.* **47**, 43-47.

Stephens, R.D.; Coley, D.R.; Warner, B.D. (2021). "Lightcurve Analysis of L4 Jovian Trojan Asteroids from the Center for Solar System Studies: 2020 October to December." *Minor Planet Bull.* **48**, 167-170.

Tonry, J.L.; Denneau, L.; Flewelling, H.; Heinze, A.N.; Onken, C.A.; Smartt, S.J.; Stalder, B.; Weiland, H.J.; Wolf, C. (2018). "The ATLAS All-Sky Stellar Reference Catalog." *Astrophys. J.* **867**, A105.

Warner, B.D., Harris, A.W., Pravec, P. (2009). "The Asteroid Lightcurve Database." Icarus **202**, 134-146. Updated 2021 May. *http://www.minorplanet.info/lightcurvedatabase.html*

ROTATION PERIOD DETERMINATION FOR ASTEROIDS 4988 CHUSHUHO AND 7393 LUGINBUHL

Alessandro Marchini, Leonardo Cavaglioni,
Chiara Angelica Privitera
Astronomical Observatory, DSFTA - University of Siena (K54)
Via Roma 56, 53100 - Siena, ITALY
marchini@unisi.it

Riccardo Papini, Fabio Salvaggio
Wild Boar Remote Observatory (K49)
San Casciano in Val di Pesa (FI), ITALY

(Received: 2022 Jan 15)

Photometric observations of two main-belt asteroids were conducted in order to determine their synodic rotation periods. For 4988 Chushuho we found P = 3.170 ± 0.001 h, A = 0.15 ± 0.02 mag; for 7393 Luginbuhl we found P = 2.602 ± 0.001 h, A = 0.08 ± 0.03 mag.

CCD photometric observations of two main-belt asteroids were carried out in 2021 October and November at the Astronomical Observatory of the University of Siena (K54), a facility inside the Department of Physical Sciences, Earth and Environment (DSFTA, 2022). We used a 0.30-m *f*/5.6 Maksutov-Cassegrain telescope, SBIG STL-6303E NABG CCD camera, and clear filter; the pixel scale was 2.30 arcsec when binned at 2×2 pixels and all exposures were 300 seconds.

Data processing and analysis were done with *MPO Canopus* (Warner, 2018). All images were calibrated with dark and flat-field frames and the instrumental magnitudes converted to R magnitudes using solar-colored field stars from a version of the CMC-15 catalogue distributed with *MPO Canopus*. Table I shows the observing circumstances and results.

A search through the asteroid lightcurve database (LCDB; Warner et al., 2009) indicates that our results may be the first reported lightcurve observations and results for 4988 Chushuho, while for 7393 Luginbuhl we found a solution in good agreement with the recent literature.

4988 Chushuho (1980 VU1) was discovered on 1980 November 6 at the Purple Mountain Observatory and named after David Chu, Shu Ho (b. 1950), who lives in Hong Kong and has devoted his energies to physical education in China [MPC 55719]. It is a main-belt asteroid with a semi-major axis of 2.406 AU, eccentricity 0.214, inclination 2.138°, and an orbital period of 3.73 years. Its absolute magnitude is H = 13.83 (JPL, 2022). The WISE/NEOWISE satellite infrared radiometry survey (Masiero et al., 2012) found a diameter $D = 3.58 \pm 0.19$ km using an absolute magnitude $H = 13.6$.

Observations were conducted over four nights and collected 231 data points. The period analysis shows a bimodal solution for the rotational period of $P = 3.170 \pm 0.001$ h with an amplitude $A = 0.15 \pm 0.02$ mag.

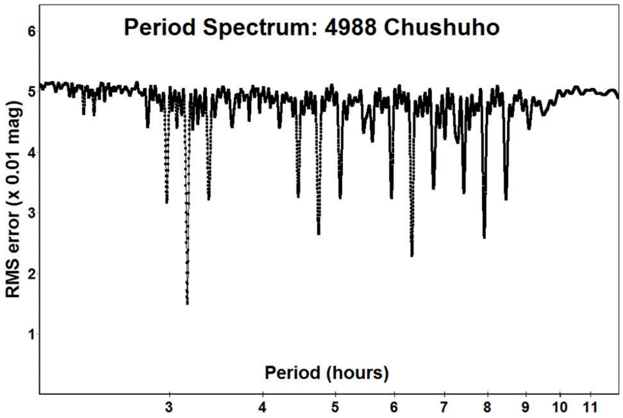

Figure 1: Period spectrum of 4988 Chushuho.

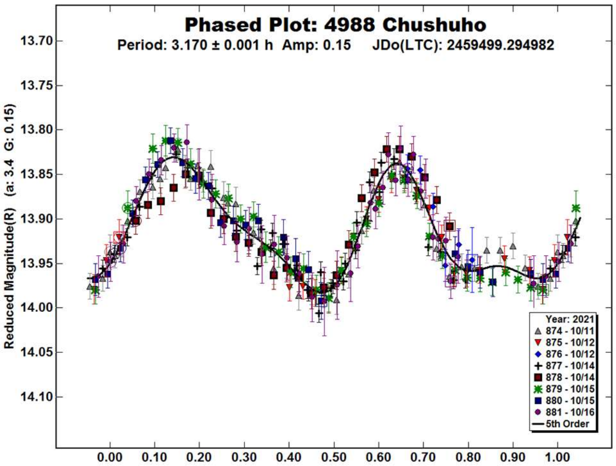

Figure 2: Phased lightcurve of 4988 Chushuho.

7393 Luginbuhl (1984 SL3) was discovered on 1984 September 28 by B.A. Skiff at the Anderson Mesa Station of the Lowell Observatory and named after Christian B. Luginbuhl (b. 1955), of the U.S. Naval Observatory's Flagstaff Station, who was largely responsible for the enactment and continued enforcement of ordinances preserving the dark skies of northern Arizona. With the discoverer, he co-authored the Observing Handbook and Catalogue of Deep-Sky Objects (Luginbuhl and Skiff, 1998). [MPC 36127] It is a main-belt asteroid with a semi-major axis of 2.240 AU, eccentricity 0.200, inclination 6.731°, and an orbital period of 3.35 years. Its absolute magnitude is H = 13.29 (JPL, 2022). The WISE/NEOWISE satellite infrared radiometry survey (Masiero et al., 2011) found a diameter $D = 5.306 \pm 0.242$ km using an absolute magnitude $H = 12.9$.

Observations were conducted over two nights and collected 71 data points. Despite the first session being carried out under bad sky conditions, the period analysis using a subset of the data that excluded an apparent large attenuation (Figure 4), shows a result for the rotational period of $P = 2.602 \pm 0.001$ h with an amplitude $A = 0.08 \pm 0.03$ mag as the most likely bimodal solution for this asteroid. It is in good agreement with the solution found by Warner and Skiff (2019) who discovered the binary nature of this asteroid. We also recorded an anomaly in the lightcurve (Figure 5), which may have been due to an eclipse or occultation event in the binary system.

Number	Name	2021/mm/dd	Phase	L_{PAB}	B_{PAB}	Period(h)	P.E.	Amp	A.E.	Grp
4988	Chushuho	10/11-10/16	3.4,0.9	23	-1	3.170	0.001	0.15	0.02	MB
7393	Luginbuhl	11/02-11/13	*5.3,3.8	47	4	2.602	0.001	0.08	0.03	MB

Table I. Observing circumstances and results. The phase angle is given for the first and last date. If preceded by an asterisk, the phase angle reached an extrema during the period. L_{PAB} and B_{PAB} are the approximate phase angle bisector longitude/latitude at mid-date range (see Harris et al., 1984). Grp is the asteroid family/group (Warner et al., 2009).

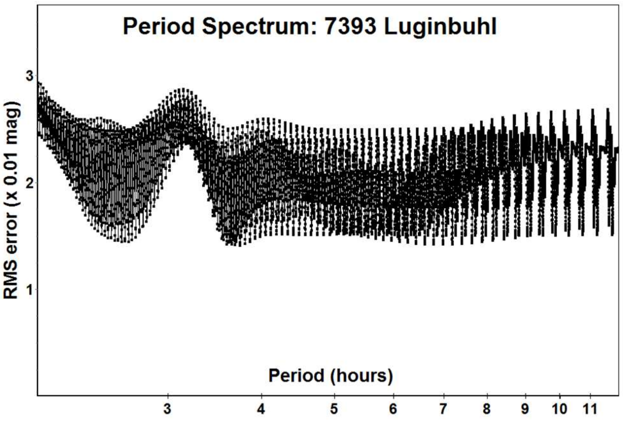

Figure 3: Period spectrum of 7393 Luginbuhl.

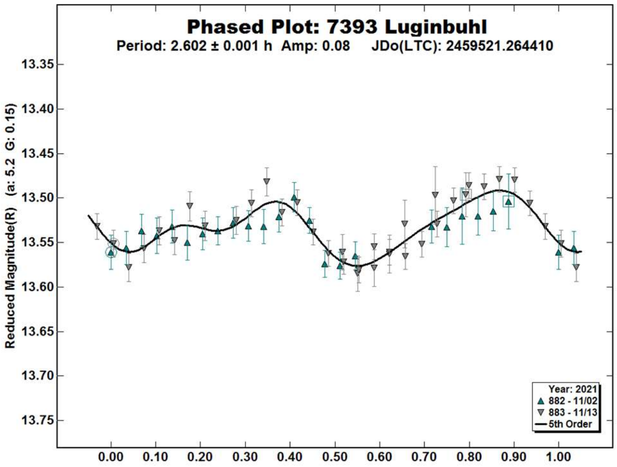

Figure 4: Phased lightcurve of 7393 Luginbuhl cleaned of the points due to a probable event.

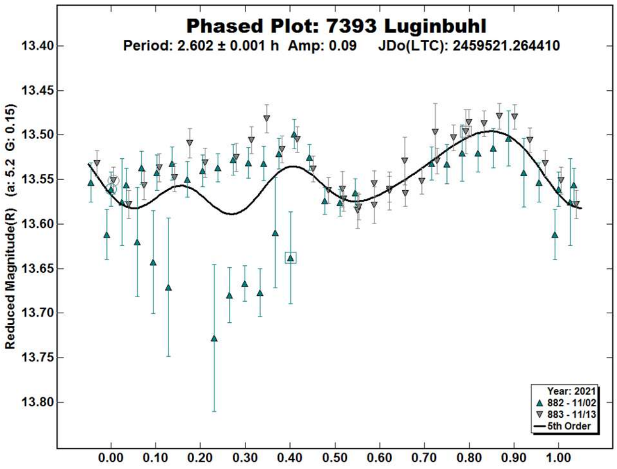

Figure 5: The phased lightcurve of 7393 Luginbuhl with all the collected points shows a probable eclipsing or occultation event.

Acknowledgements

Minor Planet Circulars (MPCs) are published by the International Astronomical Union's Minor Planet Center. *https://www.minorplanetcenter.net/iau/ECS/MPCArchive/MPCArchive_TBL.html*

References

DSFTA (2022). Dipartimento di Scienze Fisiche, della Terra e dell'Ambiente - Astronomical Observatory. *https://www.dsfta.unisi.it/en/research/labs/astronomical-observatory*

Harris, A.W.; Young, J.W.; Scaltriti, F.; Zappala, V. (1984). "Lightcurves and phase relations of the asteroids 82 Alkmene and 444 Gyptis." *Icarus* **57**, 251-258.

JPL (2022). Small Body Database Search Engine. *https://ssd.jpl.nasa.gov*

Luginbuhl, C.B.; Skiff, B.A. (1998). *Observing Handbook and Catalogue of Deep-Sky Objects.* pp 368. Cambridge University Press, Cambridge, UK.

Masiero, J.R.; Mainzer, A.K.; Grav, T.; Bauer, J.M.; Cutri, R.M.; Dailey, J.; Eisenhardt, P.R.M.; McMillan, R.S.; Spahr, T.B.; Skrutskie, M.F.; Tholen, D.; Walker, R.G.; Wright, E.L.; DeBaun, E.; Elsbury, D.; Gautier IV, T.; Gomillion, S.; Wilkins, A. (2011). "Main Belt Asteroids with WISE/NEOWISE. I. Preliminary Albedos and Diameters." *Astrophys. J.* **741**, A68.

Masiero, J.R.; Mainzer, A.K.; Grav, T.; Bauer, J.M.; Cutri, R.M.; Nugent, C.; Cabrera, M.S. (2012). "Preliminary Analysis of WISE/NEOWISE 3-Band Cryogenic and Post-cryogenic Observations of Main Belt Asteroids." *Astrophys. J. Letters* **759** L8.

Warner, B.D.; Harris, A.W.; Pravec, P. (2009). "The Asteroid Lightcurve Database." *Icarus* **202**, 134-146. Updated 2020 Oct. *http://www.minorplanet.info/lightcurvedatabase.html*

Warner, B.D. (2018). MPO Software, *MPO Canopus* v10.7.7.0. Bdw Publishing. *http://minorplanetobserver.com*

Warner, B.D.; Skiff, B.A. (2019). "(7393) Luginbuhl." *CBET* **4561**.

LIGHTCURVES AND ROTATION PERIODS OF 330 ADALBERTA, 494 VIRTUS, 530 TURANDOT, 784 PICKERINGIA, AND 1009 SIRENE

Frederick Pilcher
Organ Mesa Observatory (G50)
4438 Organ Mesa Loop
Las Cruces, NM 88011 USA
fpilcher35@gmail.com

(Received: 2022 Jan 6)

Synodic rotation periods and amplitudes are found for 330 Adalberta: 3.5553 ± 0.0001 h, 0.43 ± 0.02 mag; 494 Virtus: 40.42 ± 0.01 h, 0.21 ± 0.01 mag; 530 Turandot: 19.961 ± 0.001 h, 0.10 ± 0.01 mag; 784 Pickeringia: 13.169 ± 0.001 h, 0.19 ± 0.01 mag, and 1009 Sirene: 2.8796 ± 0.0005 h, 0.09 ± 0.02 mag. For 494 Virtus, V-R = 0.36; H(V) = 9.118 ± 0.023, G = 0.151 ± 0.039.

Observations to produce the results reported in this paper were made at the Organ Mesa Observatory with a Meade 35-cm LX200 GPS Schmidt-Cassegrain, SBIG STL-1001E CCD, unguided, clear filter. Image measurement and lightcurve construction were with *MPO Canopus* software with all calibration star magnitudes from the CMC15 catalog reduced to the Cousins R band. To reduce the number of data points on the lightcurves and make them easier to read, data points have been binned in sets of 3 with maximum time difference 5 minutes.

330 Adalberta. The only previously published rotation data set is by Alvarez and Pilcher (2014), 3.5553 h, 0.44 mag near celestial longitude 338°. New observations on four nights 2021 Oct. 11 - Nov. 8, near celestial longitude 37°, provide an excellent fit to exactly the same period, 3.5553 ± 0.0001 h, and an almost identical amplitude of 0.43 ± 0.02 mag.

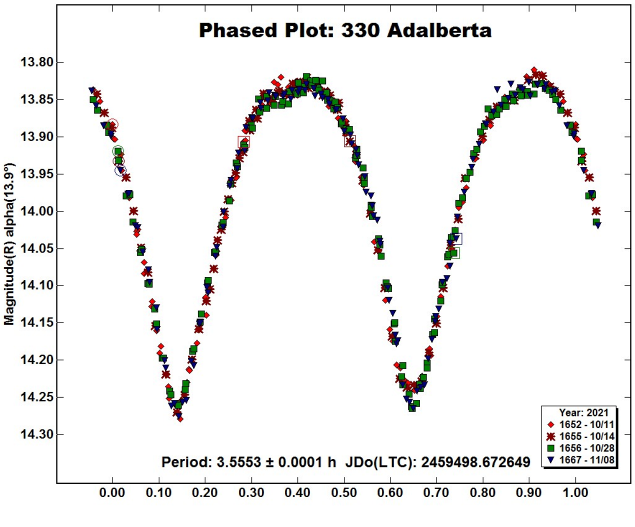

Figure 1. The lightcurve of 330 Adalberta phased to a period of 3.5553 hours.

494 Virtus. Several previously published periods are in great discordance: Behrend (2006web), 4.99 h, 0.03 mag; Warner (2006), 5.57 h, 0.12 mag near celestial longitude 16°; Behrend (2008web), 4.9903 h, 0.03 mag; Hamanowa and Hamanowa (2009), 5.57 h, 0.03 mag near celestial longitude 167°; Polakis (2018), 49.427 h, 0.05 mag near celestial longitude 139°. New observations on 15 nights 2021 Oct. 9 - Nov. 30 near celestial longitude 52° provide a good fit to a somewhat irregular bimodal lightcurve with period 40.42 ± 0.01 hours, amplitude 0.21 ± 0.01 magnitudes. This new result based on a dense data set that covers the entire double period rules out all previously published periods.

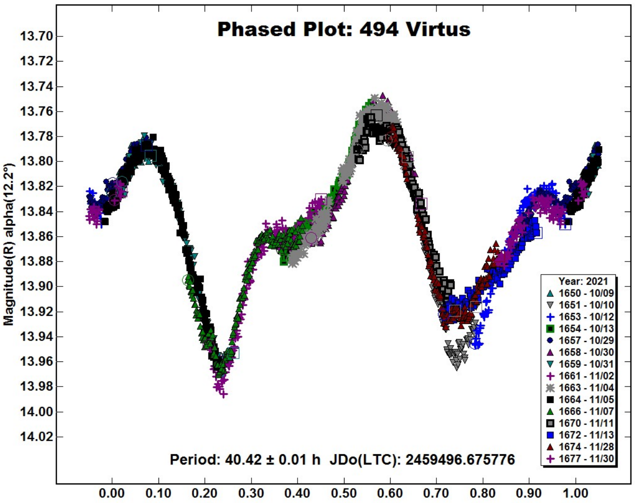

Figure 2. The lightcurve of 494 Virtus phased to a period of 40.42 hours.

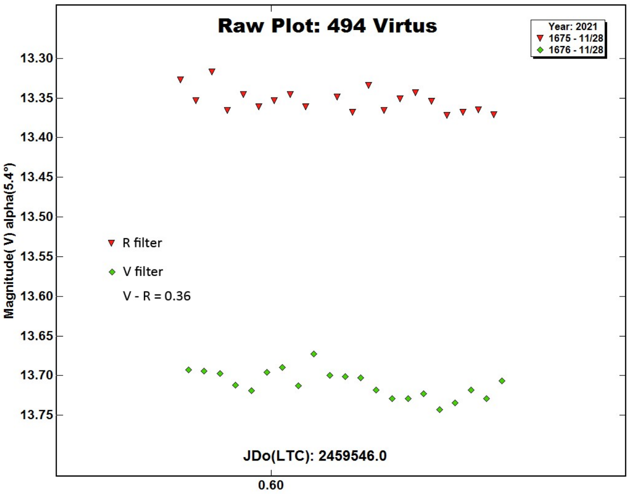

Figure 3. V and R lightcurves of 494 Virtus.

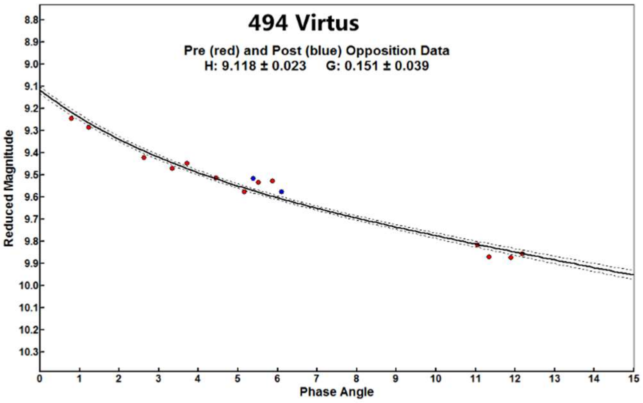

Figure 4. H-G plot for 494 Virtus in the V magnitude band.

On 2021 Nov. 28 twenty exposures were obtained alternating between the R and V filters. A raw lightcurve of both sessions shows that V-R = 0.36. An H-G plot from phase angle –12.2° to –0.8° to +6.2° in the V magnitude band shows *H* = 9.118 ± 0.023 and *G* = 0.151 ± 0.039 at mid light.

530 Turandot. The Lightcurve Data Base (LCDB; Warner et al. 2009, updated 2021 December) lists five previously published rotation periods, four of which are within 0.02 hours of the adopted value of 19.96 hours. New observations on seven nights 2021 Nov. 1 - 29 provide an excellent fit to a period of 19.961 ± 0.001 hours with an amplitude 0.10 ± 0.01 magnitudes. This value is in very good agreement with most previously published values.

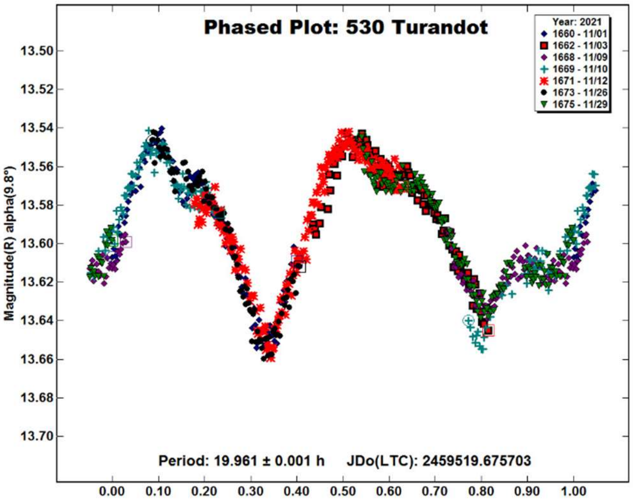

Figure 5. The lightcurve of 530 Turandot phased to a period of 19.961 hours.

784 Pickeringia. The Lightcurve Data Base (Warner et al. 2009, updated 2021 December) lists four previously published rotation periods that are all within 0.15 hours of the adopted value of 13.144 hours. New observations on four nights 2021 Nov. 6 - Dec. 6 provide an excellent fit to a period of 13.169 ± 0.001 hours, amplitude 0.19 ± 0.01 magnitudes. This value of the rotation period is consistent with other published values.

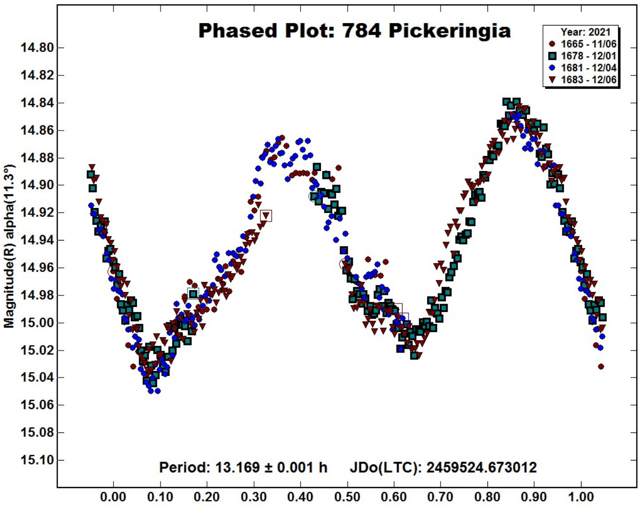

Figure 6. The lightcurve of 784 Pickeringia phased to a period of 13.169 hours.

1009 Sirene. This object has a highly eccentric and inclined orbit, *a* = 2.629, *e* = 0.454, *i* = 15.73°, H=13.9. In 2021 December it was just past perihelion and brighter than at any time in the previous several decades. Its faintness over this interval is the reason there are no previously published lightcurves.

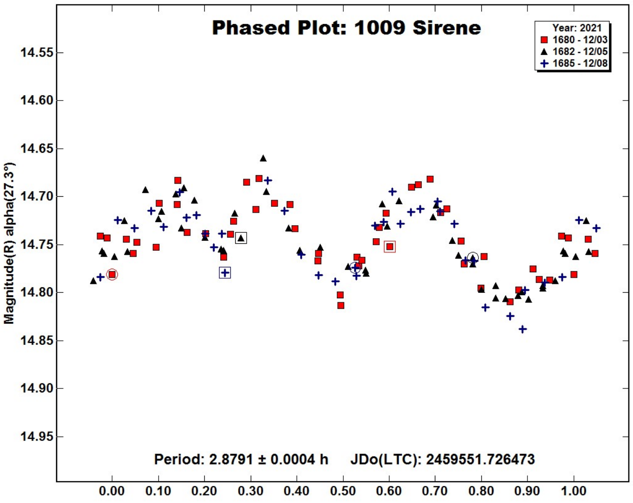

Figure 7. The lightcurve of 1009 Sirene, 2021 Dec. 3 - 8, phased to a period of 2.8791 hours

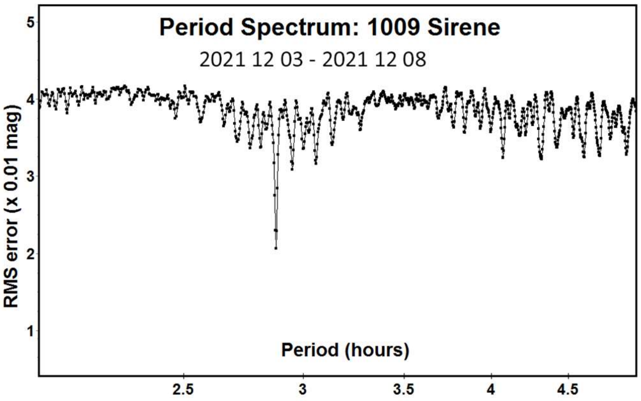

Figure 8. The period spectrum of 1009 Sirene, 2021 Dec. 3 - 8, between 2 and 5 hours.

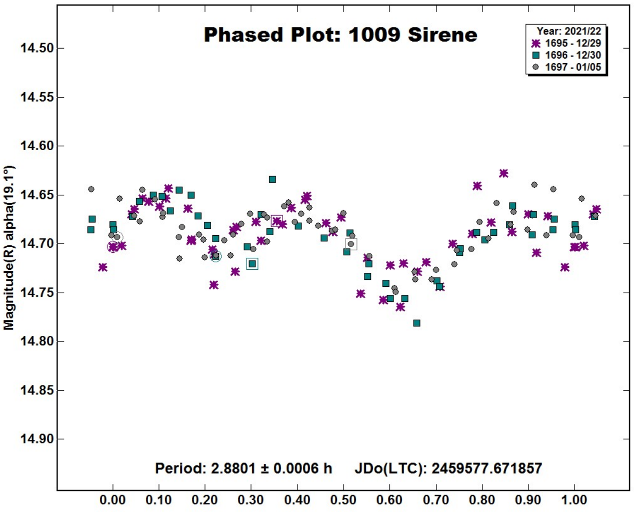

Figure 9. The lightcurve of 1009 Sirene, 2021 Dec. 29 - 2022 Jan. 5, phased to a period of 2.8801 hours.

Number	Name	20yy/mm/dd	Phase	L$_{PAB}$	L$_{PAB}$	Period(h)	P.E	Amp	A.E.
330	Adalberta	21/10/11-21/11/08	*13.9,9.2	37	-9	3.5553	0.0001	0.43	0.02
494	Virtus	21/10/09-21/11/30	*12.2,6.2	52	2	40.42	0.01	0.21	0.01
530	Turandot	21/11/01-21/11/29	*9.8,3.8	64	-10	19.961	0.001	0.10	0.01
784	Pickeringia	21/11/06-21/12/06	11.2,5.0	86	13	13.169	0.001	0.19	0.01
1009	Sirene	21/12/03-21/12/08	27.3,25.3	98	-17	2.8791	0.0004	0.09	0.02
1009	Sirene	21/12/30-22/01/05	19.1,18.6	104	-22	2.8801	0.0006	0.08	0.02

Table I. Observing circumstances and results. The phase angle is given for the first and last date. If a minimum phase angle was reached between these dates, an * is shown. LPAB and BPAB are the approximate phase angle bisector longitude and latitude at mid-date range (see Harris *et al.*, 1984).

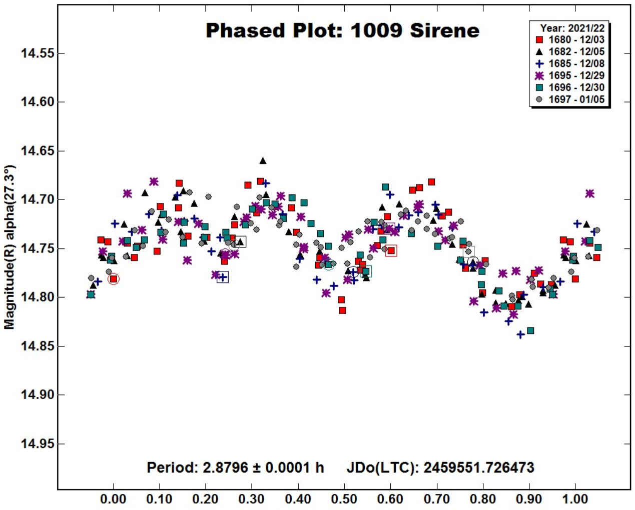

Figure 10. The lightcurve of 1009 Sirene, 2021 Dec. 3 - 2022 Jan. 5, phased to a period of 2.8796 hours.

More than 20 hours of photometric monitoring on three nights form 2021 Dec. 3-8 near celestial longitude 98°, celestial latitude -17°, and phase angle 26° provide a good fit to an asymmetric trimodal lightcurve with period 2.8791 ± 0.0004 hours, amplitude 0.09 ± 0.02 magnitudes. The period spectrum from 2 to 5 hours is presented. It shows one narrow minimum at 2.8791 hours much deeper than any other minima, strong evidence that between 2 hours and 5 hours no rotation period other than 2.8791 hours can be supported by these data. The split halves plot of the double period 5.758 hours (not presented here but available from the author on request) shows that the tenth order Fourier curves of the two halves are much closer together than the scatter of the individual data points, strong evidence against the double period. I offer two reasons to rule out one or two maxima and minima per cycle. Either would require a period less than the 2.2 hours centrifugal limit. Simple eyeballing of the lightcurve, and seeing the asymmetry of the three maxima, would also rule out a shorter period with fewer maxima and minima per rotational cycle, even if the centrifugal limit did not apply. All of these combined circumstances show that any period except 2.8791 hours can be ruled out. Hence, I claim that a period of 2.8791 hours is the correct one.

Mars-crossers do not move as rapidly across the sky as Earth crossers, but move faster than ordinary main belt asteroids. Three more sessions were obtained 2021 Dec. 29 - 2022 Jan. 5 near celestial longitude 104°, celestial latitude -22°, phase angle 19°. The lightcurve of these three sessions is somewhat noisier than the 2021 Dec. 3-8 lightcurve, but shows only a slightly different period, 2.8801 ± 0.0006 hours, and amplitude, 0.08 ± 0.02 magnitudes. The synodic periods for these two intervals differ by an amount no greater than their formal errors. The difference may not be significant. It may be useful to plot a phased lightcurve of all six sessions, which shows a mean synodic period for the interval 2021 Dec. 3 - 2022 Jan. 5 of 2.8796 hours. The real error is likely to be larger than the formal error of 0.0001 hours and I present the result as 2.8796 ± 0.0005 hours.

References

Alvarez, E.M.; Pilcher, F. (2014). "Period determination for 330 Adalberta: a low numbered asteroid with a previously unknown period." *Minor Planet Bull.* **41**, 23-24.

Behrend, R. (2006web, -2008web). Observatoire de Geneve web site. *http://obswww.unige.ch/~behrend/page_cou.html*

Hamanowa, H.; Hamanowa, H. (2009). "Lightcurves of 494 Virtus, 556 Phyllis, 657 Gunlod, 1111 Reinmuthia, 1188 Gothlandia, and 1376 Michelle." *Minor Planet Bull.* **36**, 87-88.

Harris, A.W.; Young, J.W.; Scaltriti, F.; Zappala, V. (1984). "Lightcurves and phase relations of the asteroids 82 Alkmene and 444 Gyptis." *Icarus* **57**, 251-258.

Polakis, T. (2018). "Lightcurve analysis for eleven main-belt minor planets." *Minor Planet Bull.* **45**, 269-273.

Warner, B.D. (2006). "Asteroid lightcurve analysis at the Palmer Divide Observatory - late 2005 and early 2006." *Minor Planet Bull.* **33**, 58-62.

Warner, B.D.; Harris, A.W.; Pravec, P. (2009). "The Asteroid Lightcurve Database." *Icarus* **202**, 134-146. Updated 2021 Dec. *https://www.minorplanet.info/php/lcdb.php*

PHOTOMETRY AND LIGHT CURVE ANALYSIS OF SIX ASTEROIDS BY GORA'S OBSERVATORIES

Milagros Colazo
Instituto de Astronomía Teórica y Experimental
(IATE-CONICET)
ARGENTINA
Facultad de Matemática, Astronomía y Física
Universidad Nacional de Córdoba, ARGENTINA
Grupo de Observadores de Rotaciones de Asteroides (GORA),
ARGENTINA
milirita.colazovinovo@gmail.com

Aldo Mottino, Damián Scotta, Tiago Speranza, César Fornari,
Ariel Stechina, Mario Morales, Alberto García, Francisco Santos,
Marcos Santucho, Néstor Suárez, Aldo Wilberger, Nicolás Arias,
Raúl Melia, Ezequiel Bellocchio, Matías Martini, Mateo Borello,
Carlos Galarza, Andrés Chapman, Carlos Colazo.
Grupo de Observadores de Rotaciones de Asteroides (GORA)
ARGENTINA

Observatorio Astronómico Giordano Bruno (MPC G05) Piconcillo
Córdoba, ESPAÑA

Observatorio Cruz del Sur (MPC I39) - San Justo
Buenos Aires, ARGENTINA

Observatorio de Sencelles (MPC K14) - Sencelles
Mallorca, Islas Baleares ESPAÑA

Observatorio Los Cabezones (MPC X12) - Santa Rosa
La Pampa, ARGENTINA

Observatorio Orbis Tertius (MPC X14) - Córdoba
Córdoba, ARGENTINA

Observatorio Galileo Galilei (MPC X31) - Oro Verde
Entre Ríos ARGENTINA)

Observatorio Antares (MPC X39) - Pilar
Buenos Aires ARGENTINA

Observatorio Río Cofio (MPC Z03) - Robledo de Chavela
Madrid ESPAÑA

Observatorio AstroPilar (GORA APB) - Pilar
Buenos Aires ARGENTINA

Observatorio de Aldo Mottino (GORA OAM) - Rosario
Santa Fe ARGENTINA

Observatorio Astronómico Aficionado Omega
(GORA OAO) - Córdoba
Córdoba ARGENTINA

Observatorio de Ariel Stechina 1 (GORA OAS) - Reconquista
Santa Fe ARGENTINA

Observatorio de Ariel Stechina 2 (GORA OA2) - Reconquista
Santa Fe ARGENTINA

Observatorio Cielos de Banfield (GORA OCB) - Banfield
Buenos Aires ARGENTINA

Observatorio de Damián Scotta 1
(GORA ODS) - San Carlos Centro
Santa Fe ARGENTINA

Observatorio de Damián Scotta 2
(GORA OD2) - San Carlos Centro
Santa Fe ARGENTINA

Observatorio Astronómico Municipal Reconquista
(GORA OMR) - Reconquista
Santa Fe ARGENTINA

Observatorio de Raúl Melia (GORA RMG) - Gálvez
Santa Fe ARGENTINA

(Received: 2021 Nov 29)

Synodic rotation periods and amplitudes are reported for 470 Kilia, 478 Tergeste, 548 Kressida, 666 Desdemona, 814 Tauris, and (68063) 2000 YJ66.

The periods and amplitudes of asteroid lightcurves presented here are the product of collaborative work by GORA (Grupo de Observadores de Rotaciones de Asteroides). In all the studies we have applied relative photometry assigning V magnitudes to the calibration stars.

Image acquisition was performed without filters and with exposure times of a few minutes. All images used were corrected using dark frames and, in some cases, bias and flat-fields. Photometry measurements were performed using *FotoDif* software and for the analysis, we employed *Periodos* software (Mazzone, 2012).

The lightcurve figures contain the following information: the estimated period and period error and the estimated amplitude and amplitude error. In the reference boxes, the columns represent, respectively, the marker, observatory MPC code or the GORA internal code, session date, session offset, and several data points.

Targets were selected based on the following criteria: 1) magnitudes accessible to the equipment of all participants, 2) those with favorable observation conditions from Argentina or Spain, *i.e.,* with negative or positive Declinations, and 3) objects with few periods reported in the literature and/or, in the Lightcurve Database (LCDB hereon; Warner et al., 2009) quality codes (U) of less than 3.

470 Kilia is an S-type asteroid discovered in 1901 by Carnera. Behrend (2010web) reported a period of 26.4 h. In contrast, Stephens (2009) measured a period of 290 h, and, recently, Pilcher and Polakis (2020) published a period of 296.0 ± 5 h. Our analysis yields a period of 297.655 ± 0.012 h and amplitude Δm = 0.40 ± 0.01 mag. Note that our period is in good agreement with a slow rotator, as previously proposed by Stephens and Pilcher and Polakis.

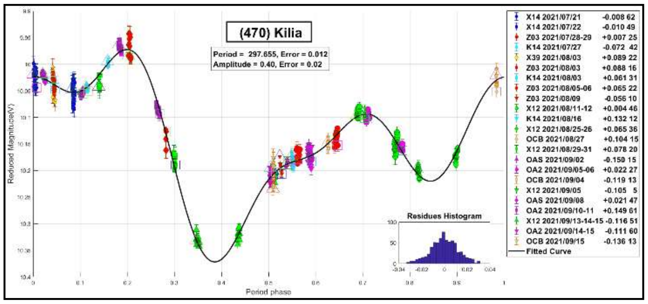

478 Tergeste is an S-type asteroid discovered in 1901 by Carnera. The period most recently reported in the literature is P = 16.105 ± 0.002 h (Marciniak et al., 2018). Previous observations, including several performed by the same author, yielded a similar period. The results we obtained are P = 16.110 ± 0.009 h and Δm = 0.19 ± 0.01 mag, in good agreement with previous results.

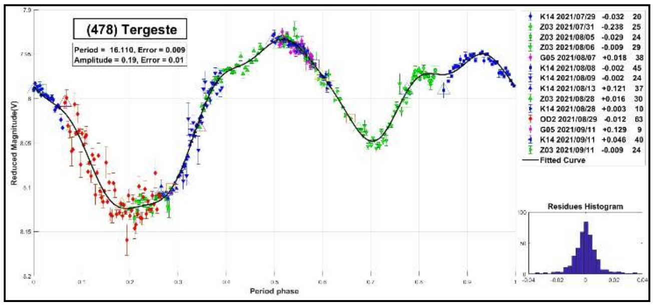

548 Kressida. This S-type asteroid was discovered in 1904 by Gotz. We measured a period of 11.930 ± 0.017 h with Δm = 0.25 ± 0.02 mag. These results agree well with those reported by Behrend (2002web) of *P* = 11.9404 ± 0.0006 h and Δm = 0.44 ± 0.02 mag. The difference between the amplitudes might be caused by the change in aspect angle between observations.

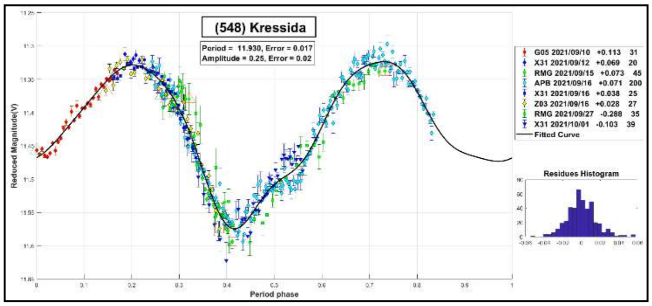

666 Desdemona was discovered in 1908 by Kopff. Behrend (2004web, 2005web, 2006web) reported three identical periods for this asteroid: 9.6 h. Nevertheless, Marciniak et al. (2015) published a period of 14.607 ± 0.004 h. We determined a period of 14.596 ± 0.005 h with Δm = 0.09 ± 0.01 mag, which is consistent with the one proposed by Marciniak et al.

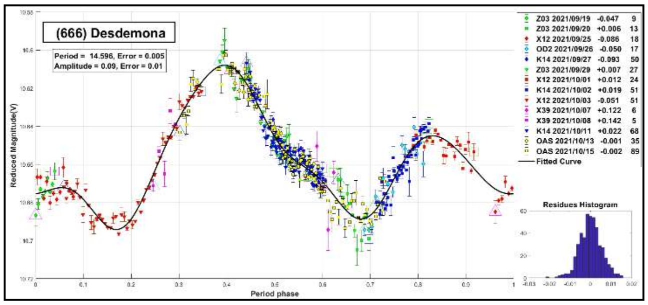

814 Tauris is a C-type asteroid that was discovered in 1916 by Neujmin. We measured a period of 36.081 ± 0.008 h with Δm = 0.15 ± 0.01 mag. Similar values were previously reported by Alkema (2013), who found *P* = 35.8 ± 0.1 h and Δm = 0.18 ± 0.03 mag.

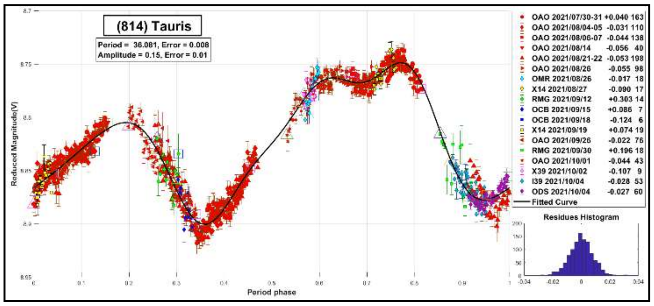

(68063) 2000 YJ66. This asteroid was discovered in 2000 from Kitt Peak Observatory, Arizona, USA, by the Spacewatch Program. It was linked to observations performed in 1964. After lightcurve analysis in 2014, Warner et al. (2015) proposed a companion for this asteroid. They reported a period of 2.1102 ± 0.0005 h and Δm = 0.14 ± 0.02 mag. Interestingly, our analysis yields rather different values. We found a period of *P* = 3.165 ± 0.016 h with Δm = 0.12 ± 0.02 mag. In view of such significant difference in the period, we believe that this case deserves further observations and analysis.

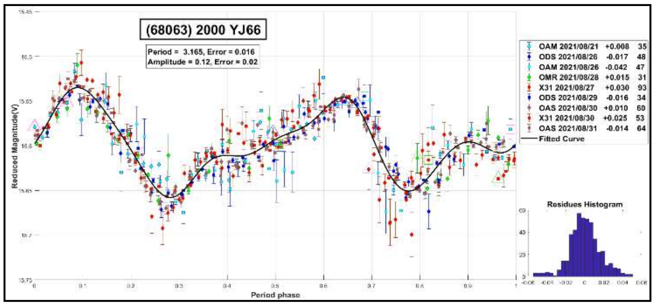

Acknowledgements

We want to thank Julio Castellano for his *FotoDif* program for preliminary analyses, Fernando Mazzone for his *Periods* program, used in final analyses, and Matías Martini for his *CalculadorMDE_v0.2* used for generating ephemerides used in the planning stage of the observations. This research has made use of the Small Bodies Data Ferret (*http://sbn.psi.edu/ferret/*), supported by the NASA Planetary System. This research has made use of data and/or services provided by the International Astronomical Union's Minor Planet Center.

Number	Name	yy/ mm/dd- yy/ mm/dd	Phase	L_{PAB}	B_{PAB}	Period (h)	P.E.	Amp	A.E.	Grp
470	Kilia	21/07/21-21/09/15	*9.5,16.5	315	6	297.655	0.012	0.40	0.02	MB-O
478	Tergeste	21/07/29-21/09/11	*10.7,8.0	332	16	16.110	0.009	0.19	0.01	MB-O
548	Kressida	21/09/10-21/10/01	*4.4,9.6	353	-5	11.930	0.017	0.25	0.02	MB-I
666	Desdemona	21/09/19-21/10/15	*10.3,6.1	12	6	14.596	0.005	0.09	0.01	MB-O
814	Tauris	21/07/30-21/10/04	*11.5,21.9	320	-24	36.081	0.008	0.15	0.01	MB-O
68063	2000 YJ66	21/08/21-21/08/31	6.2,10.5	330	6	3.165	0.016	0.12	0.02	NEA

Table I. Observing circumstances and results. The phase angle is given for the first and last date. If preceded by an asterisk, the phase angle reached an extremum during the period. L_{PAB} and B_{PAB} are the approximate phase angle bisector longitude/latitude at mid-date range (see Harris et al., 1984). Grp is the asteroid family/group (Warner et al., 2009). MB-I/O: main-belt inner/outer. NEA: near-Earth Asteroid.

Observatory	Telescope	Camera
G05 Obs.Astr.Giordano Bruno	SCT (D=203mm; f=6.0)	CCD Atik 420 m
I39 Obs.Astr.Cruz del Sur	Newtoniano (D=254mm; f=4.7)	CMOS QHY174
K14 Obs.Astr.de Sencelles	Newtoniano (D=250mm; f=4.0)	CCD SBIG ST-7XME
X12 Obs.Astr.Los Cabezones	Newtoniano (D=200mm; f=5.0)	CMOS QHY174MGPS
X14 Obs.Astr.Orbis Tertius	Newtoniano (D=200mm; f=5.0)	CMOS P1 Neptune M
X31 Obs.Astr.Galileo Galilei	RCT ap (D=405mm; f=8.0)	CCD SBIG STF8300M
X39 Obs.Astr.Antares	Newtoniano (D=250mm; f=4.7)	CCD QHY9 Mono
Z03 Obs.Astr.Río Cofio	SCT (D=254mm; f=6.3)	CCD SBIG ST8-XME
APB Obs.Astr.AstroPilar	Refractor (D=150mm; f=7.0)	CCD ZWO-ASI183
OAM Obs.Astr.de Aldo Mottino	Newtoniano (D=250mm; f=4.7)	CCD SBIG STF8300M
OAO Obs.Astr.Aficionado Omega	Newtoniano (D=150mm; f=5.0)	CMOS ZWO ASI178mm
OAS Obs.Astr.de Ariel Stechina 1	Newtoniano (D=254mm; f=4.7)	CCD SBIG STF402
OA2 Obs.Astr.de Ariel Stechina 2	Newtoniano (D=305mm; f=5.0)	CMOS QHY 174M
OCB Obs.Astr.Cielos de Banfield	Newtoniano (D=150mm; f=5.0)	CMOS QHY5L-II M
ODS Obs.Astr.de Damián Scotta 1	Newtoniano (D=300mm; f=4.0)	CMOS QHY 174M
OD2 Obs.Astr.de Damián Scotta 2	Newtoniano (D=250mm; f=4.0)	CCD Atik 314L+
OMR Obs.Astr.Municipal Reconquista	Newtoniano (D=254mm; f=4.0)	CMOS QHY5 Mono
RMG Obs.Astr.de Raúl Melia	Newtoniano (D=254mm; f=4.7)	CCD Meade DSI Pro II

Table II. List of observatories and equipment.

References

Alkema, M.S. (2013). “Asteroid Lightcurve Analysis at Elephant Head Observatory: 2013 April-July.” *Minor Planet Bulletin* **40**(4), 215-216.

Behrend, R. (2002web, 2004web, 2005web, 2006web, 2010web). Observatoire de Geneve web site.
http://obswww.unige.ch/~behrend/page_cou.html

Harris, A.W.; Young, J.W.; Scaltriti, F.; Zappala, V. (1984). “Lightcurves and phase relations of the asteroids 82 Alkmene and 444 Gyptis.” *Icarus* **57**, 251-258.

Marciniak, A.; Pilcher, F.; Oszkiewicz, D.; Santana-Ros, T.; Urakawa, S. and 19 colleagues (2015). “Against the biases in spins and shapes of asteroids.” *Planetary and Space Science* **118**, 256-266.

Marciniak, A.; Bartczak, P.; Müller, T.; Sanabria, J.J.; Alí-Lagoa, V. and 38 colleagues (2018). “Photometric survey, modelling, and scaling of long-period and low-amplitude asteroids.” *Astron. & Astrophys.* **610**, A7.

Mazzone, F.D. (2012). Periodos software, version 1.0.
http://www.astrosurf.com/salvador/Programas.html

Pilcher, F.; Polakis, T. (2020). “A Photometric Study of 470 Kilia.” *Minor Planet Bulletin* **47**, 247-248.

Stephens, R.D. (2009). “Asteroids Observed from GMARS and Santana Observatories-April to May 2009.” *Minor Planet Bulletin* **36**, 157-158.

Warner, B.D.; Harris, A.W.; Pravec, P. (2009). “The Asteroid Lightcurve Database.” *Icarus* **202**, 134-146. Updated 2021 Oct. *http://www.minorplanet.info/lightcurvedatabase.html*

Warner, B.D.; Stephens, R.D.; Harris, A.W. (2015). “A Trio of Binary Asteroids.” *Minor Planet Bulletin* **42**, 31.

COLLABORATIVE ASTEROID PHOTOMETRY FROM UAI: 2021 OCTOBER-DECEMBER

Lorenzo Franco
Balzaretto Observatory (A81), Rome, ITALY
lor_franco@libero.it

Alessandro Marchini, Riccardo Papini
Astronomical Observatory, DSFTA - University of Siena (K54)
Via Roma 56, 53100 - Siena, ITALY

Marco Iozzi
HOB Astronomical Observatory (L63), Capraia Fiorentina, ITALY

Paolo Bacci, Martina Maestripieri
GAMP - San Marcello Pistoiese (104), Pistoia, ITALY

Giorgio Baj
M57 Observatory (K38), Saltrio, ITALY

Gianni Galli
GiaGa Observatory (203), Pogliano Milanese, ITALY

Fabio Mortari, Davide Gabellini
Hypatia Observatory (L62), Rimini, ITALY

Nello Ruocco
Osservatorio Astronomico Nastro Verde (C82), Sorrento, ITALY

Luciano Tinelli
GAV (Gruppo Astrofili Villasanta), Villasanta, ITALY

Nico Montigiani, Massimiliano Mannucci
Osservatorio Astronomico Margherita Hack (A57)
Florence, ITALY

Giulio Scarfi
Iota Scorpii Observatory (K78), La Spezia, ITALY

Fabio Salvaggio
Wild Boar Remote Observatory (K49)
San Casciano in Val di Pesa (FI), ITALY

(Received: 2022 Jan 13)

Photometric observations of eight asteroids were made in order to acquire lightcurves for shape/spin axis modeling. The synodic period and lightcurve amplitude were found for 197 Arete, 359 Georgia, 796 Sarita, 901 Brunsia, 1346 Gotha, 4660 Nereus, 4935 Maslachkova and 6249 Jennifer.

Collaborative asteroid photometry was done inside the Italian Amateur Astronomers Union (UAI; 2021) group. The targets were selected mainly in order to acquire lightcurves for shape/spin axis modeling. Table II shows the observing circumstances and results.

The CCD observations of eight asteroids were made in 2021 October-December using the instrumentation described in Table I. Lightcurve analysis was performed at the Balzaretto Observatory with *MPO Canopus* (Warner, 2021). All the images were calibrated with dark and flat frames and converted to R magnitudes using solar colored field stars from CMC15 catalogue, distributed with *MPO Canopus*. For brevity, the following citations to the asteroid lightcurve database (LCDB; Warner et al., 2009) will be summarized only as "LCDB".

197 Arete is an S-type (Bus and Binzel, 2002) middle main-belt asteroid. Collaborative observations were made over seven nights. The data analysis shows a synodic period of $P = 6.608 \pm 0.001$ h with an amplitude $A = 0.12 \pm 0.02$ mag. The period is close to the previously published results in the LCDB.

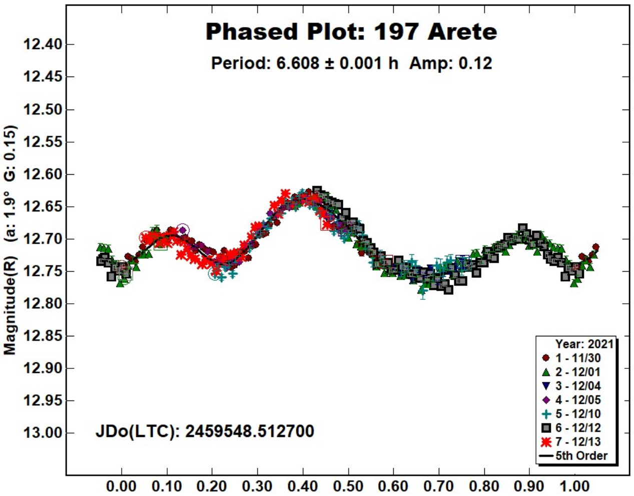

359 Georgia is an X-type (Bus and Binzel, 2002) middle main-belt asteroid. Collaborative observations were made over six nights. The data analysis shows a synodic period of $P = 5.534 \pm 0.001$ h with an amplitude $A = 0.23 \pm 0.03$ mag. The period is close to the previously published results in the LCDB.

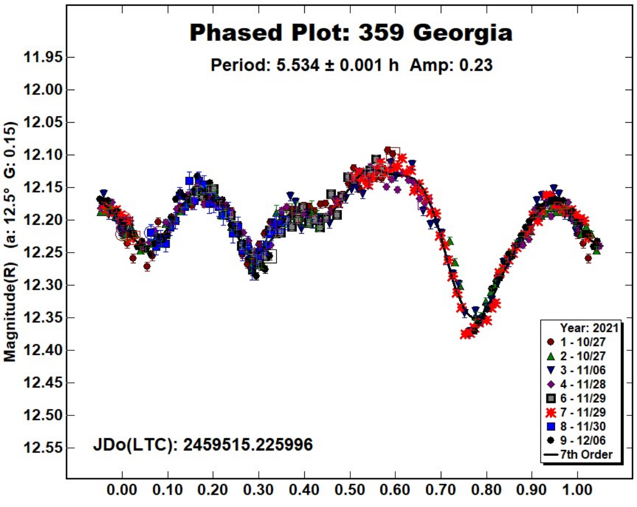

796 Sarita is an X-type (Bus and Binzel, 2002) middle main-belt asteroid. Collaborative observations were made over five nights. The data analysis shows a synodic period of $P = 8.176 \pm 0.002$ h with an amplitude $A = 0.32 \pm 0.02$ mag. The period is close to the previously published results in the LCDB.

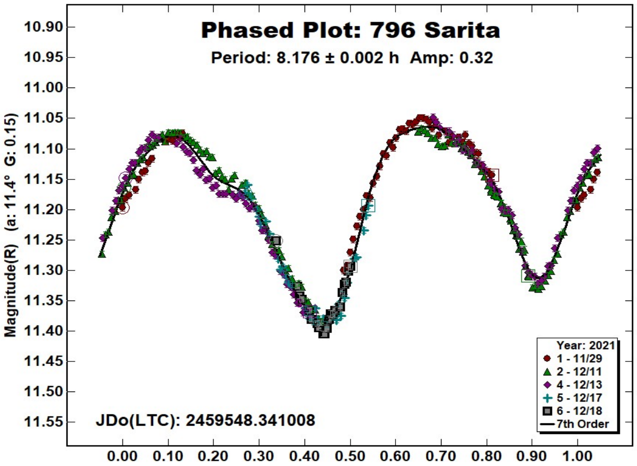

901 Brunsia is an S-type (Tholen, 1984) inner main-belt asteroid. Collaborative observations were made over six nights. We found a synodic period of P = 3.1356 ± 0.0003 h with an amplitude A = 0.19 ± 0.03 mag. The period is close to the previously published results in the LCDB.

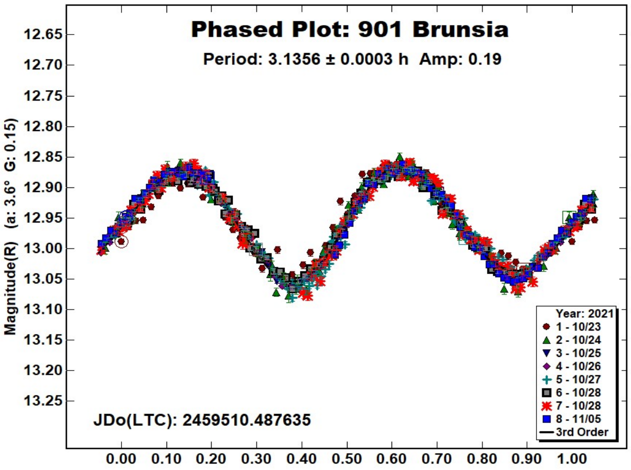

1346 Gotha is a medium albedo middle main-belt asteroid. Collaborative observations were made over eight nights. We found a synodic period of P = 2.6407 ± 0.0002 h with an amplitude A = 0.14 ± 0.02 mag. The period is close to the previously published results in the LCDB.

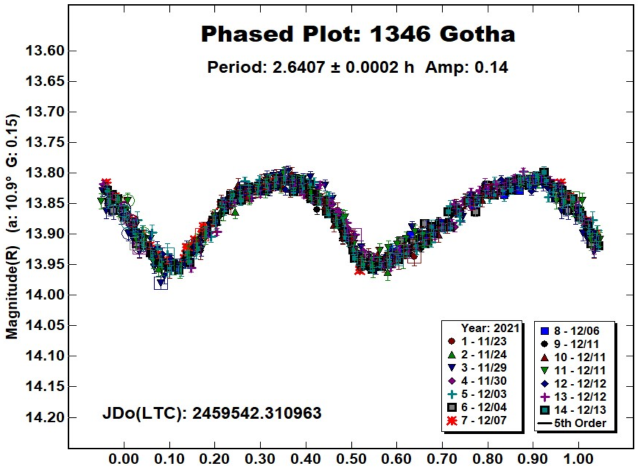

4660 Nereus is an Apollo Near-Earth asteroid classified as Potentially Hazardous Asteroid (PHA). Collaborative observations were made over seven nights using filtered (R band) and unfiltered images. The comparison star R magnitudes were obtained from the ATLAS catalog (Tonry et al., 2018), distributed with *MPO Canopus*, and no offset was applied to the sessions. We found a synodic period of P = 15.26 ± 0.01 h with an amplitude A = 1.05 ± 0.06 mag. The lightcurve shows some phase and amplitude variations, according to the tumbling nature of this asteroid (Pravec, 2021web). The period is slightly higher than the previously published results in the LCDB.

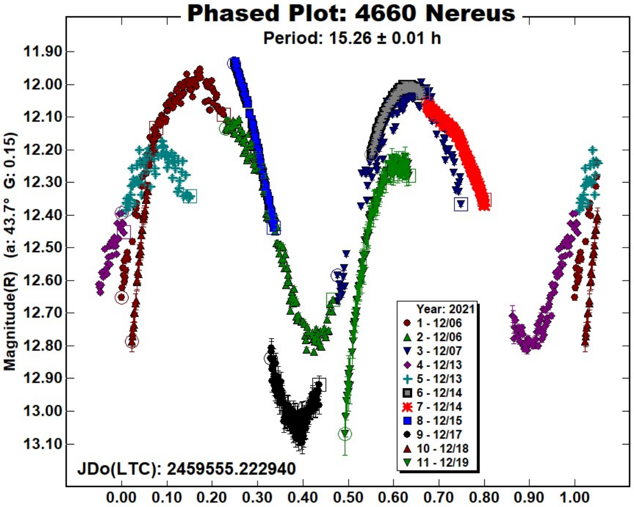

4935 Maslachkova is a medium albedo inner main-belt asteroid. Collaborative observations were made over four nights. We found a synodic period of P = 2.9019 ± 0.0001 h with an amplitude A = 0.23 ± 0.04 mag. The period is close to the previously published results in the LCDB.

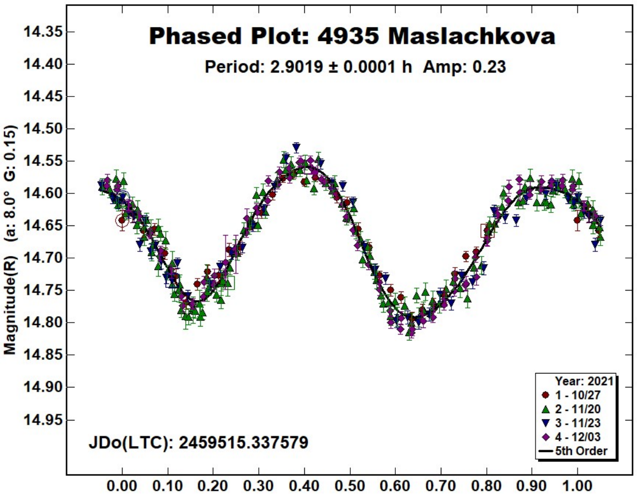

6249 Jennifer is an Xe-type (Bus and Binzel, 2002) inner main-belt asteroid. Collaborative observations were made over five nights. We found a synodic period of P = 4.958 ± 0.001 h with an amplitude A = 0.47 ± 0.03 mag. The period is close to the previously published results in the LCDB. The lightcurve shows an increasing amplitude for the last two sessions, acquired at the phase angle 22.6° and 24.6°.

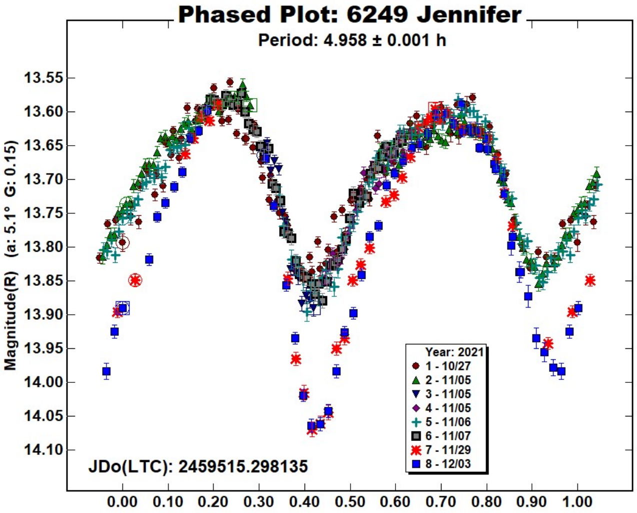

References

Bus, S.J.; Binzel, R.P. (2002). “Phase II of the Small Main-Belt Asteroid Spectroscopic Survey - A Feature-Based Taxonomy.” *Icarus* **158**, 146-177.

Harris, A.W.; Young, J.W.; Scaltriti, F.; Zappala, V. (1984). “Lightcurves and phase relations of the asteroids 82 Alkmene and 444 Gyptis.” *Icarus* **57**, 251-258.

Pravec, P. (2021web). *http://www.asu.cas.cz/~asteroid/04660.png*

Tholen, D.J. (1984). “Asteroid taxonomy from cluster analysis of Photometry.” Doctoral Thesis. University Arizona, Tucson.

Tonry, J.L.; Denneau, L.; Flewelling, H.; Heinze, A.N.; Onken, C.A.; Smartt, S.J.; Stalder, B.; Weiland, H.J.; Wolf, C. (2018). “The ATLAS All-Sky Stellar Reference Catalog.” *Astrophys. J.* **867**, A105.

UAI (2021). “Unione Astrofili Italiani” web site.
https://www.uai.it

Warner, B.D.; Harris, A.W.; Pravec, P. (2009) “The asteroid lightcurve database.” *Icarus* **202**, 134-146. Updated 2022 Jan 10. *https://minplanobs.org/alcdef/index.php*

Warner, B.D. (2021). MPO Software, *MPO Canopus* v10.8.5.0. Bdw Publishing. *http://minorplanetobserver.com*

Observatory (MPC code)	**Telescope**	**CCD**	**Filter**	**Observed Asteroids (#Sessions)**
Astronomical Observatory of the University of Siena(K54)	0.30-m MCT f/5.6	SBIG STL-6303e (2x2)	C,Rc	197(2), 796(1), 901(1), 1346(4), 4660(2), 6249(3)
HOB Astronomical Observatory (L63)	0.20-m SCT f/6.8	ATIK 383L+	C	197(4), 359(2), 901(1), 796(2), 1346(2)
GAMP (104)	0.60-m NRT f/4.0	Apogee Alta	C	1346(4), 4660(5)
M57 (K38)	0.35-m RCT f/5.5	SBIG STT1603ME	Rc	197(1), 359(2), 901(2), 4935(1)
GiaGa Observatory (203)	0.36-m SCT f/5.8	Moravian G2-3200	Rc	1346(2), 6249(2)
Hypatia Observatory (L62)	0.25-m RCT f/5.3	SBIG ST8-XE	Rc	359(1), 796(2)
Osservatorio Astronomico Nastro Verde (C82)	0.35-m SCT f/6.3	SBIG ST10XME (2x2)	C	901(2), 4935(1)
GAV	0.20-m SCT f/7.0	SXV-H9	Rc	359(3)
Osservatorio Astronomico Margherita Hack (A57)	0.35-m SCT f/8.3	SBIG ST10XME (2x2)	C	4935(2)
Iota Scorpii(K78)	0.40-m RCT f/8.0	SBIG STXL-6303e (2x2)	Rc	901(1)
WBRO (K49)	0.235-m SCT f/10	SBIG ST8-XME	Rc	1346(1)

Table I. Observing Instrumentation. MCT: Maksutov-Cassegrain, NRT: Newtonian Reflector, RCT: Ritchey-Chretien, SCT: Schmidt-Cassegrain.

Number	Name	2021 mm/dd	Phase	L_{PAB}	B_{PAB}	Period(h)	P.E.	Amp	A.E.	Grp
197	Arete	11/30-12/13	*1.9,4.0	72	-2	6.608	0.001	0.12	0.02	MB-M
359	Georgia	10/27-12/06	12.5,22.8	12	2	5.534	0.001	0.23	0.03	MB-M
796	Sarita	11/29-12/18	11.4,18.5	55	13	8.176	0.002	0.32	0.02	MB-M
901	Brunsia	10/23-11/05	*3.5,7.0	32	4	3.1356	0.0003	0.19	0.03	MB-I
1346	Gotha	11/23-12/13	10.8,13.9	64	-19	2.6407	0.0002	0.14	0.02	MB-M
4660	Nereus	12/06-12/19	43.6,103.8	110	29	15.26	0.01	1.05	0.06	NEA
4935	Maslachkova	10/27-12/03	*7.9,18.1	43	-9	2.9019	0.0001	0.23	0.04	MB-I
6249	Jennifer	10/27-12/03	*5.1,24.6	37	-1	4.958	0.001	0.47	0.03	MB-I

Table II. Observing circumstances and results. The first line gives the results for the primary of a binary system. The second line gives the orbital period of the satellite and the maximum attenuation. The phase angle is given for the first and last date. If preceded by an asterisk, the phase angle reached an extrema during the period. L_{PAB} and B_{PAB} are the approximate phase angle bisector longitude/latitude at mid-date range (see Harris et al., 1984). Grp is the asteroid family/group (Warner et al., 2009).

LIGHTCURVES FOR THIRTEEN MINOR PLANETS

Tom Polakis
Command Module Observatory
121 W. Alameda Dr.
Tempe, AZ 85282
tpolakis@cox.net

(Received: 2022 January 4)

Photometric measurements were made for 13 main-belt asteroids, based on CCD observations made from 2021 October through December. Phased lightcurves were created for 12 asteroids, while one did not yield a period solution. All the data have been submitted to the ALCDEF database.

CCD photometric observations of 13 main-belt asteroids were performed at Command Module Observatory (MPC V02) in Tempe, AZ. Images were taken using a 0.32-m *f*/6.7 Modified Dall-Kirkham telescope, SBIG STXL-6303 CCD camera, and a 'clear' glass filter. Exposure time for all the images was 2 minutes. The image scale after 2×2 binning was 1.76 arcsec/pixel. Table I shows the observing circumstances and results. All of the images for these asteroids were obtained between 2021 October and 2021 December.

Images were calibrated using a dozen bias, dark, and flat frames. Flat-field images were made using an electroluminescent panel. Image calibration and alignment was performed using *MaxIm DL* software.

The data reduction and period analysis were done using *MPO Canopus* (Warner, 2020). The 45'×30' field of the CCD typically enables the use of the same field center for three consecutive nights. In these fields, the asteroid and three to five comparison stars were measured. Comparison stars were selected with colors within the range of 0.5 < B-V < 0.95 to correspond with color ranges of asteroids. In order to reduce the internal scatter in the data, the brightest stars of appropriate color that had peak ADU counts below the range where chip response becomes nonlinear were selected. *MPO Canopus* plots instrumental vs. catalog magnitudes for solar-colored stars, which is useful for selecting comp stars of suitable color and brightness.

Since the sensitivity of the KAF-6303 chip peaks in the red, the clear-filtered images were reduced to Sloan r´ to minimize error with respect to a color term. Comparison star magnitudes were obtained from the ATLAS catalog (Tonry et al., 2018), which is incorporated directly into *MPO Canopus*. The ATLAS catalog derives Sloan *griz* magnitudes using a number of available catalogs. The consistency of the ATLAS comp star magnitudes and color-indices allowed the separate nightly runs to be linked often with no zero-point offset required or shifts of only a few hundredths of a magnitude in a series.

A 9-pixel (16 arcsec) diameter measuring aperture was used for asteroids and comp stars. It was typically necessary to employ star subtraction to remove contamination by field stars. For the asteroids described here, I note the RMS scatter on the phased lightcurves, which gives an indication of the overall data quality including errors from the calibration of the frames, measurement of the comp stars, the asteroid itself, and the period-fit. Period determination was done using the *MPO Canopus* Fourier-type FALC fitting method (cf. Harris et al., 1989). Phased lightcurves show the maximum at phase zero. Magnitudes in these plots are apparent and scaled by *MPO Canopus* to the first night. In cases where rotation periods could not be determined, raw lightcurves are presented, with "Raw" appearing in the upper right-hand corner of the plots.

Most asteroids were selected from the CALL website (Warner, 2011) In this set of observations, 2 of the 13 asteroids had no previous period analysis, 2 had U = 1, 9 had U = 2, and 1 had U = 3. The Asteroid Lightcurve Database (LCDB; Warner et al., 2009) was consulted to locate previously published results. All the new data for these asteroids can be found in the ALCDEF database.

494 Virtus was discovered by Max Wolf at Heidelberg in 1902. Several papers show short rotational periods: Behrend (2008web) 4.9903 ± 0.0004 h; Warner (2006) 5.57 ± 0.01 h; and Hamanowa (2009) 5.570 ± 0.003 h. Polakis (2018) computed a longer period of 49.427 ± 0.022 h. During six nights, 508 images were taken to determine a period of 40.13 ± 0.03 h, disagreeing with previous values. The amplitude of the lightcurve is 0.19 ± 0.02 mag.

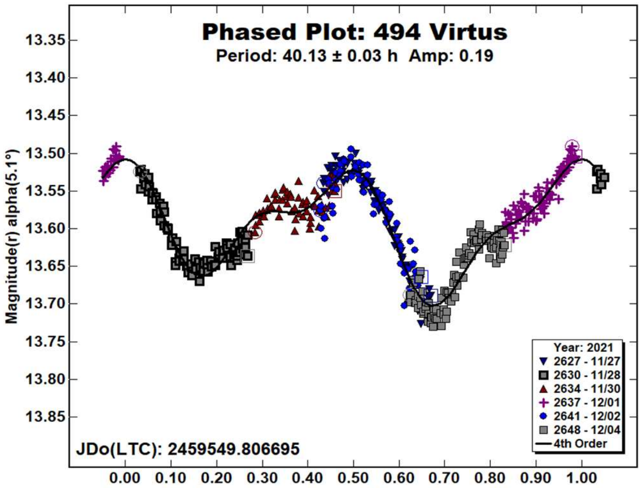

666 Desdemona. This inner main-belt asteroid was discovered by August Kopff at Heidelberg in 1908. The most recent of the many concurring period solutions are Pál et al. (2020) 14.5995 ± 0.0005 h and Dose (2022) 14.612 ± 0.014 h. This asteroid has a very eccentric orbit (*e* = 0.24), and the 2021 opposition was favorably close. A total of 219 data points were acquired during four nights, producing a period solution of 14.608 ± 0.011 h and an amplitude of 0.11 ± 0.01 mag.

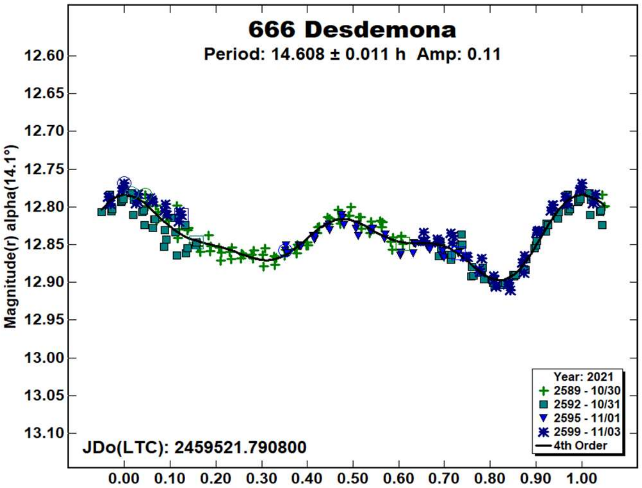

957 Camelia is one of Karl Reinmuth’s many discoveries at Heidelberg, having been announced in 1921. Warner (2001) derived a period of 5.391 ± 0.02 h, and Behrend (2020web) shows 8.984 ± 0.004 h. Obtained over seven nights, the 460 data points did not result in any minima in the period spectrum for these short periods, rather the best solution is 85.05 ± 0.11 h. The amplitude of the lightcurve is 0.20 ± 0.12 mag.

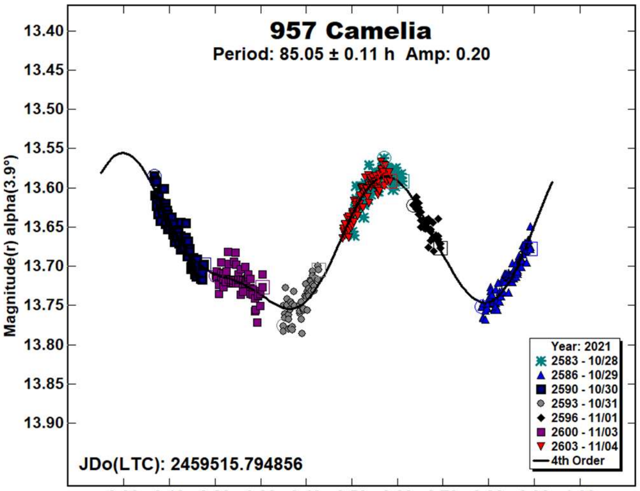

1243 Pamela is an outer main-belt asteroid, discovered by Cyril Jackson at Johannesburg in 1932. The most precise period determinations are those of Warner (2000), who published 26.017 ± 0.013 h and Garceran et al. (2016), who obtained 26.00 ± 0.01 h. During five nights, 348 images were acquired, yielding a solution of 26.01 ± 0.02 h with an amplitude of 0.46 ± 0.02 mag.

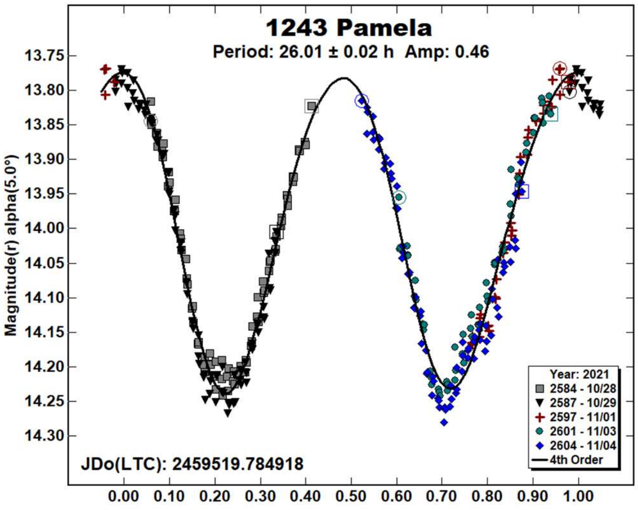

1558 Jarnefelt. Liisi Oterma made the discovery of this minor planet in Turku in 1942. Two period solutions are found in the LCDB: Hawkins and Ditteon (2016; 18.22 ± 0.06 h) and Polakis (2019; 6.252 ± 0.003 h). A total of 216 images were gathered in three nights to produce a period solution of 6.255 ± 0.007 h, in agreement with the more recent solution. The amplitude of the lightcurve is 0.13 mag, and the RMS error is 0.04 mag.

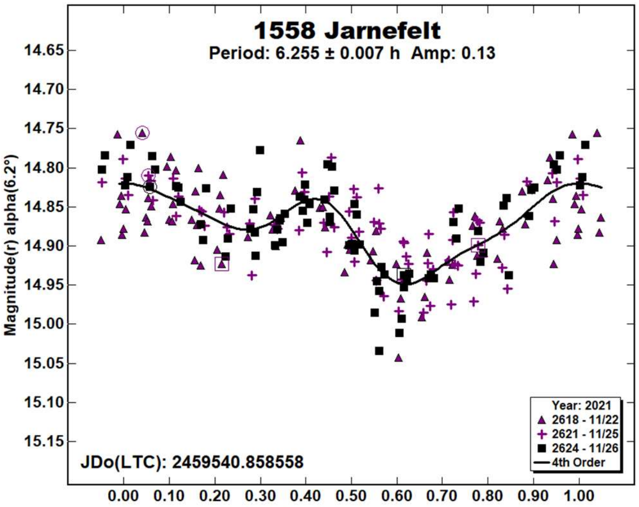

1763 Williams was discovered at Goethe Link Observatory in 1963. Durech et al. (2018) published a sidereal period of 88.030 ± 0.002 h. After eight nights, 533 images were obtained. The resulting period solution is 86.62 ± 0.15 h, in rough agreement with Durech’s value. The amplitude is 0.56 ± 0.04 mag. A curious feature resembling that of an eclipse by a companion is apparent at a phase of 0.1. Denser follow-up observations are encouraged.

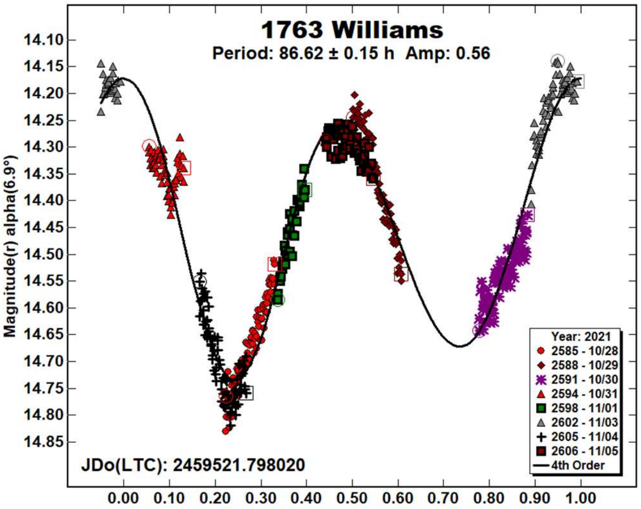

1911 Schubart. This Hilda asteroid was discovered in 1973 by Paul Wild at Zimmerwald. Stephens (2016) found a period of 11.915 ± 0.002 h and Warell (2017) published a value of 7.91 ± 0.02 h. In total, 284 observations were made on three November nights, producing a synodic period of 11.930 ± 0.013 h, which agrees with the solution by Stephens. The lightcurve has an amplitude of 0.24 ± 0.04 mag.

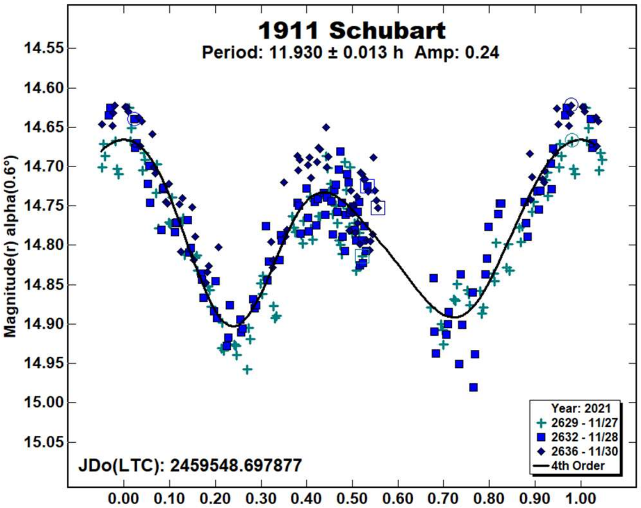

2219 Mannucci. This outer main-belt asteroid was first identified at Felix Aguilar Observatory in 1975. The only period solution in the LCDB is that of Durech et al. (2020), who published 27.4587 ± 0.0003 h. Due to its period being nearly commensurate with earth's rotation, the five observing nights were spaced over a 22-day interval. The synodic period is 27.47 ± 0.01 h, with an amplitude of 0.59 ± 0.05 mag.

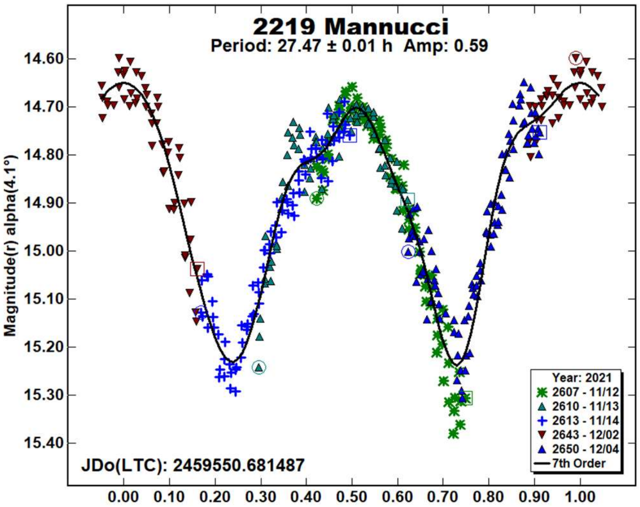

2301 Whitford was discovered at Goethe Link Observatory in 1965. Waszczak et al. (2015) showed a period of 14.275 ± 0.0049 h and Durech et al. (2020) computed 14.30151 ± 0.00006 h. During three nights, 233 images were used to obtain a similar period of 14.319 ± 0.015 h, with an amplitude of 0.43 ± 0.03 mag.

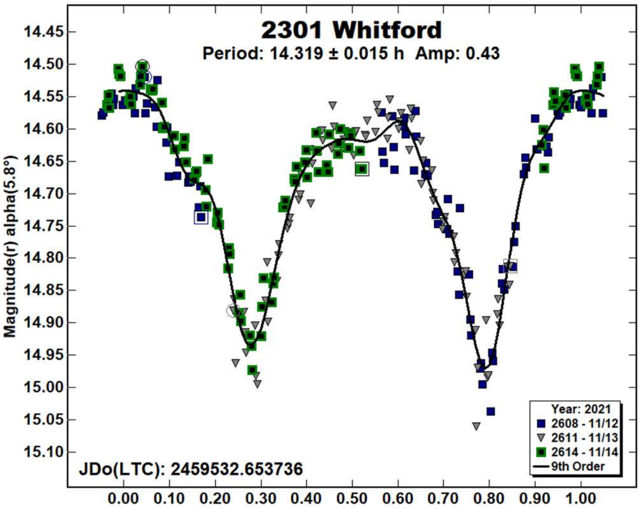

5121 Numazawa is a Flora-family asteroid discovered by Yanai and Watanabe in 1989 at Kitami. No periods appear for it in the LCDB. After three nights, it became apparent that a period would not be easily obtainable at this level of scatter. No period solution was found, and the lightcurve shown is the raw data.

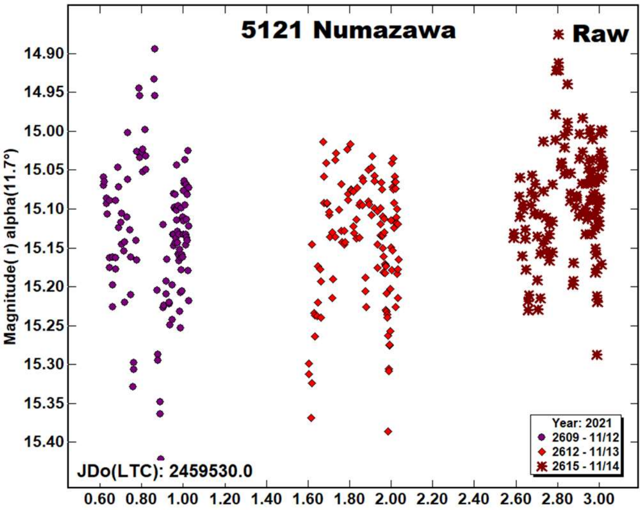

6249 Jennifer is a main-belt asteroid in a highly inclined orbit. It was first identified at Palomar in 1991 by Eleanor Helin. Many concurring period solutions may be found in the LCDB. The most recent of these is Warner (2015), who published a synodic period of 4.957 ± 0.001 h. During a single night, 128 images were gathered, yielding a period of 5.015 ± 0.013 h, with an amplitude of 0.35 ± 0.02 mag.

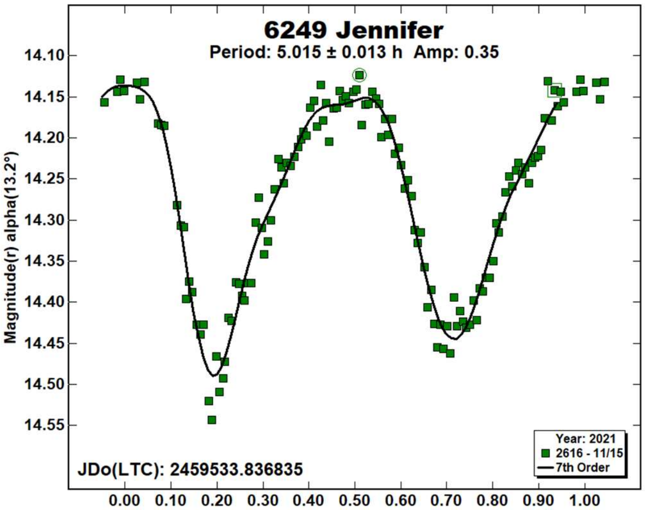

6838 Okuda. This minor planet's discovery was made by Shiimizu and Urata in 1995 at Nachi-Katsuura. Pligge et al. (2011) found a period of 8.983 ± 0.008 h and Noschese and Vecchione (2018) showed a value of 11.0537 ± 0.0012 h. During two nights, 236 data points were acquired. The resulting period is 9.006 ± 0.017 h, in agreement with Pligge. The amplitude is 0.40 mag, with an RMS error of 0.04 mag.

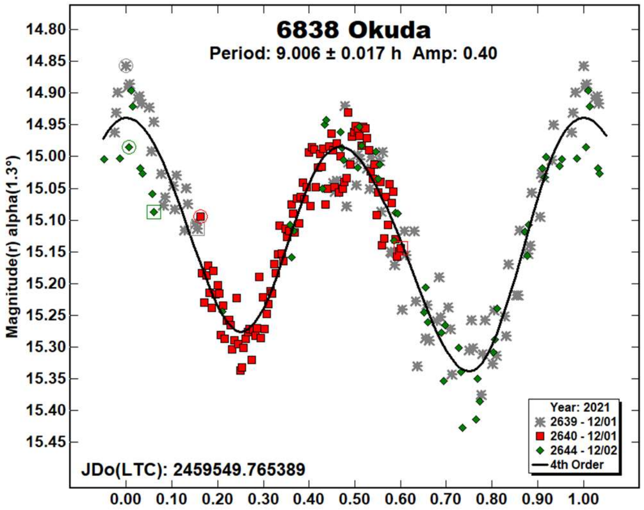

6887 Hasuo was discovered in 1951 by P.A.E. Laugier at Nice. The sole period solution in the LCDB is that of Waszczak (2015): 2.752 ± 0.0001 h. During three nights, 402 images were gathered. The synodic period is 2.752 ± 0.001 h, matching the published value. The amplitude of the lightcurve is 0.15 ± 0.05 mag.

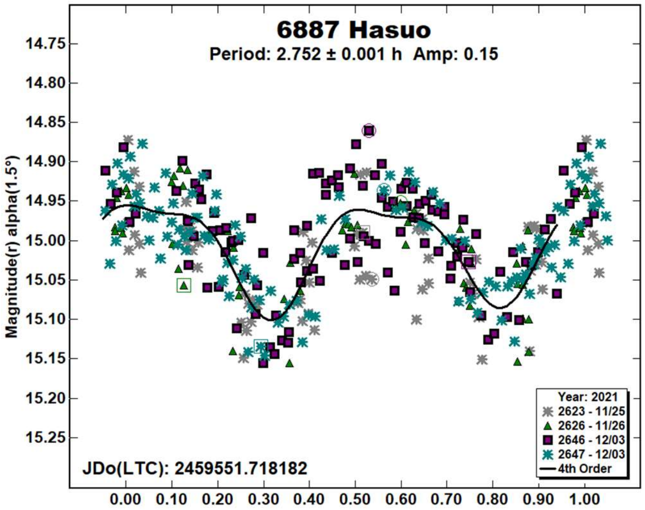

Acknowledgements

The author would like to express his gratitude to Brian Skiff for his indispensable mentoring in data acquisition and reduction. Thanks also go out to Brian Warner for support of his *MPO Canopus* software package.

References

Behrend, R. (2008web, 2020web). Observatoire de Geneve web site. *http://obswww.unige.ch/~behrend/page_cou.html*

Dose, E. (2022). "Lightcurves of Seven Asteroids." *Minor Planet Bull*. **49**, 44-47.

Durech, J.; Hanus, J.; Ali-Lagoa, V. (2018). "Photometric Observations of Seventeen Minor Planets." *Astron. Astrophys*. **617**, A57-A64.

Durech, J.; Tonry, J.; Erasmus, N.; Denneau, L.; Heinze, A.N.; Flewelling, H.; Vanco, R. (2020). "Asteroid models reconstructed from ATLAS photometry." *Astron. Astrophys*. **643**, A59-A63.

Number	Name	yy/mm/dd	Phase	L_{PAB}	B_{PAB}	Period(h)	P.E.	Amp	A.E.	Grp
494	Virtus	21/11/27-12/04	5.0,7.5	51	2	40.13	0.03	0.19	0.02	MB-O
666	Desdemona	21/11/30-12/03	25.3,26.0	22	0	14.608	0.011	0.11	0.01	MB-I
957	Camelia	21/10/28-11/04	3.9,6.0	29	7	85.05	0.11	0.20	0.01	MB-O
1243	Pamela	21/10/28-11/04	5.0,6.9	26	10	26.01	0.02	0.46	0.02	MB-O
1558	Jarnefelt	21/11/22-11/26	6.2,7.3	47	-11	6.255	0.007	0.13	0.04	MB-O
1763	Williams	21/10/28-11/05	6.9,10.9	28	6	88.62	0.15	0.56	0.04	MB-I
1911	Schubart	21/11/27-11/30	0.6,1.5	63	1	11.930	0.013	0.24	0.04	SCHU
2219	Mannucci	21/11/12-12/04	4.1,11.8	41	-4	27.47	0.010	0.59	0.05	MB-O
2301	Whitford	21/11/12-11/14	5.8,6.4	41	-9	14.319	0.015	0.43	0.03	MB-O
5121	Numazawa	21/11/12-11/14	11.7,10.6	65	9	--	--	--	--	FLOR
6249	Jennifer	21/11/15-11/15	13.0,13.2	37	-2	5.015	0.013	0.35	0.02	HUN
6938	Okuda	21/12/01-12/02	1.2,1.8	67	0	9.006	0.017	0.40	0.04	MB-M
6887	Hasuo	21/11/25-12/03	1.5,5.8	63	2	2.752	0.001	0.15	0.04	FLOR

Table I. Observing circumstances and results. The phase angle is given for the first and last date. If preceded by an asterisk, the phase angle reached an extrema during the period. L_{PAB} and B_{PAB} are the approximate phase angle bisector longitude/latitude at mid-date range (see Harris et al., 1984). Grp is the asteroid family/group (Warner et al., 2009).

Garceran, A.C.; Aznar, A.; Mansego, E.A.; Rodríguez, P.B.; de Haro, J.L.; Silva, A.F.; Silva, G.F.; Marinez, V.M., Chiner, O.R. (2016). "Nineteen Asteroids Lightcurves at Asteroids Observers (OBAS) - MPPD: 2015 April - September." *Minor Planet Bull.* **43**, 92-97.

Hamanowa, H. (2009). "Lightcurves of 494 Virtus, 556 Phyllis, 624 Hektor 657 Gunlod, 111 Reinmuthia, 1188 Gothlandia, and 1376 Michelle." *Minor Planet Bull.* **36**, 87-88.

Harris, A.W.; Young, J.W.; Scaltriti, F.; Zappala, V. (1984). "Lightcurves and phase relations of the asteroids 82 Alkmene and 444 Gyptis." *Icarus* **57**, 251-258.

Harris, A.W.; Young, J.W.; Bowell, E.; Martin, L.J.; Millis, R.L.; Poutanen, M.; Scaltriti, F.; Zappala, V.; Schober, H.J.; Debehogne, H.; Zeigler, K.W. (1989). "Photoelectric Observations of Asteroids 3, 24, 60, 261, and 863." *Icarus* **77**, 171-186.

Hawkins, S.; Ditteon, R. (2016). "Asteroid Lightcurve Analysis at the Oakley Observatory - May 2007." *Minor Planet Bull.* **35**, 1-4.

Noschese, A.; Vecchione, A. (2018). "Lightcurve Analysis and Rotation Period for 6838 Okuda." *Minor Planet Bull.* **45**, 238-239.

Pál, A.; Szakáts, R.; Kiss, C.; Bódi, A.; Bognár, Z.; Kalup, C.; Kiss, L.L.; Marton, G.; Molnár, L.; Plachy, E.; Sárneczky, K.; Szabó, G.M.; Szabó, R. (2020). "Solar System Objects Observed with TESS - First Data Release: Bright Main-belt and Trojan Asteroids from the Southern Survey." *Ap. J.* **247**, A26.

Pligge, Z.; Monnier, A.; Pharo, J.; Stolze, K.; Yim, A.; Ditteon, R. (2011). "Asteroid Lightcurve Analysis at the Oakley Southern Sky Observatory: 2010 May." *Minor Planet Bull.* **38**, 5-7.

Polakis, T. (2018). "Lightcurve Analysis for Eleven Main-belt Asteroids." *Minor Planet Bull.* **45**, 269-273.

Polakis, T. (2019). "Photometric Observations of Seventeen Minor Planets." *Minor Planet Bull.* **46**, 400-406.

Stephens, R. (2016). "Asteroids Observed from CS3: 2016 April - June." *Minor Planet Bull.* **43**, 336-338.

Tonry, J.L.; Denneau, L.; Flewelling, H.; Heinze, A.N.; Onken, C.A.; Smartt, S.J.; Stalder, B.; Weiland, H.J.; Wolf, C. (2018). "The ATLAS All-Sky Stellar Reference Catalog." *Astrophys. J.* **867**, A105.

Warell, J. (2017). "Lightcurve Observations of Nine Main-belt Asteroids." *Minor Planet Bull.* **43**, 304-305.

Warner, B. (2000). "Asteroid Photometry at the Palmer Divide Observatory." *Minor Planet Bull.* **27**, 4-6.

Warner, B. (2001). "Asteroid Photometry at the Palmer Divide Observatory: Results for 706 Hirundo, 957 Camelia, and 1719 Jens." *Minor Planet Bull.* **28**, 4-5.

Warner, B. (2006). "Asteroid lightcurve analysis at the Palmer Divide Observatory - late 2005 and early 2006." *Minor Planet Bull.* **33**, 58-62.

Warner, B.; Harris, A.W.; Pravec, P. (2009). "The Asteroid Lightcurve Database." *Icarus* **202**, 134-146. Updated 2020 Aug. *http://www.minorplanet.info/lightcurvedatabase.html*

Warner, B.D. (2011). Collaborative Asteroid Lightcurve Link website. *http://www.minorplanet.info/call.html*

Warner, B. (2015). "Asteroid Lightcurve Analysis at CS3-Palmer Divide Station: 2015 March-June." *Minor Planet Bull.* **42**, 267-276.

Warner. B.D. (2020). *MPO Canopus* software.
http://bdwpublishing.com

Waszczak, A.; Chang, C.-K.; Ofek, E.O.; Laher, R.; Masci, F.; Levitan, D.; Surace, J.; Cheng, Y.-C.; Ip, W.-H.; Kinoshita, D.; Helou, G.; Prince, T.A.; Kulkarni, S. (2015). "Asteroid Light Curves from the Palomar Transient Factory Survey: Rotation Periods and Phase Functions from Sparse Photometry," *The Astronomical Journal* **150**, 75-109.

THE ROTATION PERIODS OF 3 JUNO, 28 BELLONA, 129 ANTIGONE, 214 ASCHERA, 237 COELESTINA, 246 ASPORINA, 382 DODONA, 523 ADA, 670 OTTEGEBE, 918 ITHA, 1242 ZAMBESIA, 1352 WAWEL, 1358 GAIKA, 4155 WATANABE, AND 6097 KOISHIKAWA.

Rafael González Farfán (Z55)
Observatorio Uraniborg
Écija, Sevilla, SPAIN
uraniborg16@gmail.com

Faustino García de la Cuesta (J38)
La Vara, Valdés
Asturias, SPAIN

Esteban Fernández Mañanes
Noelia Graciá Ribes
Observatorio Estelia
Ladines, Asturias SPAIN

Javier Ruiz Fernández (J96)
Observatorio de Cantabria
Cantabria SPAIN

Javier De Elías Cantalapiedra (L46)
Observatorio en Majadahonda
Madrid SPAIN

José M. Fernández Andújar (Z77)
Observatorio Inmaculada del Molino
Sevilla SPAIN

Jesús Delgado Casal (Z73)
Observatorio Nuevos Horizontes
Camas, Sevilla SPAIN

Esteban Reina Lorenz (232)
Masquefa, Can Parellada
Barcelona SPAIN

Ramón Naves Nogues (213)
Observatorio Montcabrer
Cabrils SPAIN

E. Díez Alonso
Instituto Universitario de Ciencias y
Tecnologías Espaciales de Asturias
C/ Independencia, 13, 33004, Oviedo, SPAIN

(Received: 2022 Jan 14, Revised: 2022 Feb 14)

The lightcurves for fifteen asteroids were measured from 2020 to 2021 October: 3 Juno (7.210 h), 28 Bellona (15.699 h), 129 Antigone (4.956 h), 214 Aschera (6.833 h), 237 Coelestina (29.062 h), 246 Asporina (16.191 h), 383 Dodona (4.113 h), 523 Ada (10.031 h), 670 Ottegebe (10.042 h), 918 Itha (3.473 h), 1242 Zambesia (17.307 h), 1352 Wawel (16.936 h), 1358 Gaika (10.100 h), 4155 Watanabe (4.495 h), and 6097 Koishikawa (2.860 h).

All observations reported here were unfiltered. The images were calibrated in the standard way (bias, darks and flats). Images were measured and period analysis done using *FotoDif* (2021) and *Períodos* (2020) packages. All data were light-time corrected. The results are summarized below. Individual light curve plots along additional comments as required are also presented.

In all cases we wanted to update the data of these asteroids. Some of them had not been reviewed since 2005-2006, so we considered it was necessary new observations.

3 Juno (A804 RA). This large asteroid in the main belt was the third asteroid discovered, in 1804 by German astronomer Karl Harding. It is one of the twenty larger asteroids and one of the two larger stony (S-type) asteroids. It is estimated to contain 1% of the total mass of the asteroid belt. Our results are not different from other ones. $P = 7.210 \pm 0.005$ h, and 0.13 mag amplitude. Our data were taken between 2021 June 26-29.

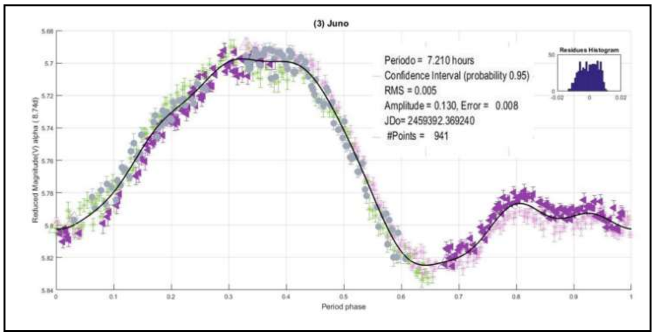

28 Bellona (A854 EA) is a large asteroid orbiting between Mars and Jupiter in the asteroid main belt. It orbits the sun every 1,690 days (4.63 years), coming as close as 2.35 au and reaching as far as 3.20 au from the sun. One of the earlier observations of this asteroid is dated in 1965 (Harris and Young, 1983). More recent results include those from Pilcher (2011; 15.706 h); a shape model has been posted on the DAMIT site (Durech, 2021). Our measurements are similar to those results: $P = 15.699 \pm 0.006$ h and 0.21 mag amplitude. Our data were taken between 2021 June 3-19 2021.

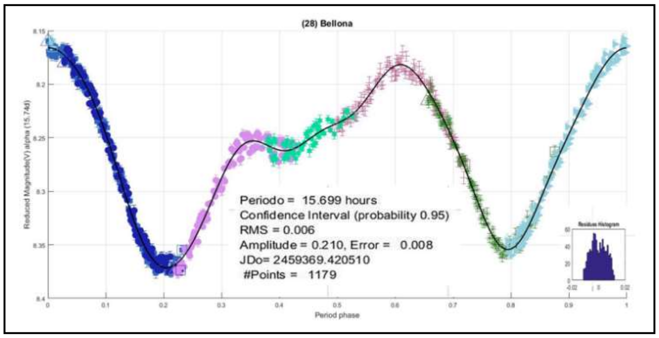

129 Antigone (A873 CA). Antigone is a large main-belt asteroid. Radar observations indicate that it is composed of almost pure nickel-iron. It was discovered by German-American astronomer C.H.F. Peters on 1873, February 5.

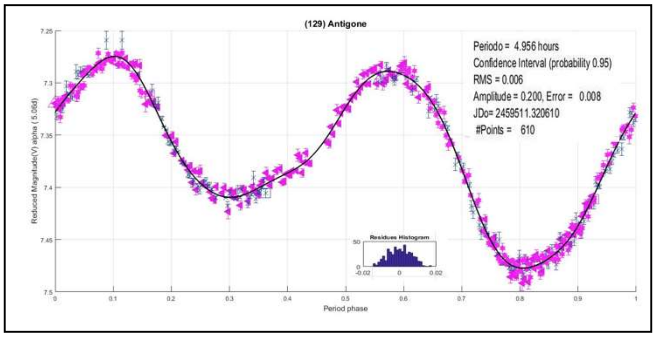

There are reports of its rotation period since 1977 (Scaltriti and Zappala, 1977). In all cases, the period has been similar to what we found: 4.956 ± 0.006 h and 0.20 mag amplitude. Our data were taken on 2021 October 23, 26, and 27.

214 Aschera (A880 DB) was discovered by Austrian astronomer John Palisa on 1880 February 29. It is classified as a rare E-type asteroid and is quite faint for an object of its type. The overall diameter is estimated to be 23 km and it has a geometric albedo of 0.52. The first known data on 214 Aschera were published in 1983 (Harris and Young, 1983) and the most recent that we could find were from Shevchenko et al. (2016). In both cases, the reported rotation periods are very similar: 6.835 h and 0.23 mag amplitude. Our measurements are in accordance with those results: *P* = 6.833 ± 0.004 h, *A* = 0.20 mag. Our data were taken between 2021 September 4-12.

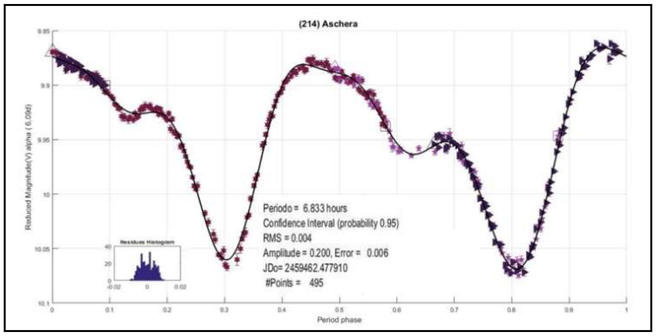

237 Coelestina (A884 MA) was discovered by Johann Palisa on 1884 June in Vienna. Behrend (2007web) reported *P* = 20 h. Other results include Stephens (2010; 29.215 h) and Hanus et al. (2016; 29.1758 h). We found *P* = 29.062 ± 0.009 h and 0.24 mag amplitude. Our data were taken between 2021 March 15-24.

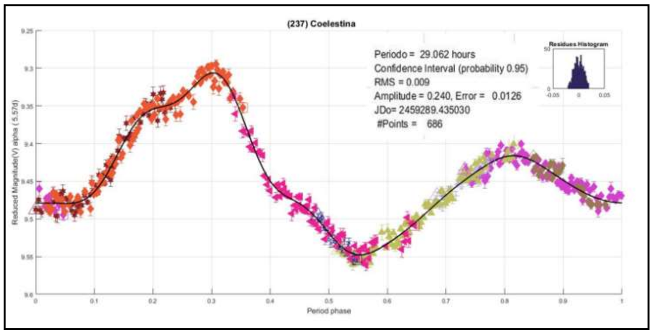

246 Asporina (A885 EA). Our data were taken between 2020 November 21 and 2022 January 18. It is classified as one of the few A-type asteroids. It was discovered by A. Borrelly on 1885 March 6 in Marseilles.

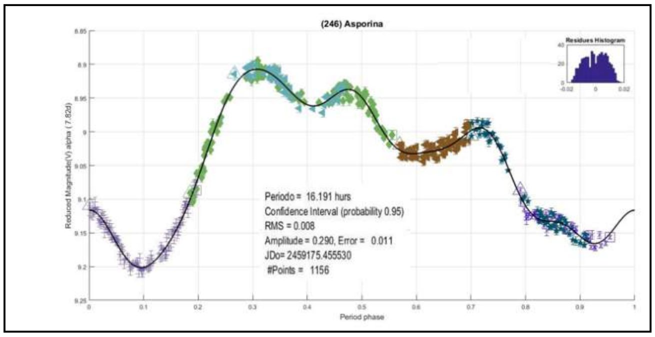

Its spectrum reveals the strong presence of the mineral olivine, a relative rarity in the asteroid belt. There are old observations and measurements on this asteroid since 1979 (Harris and Young, 1983), all reporting a similar period. Our analysis gives consistent results: *P* = 16.191 ± 0.008 h and 0.29 mag amplitude.

382 Dodona (A894 BB). Dodona is a large main-belt asteroid that was discovered by French astronomer Auguste Charlois on 1894 January 29 in Nice. It is classified as an M-type asteroid. This is another well studied asteroid, with results going back to 1986, including *P* = 4.113228 h from Michalowski et al (2004) and 4.11329 h from Behrend (2021web). Our results are *P* = 4.113 ± 0.009 h and 0.53 mag amplitude. Our data were taken between 2021 March 22 and April 7.

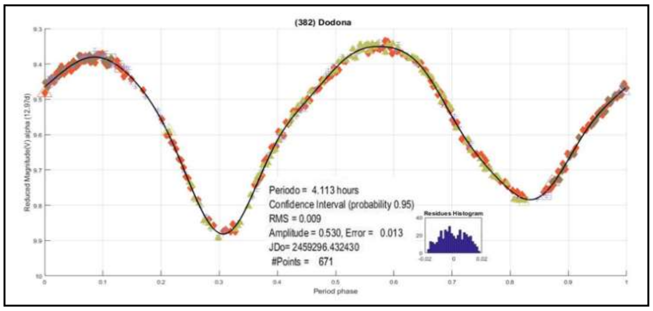

523 Ada (A904 BA) was discovered on 1904 January 29 by American astronomer Raymond S. Dugan at Heidelberg, Germany. Georgilas and Wetterer (1996) reported *P* = 9.800 h but several results published afterwards give a period of about 10.03 h, e.g., Durech et al. (2016; DAMIT web site). Our results are similar: *P* = 10.031 ± 0.006 h and 0.55 mag amplitude. Data were taken between 2020 November 22 and December 6.

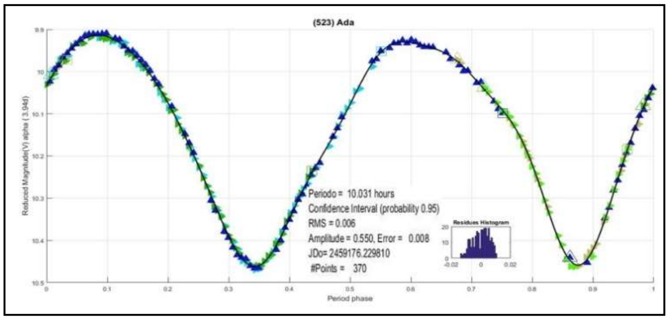

670 Ottegebe (A908 QG).

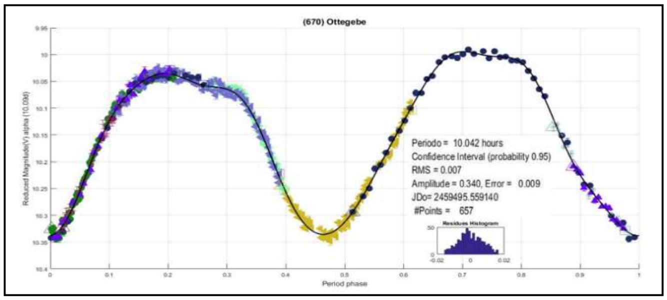

Previously published periods, e.g., Kirkpatrick et al. (2003; 10.045 h) are similar to one another. We observed this asteroid in 2021 October and our results are in good agreement: 10.042 ± 0.007 h and 0.34 mag amplitude. Our data were taken between 2021 October 7-26.

918 Itha (A919 QD) is a stony asteroid located in the outer regions of the asteroid belt. It was discovered by German astronomer Karl Reinmuth at the Heidelberg Observatory on 1919 August 22. The S-type asteroid has a notably short rotation period of only 3.5 h and measures approximately 21 km in diameter. Albers et al. (2010) reported observations but no period could be found. Oey et al. (2012) had better luck, finding P = 3.374 h, and 0.30 mag amplitude. Our results are similar: 3.474 ± 0.006 h and 0.30 mag amplitude. A shape model was found by Durech et al. (2018), which is posted on the DAMIT site. Our data were taken between 2021 September 5 - October 8.

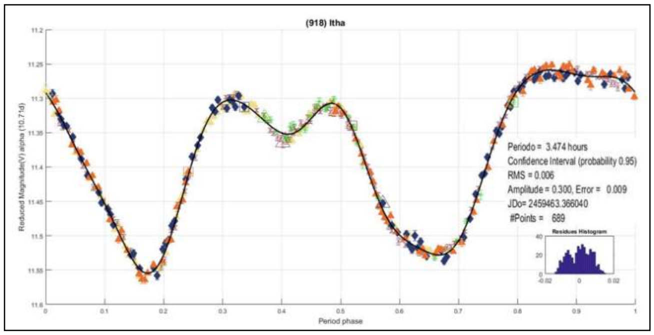

1242 Zambesia (1932 HL). This asteroid, with an estimated diameter is 48 km, orbits the Sun in the central regions of the asteroid belt. It was discovered on 1932 April 28 by South African astronomer Cyril Jackson at the Union Observatory in Johannesburg. Azan Macias et al. (2016) reported a period of P = 15.72 h. However, other observations gave different results, e.g., Behrend (2021web; 17.3148 h). Our data are similar to Behrend's: P = 17.307 ± 0.006 h and 0.14 mag amplitude. Our data were taken between 2021 January 4-27.

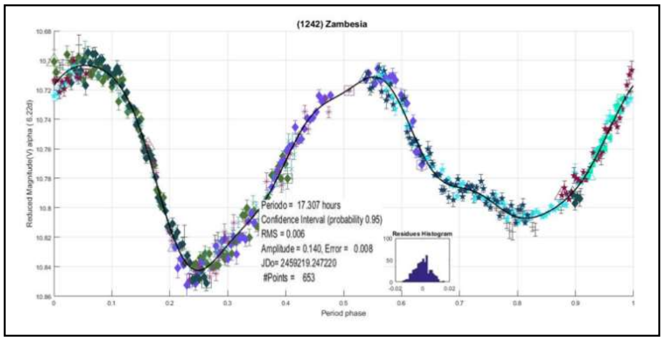

1352 Wawel (1935 CE). Brinsfield (2008) reported a period of 16.97 h. Hanus et al. (2016) later published a model of this asteroid and posted the results on the DAMIT website. Their sidereal period was 16.9543 h.

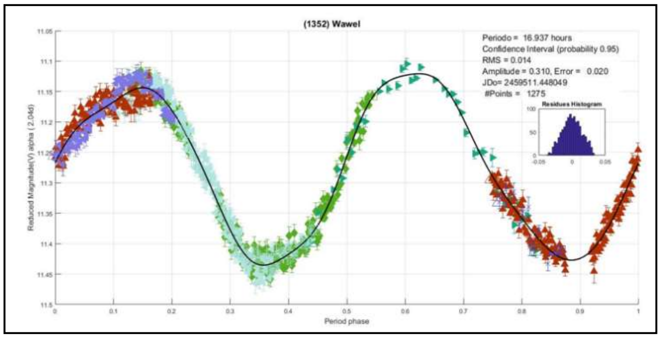

Our results are consistent with those reports: P = 16.937 ± 0.014 h and 0.31 mag amplitude. Our data were taken between 2021 October 23-27.

1358 Gaika (1935 OB). This main-belt asteroid was discovered on 1935 July 21 in Johannesburg by South African astronomer Cyril V. Jackson. Analysis of our data led to P = 10.100 ± 0.011 h and 0.70 mag amplitude. Our data were taken from 2021 October 8-10.

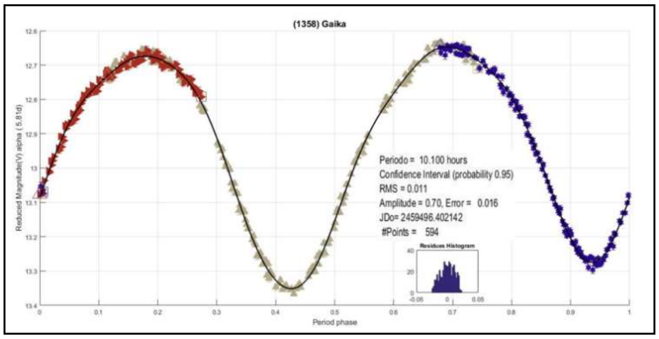

In addition, we have obtained a very preliminary model for this asteroid. We used our dense curves and six dense curves from SuperWasp (Parley et al, 2006; Pollacco et al., 2006) dated between 2008 March 15 and 2009 July 7. We found no more dense curves for Gaika. We also used sparse data from ATLAS (Heinze et al., 2018) and USNO (Flagstaff), which were available at the Asteroids Dynamics Site (AstDys-2, 2020).

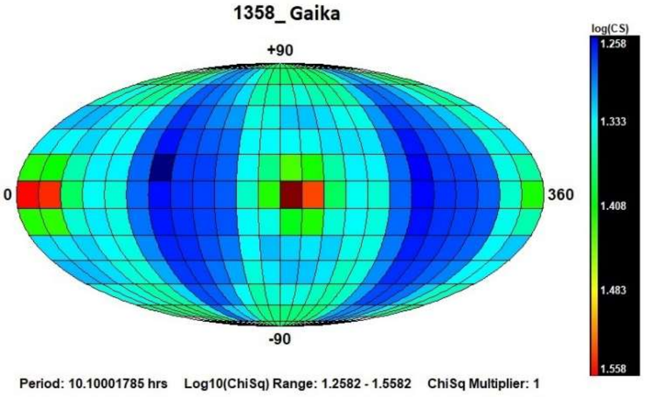

Fig 1. Pole search distribution for *1358 Gaika*

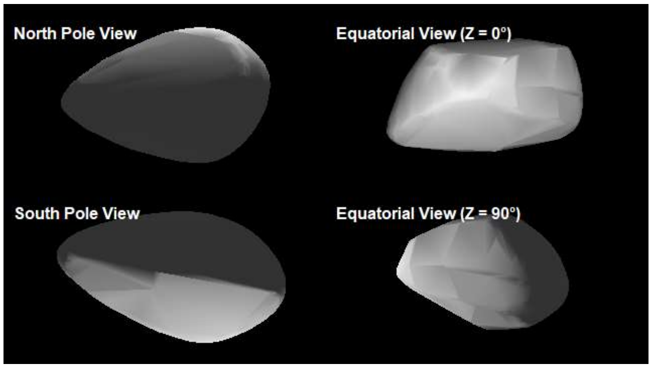

Fig 2. Shape model of *1358 Gaika* corresponding to the solution (λ, β) = (90°, +15°).

Lightcurve inversion was done with *MPO LCInvert* (BDW Publishing, 2016), which implements the procedures described in Kaasalainen and Torppa (2001) and Kaasalainen et al. (2001). We adopted a weight of 0.3 for the sparse curves (USNO and ATLAS), 0.7 for the curves from SuperWASP and 1.0 for the curves from GOAS.

We carried out a medium resolution pole search adopting P = 10.100 h, a value of 0.1 for the dark facet factor, and 50 iterations. In this way we analyzed 312 different positions of the pole in steps of 15° in latitude and longitude. The analysis suggests a region with lower $\chi 2$, centered at (λ, β) = (90°, +15°).

4155 Watanabe (1987 UB1) was discovered in 1996 by Japanese astronomer Watanabe Kazuo. Pravec et al. (2006web) reported a period of 4.4972 h. Ditteon and Hawkins (2007) were not able to determine a period and gave only an estimate of the amplitude. There is no model on the DAMIT website. In 2021 September, we observed the asteroid and made its lightcurve, finding a period P = 4.495 ± 0.012 h and 0.22 mag amplitude. Data were taken obtained 2021 September 10 - October 13.

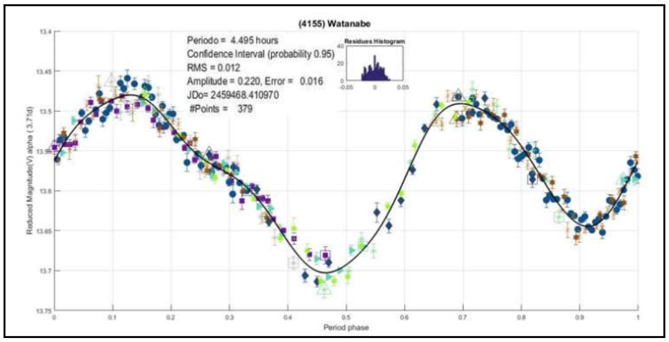

6097 Koishikawa (1991 UK2) is a Vestoid asteroid. Discovery credit goes to Endate and Watanabe (Japan) on 1991 October 29. However, the first observations were made in 1942 at the observatory of the University of Turku when the asteroid was given the provisional designation 1942 VV.

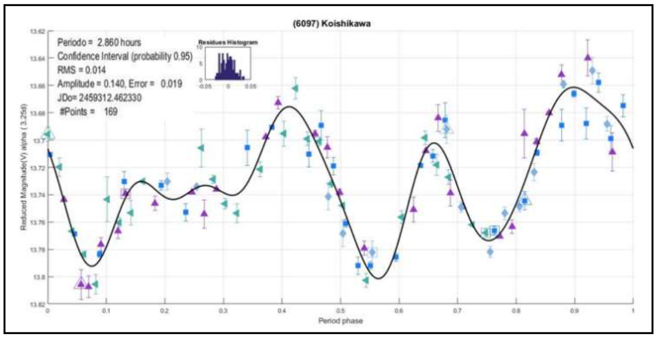

Pravec et al. (2010web) reported P = 2.85979 h and then P = 2.8598 h seven years later (Pravec et al. 2007web). More recently, Stephens and Warner (2020) found a period of 2.859 h. Our results are consistent: P = 2.860 ± 0.014 h and 0.14 mag amplitude. Data were taken between 2021 March 7-17.

Number	Asteroid	20yy mm/dd	Phase	Period(h)	P.E.	Amp	A.E.
3	Juno	21/06/26-21/06/29	8.8-9.5	7.210	0.005	0.13	0.01
28	Bellona	21/06/03-21/06/19	15.8-18.9	15.699	0.006	0.21	0.01
129	Antigone	21/10/23-21/10/27	5.1-5.5	4.956	0.006	0.20	0.01
214	Aschera	21/09/04-21/09/12	6.1-2.6	6.833	0.004	0.20	0.01
237	Coelestina	21/03/15-21/03/24	5.6-7.7	29.062	0.009	0.24	0.01
246	Asporina	20/11/21-21/01/18	7.8-16.9	16.191	0.008	0.29	0.01
382	Dodona	21/03/22-21/04/07	13.0-17.2	4.113	0.009	0.53	0.01
523	Ada	20/11/22-20/12/06	4.1-10.3	10.031	0.006	0.55	0.01
670	Ottegebe	21/10/07-21/10/26	10.1-03.7	10.042	0.007	0.34	0.01
918	Itha	21/09/05-21/10/08	10.7-8.2	3.474	0.006	0.30	0.01
1242	Zambesia	21/01/04-21/01/27	6.2-11.4	17.307	0.006	0.14	0.01
1352	Wawel	21/10/23-21/10/27	9.8-1.1	16.937	0.014	0.31	0.02
1358	Gaika	21/10/08-21/10/10	5.9-6.9	10.100	0.011	0.70	0.02
4155	Watanabe	21/09/10-21/10/13	3.7-17.9	4.495	0.012	0.22	0.02
6097	Koishikawa	21/04/07-21/04/17	3.3-8.0	2.860	0.014	0.14	0.02

Table I. Observing circumstances and results. Phase is the solar phase angle given at the start and end of the date range. If preceded by an asterisk, the phase angle reached an extrema during the period.

References

Albers, K.; Kragh, K.; Monnier, A.; Pligge, Z.; Stolze, K.; West, J.; Yim, A.; Ditteon, R. (2010). "Asteroid Lightcurve Analysis at the Oakley Southern Sky Observatory: 2009 October thru 2010 April." *Minor Planet Bull*. **37**, 152-158.

AstDys-2 (2020). Asteroids - Dynamic Site.
https://newton.spacedys.com/astdys/

Aznar Macias, A.; Carrero Garcerain, A.; Arse Mansego, E.; Briones Rodriguez, P.; Lozano de Haro, J.; Fornas Silva, G.; Mas Martinez, V.; Rodrigo Chiner, O. (2016) "Twenty-three Asteroids Lightcurves at Observadores de Asteroides (OBAS): 2015 October - December." *Minor Planet Bull.* **43**, 174-181.

BDW Publishing (2016). MPO LCInvert software.
http://www.minorplanetobserver.com/MPOSoftware/MPOLCInvert.htm

Behrend, R. (2007web, 2021web). Observatoire de Geneve web site. *https://obswww.unige.ch/~behrend/page_cou.html*

Brinsfield, J.W. (2008). "The Rotation Periods of 531 Zerlina, 1194 Aleta 1352 Wawel, 2005 Hencke, 2648 Owa, and 3509 Sanshui." *Minor Planet Bull*. **35**, 86-87.

Ditteon, R.; Hawkins, S. (2007) "Asteroid Lightcurve Analysis at the Oakley Observatory - October-November 2006." *Minor Planet Bull.* **34**, 59-64.

Durech, J.; Hanus, J.; Oszkiewsicz, D.; Vanco, R. (2016). "Asteroid models from the Lowell photometric database." *Astron. Astrophys*. **587**, A48.

Durech, J.; Hanus, J.; Broz, M.; Lehky, M. and 13 colleagues (2018). "Shape models of asteroids based on lightcurve observations with BlueEye600 robotic observatory." *Icarus* **304**, 101-109.

Durech (2021). DAMIT web site.
https://astro.troja.mff.cuni.cz/projects/damit/

FotoDif (2021). Software.
http://astrosurf.com/orodeno/fotodif/index.htm

Georgilas, S.A.; Wetterer, C.J. (1996). "CCD Photometry of 523 Ada." *Minor Planet Bull.* **23**, 41-42.

Hanus, J.; Durech, J.; Oszkiewicz, D.A.; Behrend, R. and 165 colleagues (2016). "New and updated convex shape models of asteroids based on optical data from a large collaboration network." *Astron. Astrophys*. **586**, A108.

Harris, A.W.; Young, J.W. (1983). "Asteroid rotation IV. 1979 observations." *Icarus* **54**, 59-109.

Heinze, A.N.; Tonry, J.L.; Denneau, L.; Flewelling, H.; Stalder, B.; Rest, A.; Smith, K.W.; Smartt, S.J.; Weiland, H. (2018). "A first catalog of variable stars measured by the Asteroid Terrestrial-impact Last Alert System (ATLAS)." *Astronomical Journal* **156**, id.241.

Kaasalainen, M.; Torppa, J. (2001). "Optimization Methods for Asteroid Lightcurve Inversion: I. Shape Determination." *Icarus* **153(1)**, 24-36.

Kaasalainen, M.; Torppa, J.; Muinonen, K. (2001). "Optimization Methods for Asteroid Lightcurve Inversion: II. The Complete Inverse Problem." *Icarus* **153(1)**, 37-51.

Kirkpatrick, E.; Hirsch, B.; Lecrone, C.; Schwoenk, D.; Shiery, M.; Tollefson, E.; Twarek, A.; White, S.; Wolfe, C. (2003). "Oakley Observatory lightcurves of asteroids 670 Ottegebe and 1035 Amata." *Minor Planet Bull*. **30**, 41.

Michalowski, T.; Kwiatkowski, T.; Kaasalainen, M.; Pych, W.; Kryszczyńska, A.; Dybczyński, P.A.; Velichko, F.P.; Erikson, A.; Denchev, P.; Fauvaud, S.; Szabó, Gy.M. (2004). "Photometry and models of selected main belt asteroids I. 52 Europa, 115 Thyra, and 382 Dodona." *Astron. Astrophys*. **416**, 353-366.

Oey, J.; Colazo, C.; Mazzone, F.; Chapman, A. (2012). "The Lightcurve Analysis of 918 Itha and 2008 Konstitutsiya." *Minor Planet Bull*. **39**, 1-2.

Parley, N.R.; McBride, N.; Green, S.F.; Haswell, C.A.; Clarkson, W.I.; Christian, D.J. and 18 colleagues (2005). "Serendipitous Asteroid lightcurve survey using SuperWASP." *Earth, Moon, and Planets* **97**, 261-268.

Períodos (2020) software.
http://www.astrosurf.com/salvador/Programas.html

Pilcher, F. (2011). "Rotation Period Determinations for 28 Bellona, 81 Terpsichore, 126 Velleda 150 Nuwa, 161 Athor, 419 Aurelia, and 632 Pyrrha." *Minor Planet Bull*. **38**, 156-15.

Pollacco, D.L.; Skillen, I.; Collier Cameron, A; Christian, D.J.; Hellier, C.; Irwin, J. and 22 colleagues (2006). "The WASP project and the SuperWASP cameras." *Pub. Ast. Soc. Pacific* **118**, 1407-1418.

Pravec, P.; Wolf, M.; Sarounova, L. (2006web; 2007web; 2010web). *http://www.asu.cas.cz/~ppravec/neo.htm*

Scaltriti, F.; Zappala, V. (1977). "Photoelectric photometry of the minor planets 41 Daphne and 129 Antigone." *Astron. Astrophys*. **56**, 7-11.

Shevchenko, V.G.; Belksaya, I.N.; Muinonen, K.; Penttilä, A.; Krugly, Y.N.; Velichko, F.P.; Chiorny, V.G.; Slyusarev, I.G.; Gaftonyuk, N.M.; Tereschenko, I.A. (2016). "Asteroid observations at low phase angles. IV. Average parameters for the new H, G1, G2 magnitude system." *Plan. Space Sci.* **123**, 101-116.

Stephens, R.D. (2010). "Asteroids Observed from GMARS and Santana Observatories: 2009 June - September." *Minor Planet Bull*. **37**, 28-29.

Stephens, R.D.; Warner, B.D. (2020). "Main-Belt Asteroids Observed from CS3: 2019 October to December." *Minor Planet Bull*. **47**, 125-133.

LIGHTCURVES OF SEVENTEEN ASTEROIDS

Eric V. Dose
3167 San Mateo Blvd NE #329
Albuquerque, NM 87110
mp@ericdose.com

(Received: 2022 January 15)

We present lightcurves, synodic rotation periods, and G value (H-G) estimates for seventeen asteroids.

We present asteroid lightcurve photometry results, continuing with efforts to measure lightcurves with lower amplitude and generally longer periods. The lightcurves were obtained by following the workflow process described by Dose (2020), with later improvements (Dose, 2021). This workflow applies to each image an ensemble of typically 20-60 nearby ATLAS refcat2 catalog (Tonry et al, 2018) comparison ("comp") stars as a basis for asteroid photometry. Diagnostic plots and the numerous comp stars allow for effective identification and removal of outlier, variable, and poorly measured comp stars.

The custom workflow produces a time series of asteroid magnitude estimates on Sloan r′ (SR) catalog basis, unreduced and without H-G adjustment. These magnitudes are imported directly into *MPO Canopus* software (Warner, 2021) where they are adjusted for distances and phase-angle dependence, fit by Fourier analysis including identifying and ruling out of aliases, and plotted. Phase-angle dependence is corrected with a H-G model, using the *G* value that minimizes best-fit RMS error across all nights' data.

No nightly zero-point adjustments (DeltaComps in *MPO Canopus* terminology) were made to any session herein, other than by adjusting the G value (H-G phase model). All lightcurve data herein have been submitted to ALCDEF.

Lightcurve Results

Seventeen asteroids were observed from Deep Sky West observatory (IAU V28) at 2210 meters elevation in northern New Mexico. Images were acquired with a 0.35-meter SCT reduced to f/7.7; an SBIG STXL-6303E camera cooled to -35 C and fitted with a Clear filter (Astrodon); and a PlaneWave L-500 mount. The equipment was operated remotely via *ACP software* (DC-3 Dreams, version 8.3), running plan files generated for each night by the author's python scripts (Dose, 2020). Observations often cycled among 2-4 asteroids. Exposure times targeted 4-6 millimagnitudes uncertainty in asteroid instrumental magnitude, subject to a minimum of 120 seconds to ensure suitable comp-star photometry, and to a maximum of 900 seconds. All exposures were autoguided.

FITS images were plate-solved by *PinPoint* (DC-3 Dreams) or *TheSkyX* (Software Bisque) and were calibrated using temperature-matched, median-averaged dark images and recent flat images of a flux-adjustable flat panel. Every photometric image was visually inspected; all images with poor tracking, obvious interference by cloud or moon, or having stars, satellite tracks, cosmic ray artifacts, or other apparent light sources within 10 arcseconds of the target asteroid were excluded. Photometry-ready images that pass these screens were submitted to the workflow, which applies separately measured second-order transforms from Clear filter to deliver asteroid magnitudes in Sloan r′ passband.

In this work, "period" refers to an asteroid's synodic rotation period unless otherwise noted, "SR" denotes the Sloan r' passband, and "mmag" denotes millimagnitudes (0.001 mag).

478 Tergeste. This bright outer main-belt asteroid has been reported several times to have period of about 16 hours (16.104 h, Behrend 2005web; 16.105 h, Marciniak et al., 2015; 16.107 h, Aznar Macias et al., 2017; 16.101 h, Brines et al., 2017; 16.105 h, Marciniak et al., 2018; 16.1011 h, Pál et al., 2020; 16.1 h, Behrend, 2021web) with one known early report differing (15 h, Harris and Young, 1989). Reported lightcurves have varied in LCDB uncertainty score from 1 to 3-.

We add to the consensus with our period of 16.100 ± 0.002 h, with an amplitude of 0.21 mag. Fourier fit to the present data has RMS error of 5 mmag; best G value (H-G phase model) is 0.27; in the author's hands, Fourier fit to the same data using MPC-default *G* of 0.15 never gave RMS error lower than of 13 mmag.

The lightcurve is bimodal. Despite difficulties in obtaining full phase coverage for a period very near 16 h, a synodic period of 16.10 h appears secure.

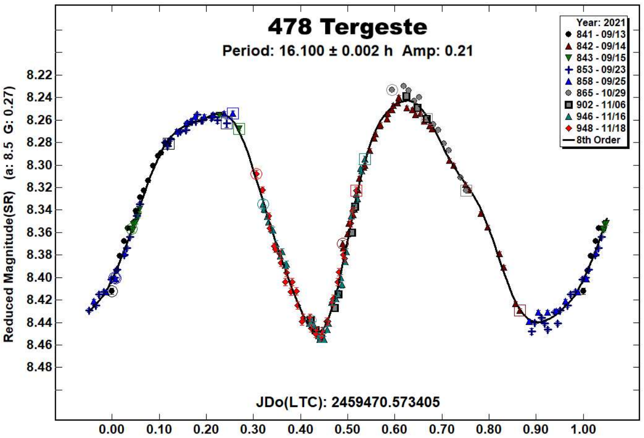

494 Virtus. This bright outer main-belt asteroid has had disparate previous reports of rotational period (4.99 h, Behrend, 2006web, 5.57 h, Warner, 2006; 4.9903 h, Behrend, 2008web; 5.57 h, Hamanowa and Hamanowa, 2009; 49.427 h, Polakis, 2018), none bearing a LCDB uncertainty score better than 2.

By contrast, we find a period of 40.431 ± 0.004 h. We were fortunate to view from a new aspect (phase angle bisector longitude) that yielded higher amplitude of 0.19 magnitude than previously reported (0.03-0.12 magnitudes). Our Fourier fit has RMS error of 5 mmag.

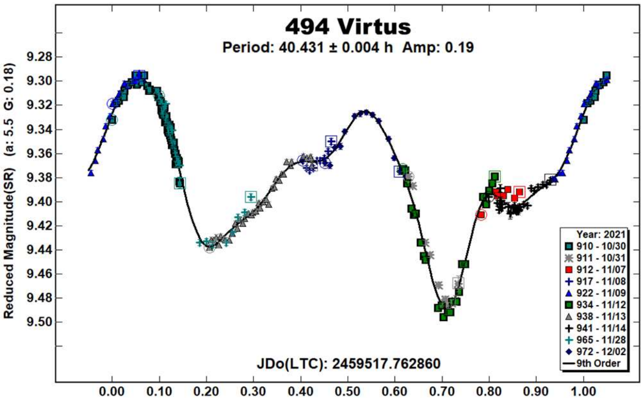

Number	Name	yyyy mm/dd		Phase	L_{PAB}	B_{PAB}	Period(h)	P.E.	Amp	A.E.	Grp
478	Tergeste	2021	09/13-11/18	8.5,18.2	334	14	16.100	0.002	0.21	0.02	MB-O
494	Virtus	2021	10/30-12/02	*5.6,6.7	52	2	40.431	0.004	0.19	0.02	MB-O
530	Turandot	2021	11/03-11/26	*9.3,3.6	64	-10	19.955	0.004	0.11	0.01	UNK
579	Sidonia	2021-22	11/20-01/10	17.4,8.1	130	8	16.290	0.001	0.10	0.01	EOS
605	Juvisia	2021-22	12/17-01/12	13.9,7.5	126	16	15.834	0.003	0.14	0.02	MB-O
764	Gedania	2021	09/10-12/05	*12.0,17.2	18	11	24.984	0.002	0.07	0.02	MB-O
858	El Djezair	2021-22	10/05-01/05	*9.1,18.0	36	-5	29.639	0.003	0.15	0.02	MB-O
1159	Granada	2021	09/17-11/23	*16.1,16.6	27	11	72.750	0.030	0.28	0.04	MB-I
1180	Rita	2021	09/14-11/07	*6.6,9.3	12	-8	14.898	0.001	0.25	0.01	HIL
1654	Bojeva	2021-22	11/30-01/10	*13.4,5.1	106	12	11.443	0.001	0.11	0.02	EOS
1748	Mauderli	2021	10/29-11/09	*3.1,1.4	44	-4	6.002	0.001	0.10	0.03	HIL
1913	Sekanina	2021-22	12/07-01/04	15.7,20.7	37	1	14.035	0.003	0.15	0.03	KOR
2599	Veseli	2021-22	10/31-01/09	*20.5,10.4	93	19	13.251	0.001	0.36	0.04	MB-I
4162	SAF	2021	11/13-11/28	9.1,14.3	36	10	3.850	0.002	0.13	0.05	MB-O
4719	Burnaby	2021	11/11-12/06	22.5,15.5	100	10	10.451	0.001	0.12	0.03	UNK
5256	Farquhar	2021	10/29-11/20	9.8,17.7	19	5	11.504	0.002	0.13	0.03	EUN
6706	1988 VD3	2021	09/12-12/04	*21.9,22.9	28	2	53.398	0.008	0.06	0.02	MB-I

Table I. Observing circumstances and results. The phase angle is given for the first and last date. If preceded by an asterisk, the phase angle reached an extrema during the period. L_{PAB} and B_{PAB} are the approximate phase angle bisector longitude/latitude at mid-date range (see Harris et al., 1984). Grp is the asteroid family/group (Warner et al., 2009).

The period spectrum disfavors candidate periods of less than 20 h.

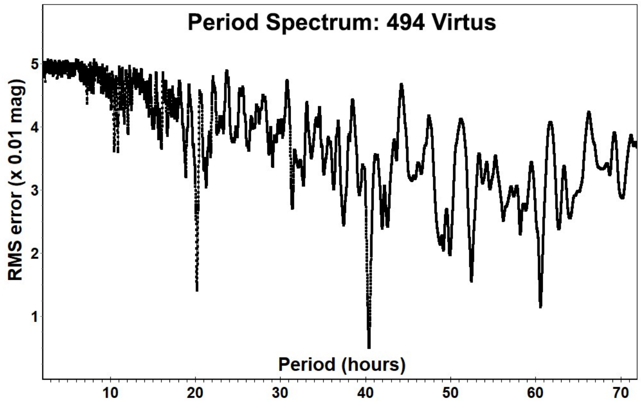

530 Turandot. This asteroid of undetermined type was found to have period of 19.955 ± 0.004 h, confirming most known, previous reports (19.95 h, Behrend, 2002web; 19.947 h, Behrend, 2005web; 19.96 h, Pilcher, 2014; 19.94 h, Colazo et al., 2021a) and differing from one early report (10.77 h, Di Martino et al., 1995), which is an alias of our solution by 1 period per 24 h. Fourier fit RMS error is 6 mmag. The *G* estimate (0.11) that we apply is made uncertain by the observations' narrow phase range.

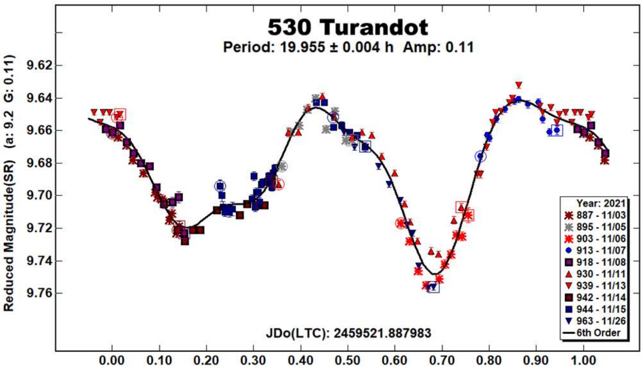

579 Sidonia. This Eos-family asteroid is approaching close consensus on its synodic period (16.286 h, Stephens, 2010; 16.2804 h, Ďurech et al., 2020; 16.279 h, Colazo et al, 2021b) after some disparate earlier reports (16.5 h, Binzel, 1987; 16.5 h, Weidenschilling et al., 1990; 18.72 h, Behrend, 2005web). We find a period of 16.290 ± 0.001 h with Fourier fit RMS error of 6 mmag. With recent reports in agreement from three apparitions, the time may be right to recompute a shape model.

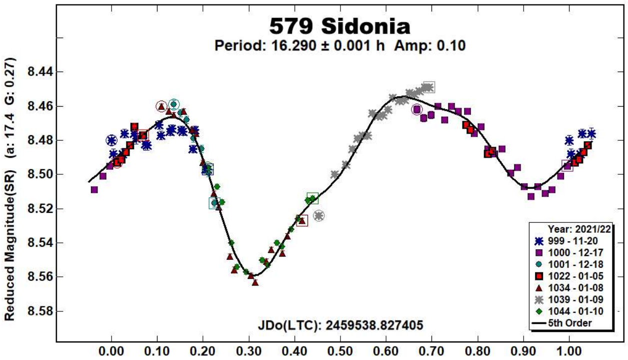

605 Juvisia. The author revisited this outer main-belt asteroid to confirm the period and to add to the viewing aspects for which data are available to future shape modeling. Our period solution of 15.834 ± 0.003 h agrees with known previous reports (15.855 h, Warner, 2000; 15.85 h, Menke, 2005; 15.93 h, Warner, 2011; 15.851, Dose, 2021; 15.844 h, Pilcher, 2021b) except one (31.6616 h, Ďurech et al., 2019). Our Fourier RMS error is 7 mmag.

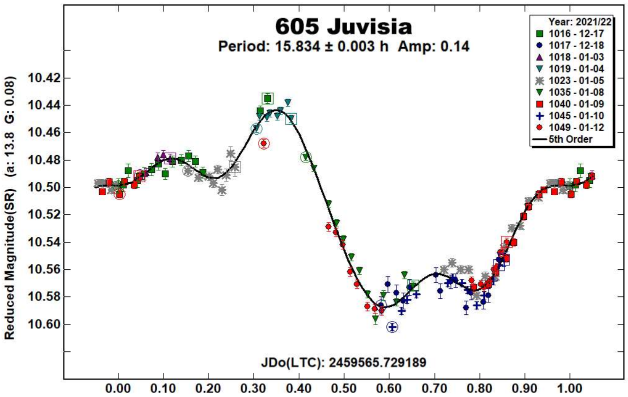

764 Gedania. This outer main-belt asteroid was found to have period of 24.984 ± 0.002 h and low amplitude of 0.07 magnitudes, confirming most known previous reports (24.9751 h, Behrend, 2006web; 24.817 h, Brinsfield, 2010; 24.97 h, Behrend, 2021web; 24.968 h, Pilcher, 2021a) but differing from two others (19.16 h, Aznar Macias et al., 2016; 25.1172 h, Pál et al., 2020). Fourier fit RMS error is 6 mmag.

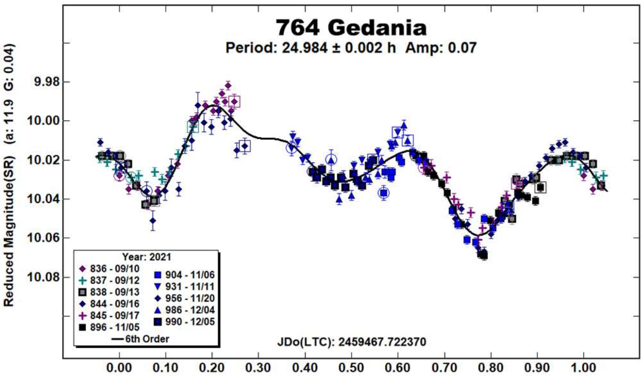

858 El Djezair. Four different periods have been reported for this outer main-belt asteroid (22.31 h, Warner, 2005; 19 h, Behrend, 2007web; 14.83 h, Polakis, 2019; 33.525 h, Colazo et al., 2021b), all with LCDB uncertainty scores of 2. We find ourselves reporting yet a fifth distinct synodic period of 29.639 ± 0.003 h, based on data taken over 12 nights. Our Fourier fit RMS error is 13 mmag. We can find no obvious aliases between our result and any of the four previous reports. The period spectrum is inconsistent with the four previous period reports.

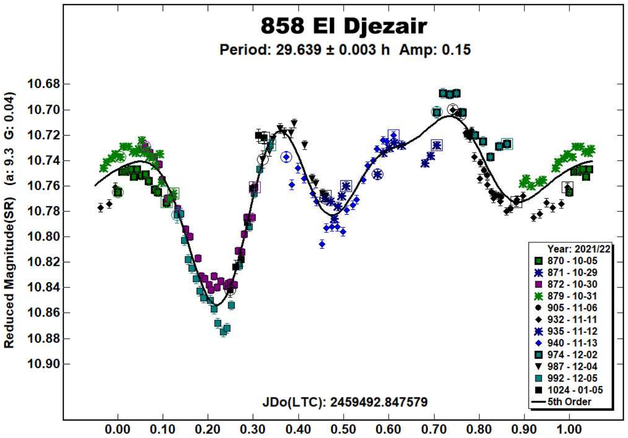

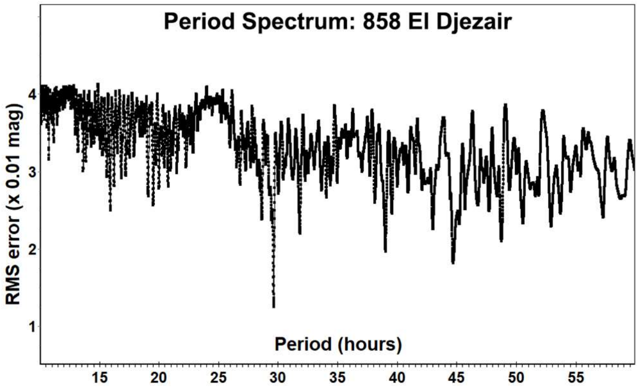

1159 Granada. All three previous period reports for this inner main-belt asteroid have LCDB uncertainty code of 2, and all differ (31 h, Binzel, 1987; 72.852 h, Waszczak et al., 2015; 77.28 h, Behrend, 2020web). We confirm the Waszczak et al. report with our period estimate of 72.75 ± 0.03 h. Fourier fit RMS error is 11 mmag.

Phase coverage is incomplete as the period is very near 3 days; for a given time of night, the phase shifts by only about 0.1 period per month. This asteroid's orbit eccentricity and inclination are modest, so it will never appear at very high or low declinations. Full phase coverage within one apparition will very likely require multi-longitude observations.

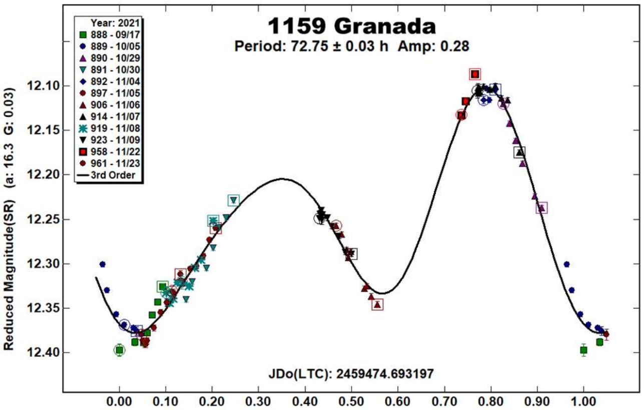

To compensate for incomplete phase coverage, we undertook twelve nights of extended-duration observations to get phase-overlapping results in the phase ranges that were available. The resulting period spectrum disfavors other solutions, including the previously reported periods of 31 h and 77.28 hours. Our second-best solution, near 36 hours, is simply the half-period, monomodal solution.

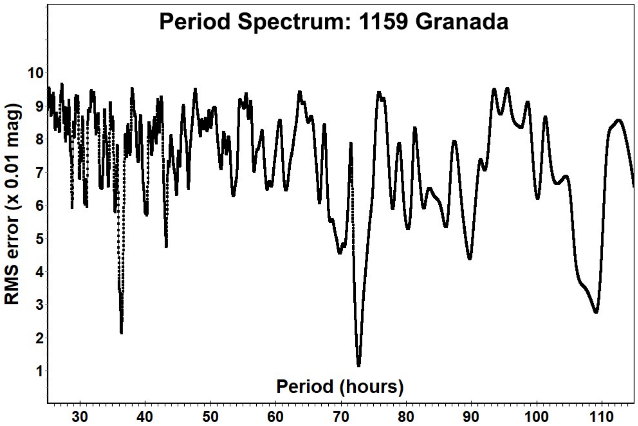

1180 Rita. This heavily studied Hilda-family asteroid was found to have period of 14.898 ± 0.001 hours. The best rotational period has been contentious, with many known reports close to our result (14.902 h, Dahlgren et al., 1998; 14.9 h, Behrend, 2006web; 14.928 h and 14.849 h, Warner and Stephens, 2018; 14.901 h, Behrend, 2020web; 14.8978 h, Ďurech et al., 2020), but others differing (14.72 h, Gonano et al., 1991; 9 h, Binzel and Sauter, 1992; 9.605 h, Polishook, 2012; 20.496 h, Slyusarev et al., 2012; 13.09 h, Warner and Stephens, 2017a; 29.78 h, Colazo et al., 2021a).

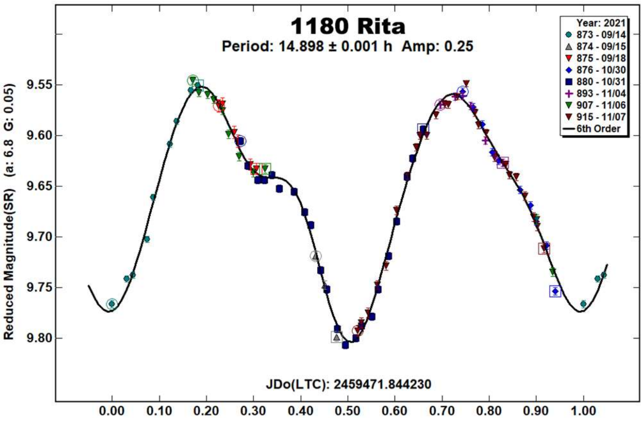

Our period spectrum contains signals at the half-, three-halves, and double durations, but it disfavors other credible candidates, including those near 9, 9.6, and 20 h. The previously reported 29.78 h is very near to twice our result.

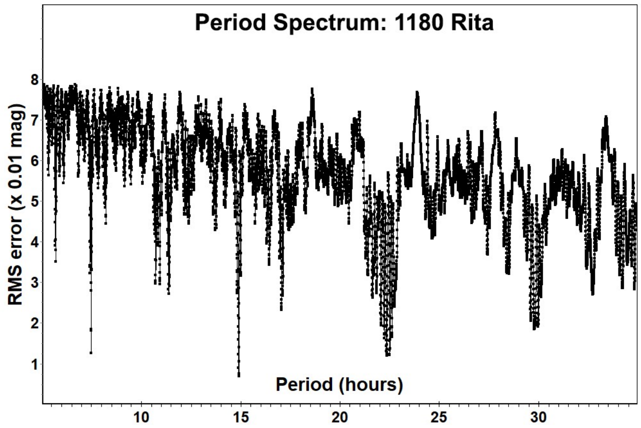

1654 Bojeva. Known period reports for this Eos-family asteroid all differ (10.5559 h, Hayes-Gehrke et al., 2016; 11.44411 h, Ďurech et al., 2020; 25.4837 h, Pál et al., 2020). We find a synodic period of 11.443 ± 0.001 h, with a Fourier fit RMS error of 7 millimagnitudes and *G* very close to the MPC-default value of 0.15. Our lightcurve is clearly bimodal.

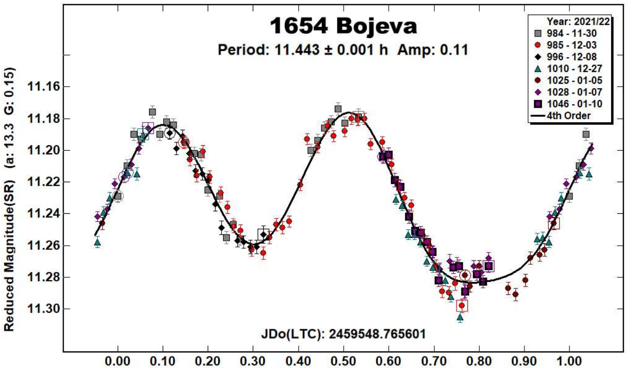

Our period spectrum disfavors periods near 10.6 or 25.5 hours, and these are not accounted for by multiples or by discernable aliasing from our value. The secondary signal seen near 23 h is twice our bimodal period.

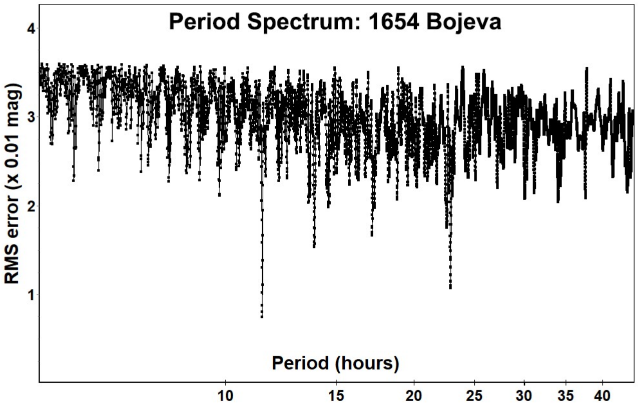

1748 Mauderli. This heavily studied Hilda has developed an increasing consensus for period very near 6 hours. Known reports are numerous (6 h, Gonano et al., 1991; 6 h, Dahlgren et al., 1998; 6.001 h, Slyusarev et al., 2012; 5.552 h, Warner and Stephens, 2017b; 5.32 and 5.551 h, Warner and Stephens, 2018; 6.012 h, Behrend, 2020web; 6.008 h, Romanishin, 2020; 6.003 h, Romanishin, 2021).

We add to the consensus with our new estimate of 6.002 ± 0.001 h. Our Fourier fit RMS error is 7 millimagnitudes; our *G* estimate of 0.31 is uncertain due to a narrow range of phase angles.

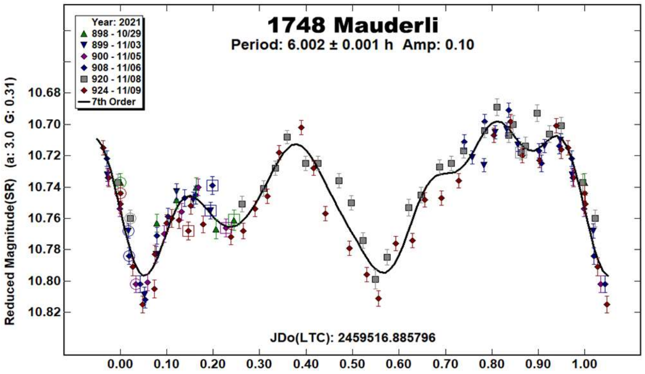

Periods near 6 hours can make for precarious period extraction due to potential cycle-counting errors and resulting aliasing, and indeed our period spectrum shows a minor alias solution near 8 hours (one cycle difference per 24 hours), as well as three-halves and double solutions near 9 and 12 hours. However, our results disfavor previously reported solutions near 5.3 and 5.55 hours.

Our lightcurve contains a remarkably sharp minimum near our phase 0.05, but shows no evidence of this asteroid's being a non-synchronous or contact binary (Romanishin, 2020).

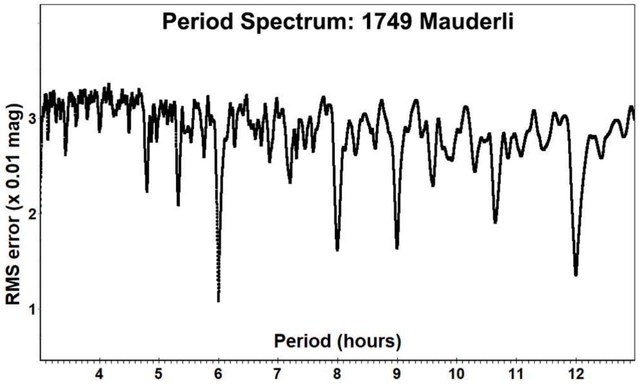

1913 Sekanina. We confirm four survey reports of synodic period (13.97 h, Chang et al., 2014; 13.985 h, Waczszak et al., 2015; 14.0313 h, Ďurech et al., 2020; 14.031 h; Erasmus et al., 2020) for this Koronis-family asteroid with our lightcurve and period estimate of 14.035 ± 0.003 h. The lightcurve is bimodal, and Fourier fit RMS error is 12 mmag.

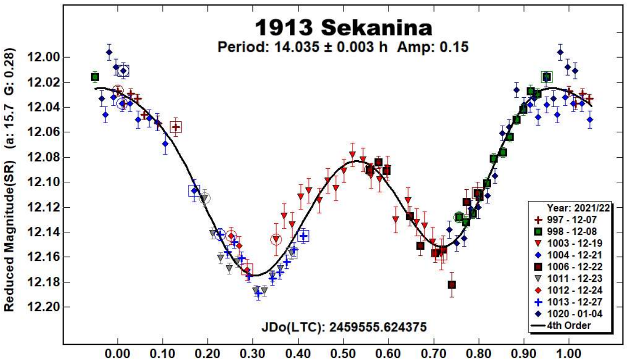

2599 Veseli. The sole known lightcurve report (Bolt and Bembrick, 2007) for this main-belt asteroid offered two period interpretations: 18.54 h, and 13.25 h which the authors preferred. These two offered periods are aliases of each other by ½ (bimodal) period per 24 hours. From 10 nights' observations, we find a period of 13.251 ± 0.001 h. Fourier fit RMS error is 13 mmag. Our period spectrum disfavors a 18.54 h period.

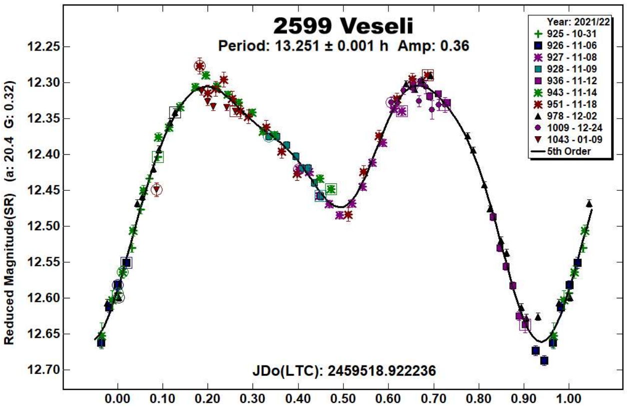

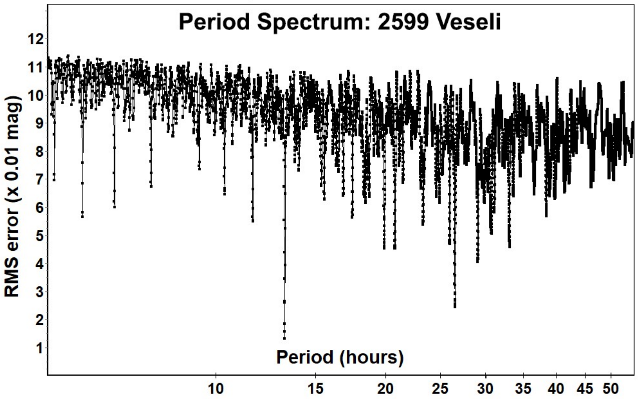

4162 SAF. For this outer main-belt asteroid, we know of only two reports of a rotational period (7.5 h, Behrend, 2002web; 15.2195 h, Pál et al., 2020), and both carry a LCDB uncertainty score of 2. We find a period of 3.850 ± 0.002 h on a monomodal basis. Fourier fit RMS error is 21 mmag. *G* value estimate of 0.03 is uncertain due to narrow phase angle range.

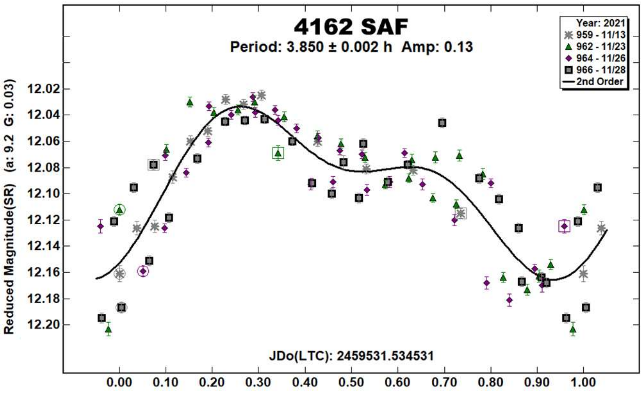

The period spectrum strongly disfavors period candidates near 15 hours, and neither it nor split-halves plots favor a bimodal lightcurve (period 7.7 hours) over the monomodal solution proposed here, though either interpretation is possible. To be certain which is correct may require lightcurve campaigns at various viewing aspects.

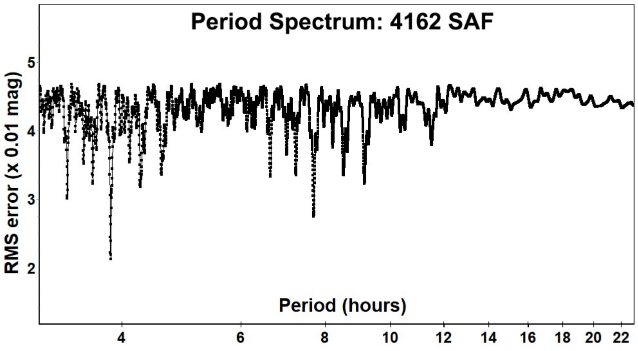

4719 Burnaby. For this asteroid of undetermined class, we find a period of 10.451 ± 0.001 h, differing from two previous reports (8.2 h, Behrend, 2009web; 13.01 h, Warner, 2013). The lightcurve is distinctly bimodal with secondary features just after each minimum. Fourier fit RMS error is 11 mmag.

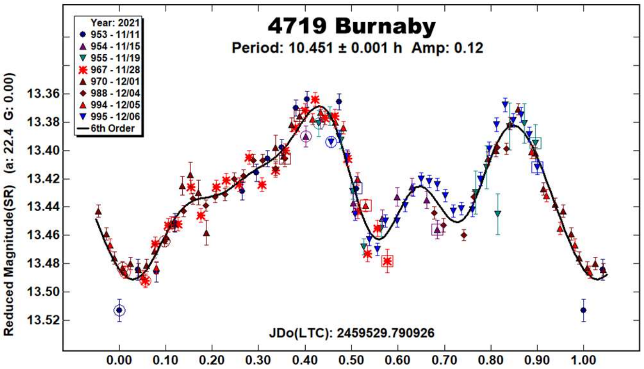

The period spectrum constructed from our data does not support either previously reported period. The 13.01 h reported period is fairly close to an alias of ½ period per 24 hours from our proposed period, and a minor signal near 13 h does appear in our spectrum.

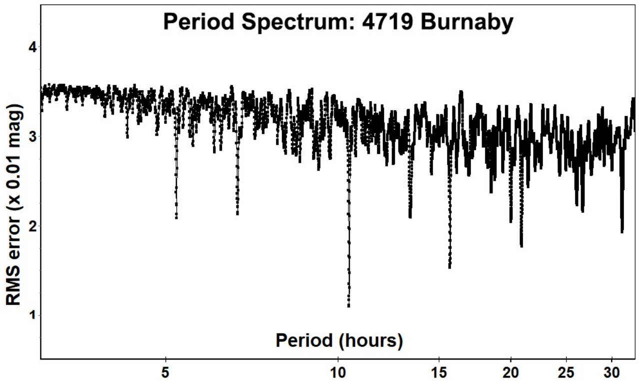

5256 Farquhar. For this Eunomia-family asteroid, we find a period of 11.504 ± 0.002 h, agreeing with one previous report (11.513 h, Odden et al., 2014) but differing from another (16.2215 h, Pál et al., 2020). Fourier fit RMS error is 14 mmag.

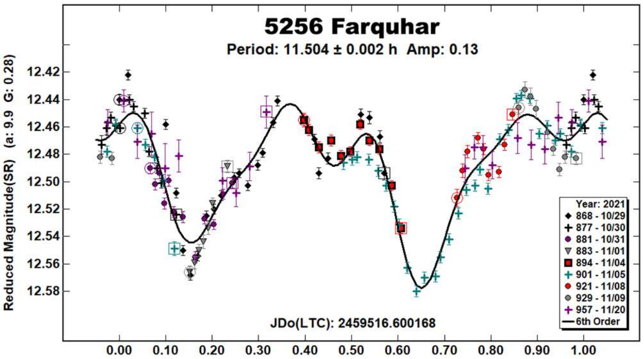

From the present data, neither the lightcurve's shape nor a split-halves plot leads us to prefer unequivocally a bimodal or monomodal solution. Based on the split-halves plot, we adopt the bimodal solution, though monomodal remains a possibility. The period's proximity to 12 (or 6) hours suggests a multi-longitude observation campaign to ensure continuous coverage through a duration of one bimodal period.

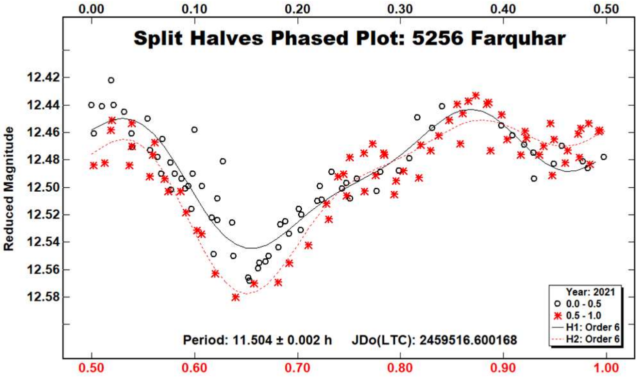

(6706) 1988 VD3. For this relatively faint inner main-belt asteroid, we find a period of 53.398 ± 0.008 h, which is close to twice that of the sole known report (27.021 h; Waszczak et al., 2015). Fourier fit RMS error is 10 mmag.

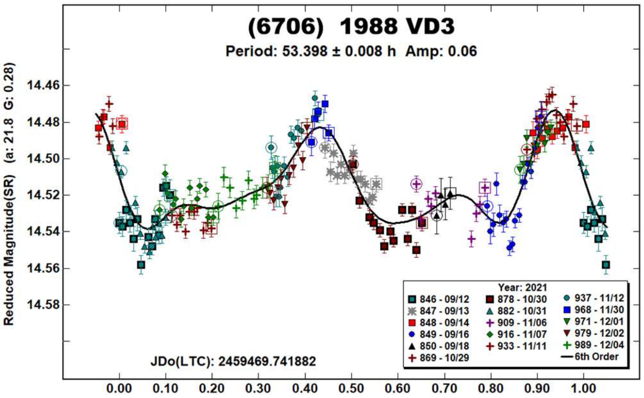

Despite being built from 16 nights of data with low Fourier fit error, our lightcurve shape, period spectrum, and split-halves plot all fail to indicate a clear preference between monomodal and bimodal solutions. Only the small, secondary maximum shapes (near our phases 0.15 and 0.70) differ enough to recommend the bimodal solution, which we adopt here.

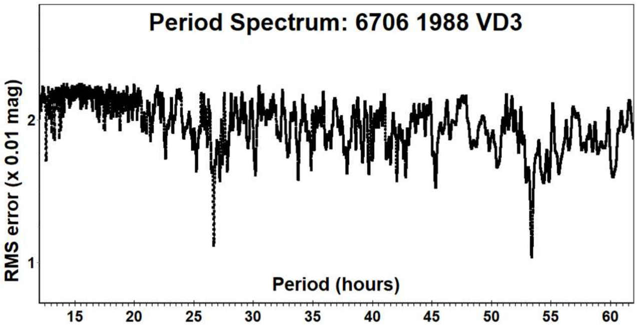

Acknowledgements

The author thanks all authors of the ATLAS paper (Tonry et al, 2018) and its numerous contributors for providing without cost the ATLAS refcat2 catalog release. This project makes extensive use of the python language interpreter and of several supporting packages (notably: pandas, ephem, matplotlib, requests, astropy, and statsmodels), all provided without cost.

References

Aznar Macias, A.; Garcerán, A.C.; Mansego, E.A.; de Haro, J.L.; Silva, A.F.; Silva, G.F.; Martinez, V.M.; Chiner, O.R. (2016). "Twenty-three Asteroids Lightcurves at Observadores de Asteroides (OBAS): 2015 October-December." *Minor Planet Bull.* **43**, 174-181.

Aznar Macias, A. (2017). "Lightcurve Analysis for Nine Main-belt Asteroids. Rotation Period and Physical Parameters from APT Observatory Group: 2016 October-December." *Minor Planet Bull.* **44**, 139-141.

Behrend, R. (2002web, 2005web, 2006web, 2007web, 2008web, 2009web, 2020web, 2021web). Observatoire de Genève web site. *http://obswww.unige.ch/~behrend/page_cou.html*

Binzel, R.P. (1987). "A photoelectric survey of 130 asteroids." *Icarus* **72**, 135-208.

Binzel, R.P.; Sauter, L.M. (1992). "Trojan, Hilda, and Cybele asteroids: New lightcurve observations and analyis." *Icarus* **95**, 222-238.

Bolt, G.; Bembrick, C. (2007). "Lightcurve Analysis of Minor Planets 2544 Gubarev and 2599 Veseli." *Minor Planet Bull.* **34**, 43.

Brines, P.; Lozano, J.; Rodrigo, O.; Formas, A.; Herrero, D.; Mas, V.; Fornas, G.; Carreño, A.; Arce, E. (2017). "Sixteen Asteroids Lightcurves at Asteroids Observers (OBAS) - MPPD: 2016 June-November." *Minor Planet Bull.* **44**, 145-149.

Brinsfield, J.W. (2010). "Asteroid Lightcurve Analysis at the Via Capote Observatory: 2009 3rd Quarter." *Minor Planet Bull.* **37** 19-20.

Chang, C.-K.; Ip, W.-H.; Lin, H.-W.; Cheng, Y.-C.; Ngeow, C.-C.; Yang, T.-C.; Waszczak, A.; Kulkarni, S.R.; Levitan, D.; Sesar, B.; Laher, R.; Surace, J.; Prince, T.A.; PTF Team (2014). "313 New Asteroid Rotation Periods from Palomar Transient Factory Observations." *Astrophys J.* **788**, 17.

Colazo, M. and 23 colleagues (2021a). "Asteroid Photometry and Lightcurve Analysis at Gora Observatories." *Minor Planet Bull.* **48**, 50-55.

Colazo, M. and 19 colleagues (2021b). "Asteroid Photometry and Lightcurve Analysis at Gora's Observatories, Part IV." *Minor Planet Bull.* **48**, 140-143.

Dahlgren, M.; Lahulla, J.F.; Lagerkvist, C.-I.; Lagerros, J.; Mottola, S.; Erikson, A.; Gonano-Beurer, M.; Di Martino, M. (1998). "A Study of Hilda Asteroids: V. Lightcurves of 47 Hilda Asteroids." *Icarus* **133**, 247-285.

Di Martino, M.; Dotto, E.; Cellino, A.; Barucci, M.A.; Fulchignoni, M. (1995). "Intermediate size asteroids: Photoelectric photometry of 8 objects." *Astron. Astrophys. Suppl. Series* **112**, 1-7.

Dose, E.V. (2020). "A New Photometric Workflow and Lightcurves of Fifteen Asteroids." *Minor Planet Bull.* **47**, 324-330.

Dose, E.V. (2021). "Lightcurves of Nineteen Asteroids." *Minor Planet Bull.* **48**, 69-76.

Ďurech, J.; Hanuš, J.; Vančo, R. (2019). "Inversion of asteroid photometry from Gaia DR2 and the Lowell Observatory photometry database." *Astron. Astrophys.* **631**, A2.

Ďurech, J.; Tonry, J.; Erasmus, N.; Denneau, L.; Heinze, A.N.; Flewelling, H.; Vančo, R. (2020). "Asteroid models reconstructed from ATLAS photometry." *Astron. Astrophys.* **643**, A59.

Erasmus, N.; Navarro-Meza, S.; McNeill, A.; Trilling, D.E.; Sickafoose, A.A.; Denneau, L.; Flewelling, H.; Heinze, A.; Tonry, J.L. (2020). "Investigating Taxonomic Diversity within Asteroid Families through ATLAS Dual-band Photometry." *Astrophys. J. Suppl. Series* **247**, 13.

Gonano, M.; Di Martino, M.; Mottola, S.; Neukum, G. (1991). "Physical study of outer belt asteroids." *Adv. Space Res.* **11**, 197-200.

Hamanowa, H.; Hamanowa, H. (2009). "Lightcurves of 494 Virtus, 556 Phyllis, 624 Hektor, 657 Gunlod, 1111 Reinmuthia, 1188 Gothlandia, and 1376 Michelle." *Minor Planet Bull.* **36**, 87-88.

Harris, A.W.; Young, J.W.; Scaltriti, F.; Zappalà, V. (1984). "Lightcurves and phase relations of the asteroids 82 Alkmene and 444 Gyptis." *Icarus* **57**, 251-258.

Harris, A.W.; Young, J.W. (1989). "Asteroid lightcurve observations from 1979-1981." *Icarus* **81**, 314-364.

Hayes-Gehrke, M.N.; Austin, D.; Bowers, C.; Cleary, A.; Dilks, A.; Dzurilla, A.; Friedenberg, M.; Isakower, S.; Davy-Coore, K.; Kee, A.; Leonhartt, G.; Rajpara, S.; Ricciardi, C.; Wolf, J.; Zohery, V. (2016). "Lightcurve Analysis of 1654 Bojeva." *Minor Planet Bull.* **43**, 122.

Marciniak, A. and 23 colleagues (2015). "Against the biases in spins and shapes of asteroids." *Planet Space Sci.* **118**, 256-266.

Marciniak, A. and 42 colleagues (2018). "Photometric survey, modelling, and scaling of long-period and low-amplitude asteroids." *Astron. Astrophys.* **610**, A7.

Menke, J. (2005). "Asteroid Lightcurve Results from Menke Observatory." *Minor Planet Bull.* **32**, 85-88.

Odden, C.E. and 17 colleagues (2014). "Lightcurve Analysis for Three Asteroids: 4000 Hipparachus, 5256 Farquhar, and 5931 Zhvanetskij." *Minor Planet Bull.* **41**, 274-275.

Pál, A.; Szakáts, R.; Kiss, C.; Bódi, A.; Bognár, Z.; Kalup, C.; Kiss, L.L.; Marton, G.; Molnár, L.; Plachy, E.; Sárneczky, K.; Szabó, G.M.; Szabó, R. (2020). "Solar System Objects Observed with TESS - First Data Release: Bright Main-belt and Trojan Asteroids from the Southern Survey." *Astrophys. J. Suppl. Series* **247**, 26.

Pilcher, F. (2014). "Rotation Period Determinations for 24 Themis, 65 Cybele, 108 Hecuba, 530 Turandot, and 749 Malzovia." *Minor Planet Bull.* **41**, 250-252.

Pilcher, F. (2021a). "Lightcurves and Rotation Periods of 49 Pales, 383 Janina, and 764 Gedania." *Minor Planet Bull.* **48**, 5-6.

Pilcher, F. (2021b). "Lightcurves and Rotation Periods of 67 Asia, 74 Galatea, 356 Liguria, 570 Kythera, 581 Tauntonia, 589 Croatia, and 605 Juvisia." *Minor Planet Bull.* **48**, 9-10.

Polakis, T. (2018). "Lightcurve Analysis for Eleven Main-belt Minor Planets." *Minor Planet Bull.* **45**, 269-273.

Polakis, T. (2019). "Lightcurves of Twelve Main-Belt Minor Planets." *Minor Planet Bull.* **46**, 287-292.

Polishook, D. (2012). "Lightcurves for Shape Modeling: 852 Wladilena, 1089 Tama, and 1180 Rita." *Minor Planet Bull.* **39**, 242-244.

Romanishin, W. (2020). "(1748) Mauderli: A Possible Binary in the Hilda Population." *Res. Notes AAS* **4**, 44.

Romanishin, W. (2021). "Lightcurves of Three Hildas." *Minor Planet Bull.* **48**, 15-16.

Slyusarev, I.G.; Shevchenko, V.G.; Belskaya, I.N.; Krugly, Yu.N.; Chiorny, V.G. (2012). "CCD Photometry of Hilda Asteroids." *Proceedings: Asteroids, Comets, Meteors*, 6398.

Stephens, R.D. (2010). "Asteroids Observed from GMARS and Santana Observatories: 2009 June - September." *Minor Planet Bull.* **37**, 28-29.

Tonry, J.L.; Denneau, L.; Flewelling, H.; Heinze, A.N.; Onken, C.A.; Smartt, S.J.; Stalder, B.; Weiland, H.J.; Wolf, C. (2018). "The ATLAS All-Sky Stellar Reference Catalog." *Astrophys. J.* **867,** A105.

Warner, B.D. (2000). "Asteroid Photometry at the Palmer Divide Observatory." *Minor Planet Bull.* **27**, 4-6.

Warner, B.D. (2005). "Asteroid Lightcurve Analysis at the Palmer Divide Observatory - Spring 2005." *Minor Planet Bull.* **32**, 90-92.

Warner, B.D. (2006). "Asteroid Lightcurve Analysis at the Palmer Divide Observatory - Late 2005 and Early 2006." *Minor Planet Bull.* **33**, 58-62.

Warner, B.D.; Harris, A.W.; Pravec, P. (2009). "The asteroid lightcurve database." *Icarus* **202**, 134-146.
https://minplanobs.org/MPInfo/php/lcdb.php

Warner, B.D. (2011). "Upon Further Review: IV. An Examination of Previous Lightcurve Analysis from the Palmer Divide Observatory." *Minor Planet Bull.* **38**, 52-54.

Warner, B.D. (2013). "Asteroid Lightcurve Analysis at the Palmer Divide Observatory: 2013 January - March." *Minor Planet Bull.* **40**, 137-145.

Warner, B.D.; Stephens, R.D. (2017a). "Lightcurve Analysis of Hilda Asteroids at the Center for Solar System Studies: 2016 December thru 2017 April." *Minor Planet Bull.* **44**, 220-222.

Warner, B.D.; Stephens, R.D. (2017b). "Lightcurve Analysis of Hilda Asteroids at the Center for Solar System Studies: 2017 April thru July." *Minor Planet Bull.* **44**, 331-334.

Warner, B.D., Stephens, R.D. (2018). "Lightcurve Analysis of Hilda Asteroids at the Center for Solar System Studies: 2018 April-June." *Minor Planet Bull.* **45**, 390-393.

Warner, B.D. (2021). *MPO Canopus* Software, version 10.8.4.11. BDW Publishing. *http://www.bdwpublishing.com*

Waszczak, A.; Chang, C.-K.; Ofek, E.O.; Laher, R.; Masci, F.; Levitan, D.; Surace, J.; Cheng, Y.-C.; Ip, W.-H.; Kinoshita, D.; Helou, G.; Prince, T.A.; Kulkarni, S. (2015). "Asteroid Light Curves from the Palomar Transient Factory Survey: Rotation Periods and Phase Functions from Sparse Photometry." *Astron. J.* **150**, 75.

Weidenschilling, S.J.; Chapman, C.R.; Davis, D.R.; Greenberg, R.; Levy, D.H.; Binzel, R.P.; Vail, S.M.; Magee, M.; Spaute, D. (1990). "Photometric geodesy of main-belt asteroids III. Additional lightcurves." *Icarus* **86**, 402-447.

CCD PHOTOMETRY OF 11 ASTEROIDS AT SOPOT ASTRONOMICAL OBSERVATORY: 2021 JULY - 2022 JANUARY

Vladimir Benishek
Belgrade Astronomical Observatory
Volgina 7, 11060 Belgrade 38, SERBIA
vlaben@yahoo.com

(Received: 2022 Jan 13, Revised: 2022 Feb 12)

CCD photometric observations carried out at Sopot Astronomical Observatory (SAO) from 2021 July to 2022 January led to establishing the lightcurve and synodic rotation period solutions for 11 asteroids.

Photometric observations of 11 asteroids were conducted at Sopot Astronomical Observatory (SAO) from 2021 July to 2022 January in order to determine their synodic rotation periods. For this purpose, two 0.35-m *f*/6.3 Meade LX200GPS Schmidt-Cassegrain telescopes were employed. The telescopes are equipped with a SBIG ST-8 XME and a SBIG ST-10 XME CCD cameras. The exposures were unfiltered and unguided for all targets. Both cameras were operated in 2×2 binning mode, which produces image scales of 1.66 arcsec/pixel and 1.25 arcsec/pixel for ST-8 XME and ST-10 XME cameras, respectively. Prior to measurements, all images were corrected using dark and flat field frames.

Photometric reduction was conducted using *MPO Canopus* (Warner, 2018). Differential photometry with up to five comparison stars of near solar color ($0.5 \le B-V \le 0.9$) was performed using the Comparison Star Selector (CSS) utility. This helped ensure a satisfactory quality level of night-to-night zero-point calibrations and correlation of the measurements within the standard magnitude framework. Field comparison stars were calibrated using standard Cousins R magnitudes derived from the Carlsberg Meridian Catalog 15 (VizieR, 2021) Sloan r' magnitudes using the formula: $R = r' - 0.22$ in all cases presented in this paper. In some instances, small zero-point adjustments were necessary in order to achieve the best match between individual data sets in terms of achieving the most favorable statistical indicators of Fourier fit.

Lightcurve construction and period analysis were performed using *Perfindia* custom-made software developed in the R statistical programming language (R Core Team, 2020) by the author of this paper. The essence of its algorithm is reflected in finding the most favorable solution for rotational period by minimizing the *residual standard error* of the lightcurve Fourier fit.

The lightcurve plots presented in this paper show so-called 2% error for rotational periods, *i.e.,* an error that would cause the last data point in a combined data set by date order to be shifted by 2% (Warner, 2012) and represented by the following formula: $\Delta P = (0.02 \cdot P^2) / T$, where P and T are the rotational period and the total time span of observations, respectively. Both of these quantities must be expressed in the same units.

Some of the targets presented in this paper were observed within the Photometric Survey for Asynchronous Binary Asteroids (*BinAstPhot Survey*) under the leadership of Dr. Petr Pravec from Ondřejov Observatory, Czech Republic.

Table I gives the observing circumstances and results.

1141 Bohmia. The only previous rotation period determination was done in the 2018-2019 apparition within the *BinAstPhot Survey* using data obtained by Pray and Benishek in 2019 January. A period of 2.8480 h (Pravec, 2019web) was found. A new period result of $P = 2.849 \pm 0.001$ h, fully consistent with the previously determined result, was derived from the SAO observations acquired on five nights in 2021 September.

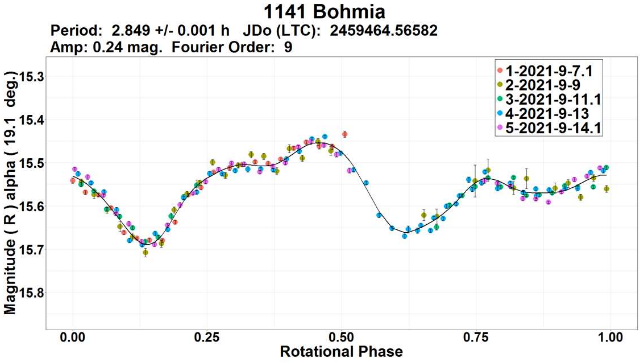

1842 Hynek. There is a significant discrepancy between the rotation period results found by Behrend in several apparitions (3.94 h, 2004web; 3.9410 h, 2007web; 3.94 h, 2014web) and the one of Pal et al. (25.3466 h, 2020). Due to the lightcurve shape changing over the observing time span, the dense SAO photometric data were divided into two groups that were analyzed separately. Rotation period values derived from these two combined data sets are highly consistent with each other (3.943 ± 0.001 h and 3.941 ± 0.005 h), as well as with the results previously found by Behrend.

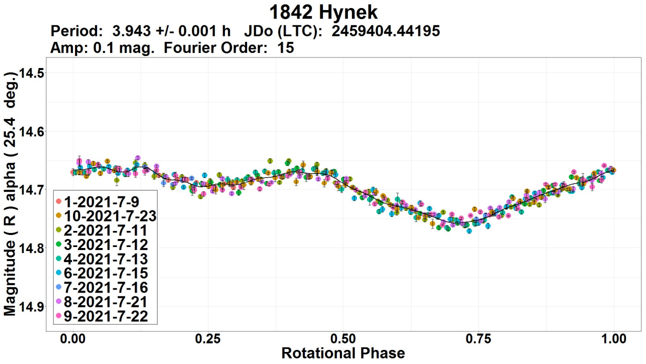

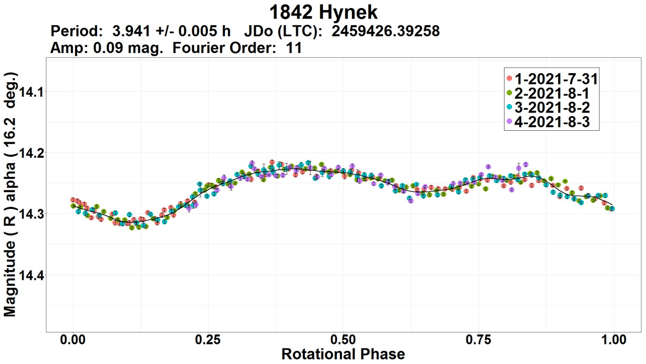

1929 Kollaa. Two previously found rotation periods by Ryan (2.980 h, 2007web) and Behrend (2.9887 h, 2008web) are in complete agreement with the rotation period value of $P = 2.982 \pm 0.004$ h, found from the SAO observations carried out on two nights in 2021 December.

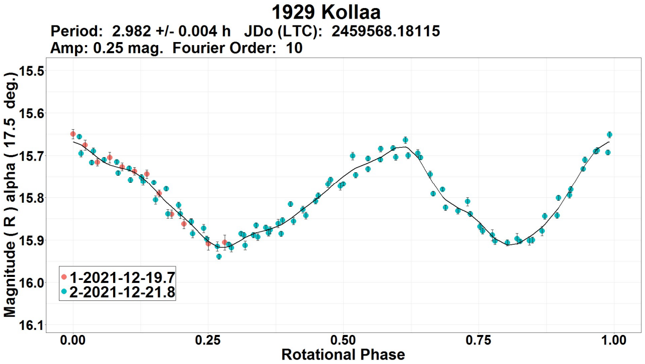

2807 Karl Marx. Period analysis using the 2021 December - 2022 January dense photometric combined data set obtained on three nights led to a bimodal lightcurve and an unambiguous period solution of *P* = 8.840 ± 0.006 h. The difference from the only previous period determination by Pal et al. (8.81893 h, 2020) is not substantial, but apparently is not exactly negligible.

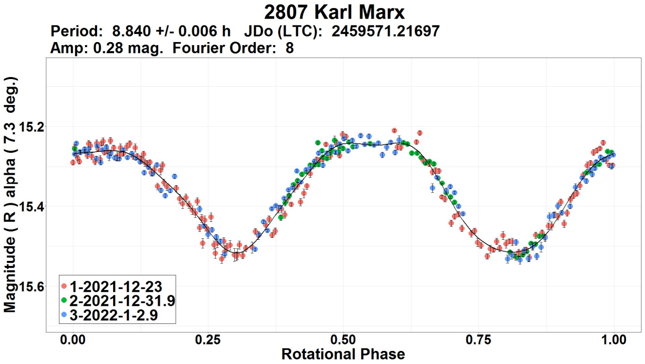

5917 Chibasai. A bimodal period solution of *P* = 2.651 ± 0.003 h resulting from the dense SAO photometric data collected on two nights in 2021 October shows very good match with all previously found results: 2.645 h (Behrend, 2004web), 2.65 h (Stephens, 2005) and Pal et al. (2.65032 h, 2020).

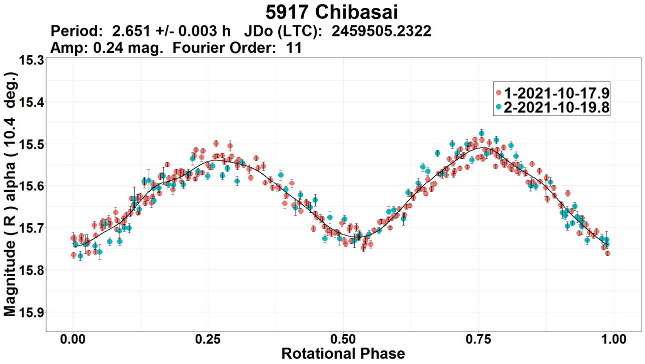

10389 Robmanning. The LCDB (Warner et al., 2009) records show two previous significantly different rotation period determinations: Hasegawa et al. (2.75 h, 2014) and Pal et al. (5.76754 h, 2020). The more recent one of these shows a close proximity to the period of *P* = 5.77 ± 0.01 h derived from the dense SAO data obtained over four consecutive nights in 2021 October. This statistically plausible result corresponds to a quadramodal lightcurve (four minima and four maxima per rotational cycle) of a relatively low amplitude (0.14 mag). A "split-halves" test shows a significant mismatch between two halves of the 5.77-hour period quadramodal lightcurve, well beyond the data scatter level; this rules out the possibility for the half-period reported by Hasegawa et al.

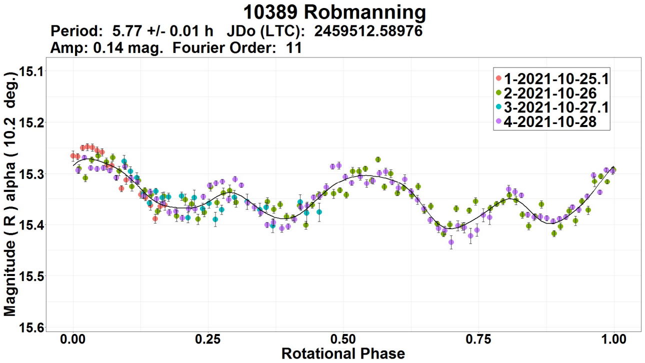

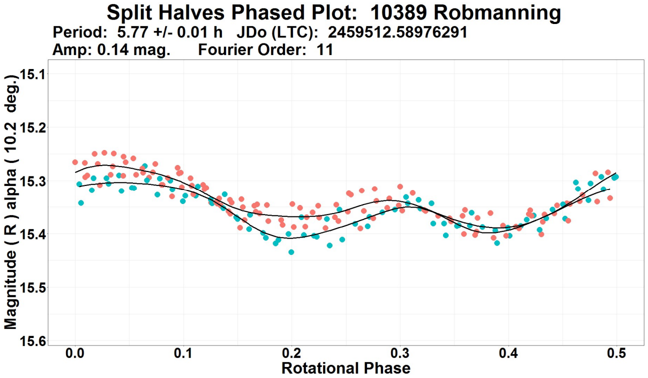

(15560) 2000 GR24. The only previously determined rotation period by Pal et al. (28.8446 h, 2020) substantially differs from the bimodal period of *P* = 2.3212 ± 0.0003 h found from the 2021 October-November SAO dense photometric data acquired on eight nights.

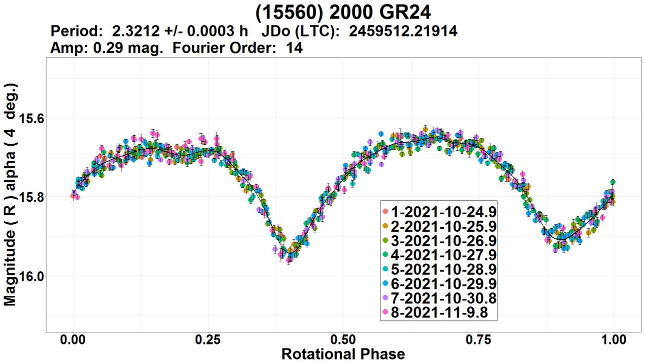

19982 Barbaradoore. The period found from the two consecutive nights 2021 October SAO data (*P* = 3.314 ± 0.007 h) is consistent with two previous result by Pravec (3.3162 h; 2010web) and Pal et al. (3.31528 h; 2020).

Number	Name	20yy/mm/dd	Phase	L_{PAB}	B_{PAB}	Period (h)	P.E.	Amp	A.E.	Grp
1141	Bohmia	21/09/07-21/09/14	19.1,15.8	13	-6	2.849	0.001	0.24	0.02	FLOR
1842	Hynek	21/07/08-21/07/23	25.4,20	329	2	3.943	0.001	0.10	0.02	MB-I
1842	Hynek	21/07/30-21/08/03	16.2,14.5	332	1	3.941	0.005	0.09	0.02	MB-I
1929	Kollaa	21/12/19-21/12/21	17.5,18.2	52	-1	2.982	0.004	0.25	0.03	V
2807	Karl Marx	21/12/22-22/01/03	*7.3,5.6	100	10	8.840	0.006	0.28	0.03	DOR
5917	Chibasai	21/10/17-21/10/19	10.4,9.8	38	16	2.651	0.003	0.24	0.03	MAR
10389	Robmanning	21/10/25-21/10/28	10.2,8.4	45	-5	5.77	0.01	0.14	0.03	FLOR
15560	2000 GR24	21/10/24-21/11/09	4.0,11.8	25	-2	2.3212	0.0003	0.29	0.03	MB-O
19982	Barbaradoore	21/10/19-21/10/21	30.2,29.9	57	31	3.314	0.007	0.24	0.02	PHO
20041	1992 YH	21/10/29-21/12/08	*14.1,9.2	60	-4	2.6205	0.0002	0.10	0.02	MB-I
27111	1998 VV34	21/09/24-21/11/01	*5.5,17.5	10	4	3.3233	0.003	0.14	0.03	MB-I
46304	2001 OZ62	21/09/24-21/09/26	2.1,1.8	3	-3	2.664	0.006	0.09	0.02	MB-I

Table I. Observing circumstances and results. Phase is the solar phase angle given at the start and end of the date range. If preceded by an asterisk, the phase angle reached an extrema during the period. L_{PAB} and B_{PAB} are the average phase angle bisector longitude and latitude. Grp is the asteroid family/group (Warner *et al.*, 2009): FLOR = Flora, MB-I/O = main-belt inner / outer, MAR = Maria, DOR = Dora, PHO = Phocaea, V = Vestoid.

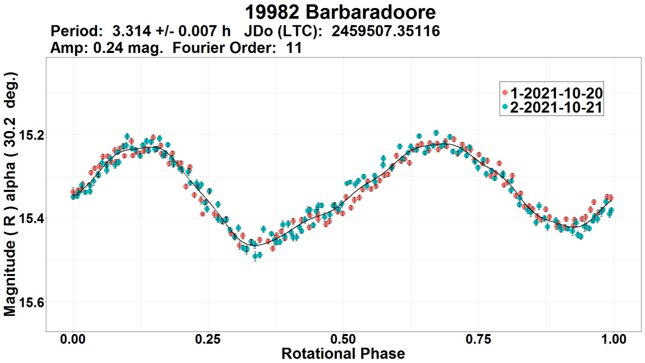

(20041) 1992 YH. No prior rotation period reports were found for this asteroid. Photometric observations at SAO were performed in a somewhat longer time span from late 2021 October until early 2021 December over a total of six nights. There was no significant change of the lightcurve shape during that time. Period analysis shows a rotation period of $P = 2.6205 \pm 0.0002$ h to be the most likely result.

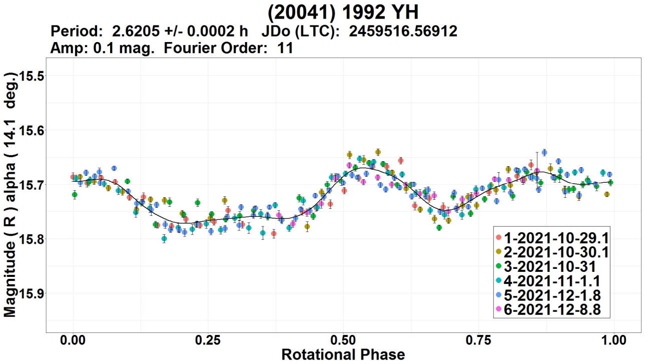

(27111) 1998 VV34. A rotation period result of $P = 3.3233 \pm 0.0003$ h was found from the six-night data obtained over a longer time span (2021 September - November). It is associated with an bimodal lightcurve with a consistent shape over the time of the observations. This result is fully consistent with the only previous result of $P = 3.323$ h Strabla et al. (2012).

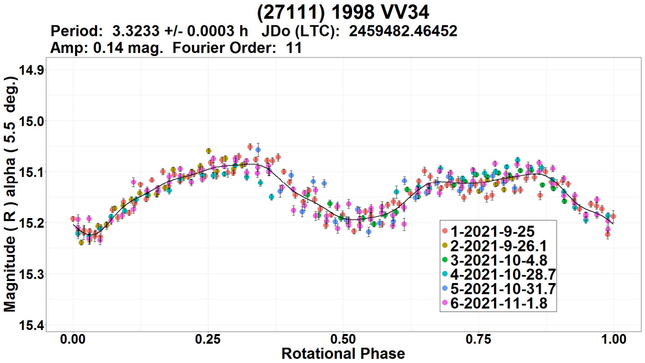

(46304) 2001 OZ62. Data taken with a dense cadence in late 2021 September led to a bimodal period solution of $P = 2.664 \pm 0.006$ h. There is good agreement with the rotation period reported by Waszczak et al. (2015) of 2.655 h, but it differs somewhat more from that found by Fauerbach and Brown (2.73 h; 2019).

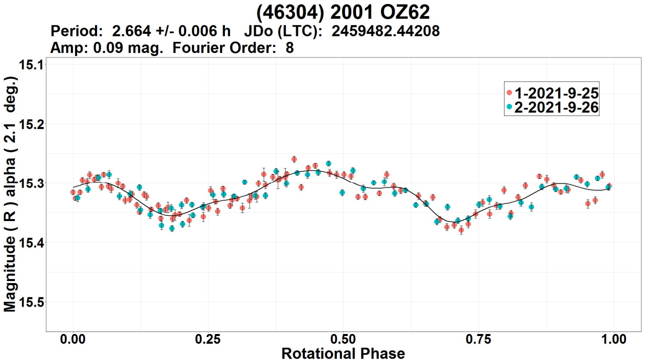

Acknowlegments

Observational work at Sopot Astronomical Observatory is supported by a 2018 Gene Shoemaker NEO Grant from The Planetary Society.

References

Behrend, R. (2004web, 2007web, 2008web, 2014web). Observatoire de Geneve web site. *http://obswww.unige.ch/~behrend/page_cou.html*

Fauerbach, M.; Brown, A. (2019). "Rotational Period Determination for Asteroids 2498 Tsesevich, (16024) 1999 CT101, (46304) 2001 OZ62." *Minor Planet Bull.* **46**, 19-20.

Hasegawa, S.; Miyasaka, S.; Mito, H.; Sarugaku, Y.; Ozawa, T.; Kuroda, D.; Nishihara, S.; Harada, A.; Yoshida, M.; Yanagisawa, K.; Shimizu, Y.; Nagayama, S.; Toda, H.; Okita, K.; Kawai, N.; Mori, M.; Sekiguchi, T.; Ishiguro, M.; Abe, T.; Abe, M. (2014). "Lightcurve survey of V-type asteroids in the inner asteroid belt." *Pub. of Astron. Soc. Japan* **66**, 5415.

Pal, A.; Szakáts, R.; Kiss, C.; Bódi, A.; Bognár, Z.; Kalup, C.; Kiss, L.L.; Marton, G.; Molnár, L.; Plachy, E.; Sárneczky, K.; Szabó, G.M.; Szabó, R. (2020). "Solar System Objects Observed with TESS - First Data Release: Bright Main-belt and Trojan Asteroids from the Southern Survey." *Ap. J. Supl. Ser.* **247**, 26-34.

Pravec, P. (2010web, 2019web). Photometric Survey for Asynchronous Binary Asteroids web site. *http://www.asu.cas.cz/~ppravec/newres.txt*

R Core Team (2020). R: A language and environment for statistical computing. R Foundation for Statistical Computing. Vienna, Austria. *https://www.R-project.org/*

Ryan, W.H. (2007web). Posting on CALL web site. *https://minplanobs.org/MPInfo/php/call.php*

Stephens, R.D. (2005). "Rotation Periods of 96 Aegle, 386 Siegena, 390 Alma, 544 Jetta, 2771 Polzunov, and (5917) 1991 NG." *Minor Planet Bull.* **32**, 2-3.

Strabla, L.; Quadri, U.; Girelli, R. (2012). "Lightcurve Analysis for Eight Minor Planets at Bassano Bresciano Observatory." *Minor Planet Bull.* **39**, 177-179.

VizieR (2021). *http://vizier.u-strasbg.fr/viz-bin/VizieR*

Warner, B.D.; Harris, A.W.; Pravec, P. (2009). "The Asteroid Lightcurve Database." *Icarus* **202**, 134-146. Updated 2021 Dec. *http://www.minorplanet.info/lightcurvedatabase.html*

Warner, B.D. (2012). The MPO Users Guide: A Companion Guide to the MPO Canopus/PhotoRed Reference Manuals. BDW Publishing, Colorado Springs, CO.

Warner, B.D. (2018). *MPO Canopus* software, version 10.7.11.3. *http://www.bdwpublishing.com*

Waszczak, A.; Chang, C.-K.; Ofek, E.O.; Laher, R.; Masci, F.; Levitan, D.; Surace, J.; Cheng, Y.-C.; Ip, W.-H.; Kinoshita, D.; Helou, G.; Prince, T.A.; Kulkarni, S. (2015). "Asteroid Light Curves from the Palomar Transient Factory Survey: Rotation Periods and Phase Functions from Sparse Photometry." *Astron. J.* **150**, A75.

LIGHTCURVE PHOTOMETRY OPPORTUNITIES: 2022 APRIL-JUNE

Brian D. Warner
Center for Solar System Studies (CS3)
446 Sycamore Ave.
Eaton, CO 80615 USA
brian@MinorPlanetObserver.com

Alan W. Harris
Center for Solar System Studies (CS3)
La Cañada, CA 91011-3364 USA

Josef Ďurech
Astronomical Institute
Charles University
18000 Prague, CZECH REPUBLIC
durech@sirrah.troja.mff.cuni.cz

Lance A.M. Benner
Jet Propulsion Laboratory
Pasadena, CA 91109-8099 USA
lance.benner@jpl.nasa.gov

We present lists of asteroid photometry opportunities for objects reaching a favorable apparition and have no or poorly-defined lightcurve parameters. Additional data on these objects will help with shape and spin axis modeling using lightcurve inversion. The "Radar-Optical Opportunities" section includes a list of potential radar targets as well as some that might be in critical need of astrometric data.

We present several lists of asteroids that are prime targets for photometry and/or astrometry during the period 2022 April through June. The "Radar-Optical Opportunities" section provides an expanded list of potential NEA targets, many of which are planned for radar observations.

In the first three sets of tables, "Dec" is the declination and "U" is the quality code of the lightcurve. See the latest asteroid lightcurve data base (LCDB from here on; Warner et al., 2009) documentation for an explanation of the U code:

http://www.minorplanet.info/lightcurvedatabase.html

The ephemeris generator on the MinorPlanet.info web site allows creating custom lists for objects reaching V ≤ 18.0 during any month in the current year and up to five years in the future, e.g., limiting the results by magnitude and declination, family, and more.

https://www.minorplanet.info/php/callopplcdbquery.php

We refer you to past articles, e.g., Warner et al. (2021a; 2021b) for more detailed discussions about the individual lists and points of advice regarding observations for objects in each list.

Once you've obtained and analyzed your data, it's important to publish your results. Papers appearing in the *Minor Planet Bulletin* are indexed in the Astrophysical Data System (ADS) and so can be referenced by others in subsequent papers. It's also important to make the data available at least on a personal website or upon request. We urge you to consider submitting your raw data to the ALCDEF database. This can be accessed for uploading and downloading data at *http://www.alcdef.org*

The database contains more than 3.9 million observations for 15,000+ objects, making it one of the more useful sources for raw data of dense time-series asteroid photometry.

Lightcurve/Photometry Opportunities

Objects with U = 3– or 3 are excluded from this list since they will likely appear in the list for shape and spin axis modeling. Those asteroids rated U = 1 should be given higher priority over those rated U = 2 or 2+, but not necessarily over those with no period. On the other hand, do not overlook asteroids with U = 2/2+ on the assumption that the period is sufficiently established. Regardless, do not let the existing period influence your analysis since even highly-rated result have been proven wrong at times. Note that the lightcurve amplitude in the tables could be more or less than what's given. Use the listing only as a guide.

An entry in bold italics is a near-Earth asteroid (NEA).

		Brightest			LCDB Data		
Number	Name	Date	Mag	Dec	Period	Amp	U
795	Fini	04 09.2	12.9	-8	9.292	0.02-0.06	1+
2328	Robeson	04 09.9	15.0	-2	18.632	0.20	2+
2689	Bruxelles	04 10.7	15.0	-6	8.71	0.05	2
5237	Yoshikawa	04 13.0	15.2	-6	3.47	0.33	2
3224	Irkutsk	04 16.5	14.3	-13	33.14	0.51	2
4544	Xanthus	04 20.2	14.9	-19	37.65	0.27	2
3580	Avery	04 22.6	15.5	-16	24.226	0.17-0.33	2
36731	2000 RR50	05 04.8	15.5	-18	7.494	0.10	1
5009	Sethos	05 05.2	15.4	-16	2.691	0.08	2
17567	Hoshinoyakata	05 08.5	15.4	-18	19.882	0.34-0.40	2
4639	Minox	05 10.6	15.5	-21	12.993	0.40	2
10212	1997 RA7	05 16.0	15.5	-20	9.154	0.88-1.05	2
3469	Bulgakov	05 16.6	14.9	-15	6.48	0.05-0.09	1
5557	Chimikeppuko	05 24.2	15.2	-29	4.168	0.35-0.46	2
5693	1993 EA	05 24.2	13.7	+15	2.496	0.05-0.13	2
3901	Nanjingdaxue	05 28.8	14.5	-45	21.4	0.21-0.28	2+
7134	Ikeuchisatoru	05 30.0	15.0	-13	20	0.15	2
3466	Ritina	05 31.4	15.0	-20	5.253	0.51	2
9900	Llull	06 02.6	14.5	-14	183.319	0.88	2
3909	Gladys	06 03.5	14.8	-9	6.83	0.04-0.15	1
30810	1990 FM	06 04.4	15.4	-16	82.259	0.48-0.55	2
10922	1998 BG2	06 06.9	14.9	-22	7.92	0.12	2
11354	1997 XY9	06 08.1	15.5	-24	6.192		2-
3326	Agafonikov	06 09.1	15.0	-29	8.118		2
2492	Kutuzov	06 14.3	15.1	-24	15.099		2-
1109	Tata	06 19.3	13.7	-23	8.277	0.06	2
6481	Tenzing	06 21.0	15.0	-35	6.517	0.13	2
7899	Joya	06 23.1	15.3	-25	85.658		2
783	Nora	06 25.4	12.7	-8	55.53	0.08-0.13	2
10347	Murom	06 30.7	15.2	-21	35.3	0.45	2-

Low Phase Angle Opportunities

The Low Phase Angle list includes asteroids that reach very low phase angles ($\alpha < 1°$). The "α" column is the minimum solar phase angle for the asteroid. Getting accurate, calibrated measurements (usually V band) at or very near the day of opposition can provide important information for those studying the "opposition effect." Use the on-line query form for the LCDB to get more details about a specific asteroid.

https://www.minorplanet.info/php/callopplcdbquery.php

The best chance of success comes with covering at least half a cycle a night, meaning periods generally < 16 h, when working objects with low amplitude. Objects with large amplitudes and/or long periods are much more difficult for phase angle studies since, for proper analysis, the data must be reduced to the average magnitude of the asteroid for each night. Refer to Harris et al. (1989) for the details of the analysis procedure.

As an aside, it is arguably better for physical interpretation (e.g., *G* value versus albedo) to use the maximum light rather than mean level to find the phase slope parameter (*G*). Maximum light better models the behavior of a spherical object of the same albedo, but it can produce significantly different values for both *H* and *G* versus using average light level, which is the method used for values listed by the Minor Planet Center. Using and reporting the results of both methods can provide additional insights into the physical properties of an asteroid.

The International Astronomical Union (IAU) has adopted a new system, H-G_{12}, introduced by Muinonen et al. (2010). It will be some years before H-G_{12} becomes widely used, and hopefully not until a discontinuity flaw in the G_{12} function has been fixed. This discontinuity results in false "clusters" or "holes" in the solution density and makes it impossible to draw accurate conclusions.

We strongly encourage obtaining data as close to 0° as possible, then every 1-2° out to 7°, below which the curve tends to be non-linear due to the opposition effect. From 7° out to about 30°, observations at 3-6° intervals should be sufficient. Coverage beyond 50° or so is not generally helpful since the H-G system is best defined with data from 0-30°.

It's important to emphasize that all observations should (must) be made using high-quality catalogs to set the comparison star magnitudes. These include ATLAS, Pan-STARRS, SkyMapper, and Gaia2/3. Catalogs such as CMC-15, APASS, or the MPOSC from *MPO Canopus* have too high of significant systematic errors.

Also important is that that there are sufficient data from each observing run such that their location can be found on a combined, phased lightcurve derived from two or more nights obtained *near the same phase angle.* If necessary, the magnitudes for a given run should be adjusted so that they correspond to mid-light of the combined lightcurve. This goes back to the H-G system being based on average, not maximum or minimum light.

The asteroid magnitudes are brighter than in others lists because higher precision is required and the asteroid may be a full magnitude or fainter when it reaches phase angles out to 20-30°.

Num	Name	Date	α	V	Dec	Period	Amp	U
340	Eduarda	04 02.7	0.62	13.7	-03	8.006	0.17-0.32	3
431	Nephele	04 07.2	0.72	13.7	-04	13.530	0.03-0.23	3
578	Happelia	04 08.1	0.73	12.8	-05	10.061	0.11-0.16	3
104	Klymene	04 08.5	0.47	13.0	-06	8.984	0.2 -0.3	3
176	Iduna	04 09.0	0.27	13.3	-08	11.288	0.14-0.43	3
795	Fini	04 09.2	0.43	12.9	-08	9.292	0.02-0.06	1+
135	Hertha	04 11.7	0.88	11.5	-10	8.403	0.12-0.30	3
720	Bohlinia	04 15.5	0.27	13.3	-09	8.919	0.16-0.46	3
79	Eurynome	04 16.0	0.04	11.6	-10	5.978	0.05-0.25	3
82	Alkmene	04 18.9	0.14	11.0	-11	12.999	0.18-0.54	3
76	Freia	04 19.7	0.13	12.8	-11	9.973	0.05-0.33	3
13	Egeria	05 04.9	0.18	9.9	-16	7.045	0.12-0.47	3
342	Endymion	05 11.1	0.19	13.8	-18	6.319	0.15-0.23	3
240	Vanadis	05 16.5	0.83	13.5	-17	10.64	0.08-0.34	3
332	Siri	05 16.5	0.67	13.3	-21	8.007	0.10-0.35	3
368	Haidea	05 16.7	0.67	13.7	-17	9.823	0.15-0.23	3
26	Proserpina	05 21.7	0.65	10.3	-22	13.110	0.08-0.21	3
534	Nassovia	05 26.8	0.79	13.7	-19	9.382	0.15-0.37	3
596	Scheila	05 28.9	0.64	11.8	-20	15.848	0.06-0.10	3
367	Amicitia	05 29.7	0.64	13.1	-20	5.055	0.25-0.90	3
3873	Roddy	05 30.8	0.61	13.9	-23	2.478	0.05-0.11	3
144	Vibilia	06 01.3	0.28	11.8	-21	13.819	0.13-0.20	3
492	Gismonda	06 03.6	0.38	14.0	-23	6.488	0.10-0.14	3
350	Ornamenta	06 17.4	0.79	13.4	-21	9.178	0.10-0.3	3
149	Medusa	06 18.0	0.72	12.9	-22	26.023	0.33-0.56	3
563	Suleika	06 18.5	0.19	12.8	-24	5.69	0.13-0.28	3
1109	Tata	06 19.3	0.14	13.8	-23	8.277	0.06	2
182	Elsa	06 21.3	0.36	12.6	-22	80.088	0.60-0.72	3
583	Klotilde	06 22.7	0.81	13.8	-21	9.213	0.17-0.30	3
222	Lucia	06 27.0	0.33	13.0	-24	7.837	0.25-0.41	3
786	Bredichina	06 28.2	0.95	12.6	-26	29.434	0.05-0.60	3-

Shape/Spin Modeling Opportunities

Those doing work for modeling should contact Josef Ďurech at the email address above. If looking to add lightcurves for objects with existing models, visit the Database of Asteroid Models from Inversion Techniques (DAMIT) web site

https://astro.troja.mff.cuni.cz/projects/damit/

Additional lightcurves could lead to the asteroid being added to or improving one in DAMIT, thus increasing the total number of asteroids with spin axis and shape models.

Included in the list below are objects that:

1. Are rated U = 3– or 3 in the LCDB.
2. Do not have reported pole in the LCDB Summary table.
3. Have at least three entries in the Details table of the LCDB where the lightcurve is rated U ≥ 2.

The caveat for condition #3 is that no check was made to see if the lightcurves are from the same apparition or if the phase angle bisector longitudes differ significantly from the upcoming apparition. The last check is often not possible because the LCDB does not list the approximate date of observations for all details records. Including that information is an on-going project.

Favorable apparitions are in bold text. NEAs are in italics.

		Brightest			LCDB Data		
Num	Name	Date	Mag	Dec	Period	Amp	U
811	Nauheima	04 01.6	14.8	-1	4.001	0.11-0.20	3
2093	Genichesk	04 02.3	15.4	+2	11.028	0.23-0.27	3
1005	Arago	04 05.1	15.0	-18	8.789	0.22-0.25	3
547	Praxedis	04 05.2	14.4	-5	9.105	0.04-0.12	3
213	Lilaea	04 05.6	12.6	+4	12.042	0.07-0.20	3
4375	**Kiyomori**	**04 06.2**	**15.3**	**+3**	**6.471**	**0.15-0.16**	**3**
431	Nephele	04 07.3	13.8	-4	13.53	0.03-0.23	3
1242	Zambesia	04 07.4	14.9	-13	17.315	0.11-0.24	3
445	Edna	04 09.4	15.0	-33	19.959	0.21-0.27	3
5484	**Inoda**	**04 11.2**	**15.3**	**+2**	**14.148**	**0.09-0.16**	**3**
4221	**Picasso**	**04 12.2**	**15.4**	**-2**	**3.111**	**0.27-0.31**	**3**
612	Veronika	04 16.4	15.4	-8	8.243	0.09-0.14	3
4029	Bridges	04 18.9	15.0	-12	3.575	0.18-0.29	3
2103	Laverna	04 19.2	14.6	-23	9.249	0.15-0.22	3
414	Liriope	04 19.3	14.9	+1	11.005	0.10-0.16	3
1656	Suomi	04 20.7	15.3	+16	2.588	0.08-0.20	3
1765	Wrubel	04 21.2	15.1	+7	5.26	0.11-0.33	3
773	Irmintraud	04 22.2	13.3	-34	6.751	0.05-0.25	3
275	Sapientia	04 23.1	11.9	-5	14.931	0.05-0.12	3-
5168	Jenner	04 23.8	15.3	-54	3.258	0.24-0.35	3
109	Felicitas	04 24.4	13.7	-19	13.191	0.06-0.17	3
1866	Sisyphus	04 25.0	14.3	+1	2.4	0.02-0.17	3
1018	Arnolda	04 25.1	14.9	-19	14.617	0.28-0.39	3
1129	Neujmina	04 25.2	15.0	-23	5.084	0.06-0.20	3
633	Zelima	04 26.3	14.6	+1	11.73	0.14-0.49	3
1416	Renauxa	04 26.5	15.4	-23	8.7	0.09-0.40	3
768	Struveana	04 26.7	15.4	-13	10.753	0.26-0.54	3-
1961	Dufour	04 28.8	15.5	-16	15.79	0.17-0.35	3-
25332	1999 KK6	04 29.0	15.5	-16	2.453	0.06-0.11	3
1262	Sniadeckia	04 30.0	14.7	+4	17.57	0.06-0.16	3
1319	**Disa**	**05 02.1**	**13.4**	**-18**	**7.08**	**0.24-0.27**	**3**
971	Alsatia	05 03.5	14.2	-3	9.614	0.17-0.29	3
948	Jucunda	05 05.5	15.4	-26	26.24	0.14-0.35	3
3306	**Byron**	**05 06.5**	**14.5**	**-15**	**7.321**	**0.18-0.84**	**3-**
323	Brucia	05 08.1	14.2	+12	9.463	0.15-0.36	3
42701	**1998 MD13**	**05 11.2**	**15.3**	**-3**	**2.603**	**0.09-0.19**	**3**
834	Burnhamia	05 12.0	12.9	-13	13.875	0.15-0.22	3
677	Aaltje	05 13.8	13.5	-27	16.608	0.10-0.37	3
240	Vanadis	05 16.5	13.6	-17	10.64	0.13-0.34	3
341	California	05 17.6	13.3	-24	18	0.43-0.92	3
2504	Gaviola	05 18.2	15.4	-24	8.738	0.25-0.31	3-
1369	Ostanina	05 18.4	14.8	-1	8.4	0.73-1.11	3
1567	Alikoski	05 21.8	14.1	-24	16.374	0.08-0.16	3
2764	Moeller	05 22.3	15.4	-23	5.953	0.24-0.51	3
2650	Elinor	05 25.6	15.2	-41	2.762	0.02-0.18	3
429	Lotis	05 26.8	13.9	-15	13.577	0.09-0.24	3
26471	Tracybecker	05 29.6	15.1	-38	2.687	0.18-0.25	3
3873	**Roddy**	**05 30.7**	**14.0**	**-23**	**2.478**	**0.05-0.11**	**3**
309	Fraternitas	05 31.0	13.8	-28	22.398	0.10-0.35	3
3800	Karayusuf	05 31.4	15.2	+0	2.232	0.10-0.19	3
4730	**Xingmingzhou**	**06 01.5**	**15.5**	**-19**	**3.396**	**0.15-0.23**	**3**
4159	Freeman	06 03.5	14.9	-14	4.402	0.23-0.40	3
1149	Volga	06 04.7	14.6	-25	27.262	0.14-0.26	3-
854	**Frostia**	**06 06.0**	**13.8**	**-11**	**37.56**	**0.33-0.38**	**3**
2729	Urumqi	06 06.8	15.2	-24	3.127	0.19-0.35	3
2166	Handahl	06 08.4	14.7	-12	7.226	0.11-0.13	3
542	Susanna	06 09.3	13.8	-5	10.069	0.11-0.30	3
2114	**Wallenquist**	**06 10.0**	**15.5**	**-24**	**5.51**	**0.22-0.30**	**3**
81	Terpsichore	06 11.9	13.5	-34	10.943	0.06-0.15	3
475	Ocllo	06 12.1	14.2	-47	7.315	0.19-0.81	3
298	Baptistina	06 14.0	14.2	-34	16.23	0.10-0.25	3
498	Tokio	06 14.9	11.7	-19	41.85	0.08-0.36	3
711	Marmulla	06 15.2	13.2	-37	2.721	0.03-0.18	3
1342	Brabantia	06 15.3	14.1	-53	4.175	0.17-0.23	3
973	Aralia	06 17.8	15.4	-45	7.366	0.20-0.25	3
1277	**Dolores**	**06 18.3**	**13.3**	**-19**	**12.676**	**0.42-0.45**	**3**
5144	Achates	06 18.7	14.6	-33	5.958	0.18-0.35	3
715	Transvaalia	06 20.0	13.9	-38	11.83	0.14-0.32	3
862	Franzia	06 21.0	14.1	-34	7.523	0.07-0.13	3
318	Magdalena	06 21.6	14.5	-9	42.65	0.06-0.11	3
643	Scheherezade	06 24.3	14.8	-17	14.161	0.23-0.37	3
70	**Panopaea**	**06 24.4**	**10.7**	**-39**	**15.805**	**0.07-0.18**	**3**
786	**Bredichina**	**06 28.0**	**12.6**	**-26**	**29.434**	**0.04-0.60**	**3-**
766	Moguntia	06 28.1	14.7	-38	4.816	0.06-0.23	3
1305	Pongola	06 30.4	14.5	-25	8.335	0.14-0.19	3-

Radar-Optical Opportunities

Table I below gives a list of near-Earth asteroids reaching maximum brightness for the current quarter-year based on calculations by Warner. We switched to this presentation in lieu of ephemerides for reasons outlined in the 2021 October-December opportunities paper (Warner et al., 2021b), which centered on the potential problems with ephemerides generated several months before publication.

The initial list of targets started using the planning tool at

https://www.minorplanet.info/php/callopplcdbquery.php

where the search was limited to near-Earth asteroids only that were V ≤ 18 for at least part of the quarter.

The list was then filtered to include objects that might be targets for the Goldstone radar facility or, if it were still operational, the Arecibo radar. This was based on the calculated radar SNR using

http://www.naic.edu/~eriverav/scripts/index.php

and assuming a rotation period of 4 hours (2 hours if *D* ≤ 200 m) if a period was not given in the asteroid lightcurve database (LCDB; Warner et al., 2009). The SNR values are estimates only and assume that the radar is fully functional.

If an asteroid was on the list but failed the SNR test, we checked if it might be a suitable target for radar and/or photometry sometime through 2050. If so, it was kept on the list to encourage physical and astrometric observations during the current apparition. In most of those cases, the SNR values in the "A" and "G" columns are not for the current quarter but the year given in the Notes column. If a better apparition is forthcoming through 2050, the Notes column in Table I contains SNR values for that time.

The final step was to cross-reference our list with that found on the Goldstone planned targets schedule at

http://echo.jpl.nasa.gov/asteroids/goldstone_asteroid_schedule.html

It's important to note that the final list in Table I is based on *known* targets and orbital elements when it was prepared. It is common for newly discovered objects to move in or out of the list. We recommend that you keep up with the latest discoveries by using the Minor Planet Center observing tools.

In particular, monitor NEAs and be flexible with your observing program. In some cases, you may have only 1-3 days when the asteroid is within reach of your equipment. Be sure to keep in touch with the radar team (through Benner's email or their Facebook or Twitter accounts) if you get data. The team may not always be observing the target but your initial results may change their plans. In all cases, your efforts are greatly appreciated.

For observation planning, use these two sites

MPC: *http://www.minorplanetcenter.net/iau/MPEph/MPEph.html*
JPL: *http://ssd.jpl.nasa.gov/?horizons*

Cross-check the ephemerides from the two sites just in case there is discrepancy that might have you imaging an empty sky.

About YORP Acceleration

Near-Earth asteroids are particularly sensitive to YORP acceleration. YORP (Yarkovsky-O'Keefe-Radzievskii-Paddack; Rubincam, 2000) is the asymmetric thermal re-radiation of sunlight that can cause an asteroid's rotation period to increase or decrease. High precision lightcurves at multiple apparitions can be used to model the asteroid's *sidereal* rotation period and see if it's changing.

It usually takes four apparitions to have sufficient data to determine if the asteroid rotation rate is changing under the influence of YORP. This is why observing an asteroid that already has a well-known period remains a valuable use of telescope time. It is even more so when considering the BYORP (binary-YORP) effect among binary asteroids that has stabilized the spin so that acceleration of the primary body is not the same as if it would be if there were no satellite.

The Quarterly Target List Table

The Table I columns are

Num	Asteroid number, if any.
Name	Name assigned by the MPC.
H	Absolute magnitude from MPCOrb.
Dkm	Diameter (km) assuming $p_V = 0.2$.
Date	Date (mm dd.d) of brightest magnitude.
V	Approximate V magnitude at brightest.
Dec	Approximate declination at brightest.
Period	Synodic rotation period from summary line in the LCDB summary table.
Amp	Amplitude range (or single value) of reported lightcurves.
U	LCDB U (solution quality) from 1 (probably wrong) to 3 (secure).
A	Approximate SNR for Arecibo (if operational and at full power).
G	Approximate SNR for Goldstone radar at full power.
Notes	Comments about the object.

"PHA" is a potentially hazardous asteroid. For good measure, consider that astrometry and photometry have been requested to support Goldstone observations. The sources for the rotation period are given in the Notes column. If none are qualified with a specific period, then the periods from multiple sources were in general agreement. Higher priority should be given to those where the current apparition is the last one V ≤ 18 through 2050 or several years to come.

References

Behrend, R. (2007web). Observatoire de Geneve web site.
http://obswww.unige.ch/~behrend/page_cou.html.

Dumitru, B.A.; Birlan, M.; Sonka, A.; Colas, F.; Nedelcu, D.A. (2018). "Photometry of asteroids (5141), (43032), (85953), (259221), and (363599) observed at Pic du Midi Observatory." *Astron. Nach.* **339**, 198-203.

Harris, A.W.; Young, J.W.; Bowell, E.; Martin, L.J.; Millis, R.L.; Poutanen, M.; Scaltriti, F.; Zappala, V.; Schober, H.J.; Debehogne, H.; Zeigler, K.W. (1989). "Photoelectric Observations of Asteroids 3, 24, 60, 261, and 863." *Icarus* **77**, 171-186.

Mahapatra, P.R.; Benner, L.A.M.; Ostro, S.J.; Jurgens, R.F.; Giorgini, J.D. Yeomans, D.K.; Chandler, J.F.; Shapiro, I.I. (2002). "Radar observations of asteroid 7335 (1989 JA)." *Planet. Space Sci.* **50**, 257-260.

Mottola, S.; Lahulla, F. (2000). "Mutual Eclipse Events in Asteroidal Binary System 1996 FG3: Observations and Numerical Model." *Icarus* **146**, 556-567.

Muinonen, K.; Belskaya, I.N.; Cellino, A.; Delbò, M.; Levasseur-Regourd, A.-C.; Penttilä, A.; Tedesco, E.F. (2010). "A three-parameter magnitude phase function for asteroids." *Icarus* **209**, 542-555.

Pravec, P.; Sarounova, L.; Rabinowitz, D.L.; Hicks, M.D.; Wolf, M.; Krugly, Y.N.; Velichko, F.P.; Shevchenko, V.G.; Chiorny, V.G.; Gaftonyuk, N.M.; Genevier, G. (2000). "Two-Period Lightcurves of 1996 FG 3, 1998 PG, and (5407) 1992 AX: One Probable and Two Possible Binary Asteroids." *Icarus* **146**, 190-203.

Pravec, P.; Wolf, M.; Sarounova, L. (2019web).
http://www.asu.cas.cz/~ppravec/neo.htm

Rubincam, D.P. (2000). "Radiative Spin-up and Spin-down of Small Asteroids." *Icarus* **148**, 2-11.

Taylor, P.A.; Nolan, M.C.; Howell, E.S.; Benner, L.A.M.; Brozovic, M.; Giorgini, J.D.; Margot, J.L.; Busch, M.W.; Naidu, S.P.; Nugent, C.; Magri, C.; Shepard, M.K. (2012). "2004 FG11." *CBET* **3091**.

Warner, B.D.; Harris, A.W.; Pravec, P. (2009). "The asteroid lightcurve database." *Icarus* **202**, 134-146.

Warner, B.D.; Stephens, R.D. (2019a). "Near-Earth Asteroid Lightcurve Analysis at the Center for Solar System Studies: 2018 September-December." *Minor Planet Bull.* **46**, 144-152.

Warner, B.D.; Stephens, R.D. (2019b). "Near-Earth Asteroid Lightcurve Analysis at the Center for Solar System Studies." *Minor Planet Bull.* **46**, 423-438.

Warner, B.D.; Harris, A.W.; Durech, J.; Benner, L.A.M. (2021a). “Lightcurve Photometry Opportunities: 2021 January-March.” *Minor Planet Bull.* **48**, 89-97.

Warner, B.D.; Harris, A.W.; Durech, J.; Benner, L.A.M. (2021b). “Lightcurve Photometry Opportunities: 2021 October-December.” *Minor Planet Bull.* **48**, 406-410.

Num	Name	H	D	Date	V	Dec	Period	Amp	U	A	G	Notes
474585	2004 HC2	19.46	0.381	04 03.6	17.0	-3				10	-	
363599	2004 FG11	21.03	0.185	04 09.8	17.1	37	7.021	0.3	2	75	20	PHA, Binary. Taylor et al. (2012). Dumitru et al. (2018).
	2015 TX143	19.76	0.332	04 17.0	17.8	63				12	–	
4544	Xanthus	17.21	1.070	04 20.2	14.9	-19	37.65	0.27	2	10	–	Behrend (2007web).
175706	1996 FG3	18.32	0.644	04 21.7	15.0	-20	3.5942	0.04 0.2	3	100	30	PHA, Binary, NHATS Mottola and Lahulla (2000). Pravec et al. (2000).
	2009 CC3	19.12	0.446	04 26.8	16.8	56				30	10	
418135	2008 AG33	19.40	0.392	05 02.5	15.8	-54				6900	1980	
467460	2006 JF42	19.20	0.430	05 10.3	13.4	-45				990	280	PHA
388945	2008 TZ3	20.46	0.240	05 10.9	16.2	-3	39.15	0.47 0.56	2+	1280	370	PHA. Pravec et al. (2019web).
	2017 VV	20.40	0.247	05 13.1	16.8	-16				55	15	
	2013 UX	22.00	0.118	05 14.8	17.7	-81				75	20	
163692	2003 CY18	18.16	0.693	05 18.2	16.0	54				60	15	
	2018 KM1	20.80	0.206	05 22.0	17.6	36				15	–	
5693	1993 EA	16.69	1.360	05 24.2	13.7	15	2.496	0.13	2	425	120	PHA. Warner and Stephens (2019b).
7335	1989 JA	17.52	0.931	05 25.8	11.1	-29	12			20200	5800	PHA. Mahapatra et al. (2002).
	2018 XR	18.58	0.571	06 17.8	15.8	-60	15.27	0.53	3	525	150	PHA. Warner and Stephens (2019a).
	2011 MU	20.28	0.261	06 19.8	16.6	8				40	10	
10302	1989 ML	19.40	0.392	06 23.6	15.9	-9	19.164	1.00 1.13	2+	40	10	Pravec et al. (2019web).
66400	1999 LT7	19.28	0.414	06 27.5	16.6	-39				45	15	

Table I. A list of near-Earth asteroids reaching brightest in the fourth quarter of 2021. * Favorable apparition. PHA: potentially hazardous asteroid. Diameters are based on $p_V = 0.20$. The Date, V, and Dec columns are the mm/dd.d, approximate magnitude, and declination when at brightest. Amp is the single or range of amplitudes. The A and G columns are the approximate SNRs for an assumed full-power Arecibo (not operational) and Goldstone radars. The references in the Notes column are those for the reported periods and amplitudes.

IN THIS ISSUE

This list gives those asteroids in this issue for which physical observations (excluding astrometric only) were made. This includes lightcurves, color index, and H-G determinations, etc. In some cases, no specific results are reported due to a lack of or poor-quality data. The page number is for the first page of the paper mentioning the asteroid. EP is the "go to page" value in the electronic version.

Number	Name	EP	Page
3	Juno	70	136
22	Kalliope	42	108
28	Bellona	70	136
129	Antigone	70	136
197	Arete	62	128
214	Aschera	70	136
237	Coelestina	70	136
246	Asporina	70	136
330	Adalberta	56	122
359	Georgia	62	128
382	Dodona	70	136
470	Kilia	59	125
478	Tergeste	59	125
478	Tergeste	75	141
494	Virtus	56	122
494	Virtus	65	131
494	Virtus	75	141
523	Ada	70	136
530	Turandot	56	122
530	Turandot	75	141
548	Kressida	59	125
579	Sidonia	75	141
605	Juvisia	75	141
666	Desdemona	59	125
666	Desdemona	65	131
670	Ottegebe	70	136
764	Gedania	75	141
784	Pickeringia	56	122
796	Sarita	62	128
814	Tauris	59	125
849	Ara	3	69
858	El Djezair	75	141
901	Brunsia	62	128
918	Itha	70	136
957	Camelia	65	131
1009	Sirene	56	122
1141	Bohmia	83	149
1159	Granada	75	141
1162	Larissa	36	102
1180	Rita	36	102
1180	Rita	75	141
1242	Zambesia	70	136
1243	Pamela	65	131
1346	Gotha	62	128
1352	Wawel	70	136
1358	Gaika	70	136
1558	Jarnefelt	65	131
1654	Bojeva	75	141
1713	Bancilhon	44	110
1748	Mauderli	36	102
1748	Mauderli	75	141
1762	Russell	5	71
1763	Williams	65	131
1774	Kulikov	40	106
1842	Hynek	83	149
1842	Hynek	83	149
1862	Apollo	17	83
1877	Marsden	36	102
1911	Schubart	65	131
1913	Sekanina	75	141
1929	Kollaa	83	149
2219	Mannucci	65	131
2232	Altaj	44	110
2301	Whitford	65	131
2458	Veniakaverin	44	110
2498	Tsesevich	10	76
2599	Veseli	75	141
2807	Karl Marx	83	149
3063	Makhaon	51	117
3200	Phaethon	17	83
3361	Orpheus	17	83
3596	Meriones	51	117
3648	Raffinetti	32	98
3942	Churivannia	47	113
4063	Euforbo	51	117
4068	Menestheus	51	117
4155	Watanabe	70	136
4162	SAF	75	141
4501	Eurypylos	51	117
4660	Nereus	17	83
4660	Nereus	62	128
4673	Bortle	47	113
4719	Burnaby	75	141
4935	Maslachkova	62	128
4988	Chushuho	54	120
5121	Numazawa	65	131
5143	Heracles	7	73
5186	Donalu	47	113
5235	Jean-Loup	32	98
5256	Farquhar	75	141
5917	Chibasai	83	149
5987	Liviogratton	4	70
6097	Koishikawa	70	136
6249	Jennifer	42	108
6249	Jennifer	62	128
6249	Jennifer	65	131
6681	Prokopovich	44	110
6706	1988 VD3	75	141
6764	Kirillavrov	15	81
6787	1991 PF15	44	110
6838	Okuda	65	131
6887	Hasuo	65	131
7145	Linzexu	40	106
7358	Oze	17	83
7393	Luginbuhl	54	120
7637	1984 DN	39	105
8080	Intel	11	77
8086	Peterthomas	36	102
8441	Lapponica	47	113
9223	Leifandersson	32	98
10389	Robmanning	83	149
11099	Sonodamasaki	40	106
11699	1998 FL105	32	98
12073	Larimer	32	98
12198	1980 PJ1	42	108
12259	Szukalski	47	113
12711	Tukmit	17	83
15121	2000 EN14	32	98
15560	2000 GR24	83	149
16024	1999 CT101	40	106
16452	Goldfinger	32	98
18863	1999 RC191	44	110
18882	1999 YN4	17	83
19982	Barbaradoore	83	149
20041	1992 YH	83	149
20460	Robwhiteley	17	83
20557	Davidkulka	32	98
27111	1998 VV34	83	149
29796	1999 CW77	32	98
35821	1999 JW50	32	98
45687	Pranverahyseni	42	108
46304	2001 OZ62	83	149
49483	1999 BP13	39	105
52800	1998 QT60	42	108
68063	2000 YJ66	59	125
87024	2000 JS66	17	83
125072	2001 UG	12	78
137062	1998 WM	17	83
137805	1999 YK5	17	83
285571	2000 PQ9	17	83
	1999 FJ21	17	83
	2018 GG	14	80
	2019 XS	17	83
	2021 LC1	24	90
	2021 RB1	24	90
	2021 US1	24	90
	2021 UW1	24	90
	2021 RS2	24	90
	2021 QB3	24	90
	2021 VL3	24	90
	2021 TT10	24	90
	2021 RG19	24	90
	2021 JQ24	17	83
	2021 RA	24	90
	2021 VQ26	24	90

THE MINOR PLANET BULLETIN (ISSN 1052-8091) is the quarterly journal of the Minor Planets Section of the Association of Lunar and Planetary Observers (ALPO, http://www.alpo-astronomy.org). Current and most recent issues of the *MPB* are available on line, free of charge from:

https://mpbulletin.org/

The Minor Planets Section is directed by its Coordinator, Prof. Frederick Pilcher, 4438 Organ Mesa Loop, Las Cruces, NM 88011 USA (fpilcher35@gmail.com). Robert Stephens (rstephens@foxandstephens.com) serves as Associate Coordinator. Dr. Alan W. Harris (MoreData! Inc.; harrisaw@colorado.edu), and Dr. Petr Pravec (Ondrejov Observatory; ppravec@asu.cas.cz) serve as Scientific Advisors. The Asteroid Photometry Coordinator is Brian D. Warner (Center for Solar System Studies), Palmer Divide Observatory, 446 Sycamore Ave., Eaton, CO 80615 USA (brian@MinorPlanetObserver.com).

The Minor Planet Bulletin is edited by Professor Richard P. Binzel, MIT 54-410, 77 Massachusetts Ave, Cambridge, MA 02139 USA (rpb@mit.edu). Brian D. Warner (address above) is Associate Editor, and Dr. David Polishook, Department of Earth and Planetary Sciences, Weizmann Institute of Science (david.polishook@weizmann.ac.il) is Assistant Editor. The *MPB* is produced by Dr. Pedro A. Valdés Sada (psada2@ix.netcom.com). The MPB is distributed by Dr. Melissa Hayes-Gehrke. Direct all subscriptions, contributions, address changes, etc. to:

Dr. Melissa Hayes-Gehrke
UMD Astronomy Department
1113 PSC Bldg 415
College Park, MD 20742 USA
(mhayesge@umd.edu)

Effective with Volume 38, the *Minor Planet Bulletin* is a limited print journal, where print subscriptions are available only to libraries and major institutions for long-term archival purposes. Effective with Volume 50, January 1, 2023 and beyond, printed issues of the *Minor Planet Bulletin* will no longer be distributed. In addition to the free electronic download of the *MPB* noted above, electronic retrieval of all *Minor Planet Bulletin* articles (back to Volume 1, Issue Number 1) is available through the Astrophysical Data System:

http://www.adsabs.harvard.edu/

Authors should submit their manuscripts by electronic mail (rpb@mit.edu). Author instructions and a Microsoft Word template document are available at the web page given above. All materials must arrive by the deadline for each issue. Visual photometry observations, positional observations, any type of observation not covered above, and general information requests should be sent to the Coordinator.

*   *   *   *   *

The deadline for the next issue (49-3) is April 15, 2022. The deadline for issue 49-4 is July 15, 2022.